Analysis of Transcranial Doppler Ultrasound Waveform Morphology for the Assessment of Cerebrovascular Hemodynamics

by

Kathryn Alexandra Zuj

A thesis
presented to the University of Waterloo
in fulfillment of the
thesis requirement for the degree of
Doctor of Philosophy
in
Kinesiology

Waterloo, Ontario, Canada, 2012

Author’s Declaration

I hereby declare that I am the sole author of this thesis. This is a true copy of the thesis, including any required final revisions, as accepted by my examiners.

I understand that my thesis may be made electronically available to the public.

Abstract

The use of transcranial Doppler (TCD) ultrasound for the assessment of cerebral blood flow velocity (CBFV) provides an indication of cerebral blood flow assuming the diameter of the insonated vessel remains constant. Studies using TCD have traditionally described cerebrovascular hemodynamics with respect to CBFV and cerebrovascular resistance (CVRi); however, a more complete assessment of the cerebral circulation can be gleaned from the analysis of within beat characteristic of the TCD velocity waveform for the determination of cerebrovascular tone. Therefore, the general purpose of the presented studies was to assess CBFV responses and within beat characteristic for the description of cerebrovascular hemodynamics after long duration spaceflight, with sustained orthostasis, in response to changes in the partial pressure of end tidal carbon dioxide ($P_{ET}CO_2$), and with NG stimulation. After long duration spaceflight, cerebrovascular autoregulation was found to be impaired along with a reduction in cerebrovascular CO_2 reactivity (Study 1). Additionally, critical closing pressure (CrCP) was found to be increased suggesting potential remodelling of the cerebrovasculature contributing to an increase in cerebrovascular tone (Study 2). With sustained orthostasis, CBFV was found to progressively decrease and to be related to reductions in $P_{ET}CO_2$ and increases in CrCP suggesting the contribution of changes in cerebrovascular tone leading to the development of syncope (Study 4). The CBFV reduction with the progression towards syncope was also associated with changes in waveform morphology such that the dicrotic notch point was less than the end diastolic value (Study 3). Mathematical modelling (RCKL) was used to further assess changes in cerebrovascular hemodynamics for physiological interpretation of changes in CBFV waveform morphology and found that the amplitude of the dicrotic notch and the calculation of the augmentation index were both significantly related to vascular compliance before and after stimulation with NG (Study 5). The use of quantitative assessments of common carotid artery (CCA) blood flow as an indicator of cerebral blood flow suggested the dilation of the middle cerebral artery (MCA) with NG (Study 5 and 6) and changes in MCA diameter with acute alterations in $P_{ET}CO_2$ (Study 6). CCA and MCA velocity wave morphology were assessed showing that with changes in $P_{ET}CO_2$, changes in CBFV velocity wave were not reflected in the CCA

trace (Study 7). In addition, further assessment of the CBFV velocity trace and the calculation of CrCP and the augmentation index suggested that with changes in $P_{ET}CO_2$ cerebrovascular compliance and cerebrovascular tension, both thought to be components of cerebrovascular tone, change independently (Study 7). Combined, the results of the presented studies suggest that changes in cerebrovascular hemodynamics can be determined from alterations in the CBFV velocity waveform morphology. However, further work is required to determine how these variations relate to specific components of cerebrovascular tone, including alterations in cerebrovascular compliance and vascular tension, and how these variables change with acute and chronic alterations in cerebrovascular hemodynamics.

Acknowledgements

To simply say “thank you” seems too small a phase to express how I feel. There are so many people to acknowledge who have supported me and contributed to the development of this thesis. It may take a village to raise a child, but it also takes a village to support a PhD student and I have had an amazing community around me. Whether it has been assistance with data collection and processing, company for coffee, or a simple word of encouragement each action has contributed to the completion of this thesis. I thank you all, as this would not have been possible without you.

Finally, I would be remiss if I didn’t mention my supervisor, Dr. Richard Hughson. It feels surreal that back in 2003 I started in his lab as an undergraduate summer NSERC student getting my first experiences with this crazy thing known as “transcranial Doppler ultrasound”. Rich: Thank you so much for all the opportunities that you have given me along this incredible journey. It hasn’t always been easy, but it has been a truly amazing and memorable experience!

Dedication

To my Mum: It’s been a long road. I love you, Mum.

Table of Contents

List of Figures

List of Tables

List of Abbreviations

ABP	Arterial Blood Pressure
AG	Artificial Gravity
AI	Augmentation Index
ARMA	Autoregressive Moving Average
ASL	Arterial Spin Labelling
BOLD	Blood Oxygen Level Dependent
BP_{MCA}	Blood Pressure at the level of the MCA
C	RCKL model output of Vascular Compliance
CA	Cerebrovascular Autoregulation
CBF	Cerebral Blood Flow
CBFV	Cerebral Blood Flow Velocity
CBFVmin-dia	Difference between the minimum and end diastolic CBFV points
CCA	Common Carotid Artery
CCA_{VR}	Common Carotid Artery Vascular Resistance
CO_2	Carbon Dioxide
CON	Control Condition
CPP	Cerebral Perfusion Pressure
CrCP	Critical Closing Pressure
CVRi	Cerebrovascular Resistance Index
ECA	External Carotid Artery
fMRI	Functional Magnetic Resonance Imaging

GCTC	Gagarin Cosmonaut Training Center
HDBR	Head-Down Bed Rest
HLU	Hind-Limb Unloading
HR	Heart Rate
ICA	Internal Carotid Artery
ICP	Intracranial Pressure
ISS	International Space Station
JSC	Johnson Space Center
K	RCKL model output of Viscoelastic Resistance
KSC	Kennedy Space Center
L	RCKL model output of Inertance
LBNP	Lower Body Negative Pressure
MAP	Mean Arterial Pressure
MCA	Middle Cerebral Artery
NASA	National Aeronautics and Space Administration
NG	Nitroglycerin
NO	Nitric Oxide
O_2	Oxygen
P1-T1	Waveform characteristic of the pulse amplitude
P2-T1	Waveform characteristic of the amplitude of the reflected wave
$PaCO_2$	Partial Pressure of Arterial CO_2
PCO_2	Partial Pressure of CO_2
PET	Positron Emission Tomography

$P_{ET}CO_2$	Partial Pressure of End Tidal CO_2
PI	Pulsatility Index
R	RCKL model output of Vascular Resistance
RAP	Resistance Area Product
RI	Resistivity Index
SPECT	Single-Photon Emission Computed Tomography
SV	Cardiac Stroke Volume
T1	Waveform inflection point equivalent to the end diastolic value
T3-T1	Waveform characteristic of the amplitude of the dicrotic notch
TCD	Transcranial Doppler Ultrasound
$TEMP_{VR}$	Temporal Artery Vascular Resistance
V_{TEMP}	Temporal Artery Blood Velocity

Chapter 1
General Introduction

1.1 Introduction

Adequate cerebral blood flow (CBF) is critical to brain function as CBF provides the means of delivery of oxygen (O_2) and glucose to cerebral tissue and the removal of carbon dioxide (CO_2). Inadequate CBF has been shown to produce cognitive impairment (Poels et al., 2008) with further declines leading to loss of consciousness (Bondar et al., 1995) and potentially death. With human populations, the use of non-invasive methods for the assessment of CBF regulation is essential for clinical application and many experimental situations. Analysis methods have been developed for use with these non-invasive measures which allow for some information to be gleaned about the cerebral circulation; however, in the words of R. Panerai: "...efforts must be made to improve the amount of information that can be extracted from existing measurement techniques," (Panerai, 2003).

A quick review of the literature will show the assessment of CBF under a wide variety of conditions and disease states including responses to spaceflight. Exposure to microgravity has been shown to promote cephalic fluid shifts (Hargens & Watenpaugh, 1996) which may contribute to remodeling of the cerebrovasculature and affect the regulation of cerebral blood flow. Recently the National Aeronautics and Space Administration (NASA) has identified idiopathic intracranial hypertension and its resultant consequences as a serious health concern for long duration spaceflight (Fogarty, 2011). In addition to change in intracranial pressure with exposure to microgravity, atmospheric conditions aboard spacecraft may also influence CBF as aboard the International Space Station (ISS) the partial pressure of CO_2, a known vasodilator of cerebral blood vessels, is greater than normal Earth atmospheric levels.

The use of transcranial Doppler ultrasound (TCD) has allowed for the assessment of cerebral blood flow velocity (CBFV) in humans. In addition to conventional assessments of CBFV, analysis of the blood velocity profile may provide additional information about the

cerebral hemodynamic environment and the consequences of long duration spaceflight on CBF and CBF regulation. The following sections will provide an overview of the assessment of CBF and the use of TCD, factors affecting cerebral hemodynamics, assessment of Doppler waveform morphology, assessment of functional cerebral hemodynamics, the influence of nitric oxide in CBF regulation including responses to changes in CO_2 and nitroglycerin stimulation, and current understanding of CBF responses to spaceflight and spaceflight analogue studies.

1.2 Assessment of Cerebral Blood Flow and Transcranial Doppler Ultrasound

Over the years, the assessment of CBF has taken many forms for both clinical and research applications. Initial work required the use of invasive techniques, primarily involving patient populations undergoing cranial surgery and utilizing flow probes for the direct assessment of cerebral arteries (Nornes & Wikeby, 1977) and carotid arteries (Lindegaard et al., 1987). Some information about cerebral blood flow responses can be determined from this type of study; however, conclusions are generally limited to the anesthetized patient population. As such, these methods are generally not practical for wide spread research or clinical applications.

The development of non-invasive methods of determining CBF has led to a greater understanding of cerebral hemodynamics in both health and disease. Several techniques have involved the use of tracer molecules as in stable xenon-enhanced computed tomography (Nariai et al., 1995) or inhalation of xenon-133 for use with single-photon emission computed tomography (SPECT). In addition to SPECT, positron emission tomography (PET) has been commonly used in the assessment of CBF. Both SPECT and PET methods require the administration of a radioactive isotope which is then monitored by detection equipment for the assessment of total and/or regional CBF (Wintermark et al., 2005). Unlike SPECT, PET measurements involve the use of metabolic tracers which allow for the determination of oxygen extraction which can then be used as an indicator of cerebral metabolism

(Wintermark et al., 2005; Powers, 1991). PET has been frequently used to validate other methods of determining CBF (Nariai et al., 1995; Poeppel et al., 2007); however the use of radioactive material among other technical considerations limit the applications of these methods for determining CBF.

Functional magnetic resonance imaging (fMRI) capitalizes on the different signals produced by oxygenated versus deoxygenated haemoglobin which can be used as an indicator of CBF without the administration of radioactive material. When subjected to a magnetic field, the free lone pair on deoxygenated haemoglobin produces a different magnetic signature in the surrounding tissue allowing for blood oxygen level dependent (BOLD) imaging (Brown, Perthen, Liu, & Buxton, 2007; Forster et al., 1998). BOLD signal increases with the presence of oxygenated haemoglobin allowing for the relative change in signal intensity to be determined (Brown et al., 2007; Forster et al., 1998). As BOLD gives an indication of oxygen levels, observed changes in BOLD signal can be the result of either a change in CBF, a change in blood volume, or a change in the oxygen utilization of cerebral tissue. The limitations inherent in BOLD imaging have led to a refined fMRI technique known as arterial spin labeling (ASL).

With ASL, a perpendicular magnetic field is applied to a "tagging" region of the body which serves to align the spins of water molecules in that region (Brown et al., 2007). Images are then recorded in an "imaging" region where the appearance of the spin oriented water molecules in blood are recorded (Brown et al., 2007). ASL provides a quantitative method for determining CBF in steady state situations and fMRI imaging techniques appear to be very promising with respect to the non-invasive determination of CBF; however, they do possess the limitations of size of measurement equipment required, length of time for assessment, and restricted application in the assessment of dynamic changes in CBF.

In 1982, Aaslid et al. (Aaslid, Markwalder, & Nornes, 1982) described the use of TCD as a non-invasive method for the assessment of CBF. TCD uses the principles of Doppler ultrasound to determine the velocity of red blood cells travelling towards or away from the Doppler probe. Briefly, and ultrasound wave of known frequency is transmitted

from the probe towards a vessel of interest, traditionally the middle cerebral artery (MCA). Sound waves are reflected off particles back towards the probe with the frequency of returning sound waves depended on the velocity of the particle from which it was reflected. Therefore, by determining the frequency shift and knowing the angle of insonation, the velocity of the moving particles, primarily red blood cells, can be determined using the Doppler Shift Equation (A):

(A) $$V = \frac{f_d \cdot C}{2 f_t \cdot \cos\theta}$$

Where V is the velocity of the moving particle, f_d is the Doppler shift frequency, C is the velocity of the sound wave through tissue, f_t is the transmitted ultrasound frequency, and θ is the angle of insonation (Hoskins, 1990). A schematic of Doppler ultrasound measurement is presented in Figure 1.1 drawn from information discussed in Reneman et al. (Reneman, Hoeks, & Spencer, 1979).

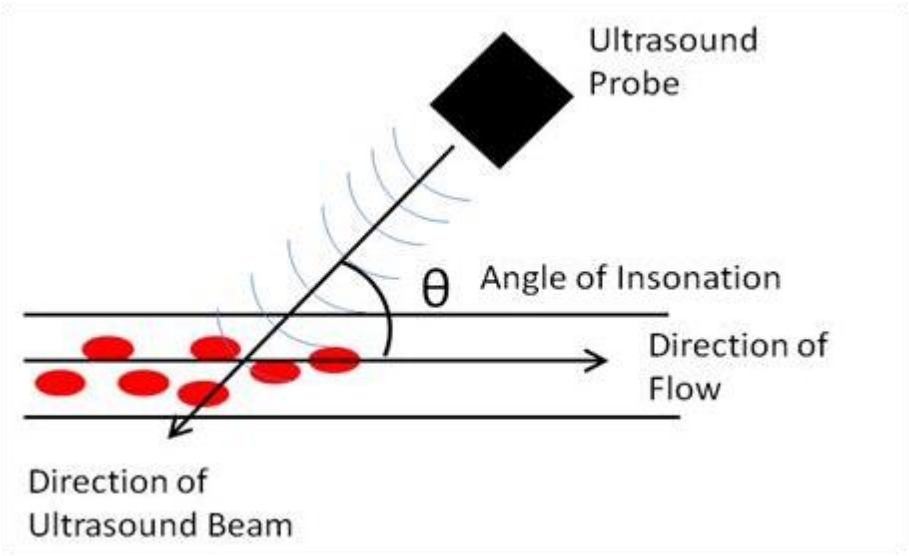

Figure 1.1: Schematic of Doppler ultrasound measurement

The ultrasound probe sends out a sound wave of known frequency that is reflected off particles back towards the probe. The frequency of the returning sound wave can be described using the Doppler shift equation (A) and is dependent on the transmitted frequency, the velocity of the particle reflected off, and the angle between the direction of the ultrasound beam and the direction of the moving particle (angle of insonation).

It should be highlighted that TCD provides measures of cerebral blood velocity and not flow. As such, TCD measures are commonly expressed as cerebral blood flow velocity (CBFV) with the assumptions made that the angle of insonation and the diameter of the MCA both remain constant with testing and, therefore, velocity measures are reflective of CBF. TCD validation studies have shown that measures of CBFV track well with changes in CBF (Poeppel et al., 2007; Dahl et al., 1992; Bishop, Powell, Rutt, & Browse, 1986; Muller, Voges, Piepgras, & Schimrigk, 1995; Ulrich, Becker, & Kempski, 1995) suggesting that the assumptions involved with the use of TCD for the assessment of CBF are valid. Studies have shown no changes in MCA diameter during experimental manipulations such as orthostatic stress and changes in arterial CO_2, when measured during cranial surgery (Giller et al., 1993), angiography (Djurberg et al., 1998), assessing the power of the TCD Doppler spectrum (Poulin & Robbins, 1996), or through the use magnetic resonance imaging (Serrador, Picot, Rutt, Shoemaker, & Bondar, 2000; Schreiber, Gottschalk, Weih, Villringer, & Valdueza,

2000; Valdueza et al., 1997). However, other work has suggested that the MCA is not a static vessel and, therefore, care needs to be taken when interpreting CBFV as CBF.

Work by Hansen et al. (Hansen et al., 2007) has shown using MRI imaging that the MCA does dilate with nitroglycerin stimulation. In another study, Valdueza et al. (Valdueza, Draganski, Hoffmann, Dirnagl, & Einhaupl, 1999) used venous outflow measures in comparison to MCA velocity measures to suggest the dilation of the MCA with hypercapnia. In addition, a more recent paper showed that changes in CBFV underestimated changes in cerebral blood flow with hypercapnia and hypocapnia suggesting the possible dilation of the MCA (Willie et al., 2012). Methodological considerations have also raised questions as to the accuracy of the observation of no changes in MCA diameter. Bondar et al. (Bondar et al., 1990), who used the Doppler spectrum power method to assess MCA diameter during parabolic flight cautioned that the values may have been affected by slight changes in the relative positions of the MCA and the ultrasound probe during the protocol thus changing the amount of ultrasound signal scattered by surrounding tissue and, therefore, altering the reflected spectrum power independent of changes in vessel diameter. Work published by Serrador et al. (Serrador et al., 2000) has frequently been used as support for the assumption that the diameter of the MCA does not change. However, the paper states that the resolution of the images analyzed in this study was unclear. The authors believed that the resolution was higher than the single pixel size of 0.47mm but this was not known. Assuming that the resolution of the images in this paper was improved to 0.25mm, this is still 10% of the diameter of an average MCA. Therefore, it is possible that this study was not able to detect small changes in MCA diameter that may have a significant influence on cerebral blood flow. To date, no studies have been conducted with improved MRI image resolution to verify results of this study.

In addition to assumptions made about MCA diameter, equation (A) shows that absolute values of CBFV are also dependent on the cosine of the angle of insonation. Therefore, as the angle of insonation approaches zero, the cosine of the angle approaches one and the accuracy of the velocity measurement increases. Conversely, as shown in Figure 1.2, as the angle of insonation becomes greater than 60°, where the error is 100%, the error of

recorded velocities increases such that small change in angle produce large errors in the calculation of velocity.

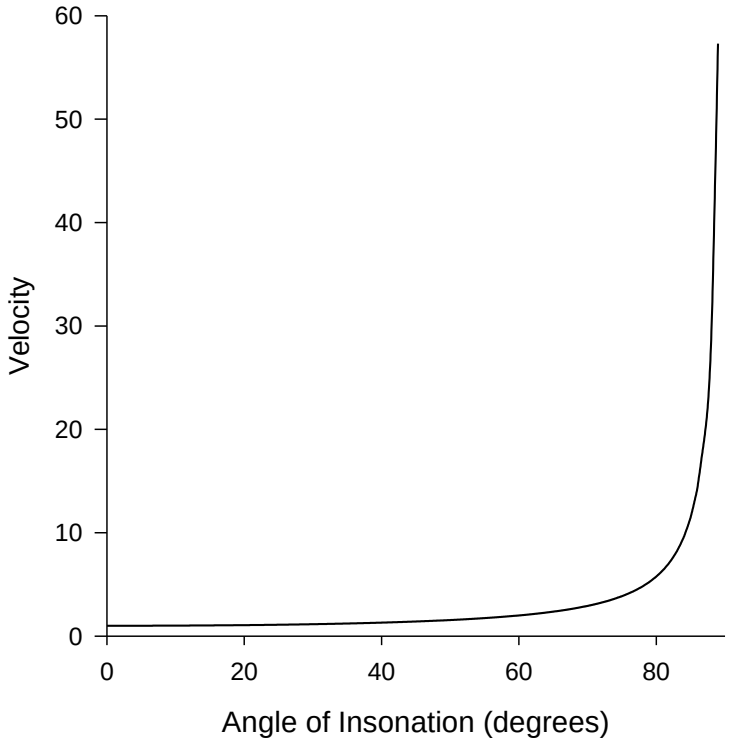

Figure 1.2: Relationship between angle of insonation and resultant calculated velocity
Using a starting velocity value of 1cm/s at an angle of 0°, this figure has been adapted from the Doppler shift equation where the calculated velocity is proportional to 1/cosθ. From the curve it can be seen that changes in the angle of insonation (θ) produce much smaller changes in velocity with angles approaching 0°.

When using TCD to assess blood flow in the MCA, the probe is placed over the temporal window where the skull bone allows for the transmission of ultrasound waves towards the cerebral blood vessels. The use of this site for ultrasound allows for an angle of insonation with the MCA approaching zero; thus decreasing potential error in the calculation of blood velocity. At least one group has attempted to use ultrasound imaging to determine the angle of insonation for the MCA, suggesting an angle of insonation for the right MCA of 30±16 degrees (Krejza et al., 2007). Assuming an angle of 30% would account for an error of

approximately 15%. Therefore, as it is not possible to measure the exact angle of insonation using TCD, care needs to be taken in the placement of the probe to ensure that the angle of insonation remains as consistent as possible.

In addition to being a relatively simple method for the assessment of cerebral blood flow velocity with the use of equipment that is potentially very portable allowing for the use in a wide variety of settings, TCD is able to generate continuous, beat-by-beat mean measures of CBFV and a velocity trace throughout the cardiac cycle. When determining blood flow during a 'steady state' condition, flow can be explained through the relationship of pressure and vascular resistance. However, a true steady state condition is never achieved as fluctuations in blood flow are known to occur within a cardiac cycle and on a beat-by-beat basis. Therefore, analysis of the beat-by-beat and within cardiac cycle variation of the TCD velocity recording may provide additional information about other factors affecting cerebral blood flow in dynamic conditions.

1.3 Factors Affecting Cerebral Blood Flow

The assessment of cerebral hemodynamics primarily requires an understanding of factors that affect blood flow. Overall blood flow is affected by a number of variables and is generally simplified to use the principles of Newtonian fluids flowing through rigid tubes. Using this simplification, hemodynamics can be explained by Poiseuille's law (B).

(B) $$Q = \frac{\Delta P \pi r^4}{8 \mu L}$$

By examining equation (B), it can be seen that flow (Q) is directly proportional to the pressure change across the system (ΔP) and the radius of the tube (r) to the fourth power. As well, flow is inversely proportional to the viscosity of the fluid (μ) and the length of the tube (L). With respect to acute changes in blood flow, it is assumed that the length of the system and the viscosity of blood do not change acutely. Therefore, flow is then described with respect to the pressure drop across the system and vascular radius, or vascular resistance such that flow is equal to the pressure gradient divided by resistance.

1.3.1 Vascular Resistance

To date, much of the research with respect to cerebral blood flow has focused on the pressure, flow, and resistance relationships. It is well known that not all blood cells within a vessel are moving at the same velocity. For simplification, it is generally assumed that blood flow is laminar with a parabolic flow profile such that faster moving particles are in the centre of the artery and slower moving particles near the wall (Ku, 1997). The different red blood cell velocities are evident in the Doppler spectrum as the intensity of the Doppler spectrum is dependent on the number of particles moving at a particular velocity. Traditionally, measures of CBFV using TCD have used the outer envelope of the Doppler spectrum representing the maximal velocity of particles within the vessel. The use of the peak envelope may not completely reflect changes in blood velocity within the vessel; however, assuming the central portion of the vessel is included in the sampling volume, it does provide a very repeatable and reproducible measure that is not artificially affected by slight shifts in probe placement or changes in vessel diameter.

The influence of blood pressure on cerebral blood flow is generally determined using a peripheral measure of arterial blood pressure (ABP). With participants resting in a supine position, pressure is thought to be equalized throughout the body; therefore, measures of ABP are used to represent cerebral perfusion pressure. Upon assuming an upright posture, pressure measures are adjusted to the height level of the TCD probe to provide an indication of pressure at the level of the brain.

Using the measures of ABP corrected to the level of the TCD probe (BP_{MCA}) and CBFV, an index of cerebrovascular resistance can be calculated as:

(C) $$CVRi = \frac{BP_{MCA}}{CBFV}$$

Where the cerebrovascular resistance index (CVRi) is equal to the ratio of arterial blood pressure at the level of the TCD and CBFV. Describing cerebral blood flow regulation with respect to CBFV and CVRi does provide some information; however, this method also presents several limitations. As with the use of CBFV as an indicator of CBF, the use of

CVRi as an indication of resistance is dependent on the assumption that the diameter of the MCA remains constant and that BP_{MCA} accurately reflects the pressure change across the cerebral circulation (perfusion pressure). In addition, the use of CVRi also assumes that flow though cerebral vessels will continue to 0mmHg, which may not be accurate as seen by the concept of critical closing pressure (Burton, 1951).

1.3.2 Cerebral Perfusion Pressure

Cerebral perfusion pressure (CPP) is the pressure promoting blood flow to the brain or, with respect to equation (B), the ΔP of the system. This value is dependent on arterial pressure, intracranial pressure (ICP), and the venous pressure exiting the cerebral circulation (Mathew, 1996; Paulson, Waldemar, Schmidt, & Strandgaard, 1989; Zhang, 2001). The venous component of CPP is generally ignored, as it is thought that the venous system provides minimal resistance to venous outflow, and that the veins are not producing a siphon effect on the cranium (Carey, Manktelow, Panerai, & Potter, 2001). It is also thought that intracranial pressure remains constant under most conditions (Carey et al., 2001; Mathew, 1996; Zhang, 2001), therefore, mean arterial pressure at the level of the brain is often used as a substitute for CPP measurements.

Work has been conducted looking at the changes in cerebral spinal fluid pressure dynamics which could influence ICP and, therefore, CPP (Haubrich et al., 2007; Hu, Alwan, Rubinstein, & Bergsneider, 2006). Studies examining ICP have primarily looked at individuals with head injuries; however, it does present a precedent for situations where CPP may be changing due to changes in ICP (Portella et al., 2005). Questions still remain on how changes in cerebral spinal fluid dynamics affect ICP, if these changes occur on an acute basis, and what exact influences these changes may have on CBF.

1.3.3 Vascular Impedance

The use of the pressure and resistance relationship to describe blood flow may be adequate over long periods of time; however, the dynamic and pulsatile nature of blood flow suggests the use of vascular impedance. In addition to vascular resistance, impedance also

incorporates in the influences of the inertia of blood and vascular elasticity or vascular compliance (Zhu, Tseng, Shibata, Levine, & Zhang, 2011; Zamir, 2005).

Static vascular compliance can be defined as the slope of the pressure-volume curve or dV/dP where dV is the change in volume for the change in pressure dP and has been shown to be affected by several variables including vascular wall composition and vascular tone (Klabunde, 2007). Several studies have attempted to examine cerebrovascular tone using the concept of critical closing pressure (CrCP). First introduced in 1951 by Burton (Burton, 1951), CrCP is defined at the pressure level where blood flow is ceased due to the theoretical collapse of small vessels. Based on the principles of Laplace's Law, Burton showed that CrCP would be dependent on both the active tension of the blood vessel, and the unstretched radius of the vessel. In the study of human cerebral circulation, direct assessment of the critical closing pressure is not possible; however, several methods have been developed that provide indications of CrCP (Panerai, Salinet, Brodie, & Robinson, 2011). Calculation of CrCP also allows for the determination of the resistance area product (RAP) described by Evans et al. (Evans, Levene, Shortland, & Archer, 1988). Calculated as the inverse of the pressure-velocity slope, RAP provides an indication of cerebrovascular resistance accounting for the influence of CrCP (Carey, Eames, Panerai, & Potter, 2001; Panerai, 2003).

In the study of CrCP, changes have been seen with alterations in CO_2 such that an increase in CO_2 produces a reduction in CrCP and an a reduction in CO_2 increases CrCP (Panerai, Deverson, Mahony, Hayes, & Evans, 1999; Ainslie, Celi, McGrattan, Peebles, & Ogoh, 2008; Panerai, 2003). Interestingly, these studies also showed no changes in RAP suggesting that alterations in cerebral blood flow with CO_2 are primarily affected by change in vascular tension and vessel radius and not necessarily vascular resistance (Panerai et al., 1999). Work by Ogoh et al. (Ogoh, Brothers, Jeschke, Secher, & Raven, 2010) showed an increase in CrCP with heavy exercise which they suggested was related to an increase in plasma norepinephrine in addition to a reduction in the partial pressure of CO_2 (PCO_2). With the progression towards syncope, Carey et al. (Carey et al., 2001) have also shown increases

in CrCP and reductions in RAP suggesting that changes in cerebrovascular tone and resistance interact in the regulation of cerebral blood flow with approaching syncope.

The influence of cerebrovascular tone in the regulation of cerebral blood flow has been studied more recently with work assessing cerebrovascular autoregulation with respect to a Windkessel model including the components of both resistance and compliance. In 2009, Zhang et al. (Zhang, Behbehani, & Levine, 2009) showed, using a three-element Windkessel model, that steady state values of cerebrovascular resistance and/or compliance may influence dynamic cerebrovascular autoregulation. These results were later supported by Chan et al. (Chan et al., 2011) using a two-element Windkessel model. In a more recent paper, Zhu et al. (Zhu et al., 2011) have suggested that transfer function analysis of pressure and CBFV recordings can be used to determine cerebrovascular impedance in the frequency domain and that alterations in cerebrovascular impedance occur with age. The results of these studies suggest that values and changes in vascular tone, cerebrovascular compliance, and in general, cerebrovascular impedance cannot be ignored in the dynamic assessment of cerebral blood flow regulation. In addition, work has shown that, in peripheral vessels, a reduction in vascular compliance has been associated with an increase in risk of vascular injury and the progression of cardiovascular disease (Seals, 2003). Therefore, the assessment of cerebrovascular tone may be important in both clinical and research settings.

1.4 TCD Waveform Analysis

Waveform analysis is not a new concept in the study of blood flow dynamics, but in some ways it is a topic that is rarely studied. It is well known that pulsatile flow will result in a waveform profile that is dependent on a number of contributing factors including driving pressure, vessel diameter, and vessel compliance. Therefore, through the assessment of TCD waveform morphology it may be possible to glean additional information about changes in cerebrovascular hemodynamics.

1.4.1 Doppler Resistance Indices

Many researchers have looked to the shape of Doppler velocity waveforms as a means of determining downstream vascular resistance. Several Doppler resistance indices have been developed for use in different situations. In a simple form, researchers have looked at the relationship between the maximum velocity point and minimum velocity point as shown in Figure 1.3. The ratio between systolic and diastolic, maximum and minimum velocity, has been used; however, some work has shown that this relationship does not adequately reflect changes in resistance (Adamson, Morrow, Langille, Bull, & Ritchie, 1990). This is especially true in high resistance vascular beds where the minimum velocity point approaches zero or is negative (Figure 1.3, panel B). In this case, researchers have suggested that the ratio be reversed to diastolic to systolic, or minimum to maximum (Arbeille, Berson, Achaibou, Bodard, & Locatelli, 1995).

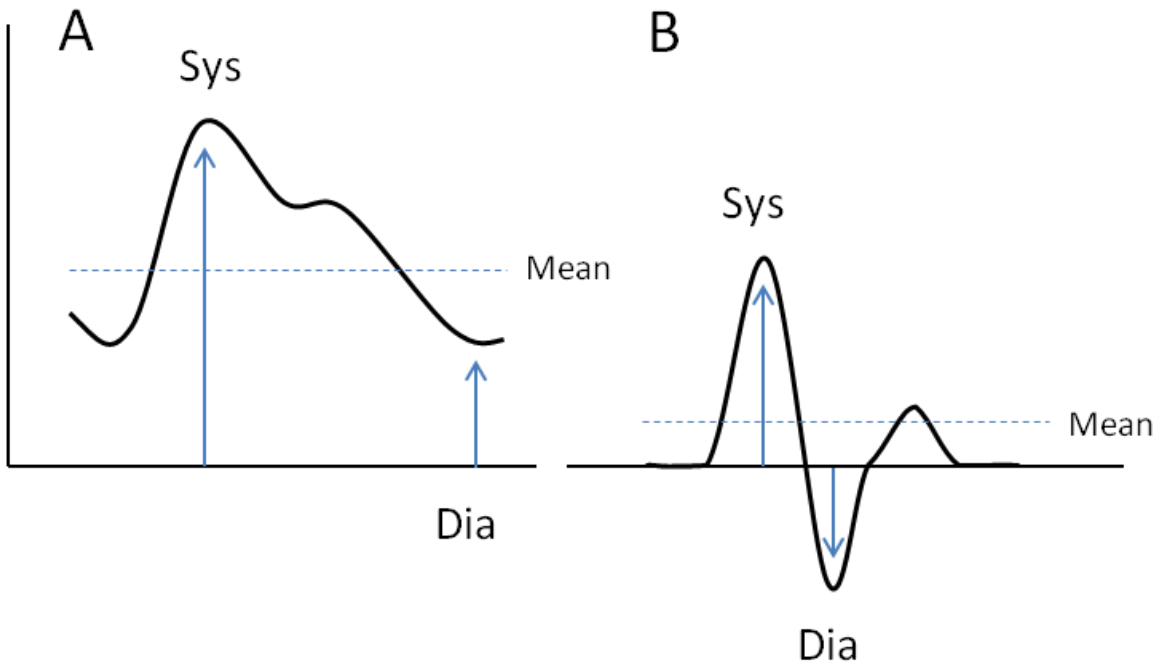

Figure 1.3: Velocity points for Doppler resistance indices

Adapted from Arbeille et al. (Arbeille et al., 1995), this figure shows a schematic of a velocity trace for a low resistance vascular bed (panel A) and a high resistance vascular bed (panel B). The figure shows a dashed horizontal line showing the mean of the velocity signals, and arrows pointing to the systolic (Sys) and diastolic (Dia) points that are used for the calculation of the Doppler resistance indices.

For use with low resistance vascular beds such as cerebral circulation, the resistivity index (RI) was developed based on the theory that as downstream resistance changes, the amplitude of the diastolic component of the wave will also change (Donald & Levi, 1976). Calculated as:

(D) $$RI = \frac{CBFVsys - CBFVdia}{CBFVsys}$$

RI calculates the proportion of the wave that is diastolic, or the minimum point (CBFVdia) with relation to the systolic, or maximum point (CBFVsys). As resistance increases, the wave becomes sharper with larger pulse amplitude (CBFVsys – CBFVdia). Therefore, the

contribution of the diastolic component of the wave is very small, increasing the RI. As resistance decreases, the contribution of the diastolic component of the wave increases thereby decreasing RI.

RI provides an indication of resistance based on two points on the Doppler waveform and the observation that the diastolic point of a velocity wave will change with changes in downstream vascular resistance. First described in 1969, the Gosling pulsatility index (PI) relates the amplitude of the velocity waveform to the mean of the wave (Hoskins, 1990). Therefore, PI is calculated as:

(E) $$PI = \frac{CBFVsys - CBFVdia}{CBFVmean}$$

In contrast to RI, PI appears to provide a more robust estimate of resistance as it incorporates the entire waveform and is not as heavily reliant on two points. Both RI and PI have been validated experimentally and appear to track well with changes in vascular resistance (Adamson et al., 1990). However, it is thought that changes in CPP may influence RI and PI independently of changes in vascular resistance (Zwiebel & Pellerito, 2005). In addition, a recent study has suggested that PI is a more complex variable reflecting multiple cerebrovascular characteristics (de Riva et al., 2012). Therefore, care needs to be taken with the interpretation of PI as factors other than cerebrovascular resistance may be influencing this value.

Other work has started to question the exact points of the velocity wave that are to be used in the calculation of the Doppler resistance indices. Traditionally, CBFVsys has been considered the maximum point of the CBFV waveform; however, Kurji et al. (Kurji et al., 2006) and Robertson et al. (Robertson, Debert, Frayne, & Poulin, 2008) have both shown CBFV waveforms that exhibit a distinct second peak which is higher than the observed first peak which the authors suggest is a wave augmentation and should not be considered as CBFVsys. Further work is required to assess this statement and to determine which points most accurately reflect downstream vascular resistance.

1.4.2 MCA Velocity Wave Inflection Points

Several studies considering the entire velocity wave over a cardiac cycle have looked to simplify the MCA velocity waveform and characterize it based on several key points (Kurji et al., 2006; Aggarwal, Brooks, Kang, Linden, & Patzer, 2008; Robertson et al., 2008; Lockhart et al., 2006). As shown in Figure 1.4, the MCA velocity wave can be characterized by several peaks (P1, P2, and P3) and troughs (T1, T2, and T3). Interpretation of the velocity wave inflection points has mainly attempted to link the observed velocity wave profile to that of the arterial pressure wave (Aggarwal et al., 2008; Robertson et al., 2008). Therefore, the first inflection point, labeled T1, represents the end diastolic value just before the start of the systolic portion of the wave. P1 represents the systolic peak and is commonly the maximum velocity point of the wave; however, studies have shown that under certain conditions P2 is greater than P1 (Kurji et al., 2006; Robertson et al., 2008). Associating the velocity wave with recordings of arterial pressure waves, P2 is thought to be the result of constructive interference from a reflected velocity wave (Nichols et al., 2008; Robertson et al., 2008). T3 is the dicrotic notch which corresponds to the closing of the aortic valve and is used as the dividing point for the portion of the wave that is influenced by systole and the diastolic component primarily influenced by downstream vascular properties (Aggarwal et al., 2008). Some work has primarily focused on the systolic portion of the wave (Aggarwal et al., 2008; Kurji et al., 2006; Robertson et al., 2008) whereas others have looked to the diastolic portion as an indicator of the vascular environment (Lockhart et al., 2006). However, by looking at the whole velocity wave profile, a greater understanding of cerebral hemodynamics may be gained.

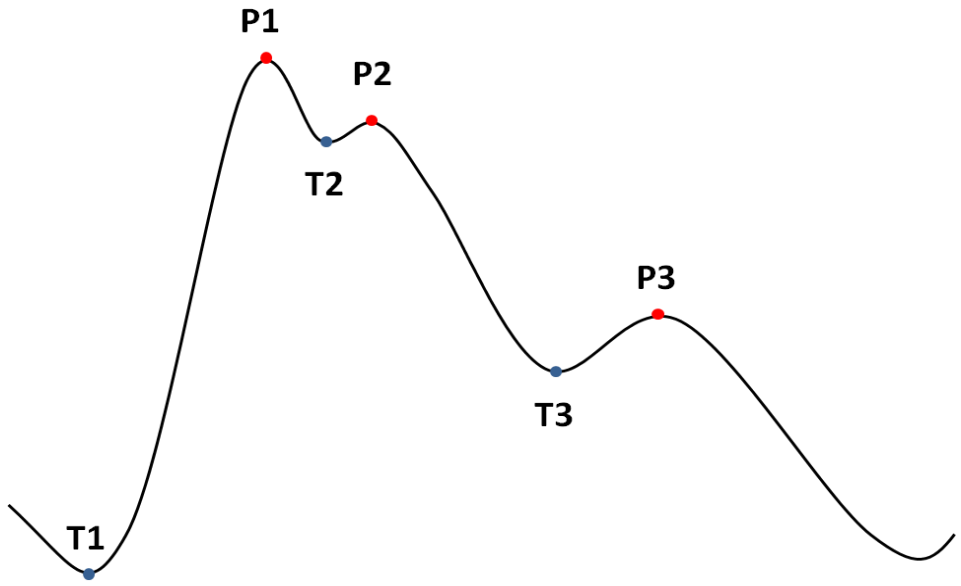

Figure 1.4: MCA velocity wave inflection points

Adapted from several sources (Kurji et al., 2006; Aggarwal et al., 2008; Robertson et al., 2008; Lockhart et al., 2006), this figure depicts a schematic of a MCA blood velocity waveform with key inflection points labeled.

In 2006, Kurji et al. (Kurji et al., 2006) used this simplified model of the MCA velocity wave to assess changes with age and increased partial pressure of end tidal CO_2 ($P_{ET}CO_2$). In this study, the group was able to demonstrate that CBFV waveforms change with alterations in $P_{ET}CO_2$ and with age such that both age and increased $P_{ET}CO_2$ showed increased P2 values. However, it is still unclear what physiological variables contribute to the observed changes in the TCD waveform.

Work by McVeigh et al. (McVeigh et al., 1999) has looked at the diastolic decay portion of a peripheral arterial blood pressure waveform to give an indication of large and small artery compliance. In another paper, this same group used the principles of the blood pressure wave analysis to assess cerebral blood velocity waves at rest and with nitroglycerin (NG) stimulation with particular focus on the points shown in Figure 1.4 (Lockhart et al., 2006). The results of this study showed waveform changes with no change being seen in P1, but significant reductions in P2, P3, T1, T2, and T3.with NG stimulation; however, again,

there was limited discussion as to what the changes in waveform morphology mean physiologically.

Aggarwal et al. (Aggarwal et al., 2008) used the points of the MCA velocity wave presented in Figure 1.4 to create a linear model of the MCA velocity wave. Point values, slopes of lines between points, and timing of points were then all assessed for velocity data collected from patient population and compared to measures of ICP from a sensor that had been inserted into the epidural space and calculated CPP. MCA waveform features were then used to discriminate between subjects separated into high, medium, and low ICP and CCP groups. The results of this study suggest that the assessment of MCA velocity wave characteristics might provide a method for determining changes in ICP or CPP.

Work by Robertson et al. (Robertson et al., 2008), similar to the paper by Kurji et al. (Kurji et al., 2006), also looked at changes in the MCA velocity wave with increased $P_{ET}CO_2$ and identified the P2 point on the CBFV velocity trace which they termed the reflected component of the velocity wave. By likening this reflected velocity wave point to the work presented by Nichols et al. (Nichols et al., 2008) with central aortic pressure waves, Robertson et al. calculated an augmentation index and suggested that the observed changes in the velocity wave were the result of alterations in cerebrovascular compliance.

In general, the studies mentioned above all demonstrated the malleability of the MCA blood velocity wave. The work by Aggarwal et al. (Aggarwal et al., 2008) showed potential links between waveform characteristics, ICP and CPP, where the work by Robertson et al. (Robertson et al., 2008) suggested alterations in waveforms related to changes in cerebrovascular compliance. Additional work is still needed to determine how the velocity wave changes under various conditions and to determine how this relates to cerebrovascular hemodynamics.

1.4.3 Carotid Artery Flow Profile

As the internal carotid artery (ICA) is the large conduit artery supplying the cerebral circulation, it follows that changes in cerebral blood velocity profile could be reflected in the ICA flow trace and potentially in the common carotid artery (CCA) which in turn supplies

the ICA. Some of the earliest TCD validation studies looked at the relationship between ICA flow and CBFV measures to verify that TCD measures were representative of changes in CBF (Lindegaard et al., 1987). Since the early TCD validation studies, other work has looked at CCA and ICA blood flow as indicators of changes in CBF (Eicke, Buss, Bahr, Hajak, & Paulus, 1999; Kleiser, Scholl, & Widder, 1995).

1.4.3.1 Wave Intensity Analysis

Recently, "wave intensity" analysis of the CCA has been used as a potential indicator of cerebrovascular properties (Bleasdale et al., 2003). In this analysis, simultaneous pressure and flow waves are measured in the CCA and analyzed to for the calculation of the intensity of forward travelling waves, or waves travelling away from the heart, versus backwards travelling waves (Bleasdale et al., 2003; Rakebrandt et al., 2009; Zhang et al., 2010; Niki et al., 2002). In a study by Bleasdale et al. (Bleasdale et al., 2003) cerebrovascular resistance was manipulated by changes in arterial PCO_2 and showed relations to the calculated reverse wave intensity of the CCA. This relationship led the authors to suggest that wave intensity may provide a non-invasive method for assessing cerebrovascular properties.

1.4.3.2 RCKL Modelling

Another approach to waveform analysis involves the use of mathematical modelling. Models can use input variables measured in one segment of the arterial tree to determine downstream vascular responses in areas that cannot be easily measured non-invasively. In 2007, Zamir et al. (Zamir, Goswami, Salzer, & Shoemaker, 2007) developed the RCKL model as a modification of the Windkessel model where resistance (R) and capacitance (C) were placed in parallel and viscoelastic resistance (K) and inertance (L) in series with C (Figure 1.5). If blood flow was a purely resistive system, the pressure wave would be identical to the flow wave (Zamir, 2005). As this is not the case, the RCKL model provides results for C, K, and L which are used to alter a modeled flow wave, based on the recorded pressure wave, so that the modeled wave matches the recorded flow wave. The R, C, K, and L parameters of this model therefore provide information about the total downstream vascular environment. This model has been successfully used with the peripheral vasculature

(Zamir et al., 2007) and may provide the opportunity to be used to assess cerebrovascular variables.

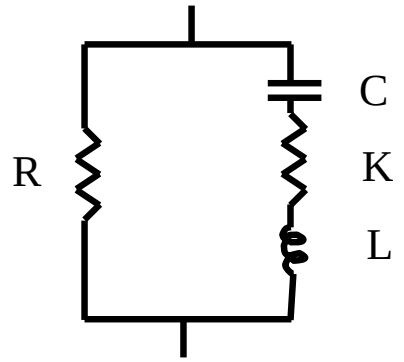

Figure 1.5: RCKL Model

Electrical circuit schematic of the RCKL model in which the resistor R is place in parallel with the capacitor C which is in series with a second resistor K and the inductor L.

The RCKL modelling approach requires the continuous assessment of blood flow and pressure within the artery of interest over a cardiac cycle. The skull provides a challenge for acquiring data non-invasively for use with this model; therefore, data must be collected from arteries supplying the cerebral circulation. In research involving cerebral blood flow, the internal carotid artery (ICA) is ideally used. However, again, the non-invasive assessment of pressure within this artery is generally not possible due to the anatomical arrangement of the vessel. Therefore, assessment of the common carotid artery (CCA) may provide adequate input for the model for the assessment of cerebral circulation. Preliminary work with this method and the CCA has been conducted with young and elderly participants with the results of this work suggesting that RCKL modeling is able to detect large changes in vascular properties with aging (Robertson, Zuj, Zamir, Hughson, & Shoemaker, 2008). However, care should be taken when interpreting these results, as the CCA is influenced by both intracranial and extracranial circulation. Further work is required with the RCKL model to determine the repeatability and validity of this model with use of CCA measures. As well, additional work needs to be conducted to help differentiate between cerebral circulation and extracranial flow to determine if the model is able to detect small, acute changes in cerebrovascular properties.

1.5 Cerebrovascular Autoregulation

The assessment of cerebral hemodynamics under resting conditions only provides a small amount of information. Cerebral blood flow regulation is a dynamic process where, in some situations, alterations in cerebrovascular properties may only be evident with changes in the regulation of cerebral blood flow.

Cerebrovascular autoregulation (CA) is the term used for the process in which vascular resistance is regulated to maintain CBF in the face of changing CPP (Panerai, 1998; Strandgaard & Paulson, 1984; Paulson, Strandgaard, & Edvinsson, 1990). With an increase in CPP a stretch is placed on the cerebral resistance vessels resulting in a vasoconstrictor response (Davis & Hill, 1999). This effectively serves to increase cerebrovascular resistance and maintain CBF. The opposite is also true in that a decrease in CPP will elicit a vasodilatory response, reducing vascular resistance and maintaining flow. CA has been shown to act rapidly within 2-5 seconds of changes in CPP and maintain CBF for perfusion pressures between 50 and 150mmHg (Panerai, 1998).

In the literature, two types of CA are frequently referred to. Static CA refers to the maintenance of CBF when faced with a constant change in CPP. Contrasted to this, dynamic CA looks at the process of regulating CBF when faced with constantly varying or acute changes in CPP values. As beat-by-beat variation is evident in most, if not all, cardiovascular variables, quantification of dynamic CA is often considered as being potentially the most physiologically relevant.

Many different tests have been proposed for the assessment of dynamic cerebral autoregulation. In 1989, Aaslid et al. (Aaslid, Lindegaard, Sorteberg, & Nornes, 1989), presented the thigh cuff method to assess dynamic CA. Using this method, cuffs were placed around the upper thigh and inflated to pressure above systolic blood pressure effectively occluding blood flow to the legs for two to three minutes. Upon cuff release the resultant reactive hyperemia to the legs serves to cause a transient decrease in ABP which is then recovered through baroreflex mechanisms. At the same time, the decrease in ABP produces a reduction in CBF which is corrected for initially through autoregulatory mechanisms. By

characterizing the decline and recovery of CBF, dynamic CA can be described and quantified. More recently, work has looked to changes in posture as an alternate method of assessing dynamic CA. Sorond et al. (Sorond, Serrador, Jones, Shaffer, & Lipsitz, 2009) have proposed the use of a sit to stand test as a method to assess CA for use with a wider population and as a test that more accurately represented challenges of day to day life. The study by this group showed similar results between the posture change method and the use of thigh cuffs (Sorond et al., 2009).

Both the thigh cuff method and posture change are based on a transient reduction in ABP resulting in changes in CBF that are then corrected through autoregulatory mechanisms. It is this relationship between ABP and CBF that has led some researchers to examine CBF with respect to spontaneous fluctuations in ABP (Zhang, Zukerman, Giller, & Levine, 1998; Edwards, Shoemaker, & Hughson, 2002; Iwasaki et al., 2007; Zhang, Zuckerman, Pawelczyk, & Levine, 1997). Analysing data within the frequency domain, cross-spectral analysis using ABP as the input and CBFV as the output variable is able to provide transfer function estimates of phase, gain, and coherence of the data with results traditionally broken down into three frequency ranges; very low frequency (VLF; 0.03-0.07Hz), low frequency (LF; 0.07-0.2Hz), and high frequency (HF; 0.2-0.3Hz) (Zhang et al., 1998). The coherence provides an indication of the linear relationship between ABP and CBFV with values greater than 0.5 being used as an indicator of linearity (Zhang et al., 1998). If coherence is above 0.5, the gain can be examined as an indicator of cerebrovascular autoregulation with higher gain values indicating an inability of cerebrovascular autoregulatory processes to dampen fluctuations in CBFV with changes in ABP. Finally, the phase provides an indication of the time relationship between the two variables with results consistently showing CBFV leading ABP (Zhang et al., 1998; Edwards et al., 2002; Zhang et al., 1997). Interestingly, the positive phase seen with this analysis suggests that changes in CBFV occur before changes in ABP which would be contradictory to the concept of CA correcting for changes in ABP. In the paper by Hughson et al. (Hughson, Edwards, O'Leary, & Shoemaker, 2001) the phase lead was examined and suggested to be a mathematical issue and a consequence of the phase lag of CVRi. This was similarly reported by Edwards et al. (Edwards et al., 2002) with both

papers showing the expected phase lag in the cross spectral analysis of the ABP→CVRi response. As the action of CA is to change cerebrovascular resistance in response to a change in pressure, assessment of the ABP→CVRi transfer function may provide a better indication of CA.

1.6 Cerebral Blood Flow and Carbon Dioxide

The pressure/flow relationships described in the assessment of CA primarily address the mechanical component of CBF regulation. Generally, these methods of assessing CBF regulation have ignored the influence of fluctuation in the partial pressure of arterial carbon dioxide ($PaCO_2$). Therefore, other methods of assessing cerebrovascular function have looked at metabolic contributions to CBF control with response to CO_2. Cerebral blood vessels have been shown to be very sensitive to changes in the partial pressure of arterial CO_2 with increases and decreases in the partial pressure of arterial CO_2 being shown to produce increases and decreases in CBF respectively (Bishop et al., 1986; Dahl et al., 1992; Dahl, Russell, Nyberghansen, Rootwelt, & Mowinckel, 1994; Muller et al., 1995; Poeppel et al., 2007; Ulrich et al., 1995). Many studies have used this reaction to arterial CO_2 as a method of assessing cerebrovascular reactivity often using modifications in breathing patterns or changes in respired gases as methods for altering end tidal CO_2 which in turn reflects changes in arterial CO_2 (Kirkham et al., 1986). Changes in CBFV have been related to the changes in CO_2 as an indication of cerebrovascular reactivity to CO_2 presenting vasomotor reactivity as a percent change in CBFV for a 1mmHg change in CO_2 with studies showing values ranging from 1.45%/mmHg to 5.28%/mmHg (Valdueza et al., 1999; Poulin, Liang, & Robbins, 1996; Hida et al., 1996; Ide, Eliasziw, & Poulin, 2003; Pandit, Mohan, Paterson, & Poulin, 2007; Ainslie et al., 2007; Clivati, Ciofetti, Cavestri, & Longhini, 1992; Claassen, Zhang, Fu, Witkowski, & Levine, 2007).

Several factors contribute to the differences in cerebral reactivity values seen. In a paper by Clivati et al. (Clivati et al., 1992) patients with chronic obstructive lung disease were compared to healthy controls showing that the patient population had a significantly reduced CO_2 reactivity which may have been related to chronic hypercapnia. In a separate

study, Ainslie et al. (Ainslie et al., 2007) showed differences in cerebral reactivity measured in the morning versus the afternoon. Ide et al. (Ide et al., 2003) looked at the relationship of CBFV to end tidal CO_2 and demonstrated a non-linear relationship with reduced cerebrovascular CO_2 reactivity in the hypocapnic range and increased sensitivity with hypercapnia. Therefore, the methodology used to assess cerebrovascular CO_2 reactivity may influence absolute values.

Another potentially confounding influence in the assessment of cerebrovascular CO_2 reactivity is the possibility of changes in ABP during CO_2 manipulations (Hetzel, Braune, Guschlbauer, & Dohms, 1999; Dumville, Panerai, Lennard, Naylor, & Evans, 1998). Recent work by Battisti-Charbonney et al. (Battisti-Charbonney, Fisher, & Duffin, 2011) suggested thresholds for changes in ABP with changes in PCO_2 and that alterations in CBF within these threshold points were due to change in CO_2 and beyond the threshold changes in CBF were due to alteration in ABP. This interpretation does present some concern as assessment of cerebrovascular autoregulation has consistently shown alterations in CBF with spontaneous fluctuations in ABP (Zhang et al., 1998; Iwasaki et al., 2007; Edwards et al., 2002; Hughson et al., 2001; Zhang et al., 1997). Regardless of the existence of a threshold value for large alterations in ABP with changes in PCO_2, CBF regulation is dependent on minor fluctuations in both ABP and CO_2 and neither variable can be ignored in the assessment of cerebral blood flow.

In 2003, Edwards et al. (Edwards, Topor, & Hughson, 2003) presented data in which autoregressive moving average (ARMA) analysis was utilized to determine independent contributions of CO_2 and ABP on CBFV. Through the use of ARMA analysis Edwards et al. showed modeled responses of CBFV and CVRi to a theoretical 1mmHg impulse and sustained increase in ABP and CO_2 (Edwards et al., 2003; Edwards, Devitt, & Hughson, 2004). Results from the Edwards et al. (Edwards et al., 2004) study suggested an increased $CO_2 \rightarrow$CVRi step response with hypocapnia and a reduced response with hypercapnia. At first glance this appears to be contrary to the results presented by Ide et al. (Ide et al., 2003); however the results from the Ide et al. study showed differences in cerebrovascular CO_2 reactivity when looking at either an increase or decrease in CO_2 whereas the Edwards et al.

paper only looked at an increase in CO_2 assuming the change in CBFV would be the same for either an increase or decrease in CO_2. Therefore, care must be taken when interpreting results as it appears that cerebrovascular CO_2 reactivity is dependent not only on starting CO_2 levels, but also on the direction of CO_2 change applied.

Recent studies have shown the potential involvement of nitric oxide (NO) and the NO system with cerebrovascular CO_2 reactivity (Lavi, Egbarya, Lavi, & Jacob, 2003; Schmetterer et al., 1997; Zimmermann & Haberl, 2003). Therefore, assessment of cerebrovascular responses to exogenous sources of NO may help in determining if changes in cerebrovascular CO_2 reactivity are due to alterations NO availability, or the vascular sensitivity to NO.

1.7 Cerebrovascular Responses to Nitroglycerin

As an NO donor, nitroglycerin (NG) is commonly used in clinical settings, alleviating symptoms of angina by reducing the work of the heart though venodilation and vasodilation of coronary arteries (Abrams, 1985; Abrams, 1996). In research settings, NG has been used as a means to determining maximal vasodilation responses to nitric oxide (Bleeker et al., 2005), as a method for expediting orthostatic tolerance tests (Raviele et al., 1994), and as a model of migraine headache (Bednarczyk et al., 2002). Several studies have looked to determine cerebral blood velocity responses to NG consistently showing reductions in velocity (Borisenko & Vlasenko, 1992; Dahl, Russell, Nyberghansen, & Rootwelt, 1989; Dahl, Russell, Nyberghansen, & Rootwelt, 1990; Micieli et al., 1997; Siepmann & Kirch, 2000; White et al., 2000). However, studies using PET and SPECT methods of determining cerebral blood flow have consistently shown no changes with NG stimulation suggesting that the observed reduction in CBFV is the results of MCA vasodilation with constant blood flow (Dahl et al., 1989; Borisenko & Vlasenko, 1992; White et al., 2000; Dahl et al., 1990). In 2007, Hansen et al. used MRI to measure the diameter of the MCA confirming that it does dilate with NG stimulation showing a 10-14% increase in vessel diameter (Hansen et al., 2007).

The observation of constant cerebral blood flow with dilation of the MCA has lead at least one group to suggest the use or sublingual NG as a method for determining cerebrovascular reactivity to NO (Borisenko & Vlasenko, 1992). Assuming that cerebral blood flow remains constant with the administration of NG and that NG works through an NO mechanism, measurement of CBFV in the MCA allows for the calculation of diameter change of the MCA. It is possible that impairments in cerebrovascular responsiveness to NO would be evident as reduced dilation responses to NG. Work has suggested the involvement of NO and the NO system in the regulation of cerebral blood flow (Lavi et al., 2003; Schmetterer et al., 1997; Zimmermann & Haberl, 2003). Therefore, the use of NG as an exogenous source of NO might provide a useful tool for determining cerebrovascular changes in cerebrovascular function.

Blood flow is the product of blood velocity and vessel cross-sectional area. As such blood flow through the MCA can be calculated as:

(F) $$CBF_{MCA} = \pi \left(\frac{MCA_{diameter}}{2}\right)^2 \times CBFV_{MCA}$$

Rearranging the equation the MCA diameter then becomes equal to:

(G) $$MCA_{diameter} = \sqrt{\frac{CBF}{\pi CBFV}} \times 2$$

The percent change in diameter can be calculated as:

(H) $$\Delta d = \frac{d_2 - d_1}{d_1} \times 100\%$$

When equation (F) is used to substitute values for d_1 and d_2, the percent change in MCA diameter is then calculated as:

(I) $$\Delta d = \left(\sqrt{\frac{CBF_2}{CBFV_2} \times \frac{CBFV_1}{CBF_1}} - 1\right) \times 100$$

In the case of NG stimulation where CBF is believed to remain constant, it follows that the following equation can then be used in the calculation of percent diameter change:

(J) $$\Delta d = \left(\sqrt{\frac{CBFV_1}{CBFV_2}} - 1\right) \times 100$$

Using this equation to calculate MCA diameter change, Dahl et al. (Dahl et al., 1989) showed a 15% increase in diameter administration of 1mg of NG where Borisenko and Vlasenko (Borisenko & Vlasenko, 1992) showed a 7.2% increase with administration of 0.25mg NG. To date limited work has been conducted to determine the usefulness of NG as a method for assessing cerebrovascular NO reactivity.

1.8 Cerebrovascular Responses to Spaceflight

Over the past century, the human drive for exploration has resulted in spaceflight. Since the first flight of Yuri Gagarin, time spent in space by astronauts has steadily increased and has emphasized the need to study the physiological effects of microgravity exposure. On Earth, the force of gravity produces a gravitational vector which draws blood and fluid towards the feet when in an upright posture. This generates a pressure gradient throughout the body such that a mean pressure of 100mmHg at heart level would translate to a pressure of approximately 200mmHg at the feet and 70mHg at the level of the brain (Hargens & Watenpaugh, 1996). In space, the gravity induced pressure gradient is eliminated and pressure is equalized effectively reducing pressure in the lower limbs and increasing pressure at the level of the brain (Hargens & Watenpaugh, 1996). In addition, exposure to microgravity results in cephalic fluid shifts (Frey, Mader, Bagian, Charles, & Meehan, 1993) which could contribute to an increase in ICP. Recently, NASA released the Human Research Roadmap in which idiopathic intracranial hypertension and its resulting effects were identified as major health risk factors associated with long duration spaceflight (Fogarty, 2011). Two recent studies have noted structural changes in the eye and optic nerve after long duration spaceflight which could result from a sustained increase in intracranial pressure (Kramer, Sargsyan, Hasan, Polk, & Hamilton, 2012; Mader et al., 2011). However, little information is known as to how idiopathic intracranial hypertension with microgravity exposure affects cerebrovascular structure or function.

Several studies have looked at orthostatic tolerance noting a high incidence of intolerance post-flight. Buckey et al. (Buckey et al., 1996) studied 14 astronauts before and after short duration spaceflight. They noted that before flight, all astronauts were able to complete a 10 minute stand test; however, after flight 9 of the 14 could no longer complete the test. In a separate study, Waters et al. (Waters, Ziegler, & Meck, 2002) also showed orthostatic intolerance post-flight with 11 of 35 unable to complete a 10 minute stand test post flight. It was also noted that orthostatic intolerance was more prevalent in female astronauts (100%) and mission specialists (7 of 16). This high incidence of orthostatic intolerance has led some researchers to study cerebrovascular responses to spaceflight. Development of pre-syncope or syncope in response to orthostasis is in essence the result of reduced cerebral blood flow (Hainsworth, 2004); therefore, the high incidence of orthostatic intolerance could be the result of altered cerebral hemodynamics with spaceflight.

Surprisingly, very limited work has been published looking at the effects of spaceflight on cerebral blood flow. In 1991, Bagian and Hackett (Bagian & Hackett, 1991) published their work using TCD to assess cerebral blood velocity during shuttle flights. This paper presented individual results from astronauts early in flight and showed no change in CBFV. Cerebral blood velocity data recorded during the Neurolab mission (STS-70) were presented in 2007 by Iwasaki et al. (Iwasaki et al., 2007) also showing no in-flight changes in CBFV. This can be contrasted to work presented by Arbeille et al. (Arbeille et al., 2001) who showed an initial increase in CBFV and values returning to pre-flight levels after 1 week and 3 months in space. This initial increase in CBFV was also accompanied by an increase in CCA blood flow which suggests that CBF is increased at the start of flight, but returns back to pre-flight levels after one week in space.

Upon return to Earth's gravitational environment, Iwasaki et al. (Iwasaki et al., 2007) again showed no change in supine resting CBFV measures. Although it appears that CBF is well maintained during and after spaceflight, it is possible that the cerebrovasculature has adapted to microgravity in such a way to potentially affect the regulation of CBF when faced with conditions such as orthostatic stress. Iwasaki et al. attempted to address this issue and interestingly found that reductions in CBFV in response to head up tilt were smaller after

spaceflight (Iwasaki et al., 2007). Additionally, spectral analysis results from this study showed changes that were consistent with improvements in dynamic cerebral autoregulation (Iwasaki et al., 2007). This provides an interesting result when considering the marked increase in orthostatic intolerance that has been demonstrated post spaceflight (Buckey et al., 1996). However, when considering the astronauts used in the study by Iwasaki et al. (Iwasaki et al., 2007), it should be noted that none of these astronauts developed orthostatic intolerance post flight; therefore it is unclear if the results from this study accurately reflect potential adaptations of astronauts who do develop orthostatic intolerance post spaceflight.

In a more recently published study of the effects of spaceflight on cerebrovascular autoregulation, Blaber et al. (Blaber, Goswami, Bondar, & Kassam, 2011) looked at cerebrovascular responses of 27 astronauts after short duration spaceflight. In this study, astronauts were separated into those who could complete a 10 minute stand test post flight and those who could not. The results suggested impairments in cerebrovascular autoregulation on landing day for only those astronauts who could not complete the 10 minutes of stand showing orthostatic intolerance. These results suggest that after short duration spaceflight, impairments in cerebrovascular autoregulation may contribute to reduced orthostatic tolerance.

One difficulty with any spaceflight research relates to the small number of people who have actually flown in space. As such, ground based analogue systems are often employed to further understanding of the physiological effects of microgravity exposure. Parabolic flight has been used as a method to examine responses during brief periods of weightlessness. A study by Bondar et al. (Bondar et al., 1990) showed an increase in CBFV with this exposure to microgravity in parabolic flight. However, the parabolic flight model presents several limitations. First, this study addressed changes in CBFV with exposures to microgravity only lasting up to 40s. Also, the microgravity sections of the flight pattern occur after exposure to a +2 Gz hypergravity session which may present confounding influences. Therefore, to examine the effects of long term exposure to microgravity a bed rest model is commonly employed.

Elimination of the head to foot gravitational vector with exposure to microgravity is associated with fluid shifts towards the head (Hargens & Watenpaugh, 1996). These fluid shifts can be mimicked in humans through the use of head down tilt bed rest (HDBR) (Frey et al., 1993). Cerebral blood velocity responses to HDBR have been mixed with studies showing increases (Kawai et al., 1993), decreases (Arbeille et al., 2001; Hirayanagi et al., 2005; Sun et al., 2005; Frey et al., 1993), and no changes in resting supine CBFV (Arbeille et al., 2001; Pavy-Le Traon et al., 2002; Zhang et al., 1997). One of the reasons for the differences in results could be related to the duration of the bed rest. In a short HDBR study, Kawai et al. (Kawai et al., 1993) demonstrated an increase in CBFV within the first nine hours of HDBR. Frey et al. (Frey et al., 1993) looked at two days of HDBR and showed reductions in CBFV. Similarly, Arbeille et al. showed reductions in CBFV and increased cerebral RI with four to five days of bed rest (Arbeille et al., 1998; Arbeille et al., 2001). However, Arbeille et al. also demonstrated that resting CBFV did not differ from baseline after longer periods of bed rest which has been confirmed in other studies (Arbeille et al., 2001; Zhang et al., 1997; Pavy-Le Traon et al., 2002).

Cerebral blood velocity responses to stresses have also been mixed post HDBR. After 24 hours of bed rest, Kawai et al. (Kawai et al., 1993) showed a significant reduction in CBFV when participants were returned to an upright posture. Similarly, Zhang et al. (Zhang et al., 1997) showed a greater reduction in CBFV with LBNP after 18 days of HDBR. However, these results are contrasted to those of Pavy-Le Traon et al. (Pavy-Le Traon et al., 2002) who showed no changes in CBFV responses to thigh cuff deflation after seven days of HDBR and the results of Arbeille et al. (Arbeille et al., 1998) who showed no changes in CBFV responses to head up tilt after 4 days of HDBR. The variability in published CBFV responses to HDBR greatly reduces the ability to draw conclusions as to how the cerebrovasculature adapts to microgravity exposure.

In an attempt to gain further insight into cerebrovascular adaptations to microgravity, animal models are also employed. Hind-limb unloading models (HLU) have been developed in which rats are suspended by their tails placing them in a head down tilt position. Fluid shifts are then theoretically similar to those experienced in spaceflight and response of

cerebral vessels can be examined. Studies of cerebral arteries in rats have shown increased basal tone (Geary, Krause, Purdy, & Duckles, 1998; Wilkerson et al., 2005) and increased vasoconstriction response after HLU (Zhang, Zhang, & Ma, 2001). This is associated with a decrease in lumen diameter and increased wall thickness indicating vascular hypertrophy (Prisby et al., 2006; Wilkerson, Muller-Delp, Colleran, & Delp, 1999). Wilkerson et al. (Wilkerson, Colleran, & Delp, 2002) also showed that observed changes in cerebral vessel morphology were associated with regionally specific reductions in cerebral blood flow. In 1998, Geary et al. (Geary et al., 1998) demonstrated that resting vessel diameter differences with HLU were abolished with L-NAME indicating the contribution of NO in the maintenance of vessel diameter. Therefore, it would appear that either a reduction in the bioavailability of NO or a reduction in the vascular smooth muscle responsiveness to NO contributed to the smaller cerebral vessel diameter after HLU.

Animal data suggests that cerebral blood vessel morphology changes with exposure to simulated microgravity. However, variability in the results of published human spaceflight and HDBR data still makes it unclear what the exact cerebrovascular responses are to spaceflight and how these compare and contrast to those of bed rest.

1.9 General Purpose of Thesis

The general purpose of this thesis was to determine cerebrovascular responses to real and simulated microgravity exposure and to determine what further information can be gained about cerebrovascular hemodynamics from the examination of the cerebral blood velocity Doppler wave profile. Cerebrovascular properties were determined after long duration spaceflight, after five days of HDBR with and without an artificial gravity countermeasure, during head up tilt and the progression towards presyncope, and under conditions that might induce changes in cerebrovascular properties including a change in $P_{ET}CO_2$ and administration of sublingual NG.

1.9.1 General Chapter Hypotheses

The first research chapter (Chapter 2) examines the cerebrovascular responses to long duration spaceflight. Based on animal data and results from HDBR studies, it was hypothesized that long duration spaceflight would result in alteration of cerebrovascular structure and function such that there would be greater reduction in CBFV with the application of a simulated orthostatic stress using lower body negative pressure and a blunting of cerebrovascular CO_2 reactivity due to changes in the nitric oxide system as previously observed in animal studies (Prisby et al., 2006; Lin et al., 2009; Wilkerson et al., 2005). However, as only CBFV was measured, no changes in supine resting values of CBFV were expected as a combination of a reduced vessel luminal diameter (Wilkerson et al., 1999; Geary et al., 1998) and reduced cerebral blood flow (Wilkerson et al., 2002) were expected to allow for the maintenance of CBFV.

The second chapter (Chapter 3) is an extension of the analysis from the study presented in Chapter 2. This section focuses on potential changes in cerebrovascular tone with exposure to long duration spaceflight. Animal studies have suggested an increase in myogenic tone of cerebral vessels after exposure to simulated microgravity (Wilkerson et al., 2005; Geary et al., 1998; Lin et al., 2009). Therefore, it was hypothesized that after long duration spaceflight there would be an increase in cerebrovascular tone and that this increase would be reflected in alterations of the MCA Doppler spectrum morphology.

Due to logistical restraints associated with human spaceflight research, head down bed rest (HDBR) is often used as an Earth-based analogue of microgravity exposure. Therefore, the following three chapters present data from 12 men who completed five days of HDBR with and without an artificial gravity countermeasure. Cerebrovascular responses to head up tilt and the progression towards syncope are presented in Chapter 4 and Chapter 5. In these chapters, it was hypothesized that after HDBR there would be alterations in the regulation of cerebral blood flow such that greater reductions in CBFV would be seen with tilt. Similar to the results of Blaber et al. (Blaber et al., 2011) individuals who develop orthostatic intolerance, as defined as the inability to complete 10 minutes of tilt post HDBR, were hypothesized to show impairments in cerebrovascular autoregulation. This work also

looked at the MCA velocity waveform profile with approaching syncope. Previous studies have shown a reduction in the dicrotic notch point of the velocity wave in patients with neurocardiogenic syncope (Albina et al., 2004) and an increase in CrCP with approaching syncope (Carey et al., 2001). Therefore, it was hypothesized that similar variation would be seen with the MCA velocity wave which will be reflective of alterations in cerebrovascular tone and related to indices of dynamic cerebrovascular autoregulation.

Assessment of the MCA velocity wave profile continues in Chapter 6 with cerebrovascular responses to sublingual nitroglycerin. Using simultaneous assessments of CCA pressure and flow, RCKL modeling was used to determine downstream vascular resistance, compliance, viscoelastic resistance, and inertance. RCKL model results were hypothesized to be related to MCA velocity waveform characteristics both before and after NG thereby allow for the physiological interpretation of changes in the MCA velocity waveform. In response to NG, it was hypothesized that the RCKL model would show an increase in cerebrovascular compliance as suggested by the response of peripheral vessels (Smulyan, Mookherjee, & Warner, 1986; Bank & Kaiser, 1998) and the calculation of CrCP (Moppett, Sherman, Wild, Latter, & Mahajan, 2008). With respect to the HDBR, it was hypothesized that at rest the RCKL model would show increased resistance and decreased vascular compliance. However, it was hypothesized that the response to NG would be consistent after HDBR as was previously shown with women after 56 days of HDBR (Zuj et al., 2012b).

The final two chapters focus on the relationships between MCA blood velocity and CCA blood flow with alterations in $P_{ET}CO_2$ and NG stimulation. In Chapter 7, CCA flow was used as a quantitative measure of cerebral blood flow to assess potential changes in MCA diameter with sublingual NG and acute changes in $P_{ET}CO_2$. It was hypothesized that with NG there would be a reduction in CBFV but no change in CCA flow indicating dilation of the MCA. With alterations in $P_{ET}CO_2$, it was hypothesized that the relationship between CCA flow and CBFV would be non-linear indicating diameter changes of the MCA.

In the final research chapter (Chapter 8) comparisons were made between the CCA and MCA blood velocity waves with changes in $P_{ET}CO_2$. In this section, it was hypothesized that the MCA velocity wave profile would show alterations in key inflection points suggesting change in cerebrovascular tone. It was also hypothesized that the changes in the MCA velocity wave would be reflected in the CCA velocity wave suggesting that CCA hemodynamics can be used as an indicator of cerebrovascular properties.

Chapter 2

Impaired cerebrovascular autoregulation and reduced CO_2 reactivity after long duration spaceflight

This chapter was published as:

Zuj KA, Arbeille Ph, Shoemaker JK, Blaber AP, Greaves DK, Xu D, and Hughson RL (2012). Impaired cerebrovascular autoregulation and reduced CO_2 reactivity after long duration spaceflight. *Am J Physiol Heart Circ Physiol* 302(12):H2592-H2598.

2.1 Overview

Long duration habitation on the International Space Station (ISS) is associated with chronic elevations in arterial blood pressure in the brain compared to normal upright posture on Earth, and elevated inspired CO_2. Although results from short duration spaceflights suggested possibly improved cerebrovascular autoregulation, animal models provided evidence of structural and functional changes in cerebral vessels that might negatively impact autoregulation with longer periods in microgravity. Seven astronauts (1 woman) spent 147±49 days on ISS. Pre-flight testing (30-60 days before launch) was compared to post-flight testing on landing day (n=4) or the morning 1 (n=2) or 2 days (n=1) after return to Earth. Arterial blood pressure at the level of the middle cerebral artery (BP_{MCA}) and expired CO_2 were monitored along with transcranial Doppler ultrasound assessment of middle cerebral artery blood flow velocity (CBFV). Cerebrovascular resistance index was calculated as $CVRi=BP_{MCA}/CBFV$. Cerebrovascular autoregulation and CO_2 reactivity were assessed from an autoregressive moving average (ARMA) model of data obtained during a test where, in a supine position, two breaths of 10% CO_2 were given 4 times during a 5min period. CBFV and Doppler pulsatility index were reduced during -20 mmHg lower body negative pressure, with no differences pre- to post-flight. The post-flight indicator of dynamic autoregulation from the ARMA model revealed reduced gain for the CVRi response to BP_{MCA} ($P=0.047$). The post-flight responses to CO_2 were reduced for CBFV ($P=0.056$) and CVRi ($P=0.017$). These results indicate that long duration missions on the ISS impaired dynamic cerebrovascular autoregulation and reduced cerebrovascular CO_2 reactivity.

2.2 Introduction

The microgravity environment, which causes cephalic fluid shifts with increased arterial pressure at the level of the brain relative to normal daily life on Earth (Hargens & Watenpaugh, 1996), might cause alterations in cerebrovascular structure and function. The impact of microgravity on human cerebrovascular function has primarily been examined during and after short duration spaceflights (Bagian & Hackett, 1991; Iwasaki et al., 2007; Blaber et al., 2011; Arbeille et al., 2001) with only a few measurements of cerebral blood flow velocity (CBFV) during or after long duration flights (Arbeille et al., 2001; Tobal, Roumy, Herault, Fomina, & Arbeille, 2001). During spaceflight, only modest changes in CBFV have been reported (Arbeille et al., 2001; Bagian & Hackett, 1991) with small increases in cerebrovascular resistance after months in space that were speculated to reflect increased sympathetic vasoconstriction (Arbeille et al., 2001). Post-flight CBFV in the supine posture was unchanged or slightly elevated from pre-flight (Blaber et al., 2011; Iwasaki et al., 2007). Post-flight measurements of dynamic cerebrovascular autoregulatory indices, reflecting vascular smooth muscle responses to changes in arterial blood pressure, were slightly enhanced in one group of astronauts (Iwasaki et al., 2007) but were reduced in astronauts with reduced post-flight orthostatic tolerance (Blaber et al., 2011).

Results from Earth-based analogs of spaceflight using head down bed rest (HDBR) have revealed increases (Kawai et al., 1993), decreases (Arbeille et al., 1998; Arbeille et al., 2001; Sun et al., 2005; Frey et al., 1993; Hirayanagi et al., 2005), or no changes (Arbeille, Kerbeci, Mattar, Shoemaker, & Hughson, 2008; Pavy-Le Traon et al., 2002; Zhang et al., 1997; Arbeille et al., 2001) in supine CBFV. After HDBR, some studies have shown a greater reduction in CBFV with lower body negative pressure (LBNP) (Zhang et al., 1997) or assuming an upright posture (Kawai et al., 1993) suggesting an impairment in the ability to regulate cerebral blood flow when faced with an orthostatic stress. However, other research has found no difference in cerebrovascular responses to tilt or LBNP (Arbeille et al., 1998; Arbeille et al., 2008) or with rapid deflation of leg cuffs (Pavy-Le Traon et al., 2002).

Animal models of spaceflight using hind limb suspension have provided convincing evidence of cerebrovascular structural and functional changes. Cerebral arteries from suspended rats have demonstrated vascular smooth muscle hypertrophy (Wilkerson et al., 1999; Lin et al., 2009; Zhang et al., 2001; Wilkerson et al., 2002) with a smaller luminal cross-sectional area (Wilkerson et al., 1999) and increased basal myogenic tone (Wilkerson et al., 2005; Geary et al., 1998; Lin et al., 2009). Further work has also shown that these changes are associated with reduced cerebral blood flow (Wilkerson et al., 2002; Wilkerson et al., 2005) and greater vasoconstrictor responses possibly acting through nitric oxide-dependent (Prisby et al., 2006; Lin et al., 2009; Wilkerson et al., 2005) or renin-angiotensin system-dependent mechanisms (Bao, Zhang, & Ma, 2007).

To date, there have been no investigations of the cerebrovascular response to carbon dioxide (CO_2) after spaceflight. Cerebrovascular CO_2 reactivity reflects endothelial function through activation of the nitric oxide system (Lavi et al., 2003; Schmetterer et al., 1997; Lavi, Gaitini, Milloul, & Jacob, 2006) that was impaired in animals by hind limb suspension (Lin et al., 2009; Prisby et al., 2006; Wilkerson et al., 2005). In addition, cerebrovascular CO_2 reactivity might also be altered as a consequence of elevated partial pressure of CO_2 in the ambient air on the International Space Station (ISS) that could chronically influence arterial CO_2 ($PaCO_2$) and cerebral acid-base balance.

We hypothesized in the current study that resting CBFV would be unchanged following long duration spaceflight but there would be greater decreases with LBNP. Further, we hypothesized that post-flight cerebrovascular autoregulation would be impaired and CO_2 reactivity would be blunted as a consequence of chronic effects of the ISS environment.

2.3 Methods

Cerebral hemodynamic data from long duration spaceflight were collected as a part of the Cardiovascular and Cerebrovascular Control on Return from the International Space Station (CCISS) project. Methods and procedures were reviewed and approved by the Office of Research Ethics at the University of Waterloo and the Committee for the Protection of

Human Subjects at Johnson Space Center. Each volunteer signed an approved consent form after receiving full verbal and written details of the experiment. The experiment conformed to the guidelines in the Declaration of Helsinki.

Seven astronauts (1 woman) with an average age of 48±4 years participated. Pre-flight data were collected 36±22 days prior to launch. Post-flight data were collected from astronauts returning via the space shuttle within 3-4 hours of landing (R+0, n=4) and, for astronauts returning via the Russian Soyuz spacecraft, the morning after landing (R+1, n=2) or two mornings after landing (R+2, n=1) for an astronaut whose return was delayed by weather. For R+0 testing, the astronauts landed on the shuttle in a supine posture and remained in that posture for transportation to the research facility and until the experiment was completed. Experiments on days R+1 and R+2 were conducted first thing in the morning. The astronauts did not assume upright posture on test day before being transported to the laboratory in a supine posture in an attempt to minimize the effects of re-adaptation to Earth's gravitational environment. The astronauts spent an average of 147±49 days in space ranging from 58 days to 199 days with all but one spending greater than 100 days on orbit.

2.3.1 Experimental Protocol and Instrumentation

Pre-flight testing for the shuttle-launched astronauts and one Soyuz-launched astronaut took place at Johnson Space Center (JSC, Houston, TX). Three of the four shuttle astronauts completed post-flight testing at Kennedy Space Center (KSC, Cape Canaveral, FL) with the other at Dryden Flight Research Center (Dryden, Edwards, CA). Pre-flight testing for two Soyuz launched astronauts and all post-flight testing was completed at the Gagarin Cosmonaut Training Center (GCTC, Star City, Russia). Due to logistics of each location, slightly different equipment was used at each of the experimental sites.

Throughout the testing periods, astronauts were equipped with a standard three lead electrocardiogram (Finometer ECG Module (JSC, KSC, Dryden), Finapres Medical, Amsterdam, the Netherlands; Hewlett-Packard (GCTC)) for the assessment of heart rate (HR). Arterial blood pressure (ABP) was continuously determined using finger photoplethysmography (Finometer (KSC, JSC, and Dryden), Portapres (JSC n=1), and

Finapres (GCTC), Finapres Medical, Amsterdam, the Netherlands) and height-corrected to heart level. The participants were also equipped with a nasal cannula for monitoring of expired CO_2 (Ohmeda 5200 CO_2 Monitor (JSC, KSC, and GCTC); ADInstruments CO_2 analyzer (Dryden)). End-tidal CO_2 values were converted to mmHg based on atmospheric temperature and pressure ($P_{ET}CO_2$). Transcranial Doppler ultrasound (Multigon Industries, New York, NY (JSC); EZDop, DWL, Compumedics, Germany (KSC); MultiFlow, DWL GmbH, Sipplingen, Germany (Dryden); CardioLab, European Space Agency (GCTC)), was used for the assessment of CBFV in the middle cerebral artery (MCA). In all locations TCD measures were conducted using a 2MHz pulsed Doppler probe that was placed over the right temporal window to allow for the insonation of the M1 segment of the MCA and the assumption of a 0° angle of insonation. Throughout the testing, the probe was held in place using a headband.

Testing that occurred at JSC, KSC, and Dryden utilized Chart software (ADInstruments Ltd.) for the continuous recording of ECG, ABP, CO_2, and TCD signals. Data recorded at GCTC also utilized Chart software for the recording of ECG, ABP, and CO_2. TCD data at GCTC were recorded on a separate system using CardioMed software (European Space Agency). Chart data were digitized at 1000Hz and CardioMed data at 100Hz. Beat-by-beat data from the CardioMed system were aligned with Chart data by introducing a common marker signal, and by pattern matching the between beat intervals from R-waves and TCD waves.

2.3.2 CO_2 and LBNP tests

Cerebral blood flow was assessed under two different conditions: lower body negative pressure (LBNP), and a CO_2 challenge using the "two-breath" test of Edwards et al. (Edwards et al., 2003). All testing took place with astronauts resting in a supine position. Two low levels of LBNP, -10 and -20 mmHg, were applied for approximately 2 min at each level while the astronauts were sealed at the waist into an airtight box. Vacuum was applied to the box to produce negative pressure promoting a shift in blood volume towards the lower limbs.

The "two-breath" method (Edwards et al., 2003) was used to assess both cerebrovascular autoregulation and cerebrovascular CO_2 reactivity. During this test, the nasal cannula was removed and a mask was held in place over the nose and mouth. A valve was turned to control whether the astronaut inspired room air or a gas mixture consisting of 10% CO_2, 21% O_2, balance N_2. Two breaths of the CO_2 gas mixture were inspired every minute for a five minute period.

2.3.3 Data Analysis

The outer envelope of the TCD Doppler spectrum was averaged over each cardiac cycle to determine mean CBFV. Similarly, arterial blood pressure tracings were averaged over a cardiac cycle to provide an indication of beat-by-beat blood pressure at the level of the MCA (BP_{MCA}). Mean CBFV and BP_{MCA} were then used to calculate an index of cerebrovascular resistance (CVRi) as CVRi = BP_{MCA} / CBFV. As an additional assessment of cerebrovascular resistance the Gosling Pulsatility index was calculated as PI = (CBFVsys-CBFVdia)/CBFVmean (Beasley, Blau, & Gosling, 1979).

During the LBNP section of the protocol, 30s averages of cerebrovascular variables were taken starting 40s before the end of each stage for the steady state assessment at rest, -10mmHg, and -20mmHg. The two-breath protocol was analyzed using autoregressive moving average (ARMA) analysis on the beat-by-beat data set as previously described (Edwards et al., 2003). PCO_2 was determined for each heart beat by taking the point on the linear interpolation for end-tidal PCO_2 corresponding to each R-wave on the electrocardiogram. Based on the best fit ARMA model parameters, step gains were calculated as the values of CBFV and CVRi 45s after the introduction of nominal inputs of 1 mmHg change in BP_{MCA} and 1 mmHg change in PCO_2 as previously described by Edwards et al. (Edwards et al., 2003).

2.3.4 Technical Issues

Technical problems reduced the sample size for certain comparisons. A CO_2 analyzer did not function during one post-flight test so the CO_2 responses of this astronaut could not be included in the ARMA analysis. In one astronaut the mean value of the TCD signal

differed by more than physiologically acceptable limits for pre- to post-flight comparisons suggesting possible differences in equipment or vessel investigation. Even so, the variability of the signals appeared to be appropriate so this astronaut's data were included when the mean values were eliminated (e.g. ARMA analysis of CBFV) but were excluded when the absolute values were important (e.g. calculation of CVRi and its subsequent analysis by ARMA). The data set of one astronaut with a very low cardiac frequency would not solve with the ARMA algorithm. This data set was linearly interpolated to double the mean sampling frequency before analysis. Testing this approach on other data sets indicated no impact on model solution.

2.3.5 Statistical Analysis

A two-way repeated measures analysis of variance was used to test pre- to post-flight effects of LBNP (SigmaStat 3.5, Systat Software Inc., Chicago, IL). The magnitudes of the impulse and step responses from the ARMA analysis were compared using a one-way repeated measures analysis of variance for pre- to post-flight effects. Statistical significance was set at $p<0.05$.

2.4 Results

There were no differences in resting CBFV, CVRi, or PI from pre- to post-spaceflight during the LBNP phase of the study (Figure 2.1). In response to LBNP, CBFV (Figure 2.1, panel A) and PI (Figure 2.1, panel C) were reduced at -20mmHg with no changes in CVRi (Figure 2.1, panel B). BP_{MCA} was not different (P=0.142) from pre- to post-flight at rest (92.9±15.0 and 99.9±8.4 mmHg) or at -20 mmHg of LBNP (92.2±13.4 and 97.4±8.8 mmHg). Also, there were no differences in $P_{ET}CO_2$ (P=0.737) at rest from pre-flight (42.3±2.5 mmHg) to post-flight (42.7±1.2 mmHg), or at -20 mmHg LBNP from pre-flight (42.4±3.0 mmHg) and post-flight (41.8±1.9 mmHg).

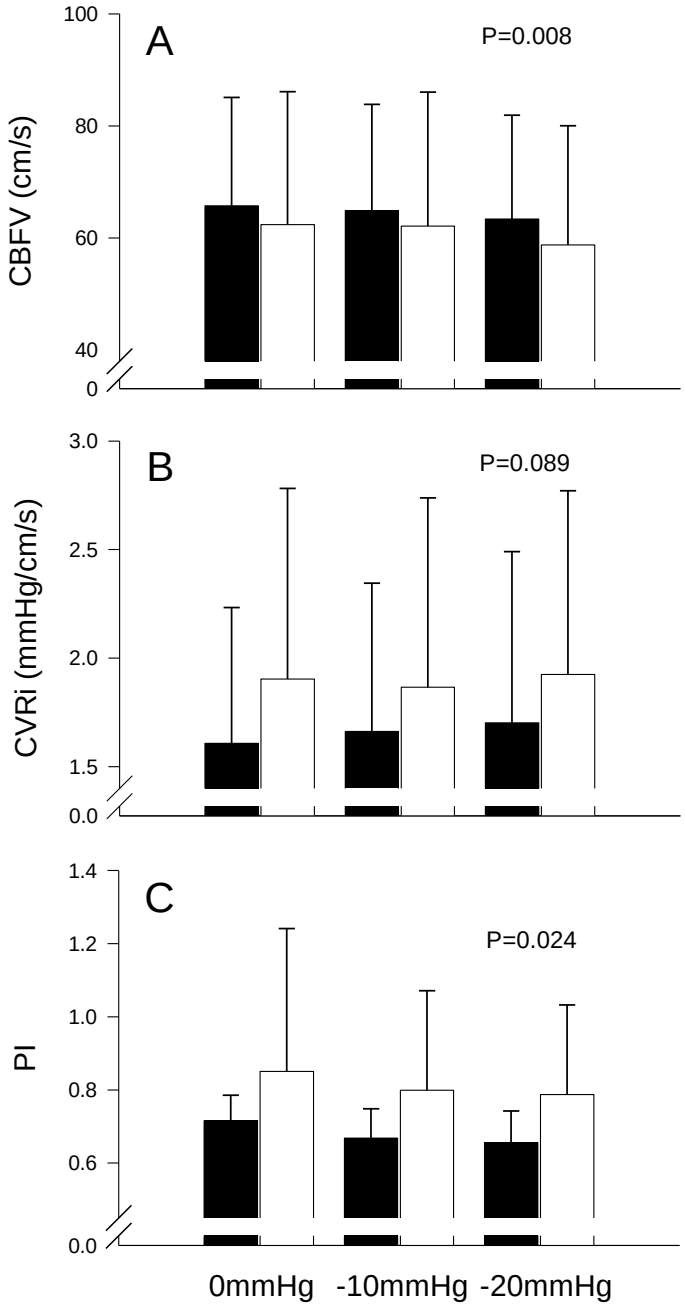

Figure 2.1: LBNP responses

The mean values (± SD, n=7) for CBFV (A), CVRi (B) and PI (C) in response to LBNP are shown for pre-flight (black) and post-flight (open). P values for the main effect of LBNP are shown on each panel. No statistical differences were seen with respect to spaceflight.

The BP_{MCA} and cerebrovascular responses to the two-breath test with intermittent increases of inspired CO_2 are displayed for a typical subject in Figure 2.2. The transient elevation in PCO_2 reduced CVRi and resulted in increases in CBFV while BP_{MCA} maintained spontaneous variations without obvious effect of PCO_2.

Group mean responses from the ARMA analyses are displayed as the time course of change to a unit input in BP_{MCA} and PCO_2 in Figure 2.3 and individual step responses in Figure 2.4. When BP_{MCA} was considered as the input signal the averaged gain value for BP_{MCA}→CBFV was not different pre- to post-flight (-0.225±0.453 vs. 0.069±0.119 cm/s/mmHg BP_{MCA}, P=0.13, Figure 2.3 A and Figure 2.4 A), but the BP_{MCA}→CVRi gain was reduced 17% after spaceflight (0.035±0.007 vs. 0.029±0.005 units/mmHg BP_{MCA}, P=0.047, Figure 2.3 C and Figure 2.4 C). The indicators of CO_2 reactivity from the responses of CBFV and CVRi revealed a strong trend for reduced CBFV response from pre- to post-flight (2.113±1.228 vs. 1.300±0.595 cm/s/mmHg PCO_2, P=0.056, Figure 2.3 B and Figure 2.4 B) and a reduction in the CVRi response (-0.038±0.018 vs. -0.027±0.012 units/mmHg PCO_2, P=0.017, Figure 2.3 D and Figure 2.4 D).

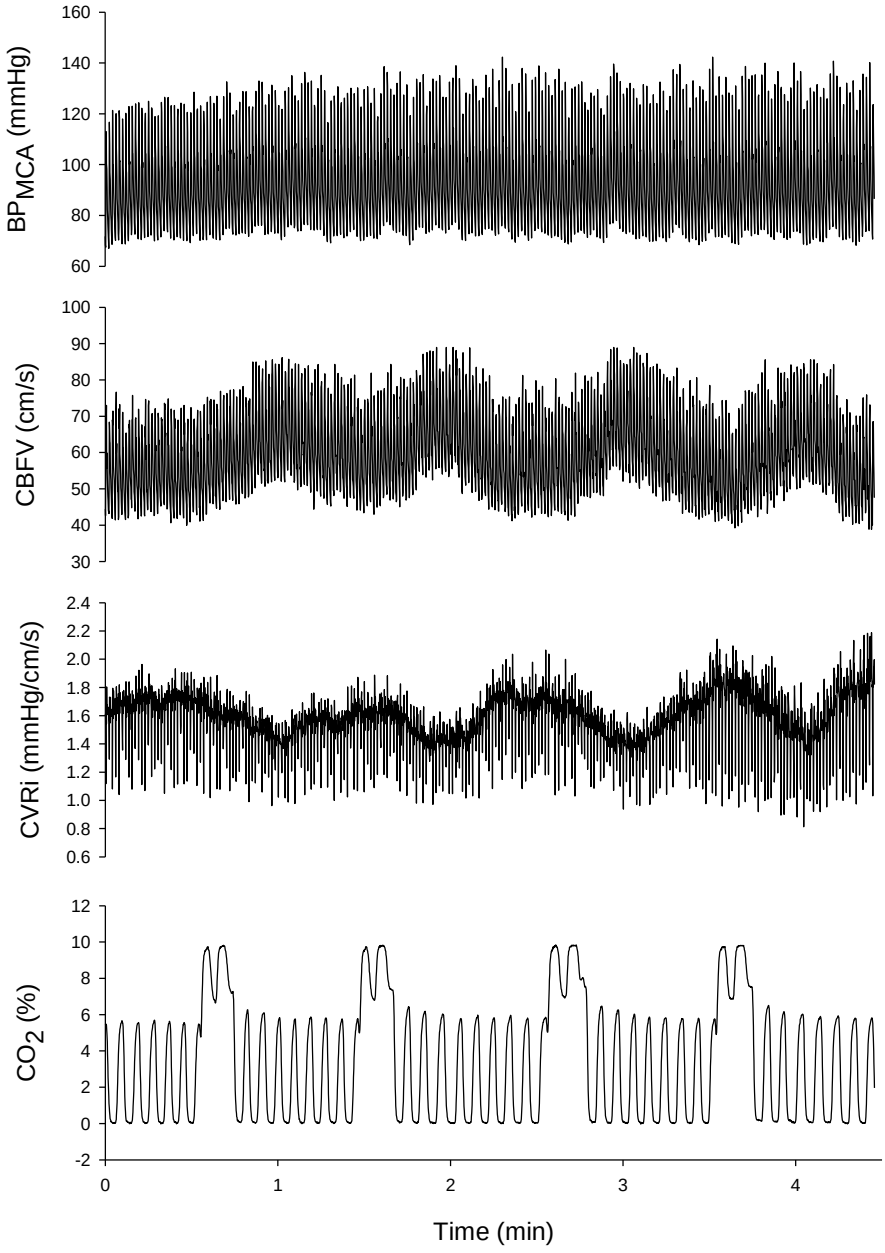

Figure 2.2: Representative "two-breath" test data set

Data set of one subject from the "two-breath" protocol. Tracing shows that, as expected, two breaths of 10% CO_2 elicited an increase in CBFV and a reduction in CVRi with minimal change in BP_{MCA}.

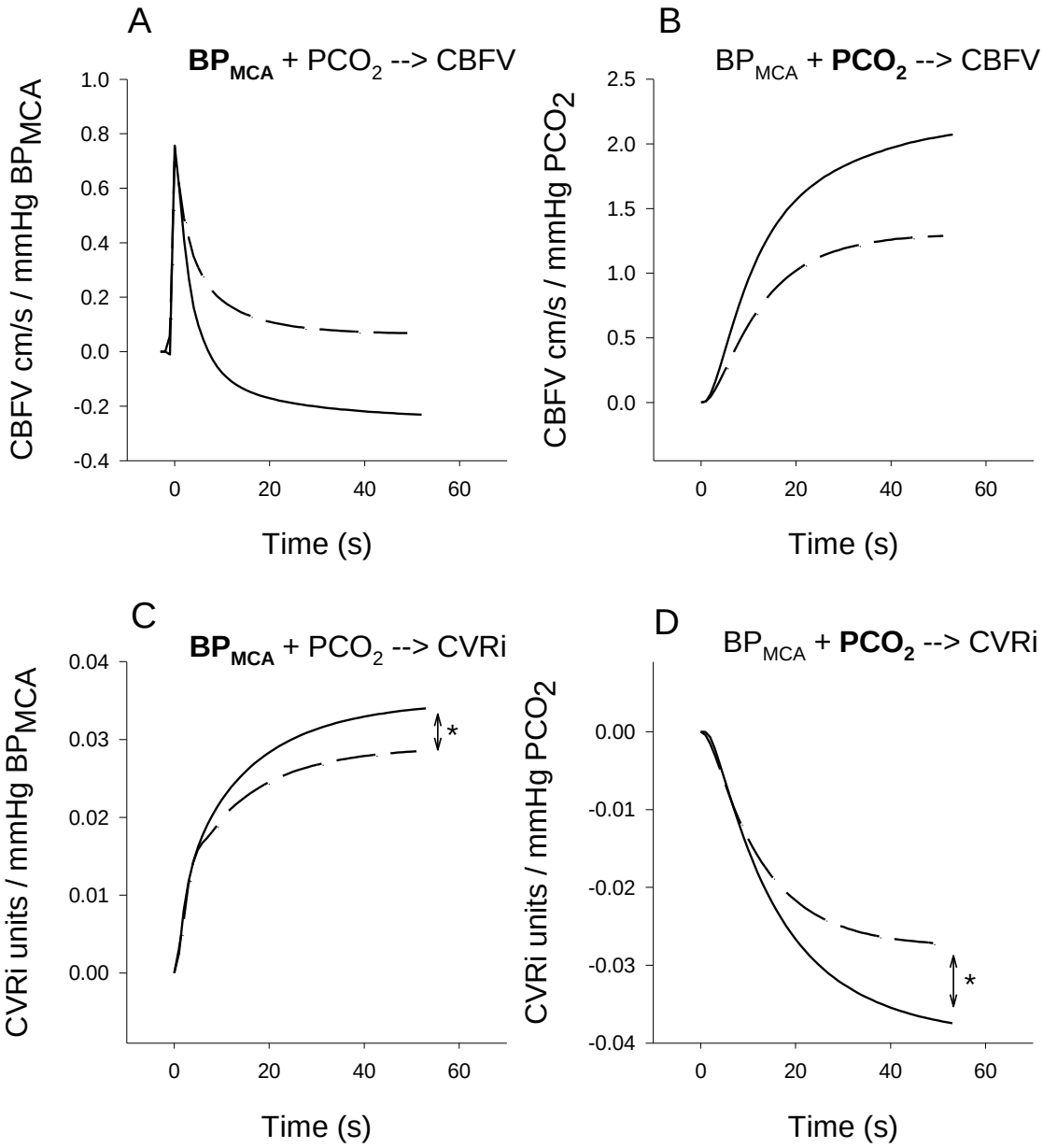

Figure 2.3:Group ARMA step responses

*The group mean ARMA analysis step responses are shown as a function of time for pre- (solid line) and post-spaceflight (dashed line). The ARMA model incorporates two inputs (BP_{MCA} and PCO_2) acting on a single output (CBFV or CVRi). The extracted solutions are shown for BP_{MCA}→CBFV (A, n=6), PCO_2→CBFV (B, n=6), BP_{MCA}→CVRi (C, n=5), and PCO_2→CVRi (D, n=5). * P<0.05 between the 45s plateau value pre- to post-flight, see Figure 2.4 for exact P-values.*

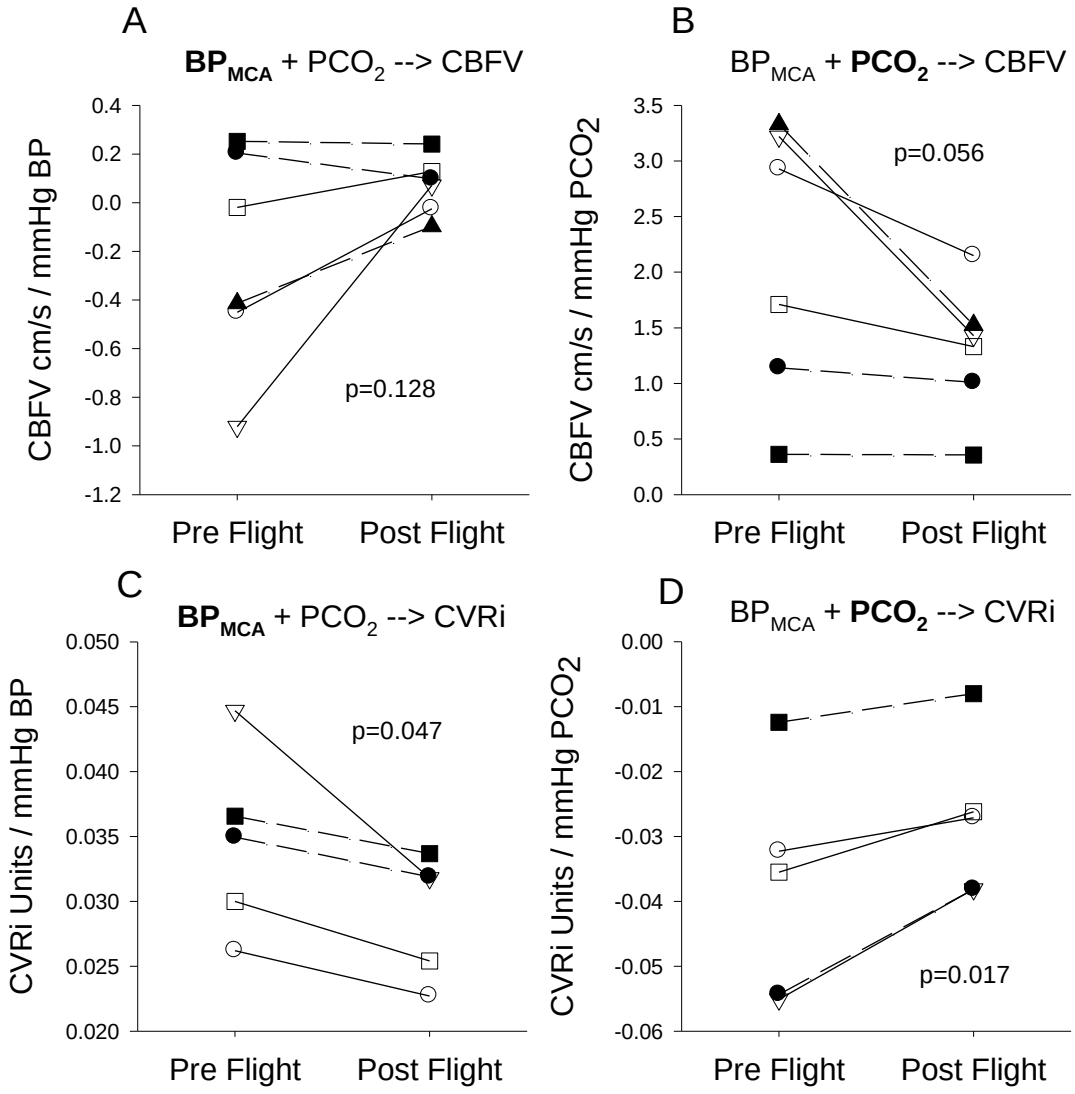

Figure 2.4: Individual ARMA step responses

Each astronaut's pre- and post-spaceflight gain values computed at 45s from the step responses of the ARMA analysis are shown for BP_{MCA}→CBFV (A, n=6), PCO_2→CBFV (B, n=6), BP_{MCA}→CVRi (C, n=5), and PCO_2→CVRi (D, n=5). Solid lines and symbols connect pre- to post-spaceflight values for shuttle landed astronauts, open symbols and dashed lines show the Soyuz landed astronauts. P-values are for pre- to post-flight comparisons.

2.5 Discussion

The major findings of this study showed that long duration spaceflight was associated with reductions in the indices of cerebrovascular dynamic autoregulation and CO_2 reactivity with no differences seen in resting CBFV or responses to low levels of LBNP. These findings, following long duration spaceflight on the ISS, were consistent with hypotheses that suggested cerebrovascular consequences from chronic elevation in cerebral blood pressure and chronic exposure to elevated atmospheric PCO_2. Our results contrast with improved dynamic autoregulation after the short duration Neurolab spaceflight mission (Iwasaki et al., 2007) but are similar to findings in astronauts who presented with orthostatic intolerance after spaceflight (Blaber et al., 2011).

2.5.1 Cerebrovascular Indicators at Rest and During LBNP

We anticipated greater reduction in CBFV during LBNP after long duration spaceflight indicative of impaired cerebral blood flow regulation, but both at rest and during LBNP the CBFV, PI, and CVRi were unchanged from pre-flight. Resting CBFV is expected to reflect the metabolic demands of the brain (Aaslid et al., 1989; Panerai, Dineen, Brodie, & Robinson, 2010) as well as the constant influence of $PaCO_2$ (Panerai et al., 2010; Mitsis, Poulin, Robbins, & Marmarelis, 2004). Our finding of no change in supine CBFV after spaceflight was consistent with other observations after short (Blaber et al., 2011; Iwasaki et al., 2007) and long duration flights (Tobal et al., 2001). The unchanged estimate of $PaCO_2$ taken from the end-tidal PCO_2 made it unlikely that alterations in CO_2 had an effect on resting cerebral blood flow.

The potential effects of long duration spaceflight on cerebrovascular structure and function have been inferred from HDBR studies with humans (Arbeille et al., 1998; Arbeille et al., 2008; Arbeille et al., 2001; Frey et al., 1993; Hirayanagi et al., 2005; Kawai et al., 1993; Pavy-Le Traon et al., 2002; Sun et al., 2005; Zhang et al., 1997) and from animal models of hind limb suspension (Geary et al., 1998; Lin et al., 2009; Wilkerson et al., 1999; Wilkerson et al., 2002; Wilkerson et al., 2005; Zhang et al., 2001). The human HDBR studies reported variable results with increases, decreases and no change in CBFV. Animal models

have revealed reduced flow (Wilkerson et al., 2002; Wilkerson et al., 2005) accompanied by significant structural changes with increased thickness of vessel walls (Lin et al., 2009; Wilkerson et al., 1999; Wilkerson et al., 2002; Zhang et al., 2001) and reduced internal dimensions (Wilkerson et al., 1999). The animal models also suggested an involvement of renin-angiotensin system in structural modifications with hind limb suspension (Bao et al., 2007; Gao et al., 2009). An up-regulation after 4-weeks, but not after 7-days, of proteins involved in the synthesis of angiotensinogen and of angiotensin-II type-1 receptors was observed in cerebral and carotid arteries, and these changes were associated with increased arterial wall thickness (Bao et al., 2007; Gao et al., 2009). Based on these results from animal models, it is possible that human cerebral arteries might also undergo structural change with prolonged exposure to microgravity. At the moment, it is not possible to rule out the possibility that, while CBFV was unchanged, cerebral blood flow might have been reduced as a function of a smaller middle cerebral artery. This can only be tested in future studies by quantitative measurements of cerebral blood flow or measures of middle cerebral artery dimensions.

In the current study, CBFV was reduced during -20 mmHg of LBNP but there was no difference in this response from pre- to post-flight. These results contrast with observations after the short duration Neurolab mission (Iwasaki et al., 2007) where there was a smaller reduction in CBFV during LBNP as well as during upright tilt compared to pre-flight. Our LBNP results after long duration spaceflight were consistent with observations from cosmonauts after 6-months in space; however, at greater levels of LBNP, cosmonauts showed a trend towards greater reductions in CBFV after flight (Tobal et al., 2001). In the current study, it is therefore possible that -20 mmHg LBNP was not sufficient to challenge cerebral blood flow regulation, as these same astronauts only showed small changes in post-flight baroreflex function in the seated posture (Hughson et al., 2011); therefore, it is still possible that changes in CBFV might have occurred with greater levels of LBNP or in assuming an upright posture. Reduced PI during LBNP reflected a relative reduction in cerebrovascular resistance (Beasley et al., 1979), but there were no apparent pre- to post-flight differences in this indicator of static cerebrovascular autoregulation.

2.5.2 Dynamic Cerebrovascular Autoregulation

Dynamic cerebrovascular autoregulation, in contrast to static autoregulation (Aaslid et al., 1989; Panerai, Dawson, & Potter, 1999), is an index of the rapid responses of the cerebrovascular system to acute changes in BP_{MCA} (Panerai et al., 1999). An inverse relationship exists between the dynamic autoregulatory index and PCO_2 (Edwards et al., 2004); therefore, it was important that resting PCO_2 was not different from pre- to post-flight and further that the simultaneous effects of BP_{MCA} and PCO_2 were accounted for by the ARMA model. The reduction in gain for CVRi relative to the change in BP_{MCA} provided an index of impaired dynamic cerebrovascular autoregulation after spaceflight. Similarly, there was a trend towards a reduced CBFV response to a change in BP_{MCA} (P=0.128). Reduced cerebrovascular dynamic autoregulation after long duration spaceflight was consistent with some (Zhang et al., 1997) but not all (Pavy-Le Traon et al., 2002) findings after HDBR, and with astronauts who had orthostatic intolerance after short duration spaceflights (Blaber et al., 2011). Altered post-flight cerebrovascular control might reflect the structural and functional changes observed in the animal models of spaceflight (Lin et al., 2009; Wilkerson et al., 1999; Wilkerson et al., 2002; Zhang et al., 2001).

2.5.3 Cerebrovascular Reactivity to CO_2

No previous investigation has examined cerebrovascular CO_2 reactivity after spaceflight. Animal studies showing reductions in nitric oxide-dependent dilation of cerebral arteries after hind limb suspension (Lin et al., 2009; Prisby et al., 2006; Wilkerson et al., 2005) suggested that the CO_2 response might be altered due to the link between CO_2 induced dilation of human cerebral arteries and nitric oxide-dependent mechanisms (Lavi et al., 2006; Fathi et al., 2011; Schmetterer et al., 1997). CO_2 reactivity was investigated in the current study by the "two-breath" method (Edwards et al., 2003) which accounts for the spontaneous variability in PCO_2 that can complicate interpretation of cerebrovascular responses (Panerai et al., 2010; Edwards et al., 2003). The reduced gain for the CBFV and CVRi responses computed with respect to the input of PCO_2 support the hypothesis that the nitric oxide-

dependent dilatory mechanisms of the cerebrovascular system might be impaired by long duration spaceflight.

The environment of ISS had an average inspired PCO_2 of 3.34mmHg during the experiments described in this study. This value is over 10-fold greater than ambient conditions on Earth. Patients with chronic hypercapnia have blunted cerebrovascular CO_2 reactivity (Clivati et al., 1992); however it is unclear if chronic exposure to increased atmospheric PCO_2, as seen on ISS, produces reductions in cerebrovascular CO_2 reactivity in a healthy population. Slightly elevated inspired CO_2 might have had a chronic effect on $PaCO_2$ and arterial acid-base which could in turn affect cerebrovascular resistance. To date, no arterial blood samples have been taken on ISS to determine if changes in $PaCO_2$ have occurred.

2.5.4 Individual Variability and Potential Implications

The responses of dynamic autoregulation and CO_2 reactivity, and the pre- to post-flight differences varied between astronauts. Finding a range of pre-flight baseline CBFV and CVRi responses to the input of BP_{MCA} (Figure 2.4 A and C) is similar to previous observations (Edwards et al., 2003). Likewise, differences between subjects in CO_2 reactivity (Figure 2.4 B and D) are expected and might be related to differences in nitric oxide-dependent dilation, but this was not directly tested. Of interest in the current study is the magnitude of change following spaceflight. One individual (open triangle, Figure 2.4) had the largest change from pre- to post-flight in both CBFV and CVRi responses to BP_{MCA} along with one of the larger changes in response to PCO_2. The other astronauts had relatively consistent changes. The functional consequences of these changes cannot be identified from the current study; however, a recent study (Blaber et al., 2011) noted that reductions in dynamic cerebrovascular autoregulation were associated with orthostatic intolerance. No tilt tolerance tests were performed by the astronauts in the current study.

Implications of individual variability in the changes in cerebrovascular dynamic autoregulation and CO_2 reactivity beyond orthostatic tolerance are not known. However, NASA has recently identified idiopathic intracranial hypertension as a risk factor for post-

flight visual problems (Fogarty, 2011; Mader et al., 2011). The current data showing a range of changes in post-flight cerebrovascular responses might provide impetus to investigate the potential for transcranial Doppler measurements to yield information on risk for these visual problems.

2.5.5 Limitations

The sample size in the current study was small. We had 7 astronauts participate in the study but technical limitations reduced our main comparison of CVRi responses to n=5. CO_2 was not available in one astronaut (this astronaut's data were eliminated from all ARMA analyses but were included in the LBNP portion of the study), and there were marked differences between pre- and post-flight CBFV in another astronaut suggesting that different arteries might have been investigated (this astronaut's data were eliminated from CVRi results but maintained for CBFV as the delta response was assumed similar independent of artery). Further, it is acknowledged that with data collection in several different locations, different equipment was used for data collection possibly contributing to variability in the results. However, the consistent pattern of response between astronauts suggests that equipment did not influence the main findings of this study.

There were also differences in the timing of the post-flight testing. Figure 2.4 indicates the individual astronauts according to their landing site which dictated whether tests were conducted on R+0 (all shuttle landings, n=3 for this figure) or were on R+1 or R+2 (Soyuz landings). For shuttle landings, all astronauts were tested within 3-4h of landing and they had not been in an upright position for more than a few seconds during transitions between the shuttle and crew transport vehicle. For Soyuz landings, crew were upright at some times on landing day during their return to Star City, but were transported the morning after their arrival to the laboratory without assuming an upright posture for longer than toilet requirements. This provided a situation as similar as possible to the shuttle crew. These preparations contributed to the similar responses observed for most astronauts.

2.6 Conclusions

The current study has shown a consistent impairment of dynamic cerebrovascular autoregulation and CO_2 reactivity in astronauts following long duration spaceflight; however, there were between person differences in the magnitude of impairment. It is unclear at the moment whether these changes have pathophysiological significance associated with the complications in vision attributed to idiopathic intracranial hypertension (Fogarty, 2011; Mader et al., 2011). Future studies should investigate pre- to post-flight changes in transcranial Doppler indices of cerebral blood flow and CO_2 reactivity to determine if they are predictors of pathophysiological complications resulting from long duration spaceflight.

Chapter 3

Assessment of middle cerebral artery Doppler waveform morphology for the determination of cerebrovascular tone after long duration spaceflight

3.1 Overview

Microgravity exposure results in cephalic fluid shifts and increased intracranial pressure that may result in remodelling of the cerebrovasculature. The purpose of this study was to examine the cerebral blood flow velocity (CBFV) waveform morphology for the determination of cerebrovascular tone before and after long duration spaceflight. Data were collected from 7 astronauts who spent a minimum of 58 days on orbit. CBFV waveform morphology was assessed based on key inflection points referring to the overall pulse amplitude of the signal, the amplitude of the reflected peak, and the amplitude of the dicrotic notch. Critical closing pressure (CrCP) and resistance area product (RAP) were calculated using a two point method involving mean and diastolic values of CBFV and arterial pressure. Waveform morphology and CrCP were assessed before and after flight at rest, after two breaths of 10% CO_2, and at -20mmHg lower body negative pressure (LBNP). The amplitudes of waveform points were increased with CO_2 and decreased with LBNP, but were not different after spaceflight. RAP was not different with CO_2, LBNP, or spaceflight. In contrast, CrCP was decreased with CO_2 and significantly increased in all three conditions after spaceflight. These results suggest that long duration spaceflight results in cerebrovascular remodelling that serves to increase tone as seen by the increase in CrCP.

3.2 Introduction

Exposure to microgravity is associated with cephalic fluid shifts (Hargens & Watenpaugh, 1996) that may promote cerebrovascular remodelling. Cerebral arteries from animal models of microgravity exposure have shown evidence of vascular smooth muscle hypertrophy (Wilkerson et al., 1999; Lin et al., 2009; Zhang et al., 2001; Wilkerson et al., 2002) associated with increased myogenic tone (Wilkerson et al., 2005; Geary et al., 1998; Lin et al., 2009), a reduction in lumen cross-sectional area (Wilkerson et al., 1999), and reduced cerebral blood flow (Wilkerson et al., 2002; Wilkerson et al., 2005).

Work with humans after spaceflight or simulated microgravity exposure has shown no changes in resting cerebral blood flow velocity or cerebrovascular resistance (Blaber et al., 2011; Iwasaki et al., 2007; Arbeille et al., 2008; Pavy-Le Traon et al., 2002; Zhang et al., 1997; Arbeille et al., 2001). However, these results are based on transcranial Doppler ultrasound (TCD) measures of cerebral blood flow velocity (CBFV) and are dependent on the diameter of the insonated vessel remaining constant after spaceflight or simulated microgravity. Currently it is unknown if this assumption is valid after spaceflight; however, additional information may be gleaned from the analysis of within beat characteristics of the CBFV trace with respect to changes in cerebrovascular tone. To date, no studies have been conducted examining potential changes in cerebrovascular tone after spaceflight.

Several methods have been proposed to assess vascular tone which could be applied to the cerebral circulation including alteration in key inflection points of the Doppler waveform (Kurji et al., 2006; Lockhart et al., 2006; Robertson et al., 2008) and the calculation of critical closing pressure (CrCP) (Moppett et al., 2008; Panerai et al., 2011; Panerai, 2003; Ogoh et al., 2010). The purpose of this study was to examine TCD recordings before and after long duration spaceflight to determine potential changes in cerebrovascular tone. It was hypothesized, that similar to results from animal models of microgravity exposure (Wilkerson et al., 2005; Geary et al., 1998; Lin et al., 2009) long duration spaceflight would result in cerebrovascular remodelling which would increase cerebrovascular tone.

3.3 Methods

Data for this study were collected as a part of the Cardiovascular and Cerebrovascular control on return from the International Space Station (CCISS) project with the general method, including instrumentation and experimental protocol having been presented in Chapter 2.

3.3.1 Data Analysis

For the assessment of velocity waveform characteristics and cerebrovascular tone, 10 cardiac cycles were averaged to produce a representative waveform at rest before the application of LBNP, at the end of -20mmHg LBNP, and after the two breaths of CO_2 at the point where the increase in CBFV was greatest. Key inflection points on the CBFV waveform were then determined as shown in Figure 3.1 and assessed with respect to the end diastolic velocity value, T1, as P1-T1, T2-T1, P2-T1, T3-T1, and P3-T1. As previously described (Robertson et al., 2008; Kurji et al., 2006), the peaks P1 and P2 of the velocity wave were used with the end diastolic value T1 for the calculation of an augmentation index as AI = (P2-T1) / (P1-T1) x 100%.

Critical closing pressure (CrCP) and the resistance area product (RAP) were calculated using a two point method previously described (Panerai et al., 2011). Using this method, the slope of the relationship between ABP and CBFV was calculated as a = (CBFVmean – CBFVdia) / (ABPmean – ABPdia). RAP was calculated as RAP = 1 / a and CrCP calculated as CrCP = ABPmean – (CBFVmean / a).

3.3.2 Statistical Analysis

A two-way repeated measures analysis of variance was used to test for the main effect of spaceflight and conditions; Resting, LBNP, and CO_2 (SigmaStat 3.5, Systat Software Inc., Chicago, IL). Statistical significance was set at $p<0.05$. Values presented are mean ± standard deviation.

3.4 Results

Analysis of MCA velocity wave inflection points, presented in Figure 3.2, showed that P1-T1 was increased with CO_2 and decreased with LBNP. Similar directional changes were seen for P2-T1, P3-T1, T2-T1, T3-T1 and AI. No differences were seen in any of these measures after spaceflight.

The results for CrCP and RAP are shown in Figure 3.3. With CO_2, CrCP was seen to decrease but was not changed with the application of -20mmHg LBNP. Post spaceflight, CrCP was increased in all three conditions. RAP was no different from baseline with either CO_2 or LBNP; however, the RAP values were different between the CO_2 and LBNP conditions. No differences in RAP were seen with spaceflight.

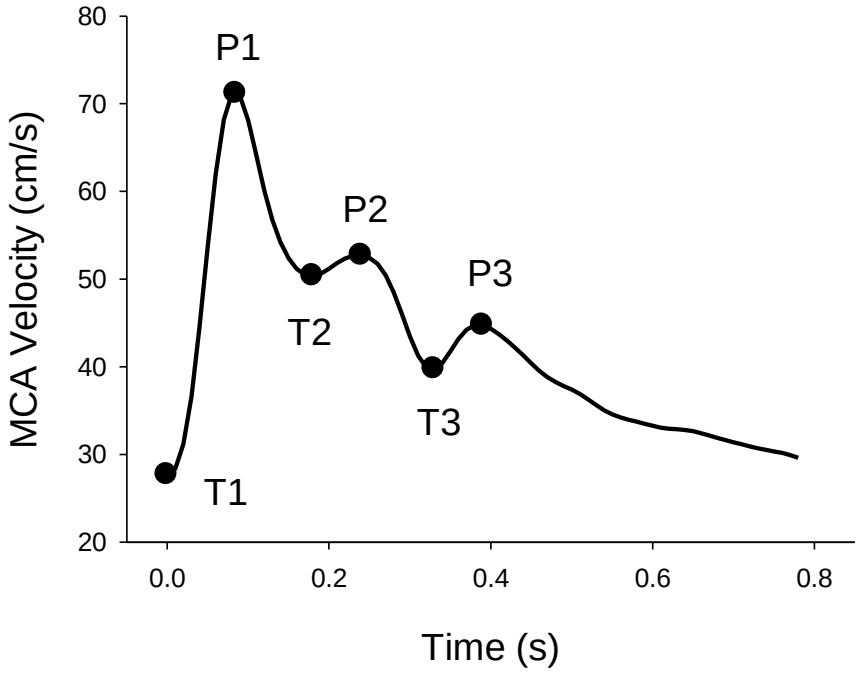

Figure 3.1: Representative velocity wave

Key inflection points indicated as the three peaks (P1, P2, P3) and three troughs (T1, T2, T3). For analysis purposed, all inflection points were expressed with respect to the T1 value.

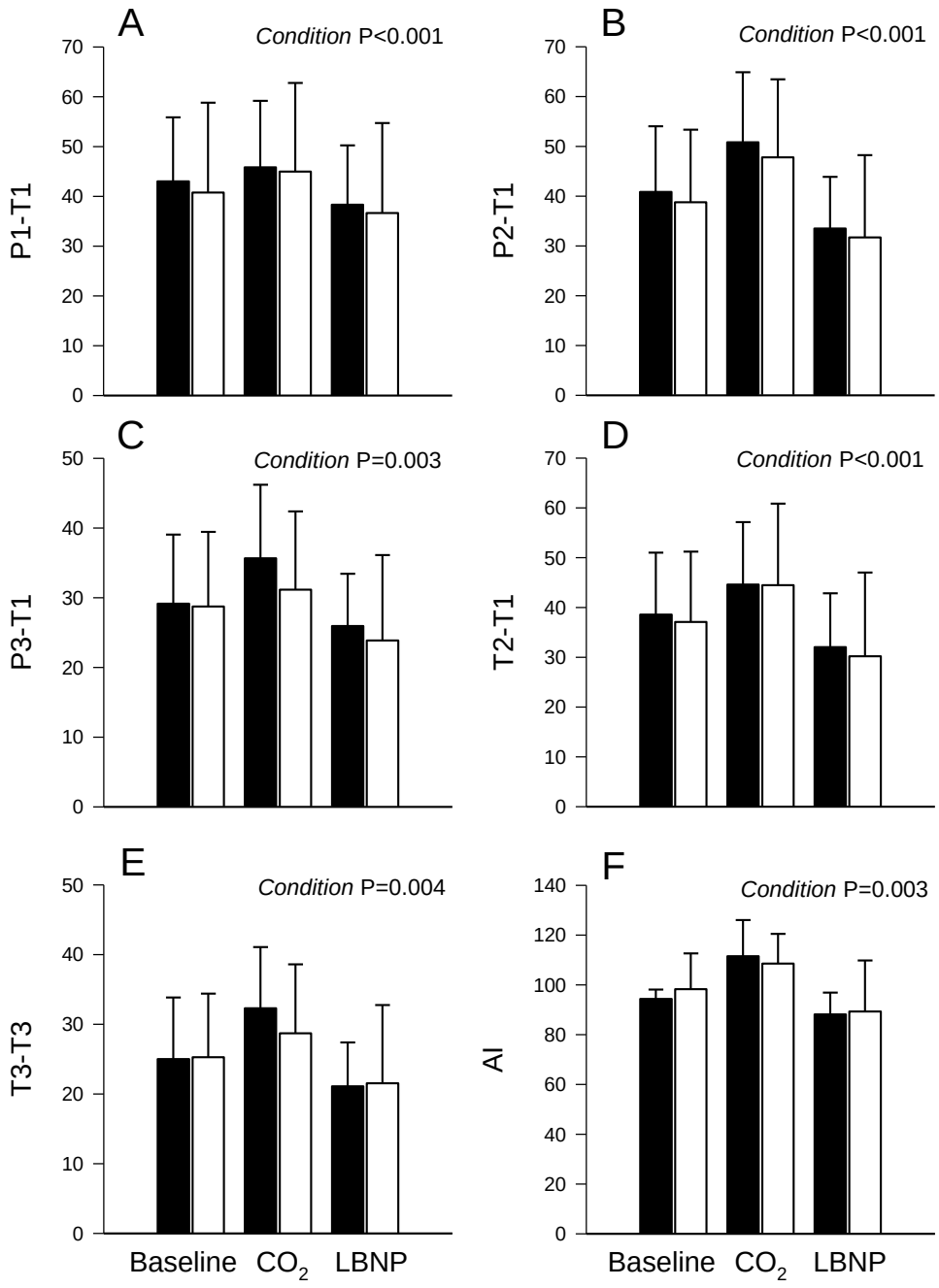

Figure 3.2: Key inflection point analysis results

Data show pre-flight (black bars) and post-flight (white bars) results for baseline rest, after the CO_2 stimulus, and with -20mmHg LBNP (conditions). P values show the main effects of condition. No effects of spaceflight were seen for any variable.

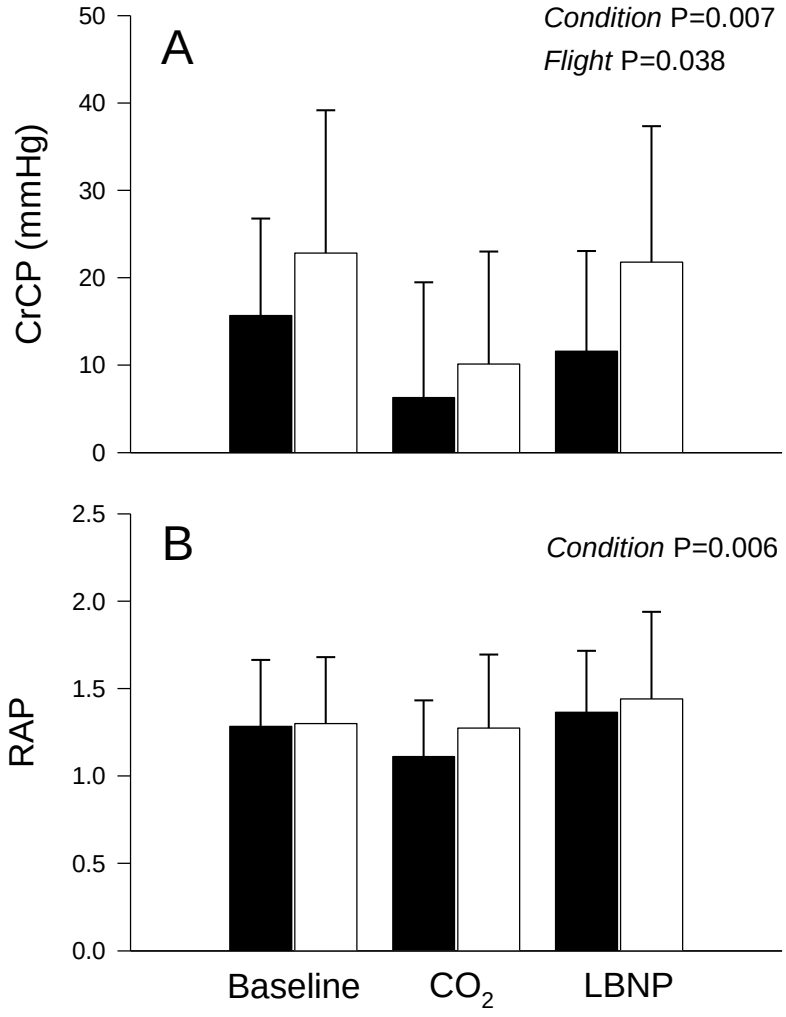

Figure 3.3: Results for calculation of CrCP and RAP

CrCP (A) and RAP (B) results for pre-flight (black bars) and post-flight (white bars) for the three conditions; baseline rest, CO_2, and -20mmHg LBNP. Statistical analysis showed the main effect of condition for both CrCP and RAP with post hoc testing indicating that for CrCP, CO_2 values were different from baseline and that a difference existed in RAP values between CO_2 and LBNP. Statistical analysis also found a main effect of spaceflight for CrCP indicating that CrCP was increased post spaceflight.

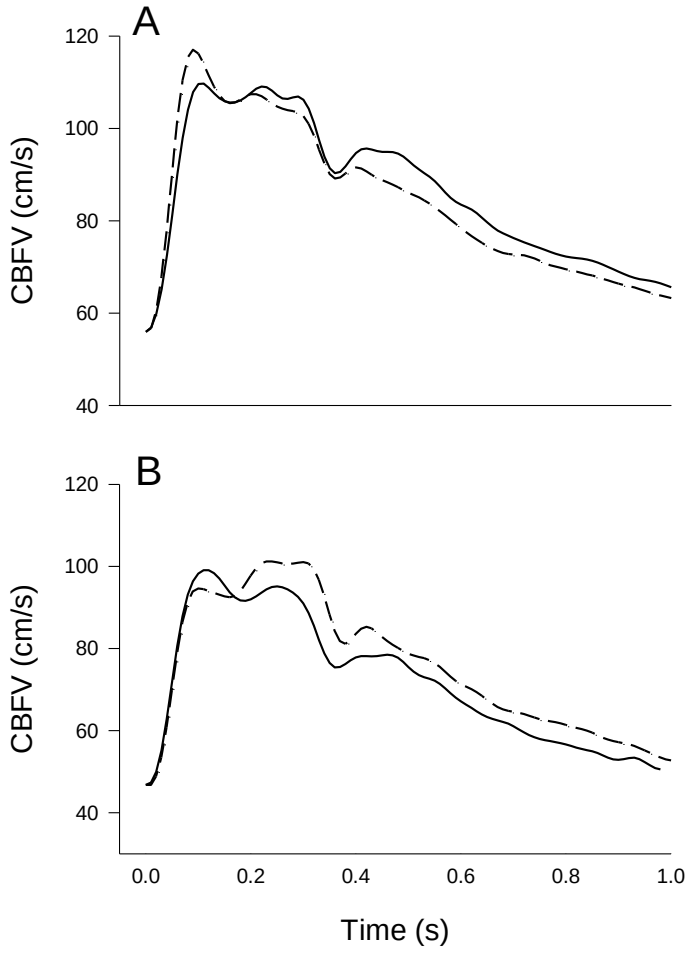

Figure 3.4:Representative MCA waveforms

Pre-flight (solid line) and post-flight (dashed line) representative MCA waveforms of two shuttle launched and landed astronauts. Pre to post spaceflight the MCA waveforms were altered, but the large amount of individual variability in the waveforms prevented any statistically significant difference.

3.5 Discussion

The current study utilized the assessment of MCA velocity wave inflection points and the calculation of CrCP in an attempt to identify potential changes in cerebrovascular tone with spaceflight. Contrary to the first hypothesis, no differences were seen in the velocity wave inflection points after long duration spaceflight. However, in support of the hypothesis,

CrCP was seen to be increased after long duration spaceflight suggesting an increase in cerebrovascular tone potentially due to vascular remodelling.

3.5.1 Cerebrovascular Remodelling with Spaceflight

To date, little information is known about the effects of long duration spaceflight on human cerebrovascular structure and function, but hypotheses have been developed (Hargens & Watenpaugh, 1996; Zhang, 2001) based on data from animal models of microgravity exposure. Cerebral arteries of rodents exposed to hind limb unloading have shown vascular smooth muscle cell hypertrophy (Wilkerson et al., 1999; Lin et al., 2009; Zhang et al., 2001; Wilkerson et al., 2002) with smaller luminal cross-sectional area (Wilkerson et al., 1999) and increased basal myogenic tone (Wilkerson et al., 2005; Geary et al., 1998; Lin et al., 2009). However, it is not known if similar adaptations occur with spaceflight, or if human arteries respond in the same fashion.

Of the studies that have attempted to assess changes in human arterial tone with microgravity exposure, the results have been mixed. In contrast to the results from animal studies, Eiken et al. (Eiken, Kolegard, & Mekjavic, 2008) showed an increased pressure distension of the tibial artery after five weeks of horizontal bed rest suggesting a reduction in vascular tone. However, Tuday et al. (Tuday, Meck, Nyhan, Shoukas, & Berkowitz, 2007) demonstrated an increase in aortic stiffness in astronauts who exhibited orthostatic intolerance after 5 to 18 days in space. Similarly, Baevsky et al. (Baevsky et al., 2007) found a reduction in pulse wave transit time during and after spaceflight which suggests an increase in vascular tone consistent with the results from animal studies.

This study is the first to examine potential changes in human cerebrovascular tone after long duration spaceflight. Based on the results from the animal studies, it was hypothesized that after long duration spaceflight, there would be cerebrovascular remodeling leading to an increase in cerebrovascular tone and that this increase in tone would be evident in changes in the MCA blood velocity waveform and changes in calculated CrCP. Consistent with this hypothesis and the results from animal data with simulated microgravity exposure, there was an increase in CrCP with long duration spaceflight suggesting an increase in

vascular tone. However, contrary to the hypothesis, there were no differences in the MCA velocity wave inflection points with respect to the end diastolic value (T1) or in the calculated augmentation index.

The lack of difference in waveform inflection points could be attributed to the small sample size of astronauts and potentially individual differences in results. Representative MCA velocity waveforms pre and post spaceflight of two male shuttle astronauts are presented in Figure 3.4. From this figure it can be seen that the velocity wave profile of individual astronauts was different pre to post flight with different directional responses for each individual.

3.5.2 Responses to CO_2 and LBNP

Results of the current study showed alterations in key inflection points of the MCA velocity wave, AI, and CrCP with CO_2 and the application of -20mmHg LBNP. The response to CO_2 was expected as previous work has shown a reduction in CrCP (Panerai et al., 1999; Panerai, 2003) and an increase in AI (Robertson et al., 2008; Kurji et al., 2006) with hypercapnia. In the current study, responses to CO_2 and LBNP were used to determine if cerebrovascular tone responses differed after long duration spaceflight. Recently, a reduction in cerebrovascular CO_2 reactivity and impaired cerebrovascular autoregulation has been observed in these astronauts (Zuj et al., 2012a). However, in the current study, no differences were found in the cerebrovascular tone responses to CO_2 or LBNP.

3.5.3 Limitations

The current study utilized transcranial Doppler measures of MCA velocity and arterial pressure measures recorded using finger photoplethysmography. When assessing MCA velocity using transcranial Doppler, care was taken to minimize any potential differences in the angle of insonation pre to post spaceflight. However, it is possible that slight differences in probe orientation may have resulted in variability in the analysis of MCA velocity wave inflection points. With respect to the calculation of CrCP, ABP recorded from the finger was used to represent cerebral perfusion pressure. However ABP measured from a peripheral site may not accurately reflect changes in pressure within the cerebral

circulation. One group has looked at the differences in CrCP calculated using finger plethysmography and carotid tonometry finding an increase in CrCP values and no negative CrCP values when tonometry and the linear regression method was used to calculated CrCP (Hsu et al., 2005). However, this paper also noted no differences between the mean and diastolic values of arterial pressure which were the points used to calculate CrCP in the current study. Therefore, it is unlikely that the site of the arterial pressure measurement would affect the calculation of CrCP with the method used in the current study.

3.6 Conclusion

The current study was the first to look at cerebral blood velocity waveforms and the calculation of CrCP and RAP after long duration spaceflight for the assessment of cerebrovascular tone. Contrary to the hypothesis, no differences in MCA velocity waveform inflection points were found after spaceflight; however, this was likely due to large variability in individual responses. Conversely, in support of the hypothesis, CrCP was increased post flight suggesting an increase in cerebrovascular tone. This result suggests that cerebrovascular remodelling may be occurring with long duration exposure to microgravity which could have an impact on the regulation of cerebral blood flow.

Chapter 4

Cerebrovascular and CO_2 responses during the progression towards syncope

4.1 Overview

Syncope from sustained orthostasis results from hypoperfusion of cerebral tissues and is normally associated with a reduction in arterial pressure at the level of the brain (BP_{MCA}) and a reduction in end tidal carbon dioxide ($P_{ET}CO_2$). In this study, it was hypothesized that cerebrovascular responses to head up tilt and the progression towards syncope, both before and after exposure to head down bed rest (HDBR), would be dominated by the reduction in $P_{ET}CO_2$ prior to an effect of BP_{MCA}. Twelve men (21-42 years of age) completed an orthostatic tolerance test consisting of head up tilt and progressive lower body negative pressure, before and after completing five days of continuous HDBR with and without an artificial gravity countermeasure. Cerebral blood velocity (CBFV), BP_{MCA}, and $P_{ET}CO_2$ were continuously recorded throughout the test. Cerebrovascular indicators: cerebrovascular resistance (CVRi), critical closing pressure (CrCP), and resistance area product (RAP) were calculated. Comparing from supine to 6-10min after the start of tilt there were reductions in CBFV (-6.3±3.7cm/s), $P_{ET}CO_2$ (-4.2±3.5mmHg), and CrCP (-18.0±6.7mmHg), an increase in RAP (0.31±0.09mmHg/cm/s), and no change in CVRi. Changes in these variables progressed and were assessed in detail over the final 15min of the test to reveal that CBFV and CrCP were significantly related to changes in $P_{ET}CO_2$ (r=0.688±0.169, and r=0.631±0.196 respectively). BP_{MCA} was not significantly reduced until the last minute of the test and was correlated with a reduction in RAP (r=0.913±0.091). No differences in responses were seen with HDBR. These results indicate that changes in $P_{ET}CO_2$ with orthostasis make an important contribution to increases in cerebrovascular tone and the reduction in CBFV during the progression toward syncope.

4.2 Introduction

Syncope occurring with prolonged orthostasis results from a reduction in cerebral perfusion and is normally associated with a large, rapid reduction in arterial blood pressure at the level of the middle cerebral artery (BP_{MCA}) (LeLorier et al., 2003; Lewis et al., 2010; Carey et al., 2001). A reduction in cerebral blood flow velocity (CBFV) with the progression towards syncope has been attributed by some researchers to a reduction in the partial pressure of arterial carbon dioxide ($PaCO_2$) (Carey et al., 2001; Cencetti, Bandinelli, & Lagi, 1997; LeLorier et al., 2003). However, other work has suggested a poor relationship between $PaCO_2$ and changes in CBFV at least during the early phase of orthostasis (Immink et al., 2006; Serrador, Hughson, Kowalchuk, Bondar, & Gelb, 2006). Both BP_{MCA} and $PaCO_2$ have a major influence on CBFV, but many studies have looked at the effects of BP_{MCA} and $PaCO_2$ in isolation or did not address the influences of $PaCO_2$ when looking at cerebrovascular responses to orthostasis thus preventing the identification of underlying mechanisms.

Assessment of cerebrovascular hemodynamics frequently relies on measurement of CBFV and calculation of cerebrovascular resistance or conductance, but these measures may not fully explain alterations in cerebrovascular properties. The calculations of critical closing pressure (CrCP) and resistance area product (RAP) have been used to further describe cerebral hemodynamic changes with exercise (Ogoh et al., 2010) and alterations in end-tidal PCO_2 ($P_{ET}CO_2$) (Ainslie et al., 2008; Panerai et al., 1999; Panerai, 2003). Carey et al. (Carey et al., 2001) showed changes in both CrCP and RAP with approaching syncope, but did not relate these changes directly to alterations in $P_{ET}CO_2$. Further analysis of CrCP and RAP may help to better describe cerebrovascular hemodynamic responses to orthostasis since CrCP is taken to reflect changes in cerebrovascular tone, while RAP, as an index of cerebrovascular resistance, does not make the assumption that cerebral perfusion pressure gradient is referenced to 0mmHg (Evans et al., 1988; Panerai, 2003).

A reduction in orthostatic tolerance has been associated with cardiovascular deconditioning from exposure to real or simulated microgravity (Arbeille et al., 2008;

Buckey et al., 1996; Zhang et al., 1997). The potential contributions of change in $P_{ET}CO_2$ and the cerebrovascular response to CO_2 have not been investigated with respect to this reduction in tolerance. Animal models provided a basis to suspect change as the nitric oxide (NO) system, linked to cerebrovascular CO_2 reactivity in humans (Lavi et al., 2003; Schmetterer et al., 1997; Lavi et al., 2006), is down-regulated with simulated microgravity (Prisby et al., 2006; Lin et al., 2009; Wilkerson et al., 2005). Recent observations of reduced cerebrovascular CO_2 reactivity in astronauts returning from long duration spaceflight (Zuj et al., 2012a) further suggest that these factors should be investigated following head-down bed rest (HDBR). To date, no studies have been conducted examining the relationship between blood pressure, $P_{ET}CO_2$, and cerebral blood flow with the progression towards syncope before and after exposure to simulated microgravity.

The following study provided the opportunity to examine cerebrovascular responses to head up tilt and the progression towards syncope both before and after exposure to simulated microgravity with particular emphasis on the influences of changes in arterial pressure and $P_{ET}CO_2$. It was hypothesized that with the progression towards syncope, there would be a reduction in CBFV that was related primarily to the change in $P_{ET}CO_2$ and not BP_{MCA} and that the reduction in CBFV would be associated with an increase in CrCP indicating increased cerebrovascular tone. Post-HDBR, it was hypothesized that these relationships would remain consistent but changes would occur sooner after tilt due to a reduction in orthostatic tolerance.

4.3 Methods

4.3.1 Experimental Protocol

Twelve, healthy men (21-42 years of age) completed five days of continuous 6° head down bed rest (HDBR) with and without an artificial gravity countermeasure. The study was designed so that all men participated in random order in both the control (CON) condition and the artificial gravity (AG) condition with each testing session separated by 30 days. All experimental procedures were approved by the Comité Consultatif de Protection des

Personnes dans la Recherche Biomédicale, Midi-Pyrenees (France), and local ethics committees, including the Office of Research Ethics, University of Waterloo. The entire protocol was in accordance with the declaration of Helsinki. Each subject signed a consent form after receiving full disclosure of the experimental protocol and was aware of his right to withdraw from the study for any reason without prejudice.

A short arm centrifuge was used to generate the AG countermeasure with a head to foot force vector of 1g at the centre of mass of the participant. The protocol consisted of intermittent application of force where five minutes of centrifugation was repeated six consecutive times for each of the five days of HDBR.

Orthostatic tolerance, tilt testing was conducted two days before the start of HDBR (pre-HDBR) and as the first transition to an upright posture after the five days of HDBR (post-HDBR). After five minutes of baseline data collection in the supine position, participants were passively tilted to an 80° head up position where they were required to stand quietly for 30 minutes. If signs of orthostatic intolerance did not occur within this time, lower body negative pressure (LBNP) was progressively applied with step decreases of -10mmHg every three minutes. Testing continued until one or more of the following test termination criteria were met; systolic blood pressure <70mmHg, a sudden drop in HR (>15 bpm), severe light headedness, nausea, or the request of the subject to terminate the test.

A standard three lead electrocardiogram (Roxon Medi-Tech Ltd., St. Leonard, QC, Canada) was used for the assessment of heart rate (HR). Finger photoplethysmography (Nexfin, BMEYE B.V., Amsterdam, Netherlands) was used for the continuous assessment of arterial blood pressure (ABP). Values recorded in the finger were corrected to heart level. Post processing of the blood pressure signal involved the correction of recorded values to a manual blood pressure measure, taken by a trained experimenter before the start of the tilt test with the subjects resting in a supine position. An additional height correction was also applied during post processing to determine arterial pressure at the level of the middle cerebral artery (BP_{MCA}). Participants were equipped with a nasal cannula for monitoring of expired CO_2 (Ohmeda 5200 CO_2 Monitor, Madison, WI, USA). Values were recorded as

percent CO_2 to be later converted to mmHg based on ambient temperature and barometric pressure. HR, BP_{MCA}, and CO_2 data were collected at 1000Hz using Chart software (ADInstruments Ltd., Colorado Springs, CO, USA).

Blood flow velocity in the middle cerebral artery (CBFV) was determined using transcranial Doppler ultrasound (TCD). A 2MHz pulsed Doppler probe was placed over the right temporal window which allowed for the insonation of the M1 segment of the right middle cerebral artery (MCA) and the assumption of 0° for the angle of insonation. A head band was used to hold the probe in place throughout the testing. Doppler signals were collected using CardioLab hardware (CNES device, European Space Agency, France) and were recorded at 100Hz using CardioMed software (CNES - European Space Agency, France).

4.3.2 Cerebrovascular Variables

Mean CBFV values were calculated from the outer envelope of the Doppler spectrum over a cardiac cycle. The Doppler recording was also assessed to determine maximum (systolic) and minimum (end diastolic) values for each cardiac cycle. An index of cerebrovascular resistance (CVRi) was calculated as $CVRi = BP_{MCA} / CBFVmean$. The Gosling Pulsatility index was also calculated as an additional assessment of cerebrovascular resistance as $PI = (CBFVsys – CBFVdia) / CBFVmean$ (Beasley et al., 1979).

Further analysis was conducted with the CBFV waveform for the calculation of critical closing pressure (CrCP) and resistance area product (RAP). Following the methods described in a recent critical analysis (Panerai et al., 2011), CrCP was calculated for each beat using mean and diastolic values for CBFV and arterial blood pressure at the level of the MCA (BP_{MCA}). The slope of the relationship between CBFV and BP_{MCA} was calculated as $a = (CBFVmean – CBFVdia) / (MAP_{MCA} – DBP_{MCA})$. RAP was then calculated as $RAP = 1 / a$ and CrCP calculated as $CrCP = MAP_{MCA} – (CBFVmean / a)$. Previous studies of head-up tilt and sustained orthostasis have used a linear regression method for assessing CrCP and RAP (Stewart et al., 2012; Carey et al., 2001). However, in this study, the two point method using mean and diastolic values of CBFV and BP_{MCA} was chosen as it has recently been shown to

have greater repeatability and fewer instances of negative CrCP values being calculated (Panerai et al., 2011).

4.3.3 Data Analysis

This study reports on data collected during the control and artificial gravity condition; however the original design of the study included two artificial gravity conditions with pre-HDBR data collected three times for each subject. Post-HDBR data for the second artificial gravity condition were not included in the present analysis as only a small number of individuals completed the entire protocol. Previous work has demonstrated good reproducibility of tilt responses (LeLorier et al., 2003) and statistical analysis of these data (not shown) showed no differences between the pre-HDBR responses defined as the difference between a five minute average taken at supine baseline, a five minute average from minutes 6 to 10 of the tilt, and the last minute of the test. Therefore, for analysis purposes, pre-HDBR was considered as the average of all three pre-HDBR data collections.

Variables were assessed beat-by-beat then averaged every 10 seconds after the transition to the tilted position. $P_{ET}CO_2$ values were linearly interpolated to determine values for each heart beat. Tilt responses were assessed as the difference between a five minute average taken during supine rest and a five minute average taken between minutes 6 and 10 of the tilt. For some tests, following HDBR, the participant was unable to complete 10 minutes of the stand test. Therefore, tilt values were taken as the average from five minutes post tilt excluding last minute of the test.

4.3.4 Statistical Analysis

The analysis of cardiovascular responses to tilt was performed in several ways. First, a two-way repeated measures ANOVA (SigmaStat 3.5, Systat Software Inc., Chicago, IL) was used to compare supine baseline with early tilt defined as the average of values between minutes 6 and 10 of the tilt. Secondly, the end of tilt responses were assessed as percent changes over the final 15 minutes of the test with a one-way repeated measures analysis of variance being used to assess each minute value. Finally, linear regression analysis was used on data from each individual to explore possible interrelationships between different

variables. From the data in the final 15 minutes of the test, two distinct sections were identified based on the point at which BP_{MCA} became different from the value at 15 minutes. BP_{MCA} was not different until 1min before syncope; therefore, regressions were performed on data between minutes 15 and 2, and 2 and 0 separately to determine relationships between $P_{ET}CO_2$, BP_{MCA}, CBFV, CrCP, and RAP. Data for the linear regressions are presented as the Pearson product moment correlation (r).

All values are shown as mean ± standard deviation unless otherwise stated. Significance was set at $P<0.05$ for the repeated measures analysis of variance, $P<0.001$ for linear regression analysis between minutes 15 and 2, and $P<0.01$ for linear regression analysis between minutes 2 and 0.

4.3.5 Analysis Limitations

Data were available for all twelve individuals pre-HDBR; however, post-HDBR some data were not available for the planned analyses. For the comparison of early tilt responses (average between 5 and 10 minutes post tilt), three individuals in the CON condition and one in the AG condition experienced syncope within five minutes of tilt, and one person had an unrelated medical complication. Therefore, only 7 of 12 individuals were included in the repeated measures analysis. The linear regression analysis was not attempted in the post-HDBR tests as three additional tests were terminated due to a power outage, equipment failure, and a request by the participant to stop the test that was not related to the onset of presyncopal symptoms.

4.4 Results

Analysis of the cerebrovascular responses to tilt, presented in Figure 4.1, show the difference from the five minute average taken during supine rest and minutes 6-10 after tilt. A reduction in CBFV (panel A), $P_{ET}CO_2$ (panel B), BP_{MCA} (panel D) and CrCP (panel E) were seen along with an increase in RAP (panel F) and no significant changes for CVRi (panel C) or PI (data not shown). No differences were found between pre-HDBR responses and post-HDBR for either the CON or AG condition.

The changes in CBFV, $P_{ET}CO_2$, and BP_{MCA} during the last 15 minutes before syncope pre-HDBR are presented in Figure 4.2. CBFV and $P_{ET}CO_2$ progressively decreased with significant reduction from the value at 15 minutes by 4min (-10.8±7.0%) and 5min (-10.1±7.2%) before syncope respectively. Conversely BP_{MCA} was only different 1 minute before and at syncope where BP_{MCA} was reduced by -8.0±6.0% and -35.1±11.8% respectively.

Three separate indicators of cerebrovascular resistance were examined over the final 15 minutes before syncope for the pre-HDBR tests (Figure 4.3). CVRi progressively increased and was statistically increased from minute 15 in the last minute before syncope with a sharp decrease to the end test value that was not statistically different from minute 15. Both RAP and PI were not significantly different until the last point of the test where there was a reduction in RAP, but a dramatic increase in PI.

Linear regression analysis results are presented in Table 4.1. Pre-HDBR, significant relationships were found between CBFV and BP_{MCA} for only 4 of 12 people, while the relationship between CBFV and $P_{ET}CO_2$ was significant in 10 of 12 people. This is in contrast to the last two minutes of the test where only 3 of 12 people had significant relationships between CBFV and $P_{ET}CO_2$ whereas 9 of 12 had CBFV significantly related to the change in BP_{MCA}.

Table 4.1: Correlation coefficients for the linear regression assessing the relationship between BP_{MCA} and $P_{ET}CO_2$ with CBFV, CrCP, and RAP during the last 15 minutes before syncope

	Time = 15 to 2 minutes		Time = 2 to 0 minutes	
	BP_{MCA}	$P_{ET}CO_2$	BP_{MCA}	$P_{ET}CO_2$
CBFV	0.566±0.137 (4)	0.688±0.169 (10)	0.881±0.075 (9)	0.855±0.076 (3)
CrCP	0.525±0.106 (4)	0.631±0.196 (7)	0.926±0.053 (2)	0.783±0.052 (2)
RAP	0.653±0.141 (9)	0.662±0.171 (6)	0.913±0.091 (8)	0.802±0.110 (3)

Values are the Pearson product moment correlation (mean ± SD) for the individuals showing significant relationships. The number of individuals out of 12 with significant relationship is presented in parentheses.

A visual display of the interrelationships between $P_{ET}CO_2$, BP_{MCA}, CrCP, and RAP is shown in Figure 4.4 for pre-HDBR tests (note the inverted scale for CrCP). Linear regressions were performed on data pairs for these variables between 15 and 2 minutes before syncope for each individual. RAP-BP_{MCA} was significant for 9 of 12 people whereas CrCP-BP_{MCA} was significant for only 4 of 12 people (Table 4.1). RAP-$P_{ET}CO_2$ was significant for 6 of 12 people and the relationship between CrCP-$P_{ET}CO_2$ was significant for 7 of the 12 subjects (Table 4.1). During the last two minutes of the test only RAP-BP_{MCA} was significant in 8 of 12 people (Table 4.1).

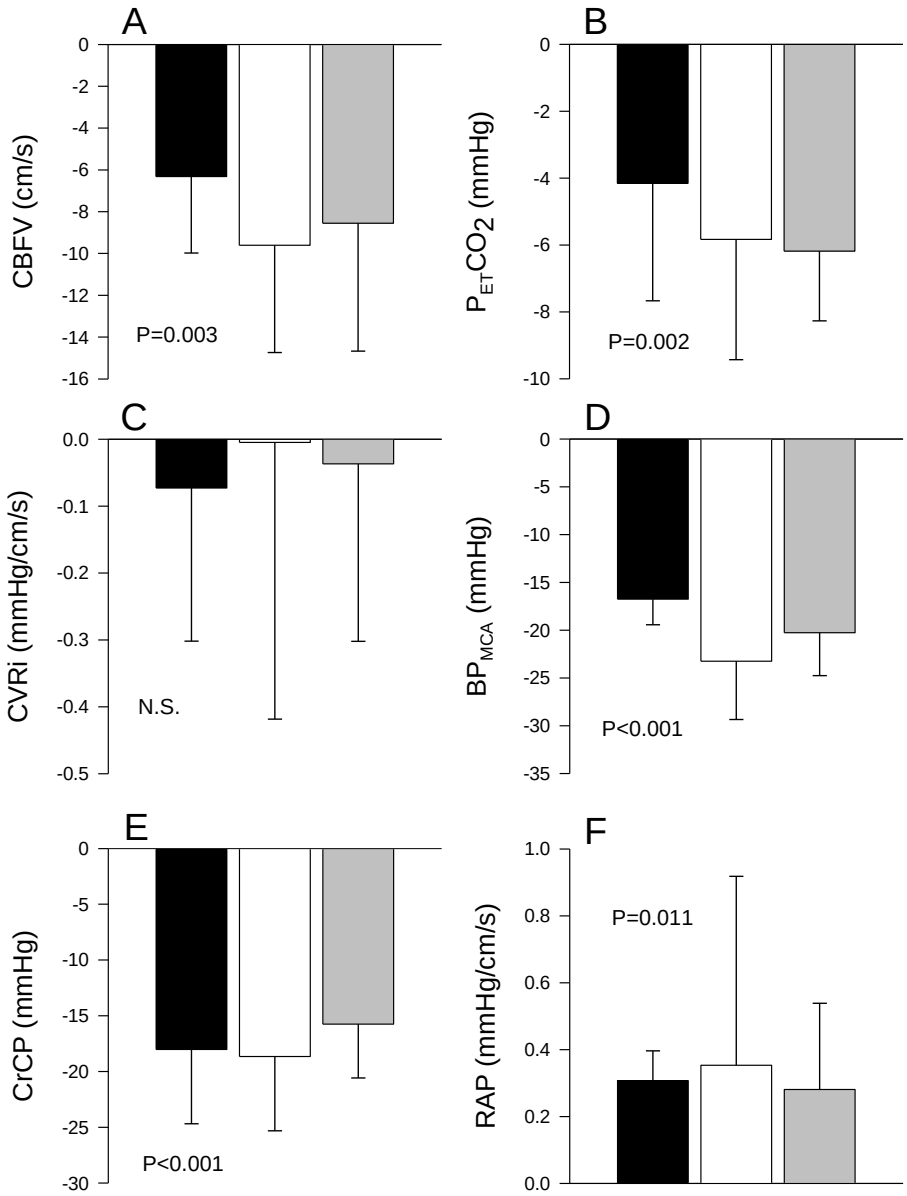

Figure 4.1:Delta tilt responses

The early tilt responses are shown as the difference from a five minute average taken during supine rest and a five minute average of minute six to ten of the tilt for individuals who completed greater than 5 minutes of tilt in both the CON and AG conditions (n=7): pre-HDBR (black bars), post-HDBR control (white bars), and post-HDBR artificial gravity (grey bars). Values are mean ± SD. No statistically significant differences were found between the conditions. P values indicate differences from supine rest for each variable.

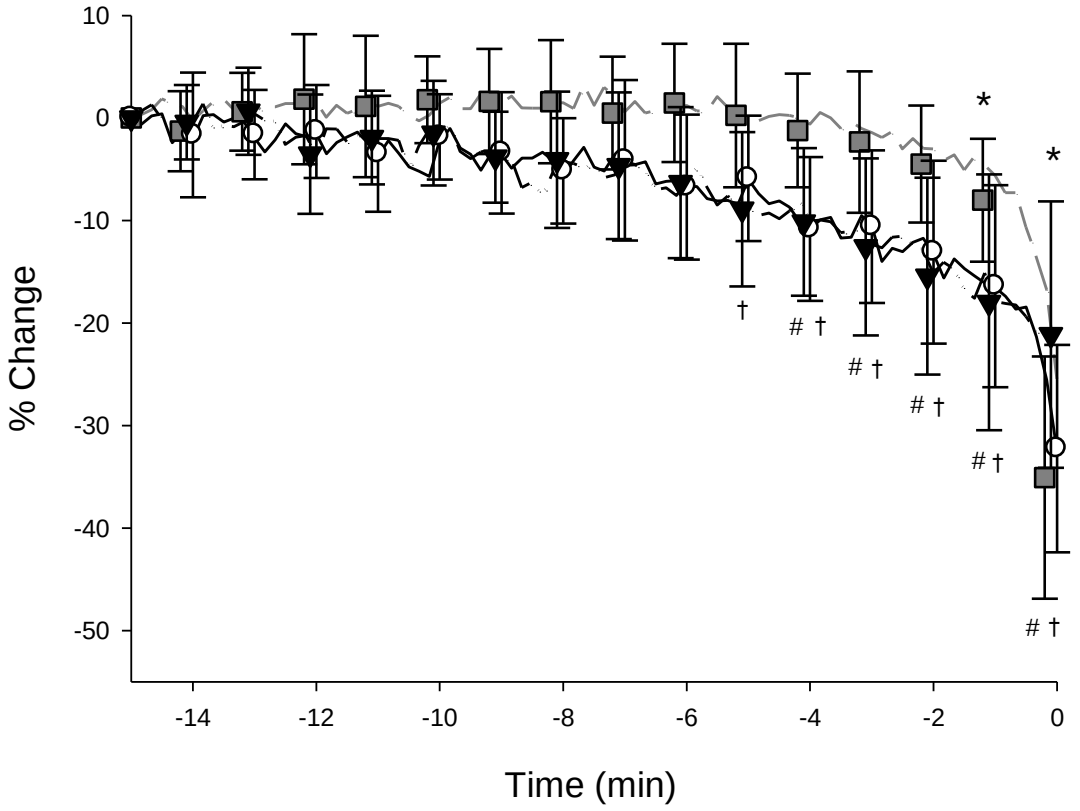

Figure 4.2: Percent change CBFV, $P_{ET}CO_2$, and BP_{MCA}

*The percent change in CBFV (solid line, ○), BP_{MCA} (dashed grey line, ■), and $P_{ET}CO_2$ (dash-dotted line, ▼) over the last 15 minutes of the tilt test (presyncope at t=0) for pre-HDBR (n=12). Points on the line show mean values ± SD, with values that are significantly different from 15 minutes before syncope denoted by * for BP_{MCA}, # for CBFV, and † for $P_{ET}CO_2$ (P<0.05).*

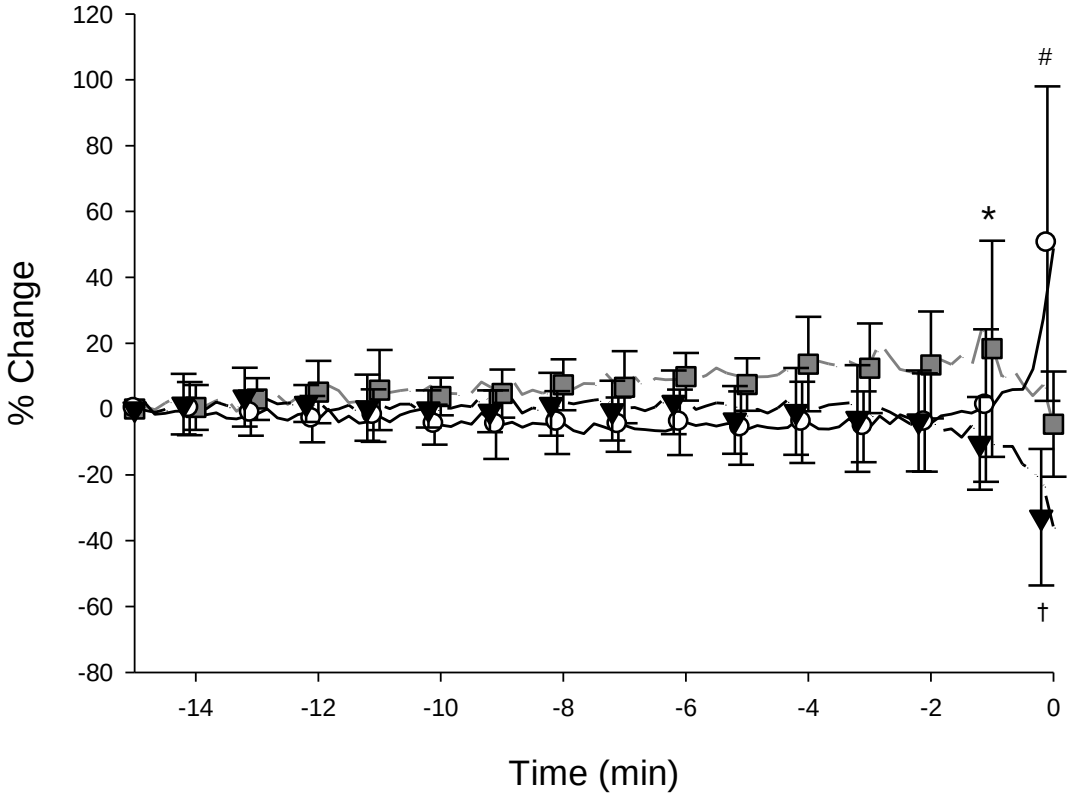

Figure 4.3: Percent change CVRi, RAP, and PI

*Three cerebrovascular resistance indicators are shown as percent change in CVRi (dashed grey line, ■), PI (solid line, ○), and RAP (dashed-dotted line, ▼) over the last 15 minutes of the tilt test (presyncope at t=0) for pre-HDBR (n=12). Points on the line are mean values ± SD, with points significantly different from 15 minutes before syncope denoted by * for CVRi, # for PI and † for RAP (P<0.05).*

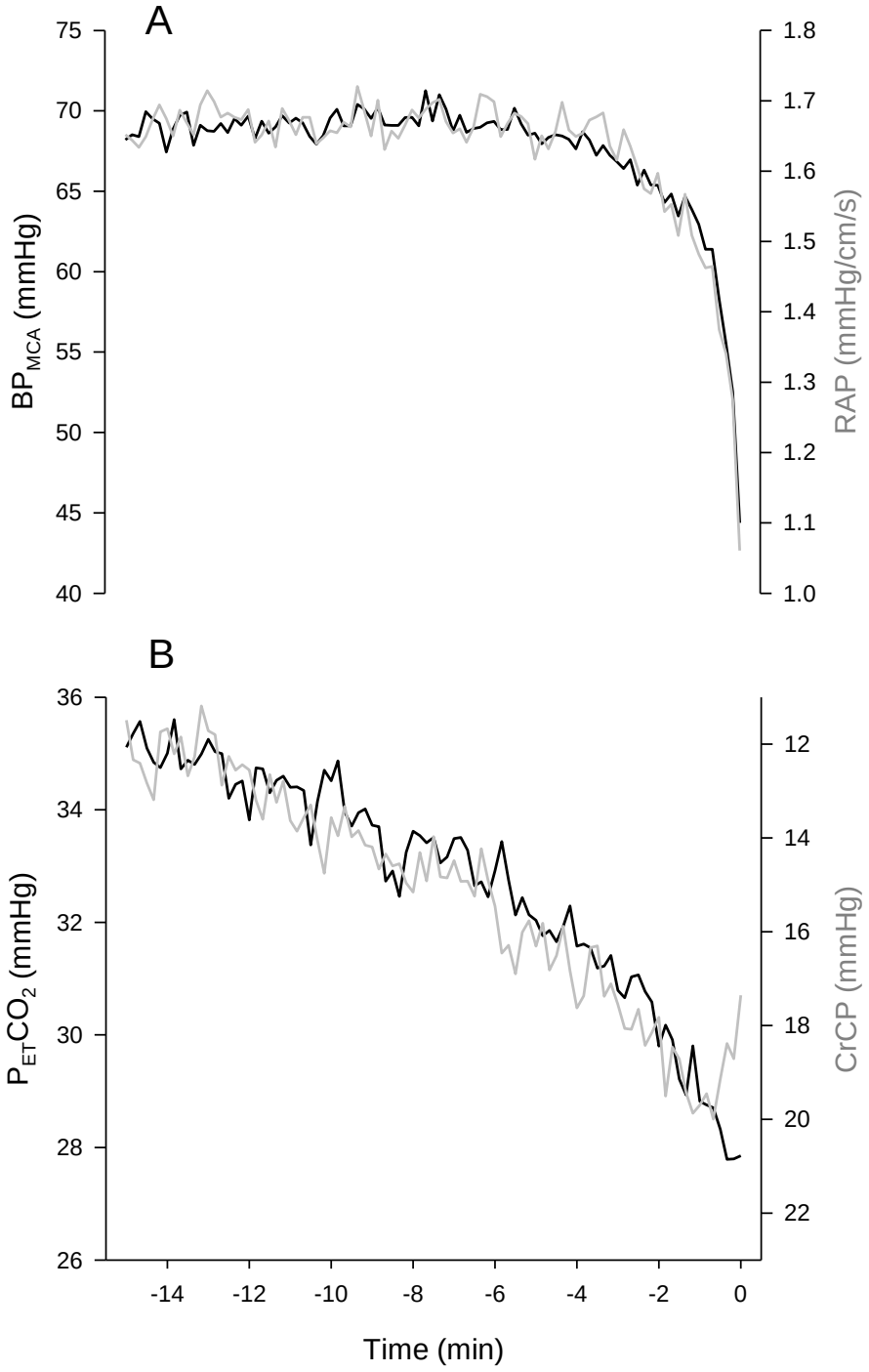

Figure 4.4: Progressions of BP_{MCA}, RAP, $P_{ET}CO_2$, and CrCP

Interrelationships between variables for the last 15 minutes of the tilt tests for pre-HDBR (n=12). A. BP_{MCA} (black line) and RAP (grey line); B. $P_{ET}CO_2$ (black line) and CrCP (note the inverted scale).

4.5 Discussion

This study provided an in depth look at cerebrovascular responses during the final 15 minutes of an orthostatic challenge resulting in presyncopal symptoms. In support of the first hypothesis, it was observed that while BP_{MCA} was unchanged until the final minute before syncope, CBFV and $P_{ET}CO_2$ were significantly reduced earlier with 10 of 12 individuals having significant linear relationships between these variables. These findings are consistent with some previous research (Cencetti et al., 1997; Carey et al., 2001; LeLorier et al., 2003) but challenge the suggestion based on examination of the early phase of head-up tilt (Serrador et al., 2006) and standing (Immink et al., 2006) that changes in CBFV are independent of $P_{ET}CO_2$. The results of the current study also supported the second hypothesis revealing an increase in CrCP that was linearly related to the reduction in $P_{ET}CO_2$ suggesting a progressive increase in cerebrovascular tone that was coupled to the reduction in CBFV. In contrast, RAP, an indicator of cerebrovascular resistance, was unchanged until there was a large drop in BP_{MCA} just prior to syncope. After HDBR, there were no differences in the cerebrovascular responses compared to pre-HDBR; but, 7 of 12 in the CON condition and 2 of 12 in the AG condition experienced presyncopal symptoms in the first 10 minutes of tilt after HDBR. Potential benefits of the artificial gravity countermeasure were not observed with respect to the indicators of cerebrovascular function during tilt.

4.5.1 Early Tilt Cerebrovascular Responses

The early responses to tilt were assessed by comparing supine resting values of cerebrovascular variables to an average taken between minutes 5 and 10 after tilt. Responses were consistent with other research observing reductions in BP_{MCA}, CBFV, and $P_{ET}CO_2$ after the transition to an upright posture (Immink et al., 2006; O'Leary et al., 2007; Cencetti et al., 1997; Serrador et al., 2006). The absence of significant change in CVRi or PI was somewhat unexpected as BP_{MCA} was reduced by ~20mmHg and autoregulatory processes were expected to reduce cerebrovascular resistance to maintain CBFV; however, the reduction in $P_{ET}CO_2$ would have an opposite effect on cerebrovascular resistance as detected by an increase in RAP. The reduction in $P_{ET}CO_2$ would also be expected to increase CrCP (Carey

et al., 2001), but a large decrease in CrCP occurred with the reduction in BP_{MCA} during tilt potentially reducing vascular tone and minimizing the decrease in CBFV.

The observed increase in RAP and large reduction in CrCP in the current study during 80° head-up tilt contrast with a recent report of no change in RAP and smaller changes in CrCP during an incremental tilt study up to 75° (Stewart et al., 2012). It might be that vascular tone (CrCP) and RAP contributed differently to cerebrovascular regulation with 80° head-up tilt compared to incremental tilt to 75°. However, the differences in calculation method for CrCP and RAP, with the two point method involving the mean and diastolic values in the current study as opposed to the linear regression method (Stewart et al., 2012), which has the potential for producing negative values for CrCP (Panerai et al., 2011), could account for these findings.

4.5.2 Sustained Tilt Cerebrovascular Responses

Over the final 15 minutes of the tilt before syncope, BP_{MCA} was well maintained until the last minute. In contrast, $P_{ET}CO_2$ and CBFV were reduced 5 and 4 minutes before syncope respectively. We utilized the two regions based on unchanged versus changed BP_{MCA} to further investigate relationships between variables. One set of regressions was computed for the period of constant BP_{MCA} (15 to 2 minutes before syncope), the second set when BP_{MCA} was changing (last two minutes of the test). These analyses confirmed distinct regions over which changes in $P_{ET}CO_2$ or BP_{MCA} were related to alterations in cerebral hemodynamics. From 15 to 2 minutes before syncope, the reduction in CBFV was primarily related to the decline in $P_{ET}CO_2$, while in the final two minutes before syncope, the reduction in CBFV was associated with the decrease in BP_{MCA}.

Changes in BP_{MCA} and $P_{ET}CO_2$ potentially impact CBFV through changes in vascular resistance and vascular tone. Three indications of cerebrovascular resistance, CVRi, RAP, and PI, were calculated in the current study. Through most of the final 15 minutes of tilt the resistance indicators were relatively stable but then presented slightly different patterns with the progression towards syncope. Previous studies, primarily looking at CVRi responses, have observed paradoxical increases in cerebrovascular resistance before syncope (Serrador

et al., 2006; Bondar et al., 1995; Levine, Giller, Lane, Buckey, & Blomqvist, 1994) with explanations including sympathetic nervous system mediated mechanisms (Bondar et al., 1995; Serrador et al., 2006) and changes in arterial CO_2 (Serrador et al., 2006; Blaber, Bondar, Moradshahi, Serrador, & Hughson, 2001). CVRi was increased only at 1 minute before syncope then decreased at syncope. However, the use of CVRi as an indicator of cerebrovascular resistance is dependent on CBFV being proportional to cerebral blood flow which may not be the case if the diameter of the insonated vessel is changing. Its calculation is also dependent on the assumption that the pressure gradient is referenced to 0 mmHg venous pressure. Therefore, two other independent indicators of vascular resistance were also assessed. With respect to the Doppler resistance index PI, it would appear that it is likely that values are only representative of cerebrovascular resistance until the last minute of the test where there is a marked reduction in arterial pressure and a large increase in PI. Conversely, the profile of RAP was consistent with what would be expected with functioning cerebrovascular autoregulation, in that there was only a marked reduction in resistance when arterial pressure was dropping, but this was independent of the impact of PCO_2. This profile of RAP decreasing in the final minute before syncope is similar to the pattern described by Carey et al. (Carey et al., 2001).

The indication of cerebrovascular tone derived from the CrCP increased progressively over the final 15 minutes prior to syncope in direct proportion to the reduction in $P_{ET}CO_2$. Although the direction of change was similar to that described by Carey et al. (Carey et al., 2001), the timing and potential functional consequences were different as the data of Carey et al. (Carey et al., 2001) showed increases in CrCP only in the final 60 seconds of the test. Conversely, in the current study the progressive increase in CrCP was followed in the final minute before syncope by a reduction (see Figure 4.4 B, noting the inverted scale for CrCP). The increase in CrCP was associated with the reduction in $P_{ET}CO_2$ whereas the final decrease in CrCP was associated with the rapid decline of BP_{MCA}, and is consistent with the reduction in CrCP noted in the early phase of the tilt of the current experiment when BP_{MCA} was reduced from the supine baseline. Previous work has shown increases in CrCP with reductions in CO_2 (Panerai et al., 1999; Panerai, 2003; Ainslie et al., 2008); however this

study is the first to suggest that over the last 15 minutes before syncope increased cerebrovascular tone was associated with a reduction in $P_{ET}CO_2$ which could contribute to reduced cerebral blood flow. The significance of the increase in CrCP with the approach of syncope is that there is a simultaneous reduction in diastolic blood pressure so that the closure of cerebral vessels could occur through part of the cardiac cycle reducing CBFV (Carey et al., 2001).

4.5.3 Effects of HDBR and the Artificial Gravity Countermeasure

Contrary to the hypothesis that CBFV would show greater reductions post-HDBR, there were no differences in the early phase tilt responses compared to pre-HDBR for either CON or AG conditions. However, four of the individuals who were unable to complete 5 minutes of tilt post-HDBR were excluded from the analysis. It is possible that these individuals did have impaired cerebral blood flow regulation post-HDBR, but it is unclear from the current analysis. Of the remaining subjects, tilt tolerance was reduced and analysis of relationships between variables was compromised due to the short data sets. For the individuals who sustained tilt for relatively longer periods of time post-HDBR, it would appear that changes in BP_{MCA} dominated the responses potentially suggesting that cerebrovascular autoregulation was overriding any PCO_2 effects with the shorter duration of tilt.

4.5.4 Limitations

In the current, study $P_{ET}CO_2$ was measured as a surrogate for $PaCO_2$ with the progression towards syncope. The relationship between $P_{ET}CO_2$ is altered during postural transitions, but it is unknown if the relationship then remains constant with sustained orthostasis (Immink et al., 2006; Serrador et al., 2006) since further changes in the ventilation perfusion ratio could occur as cardiac output is reduced with prolonged tilt (Guinet et al., 2009).

The use of transcranial Doppler ultrasound for the assessment of cerebral blood flow is dependent on the diameter of the insonated vessel remaining constant. Studies have shown that the diameter of the middle cerebral artery remains constant with changes in $P_{ET}CO_2$ and

the application of a mild orthostatic stress (Giller et al., 1993; Serrador et al., 2000). However, it is possible that prolonged orthostatic stress and reduced PCO_2 could have reduced the MCA diameter so that measures of CBFV might underestimate the decrease in cerebral blood flow. The MCA diameter and cerebrovascular properties might also change with HDBR as seen in animal models of hindlimb suspension (Wilkerson et al., 1999; Lin et al., 2009), but this seems unlikely with 5 days of HDBR in humans. Regardless, these issues raise a need for caution in interpreting the observed changes in CBFV as alterations in cerebral blood flow.

4.6 Conclusion

This study examined the cerebrovascular responses to head up tilt with particular emphasis on the contributions of changes in arterial blood pressure and $P_{ET}CO_2$ both before and after exposure to five days of HDBR with and without an artificial gravity countermeasure. Analysis of data showed that the reductions in CBFV were strongly correlated to decreases in $P_{ET}CO_2$ during the period from 15 to 2 minutes before the onset of syncope. The mechanism underlying the decrease in CBFV appeared to be related to a progressive increase in CrCP as indicators of cerebrovascular resistance obtained from CVRi, RAP and Doppler PI were unchanged over that similar period. In the final two minutes prior to syncope, RAP was the only cerebrovascular resistance indicator that reflected the anticipated decline in cerebrovascular resistance that occurred as BP_{MCA} was reduced. These results suggested that the progressive reduction in $P_{ET}CO_2$ with sustained orthostatic challenge reduced CBFV through an increase in cerebrovascular tone assessed by CrCP, and that RAP provides a valuable index of cerebrovascular resistance changes to counter the effects of changes in BP_{MCA}. The increase in cerebrovascular tone rather than an increase in resistance contributed to the reduction in cerebral blood flow and eventual development of syncope.

Chapter 5

Middle cerebral and temporal artery Doppler spectrum morphology changes with orthostasis before and after five days head down bed rest

5.1 Overview

A marked reduction in orthostatic tolerance has been noted with exposure head down bed rest (HDBR). As syncope from prolonged orthostasis ultimately results from cerebral hypoperfusion, examining cerebrovascular responses to tilt and the progression towards syncope may provide additional indications about the mechanisms involved in the reduction in orthostatic tolerance. Therefore, the purpose of this study was to assess cerebrovascular responses to tilt before and after HDBR with respect to potential changes in middle cerebral and temporal artery blood velocity traces with the progression towards syncope and indices of dynamic cerebrovascular autoregulation. Data for this study were collected from 12 men who completed an orthostatic tolerance test consisting of head up tilt and progressive lower body negative pressure before and after 5 days of HDBR with and without an artificial gravity countermeasure. Doppler ultrasound was used to assess middle cerebral artery (CBFV) and temporal artery blood velocity (V_{TEMP}) with the velocity traces assessed for the appearance of a negative component in the V_{TEMP} trace and the difference between the dicrotic notch and end diastolic values of CBFV. During supine rest indices of dynamic cerebrovascular autoregulation were determined using cross-spectral analysis for the input variable of arterial pressure and the output of CBFV and cerebrovascular resistance (CVRi). With tilt, V_{TEMP} and CBFV decreased with no change in CVRi but an increase in temporal artery vascular resistance with no differences after HDBR. Both pre- and post-HDBR, within five minutes before syncope, a negative component of V_{TEMP} appeared and the dicrotic notch point of the CBFV trace became less than the end diastolic value. No differences in dynamic cerebrovascular autoregulation were found with HDBR and values were not related to V_{TEMP} or CBFV wave morphology. The minimum values of V_{TEMP} was found to be related to vascular resistance, where the change in CBFV was not as strongly related to CVRi suggesting the potential contribution of other variables including changes in cerebrovascular tone.

5.2 Introduction

In the assessment of blood flow, analysis of Doppler spectrum morphology may provide additional information about changes in cerebrovascular hemodynamics. Analysis of Doppler spectrum morphology could also be useful in the identification of potential indicators of approaching syncope which would assist in assessment in both clinical and research settings. Assessing orthostatic tolerance requires the use of tolerance tests in which an individual is subjected to orthostatic stress and tolerance quantified based on the duration and magnitude of exposure withstood by the subject. It has also been noted that cardiovascular changes during orthostasis mimic those of hemorrhage (Cooke, Ryan, & Convertino, 2004). Recently we have published work demonstrating changes in temporal artery Doppler spectrum morphology with the progression towards syncope (Arbeille, Zuj, Shoemaker, & Hughson, 2012). In this paper, it was found that in two thirds of cases, the temporal artery Doppler spectrum showed a change in morphology in which a negative component appeared and allowed for the early detection of approaching syncope. The purpose of the following paper was to further characterize changes in temporal artery Doppler spectrum morphology with the progression towards syncope both before and after exposure to five days of head down bed rest with and without an artificial gravity countermeasure. The second purpose of this study was to characterize changes in cerebral blood velocity Doppler spectrum morphology with relation to changes in the temporal artery Doppler spectrum morphology and indications of dynamic cerebrovascular autoregulation.

Exposure to real or simulated microgravity has been shown to be associated with cardiovascular deconditioning reduced orthostatic tolerance (Arbeille et al., 2008; Buckey et al., 1996; Zhang et al., 1997). Some studies have suggested that this change in orthostatic tolerance could be related to reductions in dynamic cerebrovascular autoregulation (Zhang et al., 1997; Blaber et al., 2011; Zuj et al., 2012a), where other work has suggested the contribution of impaired peripheral vasoconstriction responses (Buckey et al., 1996; Arbeille et al., 2008). To date, no studies have looked at alterations in middle cerebral or temporal artery Doppler waveform morphology with exposure to real or simulated microgravity, or how these variables might relate to changes in orthostatic tolerance.

As syncope is ultimately the result of cerebral hypoperfusion, changes in the middle cerebral artery blood velocity waveform may be indicative of approaching syncope. In 2004, Albina et al. (Albina et al., 2004) published a paper in which the qualitative assessment of transcranial Doppler (TCD) waveforms during tilt testing. The results of this paper found that patients with a history of neurocardiogenic syncope consistently showed a deepening of the dicrotic notch in the Doppler waveform. However, no attempt was made to quantify this change, determine if it occurred at a consistent point before the onset of syncope, or relate this qualitative observation to quantitative assessments of cerebrovascular properties.

In the current paper, it was hypothesized that, similar to previously reported results (Arbeille et al., 2012), a negative component of the temporal artery Doppler velocity trace would appear approximately five minutes before the onset of syncope. It was also hypothesized that this change would be associated with a reduction in the dicrotic notch portion of the middle cerebral artery blood velocity trace. After exposure to five days of simulated microgravity, it was hypothesised that there would be a reduction in orthostatic tolerance associated with impaired dynamic cerebrovascular autoregulation. With respect to Doppler waveform morphology, it was hypothesized that the appearance of the negative component would appear closer to syncope in those individuals with reduced orthostatic tolerance, indicating an impairment of peripheral vasoconstriction during orthostasis. Conversely, it was also hypothesized that the alterations in the middle cerebral artery blood velocity trace would occur earlier in the orthostatic tolerance test and be associated with a greater reduction in cerebral blood flow velocity and impaired cerebrovascular autoregulation.

5.3 Methods

Data for this study were collected as part of the same experiment described in Chapter 4. Therefore the experimental protocol is as previously described with data analysis as follows.

5.3.1 Vascular Measures

Transcranial Doppler ultrasound (TCD) was used for the assessment of cerebral blood flow velocity (CBFV). A 2MHz pulsed Doppler probe was placed over the right temporal window which allowed for the insonation of the right middle cerebral artery (MCA). A head band was used to hold the probe in place throughout the testing. On the left side of the head, an 8MHz pulsed Doppler probe was attached to the TCD head set which allowed for the assessment of blood velocity in the temporal artery (V_{TEMP}). Supplying extracranial tissues, the temporal artery is a branch of the facial artery that originates from the external carotid artery. Approximately 1cm above the mandible, anterior to the ear, the Doppler probe was oriented to maximize the V_{TEMP} signal amplitude. Doppler signals were conducted using CardioLab hardware (CNES – European Space Agency device, France) and were recorded at 100Hz using CardioMed software (CNES - European Space Agency, France).

For MCA and temporal artery Doppler recordings, mean velocity values (CBFV and V_{TEMP} respectively) were calculated as the mean of the outer envelope of the Doppler spectrum over a cardiac cycle. For each of the Doppler recordings, maximum (systolic) and minimum (diastolic) values were determined for each cardiac cycle. In addition to the minimum value, the end diastolic value of the MCA trace was also determined. Vascular resistance was calculated as $TEMP_{VR} = MAP_{TEMP} / V_{TEMP}$ and $CVRi = MAP_{MCA} / CBFV$ for the temporal artery and MCA respectively where MAP_{TEMP} and MAP_{MCA} represent the mean arterial pressure height corrected to the levels of the temporal artery and MCA. The ratio of mean velocity values ($CBFV / V_{TEMP}$) was used as a method of assessing the redistribution of cardiac output (Arbeille et al., 1998; Arbeille et al., 2008).

5.3.2 Data Analysis

This study reports on data from the control condition and one artificial gravity condition; however, the original study design included two artificial gravity countermeasure protocols and, therefore, pre-HDBR data were collected for each subject three times. Previous work has demonstrated good reproducibility of tilt responses (LeLorier et al., 2003) and statistical analysis of this data (not shown) showed no differences between the pre-

HDBR responses; therefore, for analysis purposes, pre-HDBR was considered as the average of all pre-HDBR data collections.

Variables were assessed beat-by-beat and then averaged for every minute during the test. To assess the responses to tilt averages were taken over the first five minutes of the test (Supine) and minutes 6-10 of the tilt (Tilt). For some test, participants were unable to remain standing for 10 minutes of tilt. For these individuals, the tilt value was taken as the average from minute 5 to a point before the last two minutes of the test.

Beat-by-beat data was also averaged every 10s of the test and used to assess timing of changes in hemodynamic variables with the progression towards syncope. This data was analyzed to determine the time point before presyncope where the temporal velocity trace showed a negative component and the point where the dicrotic notch of the MCA velocity wave was less than the end diastolic value with examples of these wave changes being shown in Figure 5.1. The time point for V_{TEMP} was determined as the point in the V_{TEMP} minimum data where three consecutive 10s averages showed values less than (more negative) -0.5cm/s and was not followed by a section of three or more 10s averages greater than -0.5cm/s. Similar criteria was used for determining the time point for CBFV with the point where the difference between CBFV minimum and CBFV end diastole (CBFVmin-dia) was greater than 0.75cm/s for three consecutive 10s averages and was not followed by 3 or more 10s averages with differences less than 0.75cm/s. The values of -0.25cm/s and 0.75cm/s were arbitrarily chosen to eliminate potential variations in data due to signal noise.

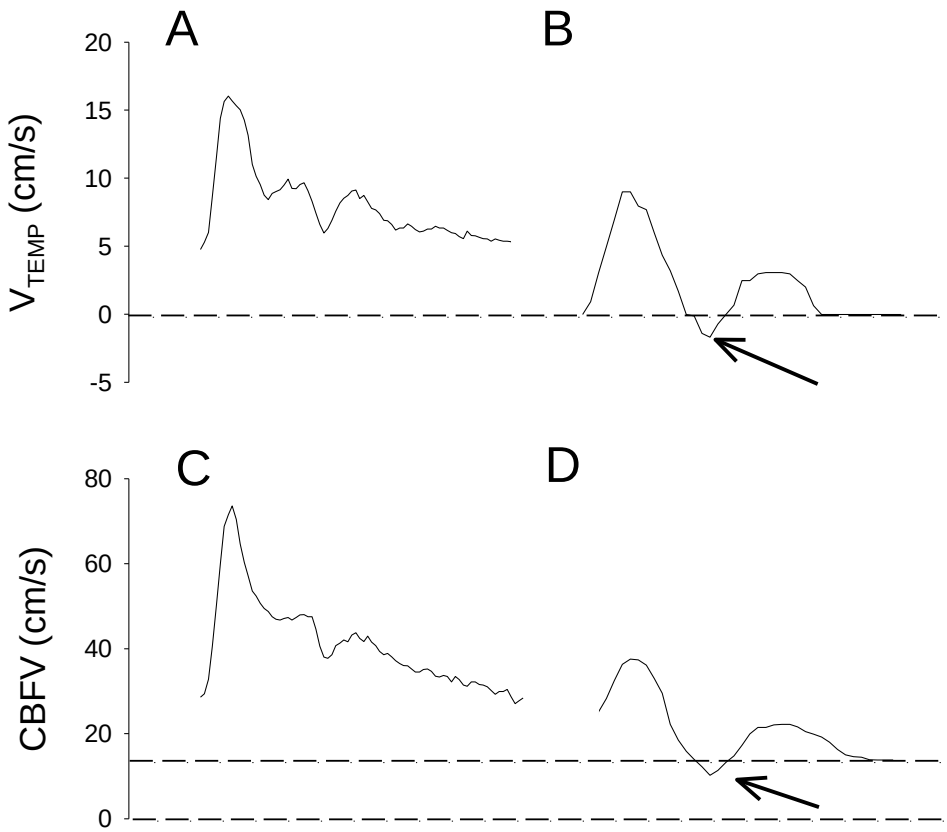

Figure 5.1: Representative temporal artery and MCA velocity waves

Figure shows tracings at rest (A and C) and near syncope (B and D). Both waves show similar morphological changes; however the temporal artery shows a negative component where the MCA is consistently positive with the dicrotic notch less than the end diastolic value.

Dynamic cerebrovascular autoregulation was assessed during the first five minutes of the test while participants rested in the supine position. For this analysis a transfer function method was used similar to previously reported (Edwards et al., 2002). Data for the five minutes of supine rest were assessed beat-by-beat then re-sampled at a frequency of 1Hz using linear interpolation. Linear trends were removed and cross-spectral analysis was performed for the input variable of MAP and the output of either CBFV or CVRi using Welch's method (Matlab, Math Works, USA). Transfer function gain, coherence, and phase

were determined in three frequency regions; very low frequency (VLF: 0.03-0.07 Hz), low frequency (LF: 0.07-0.2 Hz), and high frequency (HF: 0.2-0.3 Hz).

5.3.3 Statistical Analysis

Mean velocity, vascular resistance, and the velocity ratio were all assessed using a two way repeated measure analysis of variance (SigmaStat 3.5, Systat Software Inc., Chicago, IL). Alterations in the timing of the appearance of the temporal artery negative velocity and potential changes in the timing point where the dicrotic notch was less than the end diastolic velocity value of the MCA velocity trace were assessed using a one way repeated measures analysis of variance (SigmaStat 3.5, Systat Software Inc., Chicago, IL). V_{TEMP} minimum and CBFVmin-dia were tested for potential relationships with arterial pressure, cardiac stroke volume, and vascular resistance using linear regression. Unless otherwise stated, all values show mean ± standard deviation. For all statistical analysis, significance was set at $p<0.05$.

5.4 Results

Analysis of the velocity, resistance, and ratio responses to tilt showed that with tilt (average of minutes 6-10) there were significant reductions in CBFV (Figure 5.2 A) and V_{TEMP} (Figure 5.2 B) with no changes in CVRi (Figure 5.2 C) and a significant increase in $TEMP_{VR}$ (Figure 5.2 D). The ratio of CBFV to V_{TEMP} (Figure 5.2 E) was also significantly increased with tilt, indicating that although there were reductions in both CBFV and V_{TEMP}, there was a greater reduction in V_{TEMP}. No differences were seen between pre-HDBR responses and post-HDBR for either the CON or AG condition.

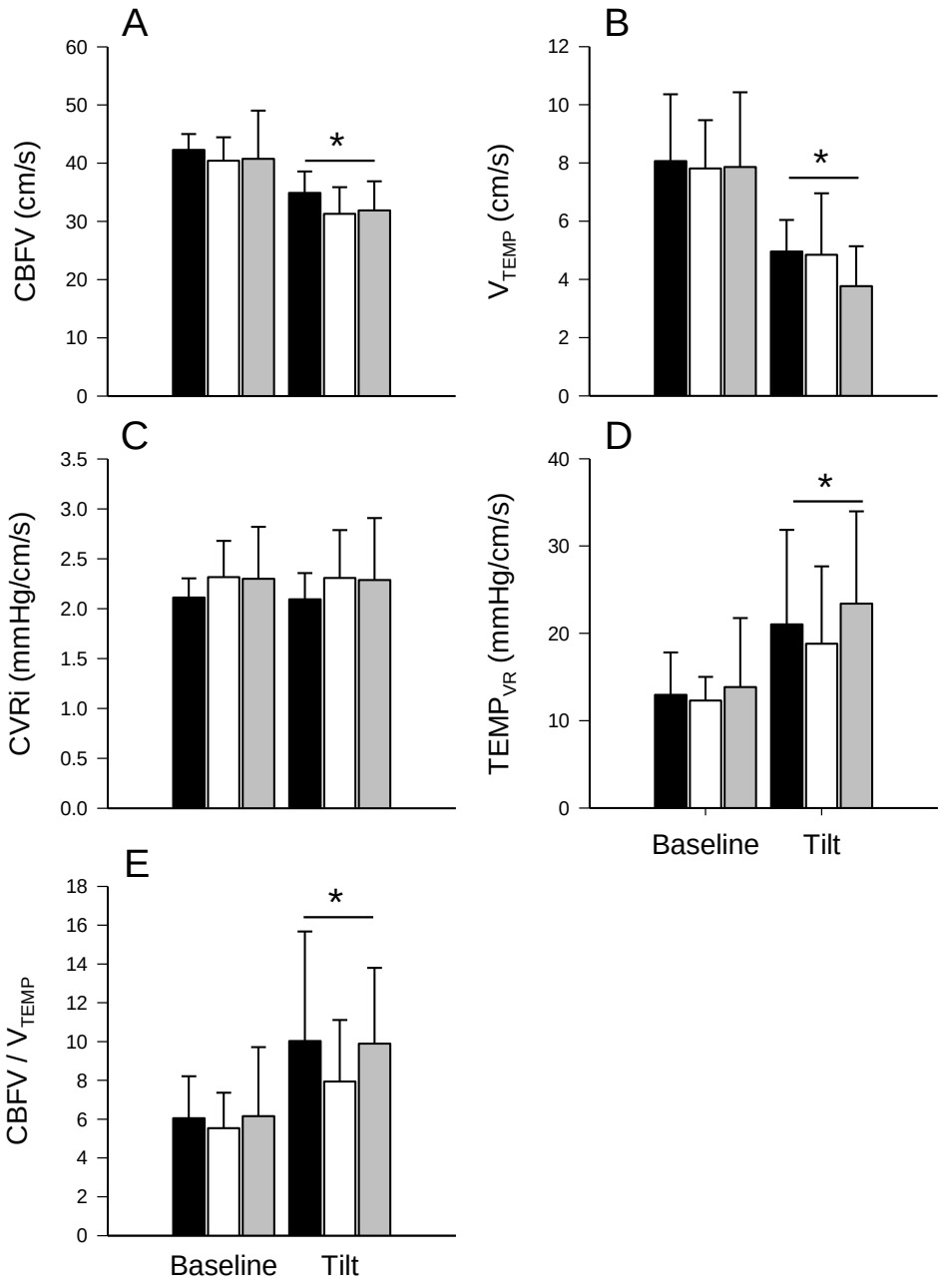

Figure 5.2: Responses to tilt

*Results (mean ± SD) for CBFV (A), V_{TEMP} (B), CVRi (C), $TEMP_{VR}$ (D), the ratio between CBFV and V_{TEMP} (E) at supine rest (baseline) and minutes 6-10 of the tilt (tilt) for pre HDBR (black bars), CON (white bars), and AG (grey bars) (n=7). Differences from supine values are denoted by * at $p<0.05$. No effects of HDBR were seen for any of the variables.*

Assessment of dynamic cerebrovascular autoregulation was conducted during the five minutes of supine rest before tilt. Results from this analysis, presented in Table 5.1 showed no effects of HDBR. Further analysis was conducted with respect to the CON condition. In this case, individuals were grouped based on those who were able to complete 10 minutes of tilt (tolerant) and those unable to complete 10 minutes of tilt (non-tolerant). Pre HDBR, all subjects were able to complete 10 minutes of tilt. Post HDBR in the CON condition, only five of the 12 subjects were able to complete more than 10 minutes of tilt. Data from these two groups are also presented in Table 5.1. Analysis showed no differences in pre HDBR versus post HDBR dynamic cerebrovascular autoregulation variables for either the tolerant or intolerant individuals.

On average, the negative component of temporal negative velocity occurred 7.17±8.84 (n=12) minutes before the onset of presyncope. Post-HDBR the negative component appeared 9.85±13.67 (n=11) and 8.14±12.95 (n=7) minutes before presyncope for CON and AG respectively with no difference being seen between pre-HDBR, CON, and AG ($p>0.05$). However, it should be noted that these values included data from three subjects who showed negative velocity much earlier than 10 minutes before presyncope. When data from these individuals were excluded from the analysis, the negative component of V_{TEMP} appeared 1.93±1.75 (n=8), 3.21±2.93 (n=7), and 3.53±4.74 (n=6) minutes before presyncope for pre-HDBR, CON, and AG respectively with no differences between pre-HDBR, CON, and AG.

Assessment of the difference between the dicrotic notch of the MCA velocity trace and the end diastolic values showed that with the progression towards syncope, the dicrotic notch became lower than the end diastolic value in 11 of 12 individuals. For these 11 individuals, the MCA velocity wave dicrotic notch became less than the end diastolic value on average 5.7±4.2 minutes before presyncope pre-HDBR. Post-HDBR this wave profile was seen on average 5.8±6.2 minutes and 11.5±12.5 minutes for CON and AG respectively. It should be noted that in the AG condition this average included two individuals who showed the smaller dicrotic notch values at 21 and 36 minutes before presyncope. When these

individuals were removed from the average, it became 5.6±5.2 minutes before presyncope. No differences with HDBR were seen with these values.

Analysis of the 10s averages for the last 15 minutes of the test suggest a good agreement between the temporal artery diastolic velocity and temporal artery vascular resistance (Figure 5.3 A). The graph of the difference between the minimum MCA velocity and the end diastolic value showed values around 0 until the last five minutes of the test. At this point, the minimum value on the MCA velocity trace, corresponding to the dicrotic notch, was less than the end diastolic value. This value also appeared to be inversely related to CVRi (Figure 5.3 B) until the last minute of the test where the two signals diverged with a dramatic decrease in CVRi and the continual increase of CBFVmin-dia. (becoming more negative).

Table 5.1: Transfer function gain and phase for the MAP-->CBFV and MAP-->CVRi relationships

					Pre-HDBR		Post-HDBR	
		PRE	CON	AG	Tolerant	Non-tolerant	Tolerant	Non-tolerant
MAP→CBFV								
Gain	VLF	0.306±0.177$^{(9)}$	0.299±0.184$^{(9)}$	0.312±0.261$^{(9)}$	0.300±0.260$^{(4)}$	0.344±0.127$^{(6)}$	0.224±0.134$^{(4)}$	0.295±0.245$^{(6)}$
	LF	0.385±0.113$^{(10)}$	0.344±0.131$^{(10)}$	0.434±0.124$^{(10)}$	0.402±0.010$^{(5)}$	0.401±0.145$^{(6)}$	0.366±0.146$^{(5)}$	0.328±0.115$^{(6)}$
	HF	0.567±0.204$^{(11)}$	0.484±0.220$^{(11)}$	0.575±0.189$^{(11)}$	0.493±0.215$^{(5)}$	0.650±0.182$^{(7)}$	0.442±0.192$^{(5)}$	0.558±0.252$^{(7)}$
Phase	VLF	48.05±21.81$^{(9)}$	46.95±19.84$^{(9)}$	47.99±32.36$^{(9)}$	42.97±32.75$^{(4)}$	51.92±8.97$^{(6)}$	51.20±21.74$^{(4)}$	51.68±26.76$^{(6)}$
	LF	47.60±11.50$^{(10)}$	43.15±14.02$^{(10)}$	40.82±8.20$^{(10)}$	42.79±4.33$^{(5)}$	50.68±13.95$^{(6)}$	39.80±13.00$^{(5)}$	47.98±14.46$^{(6)}$
	HF	10.32±24.89$^{(11)}$	12.95±26.72$^{(11)}$	7.75±14.97$^{(11)}$	9.03±30.12$^{(5)}$	10.05±20.93$^{(7)}$	12.77±27.01$^{(5)}$	12.63±26.56$^{(7)}$
MAP→CVRi								
Gain	VLF	0.012±0.008$^{(6)}$	0.017±0.005$^{(6)}$	0.021±0.004$^{(6)}$	0.012±0.009$^{(5)}$	0.009±0.003$^{(4)}$	0.019±0.007$^{(5)}$	0.019±0.005$^{(4)}$
	LF	0.008±0.007$^{(11)}$	0.009±0.008$^{(11)}$	0.004±0.006$^{(11)}$	0.006±0.005$^{(5)}$	0.009±0.007$^{(7)}$	0.005±0.008$^{(5)}$	0.012±0.007$^{(7)}$
	HF	0.004±0.009$^{(5)}$	-0.001±0.015$^{(5)}$	-0.009±0.006$^{(5)}$	0.003±0.013$^{(5)}$	0.001±0.009$^{(4)}$	-0.001±0.014$^{(5)}$	0.007±0.005$^{(4)}$
Phase	VLF	-52.55±24.61$^{(6)}$	-38.69±14.58$^{(6)}$	-36.12±11.72$^{(6)}$	-50.88±26.31$^{(5)}$	-61.52±11.97$^{(4)}$	-42.39±14.12$^{(5)}$	-33.36±10.52$^{(4)}$
	LF	-67.07±16.29$^{(11)}$	-63.85±22.12$^{(11)}$	-78.50±14.95$^{(11)}$	-68.34±13.99$^{(5)}$	-66.01±17.59$^{(7)}$	-73.57±27.14$^{(5)}$	-57.21±13.97$^{(7)}$
	HF	-53.95±65.21$^{(5)}$	-74.77±98.60$^{(5)}$	-121.57±22.54$^{(5)}$	-55.91±67.73$^{(5)}$	-61.48±69.87$^{(4)}$	-71.12±85.71$^{(5)}$	-65.44±18.04$^{(4)}$

Values are means ± SD with number of observations in superscript parentheses. Values are calculated for pre-HDBR (PRE), post-HDBR without countermeasures (CON), and post-HDBR with the artificial gravity countermeasure (AG). Values for PRE and CON are further separated into those individuals who in the CON condition could complete 10 minutes of tilt pre-HDBR and post-HDBR (Tolerant) and those who completed 10 minutes of tilt pre-HDBR, but not post-HDBR (Non-tolerant). No significant differences were found for any value.

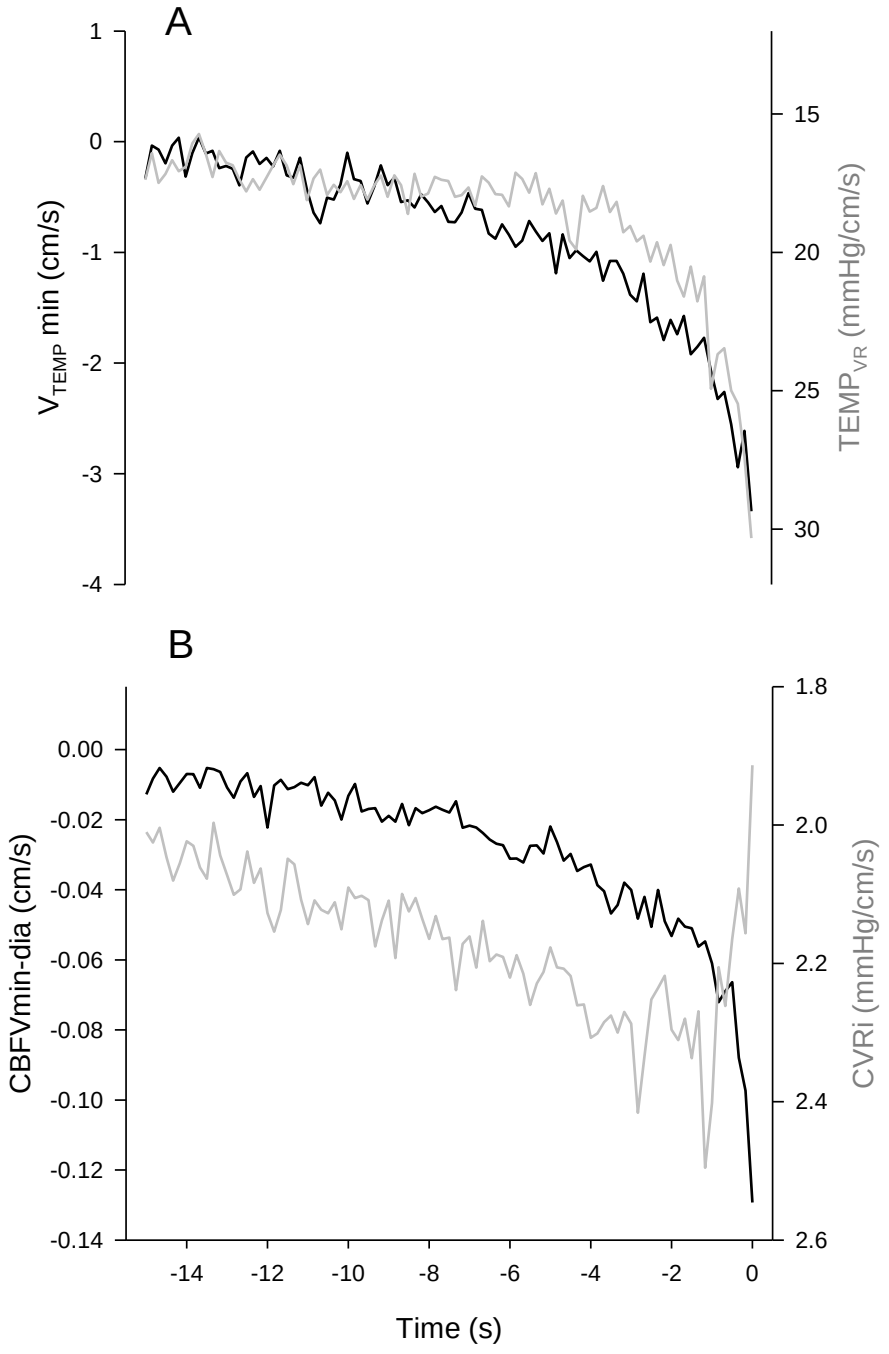

Figure 5.3: V_{TEMP} and CBFV in last 15 minutes

Graphs showing last 15 minutes of the tests for all subjects pre-HDBR, where syncope occurred at time 0 on the graph. Changes in V_{TEMP} minimum (A) and CBFVmin-dia (B) appeared to mirror those of $TEMP_{VR}$ CVRi (note the inverted scales of $TEMP_{VR}$ and CVRi).

Linear regressions analysis was done for each subject to further examine the changes in the minimum value of the temporal velocity trace and CBFVmin-dia. A summary of average results are presented in Table 5.2 with average R^2 values presented for subjects showing significant relationships ($P<0.001$). Briefly, regression analysis suggested that changes in the minimum V_{TEMP} values were related to alterations in vascular resistance ($TEMP_{VR}$), cardiac stroke volume (SV), and arterial pressure (BP_{MCA}). Similarly, the difference between the dicrotic notch and end diastole of CBFV showed significant relations to alterations in SV and BP_{MCA} with a weaker association with vascular resistance (CVRi).

Table 5.2: Correlation coefficients for linear regressions assessing the relationships of V_{TEMP} min and CBFVmin-dia with respect to BP_{MCA}, vascular resistance (VR), and cardiac stroke volume (SV)

	BP_{MCA}	VR	SV
V_{TEMP} min	0.436±0.164 (11)	0.435±0.186 (11)	0.505±0.224 (10)
CBFVmin-dia	0.481±0.210 (12)	0.316±0.164 (7)	0.542±0.287 (10)

Values are the Pearson product moment correlation squared (mean ± SD) with the number of individuals out of 12 with significant relationships in parentheses.

5.5 Discussion

This study provided the opportunity to examine morphological changes in the temporal artery and middle cerebral artery blood velocity wave profiles with the progression towards syncope and the comparison morphological changes to other measured hemodynamic variables both before and after exposure to five days of HDBR. The major finding of this study was that, in the majority of subjects, the Doppler spectrum morphology profiles of both the temporal artery and middle cerebral artery showed consistent alterations with the progression towards syncope with definitive changes occurring less than five minutes before the onset of syncope both before and after exposure to five days of continuous HDBR. Analysis also suggested that the alterations in the V_{TEMP} velocity profile

were associated with changes in vascular resistance and arterial pressure, where alterations in the CBFV velocity profile were associated with change in cardiac stroke volume and arterial pressure.

5.5.1 Doppler Spectrum Morphology

Previous work has suggested that the appearance of temporal artery negative velocity can be used as an indicator of approaching syncope (Arbeille et al., 2012). It has been previously demonstrated that in 66% of cases, negative temporal artery velocity appeared on average 5 minutes before the end of the test. This study emphasized that the negative velocity indicated increased vascular resistance in the final phase before the onset of presyncope and is a sign that is easily detectable in real time. In the current study, a more quantitative assessment of the appearance of temporal negative velocity in that three consecutive ten second averages were required with the minimum temporal velocity value less than 0.5cm/s. With the analysis used in this study, negative temporal artery velocity tended to appear earlier in the test when all individuals were considered. However, when three individuals who showed the appearance of temporal artery negative velocity early in the test were excluded from the analysis, similar to previously reported, the temporal negative velocity appeared much closer, approximately 2 minutes before the onset of syncope.

Several things could account for this discrepancy in results for the timing of the definitive morphological change of the temporal artery velocity profile. One of the primary issues is in the selection of the point where negative velocity appears. In the previous study, the negative velocity appearance was determined through quasi-qualitative assessment of the Doppler trace in order to determine if the appearance of temporal negative velocity could be used as a real time indicator for the onset of syncope. In this study, velocity was strictly quantitatively assessed; therefore, it is possible that in the analysis for this study, small variations in signal quality produced down spikes/noise in the V_{TEMP} signal that could have produced 10 second averages less than -0.5cm/s or that oscillations in the velocity signal would show negative velocity in real time, but would average to a value greater than -0.5cm/s and thus be excluded in the current analysis. With respect to the results from the

previous paper and this paper, it would appear that the appearance of negative temporal artery velocity is a good signal for use in real time during orthostatic tolerance testing, however, further work with recording of temporal artery blood velocity is required to determine the appropriate quantitative threshold to use when assessing temporal artery negative velocity and vascular resistance.

This study also showed that with the progression towards syncope, the MCA velocity waveform showed morphological alterations in which the value of the dicrotic notch of the signal became smaller than the end diastolic velocity value. Previous work has demonstrated this type of waveform alteration with respect to patients with a history of neurocardiogenic syncope (Albina et al., 2004); however, no work has been done to determine if this response is consistent with the approach of syncope in patient or non-patient populations, or how this change relates to other cerebrovascular variables. Figure 5.1 shows a representative velocity waveform from the temporal artery (top) and the middle cerebral artery (bottom) during supine rest (left) and during the last minute before syncope (right). At rest the two velocity waves show similar profiles with continuous positive velocity; however, with the approach to syncope, the temporal velocity wave shows a negative component corresponding to the dicrotic notch. Whereas, the MCA velocity wave continues to show positive velocity with the dicrotic notch less than the end diastolic value. Relating these two waveform profile changes would suggest that the deepening of the dicrotic notch of the MCA velocity and the negative component of the temporal artery velocity wave could be associated with changes in downstream vascular resistance.

Previous work with the Doppler resistance indices of vascular resistance and direct measures of vascular resistance have shown alterations in the diastolic component of the velocity waveform such that there is a reduced positive diastolic value with increasing resistance (Adamson et al., 1990), transitioning to a negative component in high resistance vascular beds (Arbeille et al., 1995). In the current study, changes in temporal artery minimum velocity seemed to track well with alteration in vascular resistance. Linear regression analysis conducted for each individual using 10s averages from the last 15min of the test showed significant relationships between changes in V_{TEMP} minimum and $TEMP_{VR}$.

Conversely, although the alterations in the CBFV waveform were similar morphologically to the changes in V_{TEMP}, changes in CBFV only showed week relations to alterations in CVRi suggesting that other variables, including absolute cerebral blood flow and changes in vascular tone, could have contributed to this observed change.

Part of this difference could be related to the influence of cerebrovascular autoregulation. Located at the same height above the heart, both the MCA and temporal artery are subjected to similar hydrostatic forces. However, blood flow in the MCA is also affected by the influences of cerebrovascular autoregulation serving to reduce vascular resistance with reductions in perfusion pressure thus allowing for the maintenance of cerebral blood flow. Whereas, blood flow in the temporal artery does not experience the protective effects of cerebrovascular autoregulation and is influenced by sympathetic vasoconstriction which serves to reduce blood flow in this vascular territory. In this case, where the changes in V_{TEMP} morphology appear to be related to alterations in downstream vascular resistance, the changes in CBFV may be indicative of reduced total flow in an area of low vascular resistance with alterations in cerebrovascular tone.

5.5.2 Cerebrovascular Autoregulation

In the present study, dynamic cerebrovascular autoregulation was determined using cross-spectral analysis. Contrary to our hypotheses, the results of this study showed no changes in autoregulation after five days of HDBR in either the CON or AG conditions. In addition, when subjects were grouped into those who could complete 10 minutes of tilt after 5 days of HDBR in the CON condition (tolerant) and those who could not complete 10 minutes of tilt (non-tolerant) there was again no differences in the effects of HDBR between the two groups.

Previous studies investigating cerebral blood flow responses before and after exposure to real or simulated microgravity have shown varied responses. In response to LBNP or assuming a head up posture, studies have found greater reductions in CBFV potential indicating an impaired ability to regulate cerebral blood flow (Kawai et al., 1993; Zhang et al., 1997). However, other work has shown no change in the CBFV response to tilt

or LBNP (Arbeille et al., 1998; Arbeille et al., 2008) or with rapid deflation of leg cuffs (Pavy-Le Traon et al., 2002). In the assessment of dynamic cerebral autoregulation, work by Zhang et al. (Zhang et al., 1997) showed a trend towards a higher coherence between MAP and CBFV post HDBR suggesting an impairment in autoregulation. This is in agreement with more recent studies which showed impaired dynamic cerebrovascular regulation after long duration spaceflight (Zuj et al., 2012a). However, studies looking at dynamic cerebrovascular autoregulation after short duration flight have shown no changes (Iwasaki et al., 2007), or impairments in only those astronauts who also showed orthostatic intolerance after flight (Blaber et al., 2011). Therefore, it was hypothesized that impairments in cerebrovascular autoregulation would also be seen in those individuals unable to complete 10 minutes of stand post HDBR. Although 7 of 12 individuals were unable to complete 10 minutes of stand in the CON condition, compared to 2 of 11 in the AG condition, the results of this study did not find any effects of HDBR on autoregulation in these groups. The reduced orthostatic tolerance with maintenance of cerebrovascular autoregulation seen in this study tends to suggest that although some previous work has demonstrated impairments post spaceflight and HDBR it does not appear to be a primary cause of the development of orthostatic intolerance.

As differences in orthostatic tolerance were seen in this study analysis was conducted to see if changes in tolerance were related to variation in the timing of Doppler spectrum morphology changes. Contrary to our hypothesis, no differences were seen in the timing of Doppler morphology changes with respect to the onset of syncope pre to post HDBR in either the CON or AG group. However, tests were shorter post HDBR with syncope occurring sooner after tilt, changes in Doppler morphology occurred earlier after tilt. Also contrary to the hypothesis, no differences in the timing of Doppler resistance indices were found between tolerant and non-tolerant individuals. These results would suggest that after five days of bed rest, alterations in cerebral blood flow did not contribute to reduced orthostatic tolerance. In addition, temporal artery vasoconstriction, indicative of peripheral vasoconstriction, also appeared to remain constant, again suggesting additional factors, potentially including regional differences in blood flow regulation.

5.5.3 Limitations

This study used recordings of middle cerebral artery and temporal artery blood velocity as indicators of blood flow in the vascular territories which in turn is used for the calculation of vascular resistance. As flow is the product of velocity and vessels cross-sectional area, changes in the diameter of insonated vessels may confound the results of this study. Previous work has shown that the diameter of the MCA remains stable with changes in $P_{ET}CO_2$ and mild orthostatic stress (Giller et al., 1993; Serrador et al., 2000); however no work has been done to determine if the diameter of the MCA changes after real or simulated microgravity in humans. Work with animal models suggests a reduction in MCA lumen diameter (Wilkerson et al., 1999) with vascular smooth muscle hypertrophy (Wilkerson et al., 2002; Wilkerson et al., 1999; Lin et al., 2009; Zhang et al., 2001) and increased myogenic tone (Wilkerson et al., 2005; Geary et al., 1998; Lin et al., 2009). Therefore, it is possible that the lack of change in CBFV seen in the study is the result of reduced cerebral blood flow through a smaller middle cerebral artery. However, this is unlikely as the bed rest period was only 5 days.

It is unknown what effects tilt and the progressions towards syncope have on the diameter of the temporal artery. However, with the increased sympathetic activity associated with tilt (O'Leary, Kimmerly, Cechetto, & Shoemaker, 2003) vasoconstriction of the temporal artery would be expected. If this is the situation, then our assessments of reduced temporal artery blood flow and increased vascular resistance would be underestimating actual changes. Regardless, any potential changes in temporal artery diameter would not change the observation that the temporal artery velocity waveform develops a negative component approximately two minutes before the onset of syncope or that this change in velocity waveform morphology seems to be related to changes in vascular resistance.

5.6 Conclusions

The results of this study found that both the temporal artery and middle cerebral artery Doppler spectrum morphologies showed consistent changes before the onset of

syncope and that these alterations were not different after exposure to five days of HDBR. Analysis of the temporal artery Doppler velocity waveform showed the appearance of a negative component on average two minutes before the onset of syncope and a change in the MCA velocity waveform such that the dicrotic notch point became less than the end diastolic value. Regression analysis suggested that the change in the temporal artery blood velocity waveform was related to alterations in vascular resistance, where the changes in the MCA velocity trace were more depended on blood flow. Although there was a reduction in orthostatic tolerance after five days of HDBR, there were no changes in either the indices of cerebrovascular autoregulation, CBFV and V_{TEMP} responses to tilt, or the alteration in Doppler waveform morphology with the progression towards syncope. These results indicate that cerebral blood flow regulation is well maintained and does not contribute orthostatic intolerance after five days of HDBR. In addition, although both the MCA and temporal artery blood velocity profiles showed similar morphological changes, it would appear that V_{TEMP} is influenced by vascular resistance, where CBFV is influenced by overall cerebral blood flow and the potential contributions of changes in cerebrovascular tone.

Chapter 6

The calculation of cerebrovascular tone and changes in middle cerebral artery diameter with nitroglycerin before and after head down bed rest

6.1 Overview

Within beat characteristics of the middle cerebral artery (MCA) velocity trace may provide an indication of changes in cerebrovascular tone. However, little work has been conducted to determine how changes in the velocity trace relate to other indicators of cerebrovascular resistance and compliance especially in situations where the diameter of the MCA may be changing. The purpose of this study was to assess potential changes in the MCA velocity trace with nitroglycerin (NG) and head down bed rest (HDBR) in relation to change in the common carotid artery (CCA) velocity profile and calculated indicators of cerebrovascular resistance (R), compliance (C), viscoelastic resistance (K), and intertance (L). Before and after HDBR, MCA velocity, CCA velocity, CCA diameter, and CCA pressure were assessed at rest and after NG. R, C, K, and L were determined using a mathematical model (RCKL) with the inputs of CCA pressure and flow. Results showed that after 5 days of HDBR there were no changes in resting CCA or calculated MCA diameter. In response to NG, both the CCA and MCA were seen to dilate with no differences after HDBR. Results from the RCKL model showed a reduction in R and an increase in C with NG with no differences at rest or with NG after HDBR. Assessment of velocity waves showed that with NG, both the CCA and MCA velocity waves exhibited similar changes. Comparison to the RCKL model results, found that the augmentation index and the amplitude of the dicrotic notch of the MCA velocity wave were significantly related to C both before and after NG. The results of this study demonstrate that cerebrovascular tone and the diameter of the MCA are well maintained after 5 days of HDBR. In addition assessment of the MCA velocity trace and RCKL modeling suggest that NG results in an increase in cerebrovascular compliance that is reflected in changes in the MCA velocity wave profile.

6.2 Introduction

Transcranial Doppler (TCD) measurement of cerebral blood flow velocity (CBFV) is frequently used as a method for non-invasively assessing cerebrovascular hemodynamics. In addition to the calculation of mean CBFV, analysis of within beat changes of the CBFV waveform have been used to describe cerebrovascular resistance and tone. However, in situations where the insonated vessel is changing the relation of within beat characteristics to cerebrovascular tone may be altered. Therefore, the purpose of this study was to use measures of common carotid artery (CCA) blood flow and pressure to model the cerebral circulation and relate within beat variations in CBFV to the model outputs of cerebrovascular hemodynamics.

Previous work has shown a consistent drop in CBFV with nitroglycerin stimulation (Borisenko & Vlasenko, 1992; Dahl et al., 1989; Dahl et al., 1990; Micieli et al., 1997; Siepmann & Kirch, 2000; White et al., 2000) that has been shown to be due to a dilation of the middle cerebral artery (Hansen et al., 2007). In addition to changes in CBFV and diameter of the MCA, studies have also noted changes in the CBFV waveform (Lockhart et al., 2006) and reduction in critical closing pressure suggesting alterations in cerebrovascular tone (Moppett et al., 2008). Therefore, stimulation with NG presents an experimental model to assess changes in cerebrovascular tone with changes in MCA diameter.

Exposure to real and simulated microgravity is associated with cephalic fluid shifts (Hargens & Watenpaugh, 1996) that may alter the structure and function of cerebral blood vessels. Studies of humans have shown no change (Arbeille et al., 2008; Pavy-Le Traon et al., 2002; Zhang et al., 1997; Arbeille et al., 2001) increased (Kawai et al., 1993), and decreased (Arbeille et al., 1998; Arbeille et al., 2001; Sun et al., 2005; Frey et al., 1993; Hirayanagi et al., 2005) cerebral blood velocity measured by transcranial Doppler ultrasound following head-down bed rest (HDBR). However, measures of cerebral blood velocity may not accurately reflect cerebral blood flow if the diameter of the insonated artery changes. To date, no studies have been conducted in humans to quantitatively assess cerebral blood flow before and after HDBR.

In 2007, Zamir et al. (Zamir et al., 2007) presented a mathematical model for the assessment peripheral vascular properties. Based on a modified Winkessel model, the RCKL model placed vascular resistance (R) in parallel with vascular compliance (C) which was in series with viscoelastic resistance (K) an inertance (L). In a pilot study, the RCKL model was used with measures of CCA blood flow and pressure to show changes in cerebrovascular properties with aging (Robertson et al., 2008). Therefore, this study utilized the RCKL model to assess change in cerebrovascular properties to NG and HDBR and related the model outputs to assessments of within beat CBFV properties.

In this study, it was hypothesized that NG would result in an increase in cerebrovascular compliance that would be reflected in both the MCA velocity and CCA flow profiles and with RCKL model outputs. Post HDBR, it was hypothesized that RCKL modeling would show an increase in vascular resistance and a reduction in vascular compliance, but no differences in the response to NG.

6.3 Methods

6.3.1 Experimental Protocol

Data for this study were collected from twelve healthy men 32±8 years of age (mean ± SD). The men participated in the study which involved five consecutive days of 6° head down bed rest (HDBR) with and without an artificial gravity countermeasure. The study was a cross-over design in which each man completed HDBR without countermeasures (CON) and with the artificial gravity (AG) countermeasure in random order with each session separated by 30 days. All experimental procedures were approved by the Comité Consultatif de Protections des Personnes dans la Recherche Biomédicale, Midi-Pyrénées (France), and local ethics committees, including the Office of Research Ethics, University of Waterloo. After receiving full disclosure of the experimental protocol, each participant signed a consent form and was aware of his right to withdraw from the study for any reason without prejudice. The entire protocol was in accordance with the declaration of Helsinki.

The AG countermeasure consisted of short arm centrifugation designed to create a head to foot force vector with a magnitude of 1g at the centre of mass of the participant. Centrifugation was applied for five minutes and repeated six times for a cumulative time of 30 minutes of AG per day. Due to medical issues during the study, one participant did not complete the AG protocol; therefore, data were collected for all twelve individuals in CON and only eleven for AG.

All measures for the response to nitroglycerin (NG) were collected in a supine position. Baseline recordings were conducted after which 0.3mg of NG (Natispray, Proctor & Gamble Pharmaceuticals, France) was administered sublingually. Data were continuously collected for ten minutes after NG administration.

6.3.2 Vascular Measures

Throughout the protocol, TCD (CardioLab, ESA-CNES device) was used for the assessment of CBFV. A 2MHz, pulsed Doppler probe was placed over the right temporal window allowing for the insonation of the M1 segment of the MCA. The probe was held in place throughout the test via the use of custom designed head gear. The outer envelope of the Doppler spectrum was determined and digitally recorded for later processing. Data were recorded using CardioMed (ESA-CNES, France) software and the outer envelope digitized at 100Hz.

Echo Doppler ultrasound (ATL HDI 5000, Philips, France) was used for the assessment of CCA diameter. A linear transducer was placed over the right CCA and longitudinal B-mode images were obtained with simultaneous Doppler velocity. B-mode images, Doppler spectrum, and Doppler audio were recorded using digital video tape for later processing.

Blood pressure waveforms were obtained from the left CCA with the use of a hand held Millar pressure transducer. Arterial blood pressure was continuously monitored using finger photoplesthysmography (Nexfin, BMEYE B.V, Amsterdam, Netherlands). Due to variation in hold-down pressure with the use of the Millar pressure transducer, Millar diastolic pressure values were corrected to recorded finger diastolic pressure values.

6.3.3 Data Analysis

Mean arterial pressure (MAP) was determined as the mean over a cardiac cycle of the arterial blood pressure recorded at the finger. The outer envelope of the MCA and CCA velocity traces were individually averaged over a cardiac cycle to provide beat-by-beat CBFV and CCA velocity values. CCA blood flow was calculated from the resultant velocity and mean CCA diameter calculated from the recorded ultrasound video. For both the MCA and the CCA, vascular resistance was calculated as CVRi = MAP/CBFV and CCA_{VR} = MAP/CCA flow respectively.

The change in MCA diameter with NG was calculated using two methods. First, the percent diameter change was calculated assuming cerebral blood flow remained constant with NG stimulation using the equation (Borisenko & Vlasenko, 1992):

(Equation 1) $$\Delta d\% = \left(\sqrt{\frac{CBFV_1}{CBFV_2}} - 1\right) \times 100$$

Where $CBFV_1$ is the mean resting CBFV value and $CBFV_2$ is the mean CBFV value five minutes after the administration of NG. Values for CCA flow were also determined in this study and can be considered surrogate measures of cerebral blood flow. Therefore, changes in MCA diameter were also calculated by:

(Equation 2) $$\Delta d\% = \left(\sqrt{\frac{CCA_2}{CBFV_2} \times \frac{CBFV_1}{CCA_1}} - 1\right) \times 100$$

Where again, $CBFV_1$ is the mean baseline CBFV value and $CBFV_2$ is the mean CBFV value five minutes after the administration of NG. Similarly, CCA_1 is the mean common carotid flow value during supine rest and CCA_2 is the mean common carotid flow value five minutes after the administration of NG.

For the assessment of velocity wave characteristics of the MCA and CCA waveforms, 10 to 20 consecutive cardiac cycles were averaged to produce a representative velocity waveform. The resultant representative waves were then assessed for potential variation in key inflection points (T1, P1, P2, T3, P3, Figure 6.2) with respect to the end diastolic velocity (T1). In addition, the augmentation index was calculated as previously described

(Kurji et al., 2006; Robertson et al., 2008) as AI = (P2-T1) / (P1-T1) x 100%. CrCP was calculated for each beat, as previously described (Panerai et al., 2011) using mean and diastolic values for CBFV and arterial blood pressure. The slope of the relationship between CBFV and arterial pressure was calculated as a = (CBFVmean – CBFVdia) / (MAP – DBP). RAP was then calculated as RAP = 1 / a and CrCP calculated as CrCP = MAP – (CBFVmean / a).

For the assessment of vascular properties downstream from the CCA, a mathematical model was used which was previously presented by Zamir et al. (Zamir et al., 2007) to describe characteristics of peripheral vessels. Briefly, in the current study simultaneous recordings of CCA pressure and flow were assessed at baseline and after NG stimulation and used as inputs to the RCKL model. Values for downstream vascular resistance (R), compliance (C), viscoelastic resistance (K), and inertance (L) were determined as model outputs.

6.3.4 Statistical Analysis

Unless otherwise stated, values presented show the mean ± SD. Data were assessed using a two-way repeated measures analysis of variance for the main effects of HDBR and NG (SigmaStat 3.5, Systat Software Inc., Chicago, IL). The potential relationships of waveform inflection points, CrCP, and RAP with RCKL model outputs were assessed using linear regressions (SigmaStat 3.5, Systat Software Inc., Chicago, IL). For all tests, significance was set at $P<0.05$.

6.3.5 Analysis Limitations

During this study, one individual did not complete the AG condition due to medical considerations. Therefore, two-way repeated measures ANOVA assessment of NG responses before and after HDBR, only 11 subjects were included. However, relationships between RCKL model results and MCA velocity waveform inflection points were conducted using all 12 subjects.

6.4 Results

In response to NG, CBFV was seen to decrease (Figure 6.1 B) with a corresponding increase in CVRi (Figure 6.1 D). Conversely, there was no change in CCA flow (Figure 6.1 A) with a reduction in CCA_{VR} (Figure 6.1 C) suggesting that the changes in CBFV and CVRi were due to changes in MCA diameter. With HDBR, there were no differences in resting values or responses to NG for any of these variables.

With HDBR, there were no changes in resting diameter of the CCA or MCA calculated with the assumption of constant CBF or using CCA flow as a surrogate of cerebral blood flow (Table 6.1). In response to NG, dilation was seen of the CCA with no changes after HDBR. Similarly, the MCA also showed dilation in response to NG with both calculation methods. Post HDBR, the dilation response of the MCA was larger in the CON condition when no change in cerebral blood flow was assumed with NG (P=0.016); however, no differences in the dilation response were seen when CCA flow was used as a quantitative indication of cerebral blood flow.

Changes were seen in both the CCA and MCA Doppler spectrum morphology with NG stimulation (Table 6.2). Waveforms presented in Figure 6.2 show data from one subject pre-HDBR with the baseline wave shift so that initial points at time 0 were equal. For both the CCA and MCA velocity waveforms, there were significant reductions in P1-T1, P2-T1, and T3-T1 with NG stimulation. For the MCA velocity trace P3-T1 was also reduced, but this did not reach significance with the CCA velocity trace (P=0.08). There was a significant reduction in AI for both the CCA and MCA with NG stimulation (Table 6.2). No differences at rest or with NG stimulation were seen after HDBR. The calculation of CrCP showed no changes with NG where RAP was seen to increase (Table 6.3). There were no effects of HDBR for either variable.

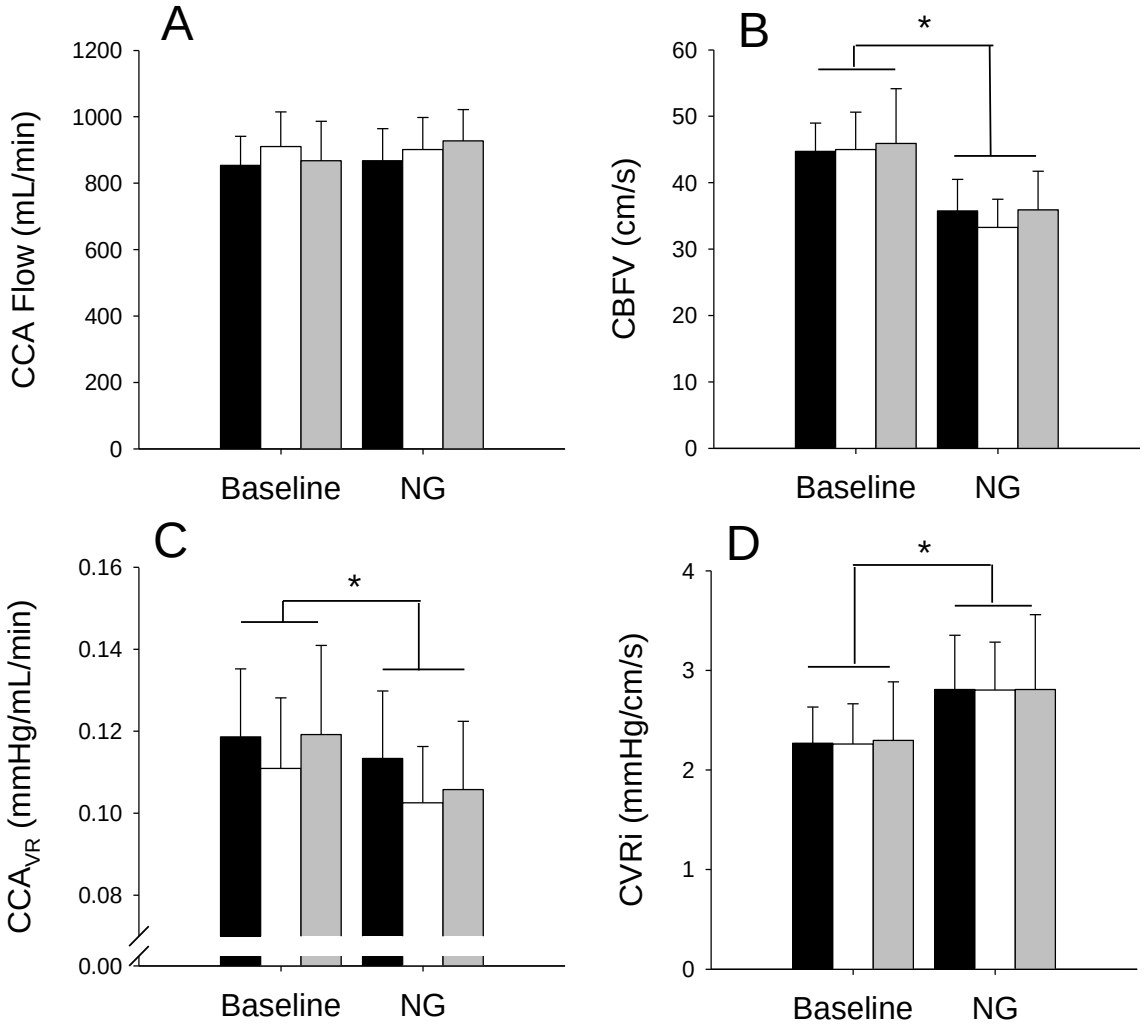

Figure 6.1: Cerebral and carotid responses to NG

Values at baseline and in response to NG for changes in CCA blood flow (A), CBFV (B), CCA_{VR} (C), and CVRi (D). Bars represent PRE (black), CON (white), and AG (grey) (mean ± SD, n=11). Statistical analysis showed significant decreases in CCA_{VR} and CBFV and an increase in CVRi with NG stimulation (P<0.05). No effects of HDBR were seen.*

Table 6.1: Calculated percent change in vessel diameter with NG and HDBR

	Condition	CCA	MCA (no change CBF)	MCA (CCA Flow)
% Change HDBR	CON	0.56 ± 4.81	-0.68 ± 5.93	2.74 ± 6.86
	AG	-0.89 ± 3.82	-0.54 ± 7.14	0.21 ± 8.64
% Change NG	PRE	6.54 ± 3.28	12.37 ± 3.42	13.06 ± 5.49
	CON	6.47 ± 4.06	16.41 ± 4.52*	16.66 ± 7.30
	AG	8.56 ± 4.69	13.04 ± 2.98	17.28 ± 7.67

*Values show the mean ± SD (n=11) for each calculated percent change in vessel diameter. Percent changes are presented for the CCA and the MCA diameter calculated assuming no changes in cerebral blood flow and using CCA flow as a surrogate for cerebral blood flow. No statistically significant changes in resting diameter were seen with HDBR. Diameter changes with NG that are statistically different from PRE are denoted by * (P<0.05).*

Table 6.2: Velocity wave inflection points with NG and HDBR

			AI (%)	P1-T1 (cm/s)	P2-T1 (cm/s)	T3-T1 (cm/s)	P3-T1 (cm/s)
MCA	PRE	Baseline	65.63±9.76	36.39±6.16	23.54±3.72	13.12±2.94	18.47±2.96
		Nitro	44.79±9.76*	28.45±6.03*	12.44±2.61*	5.55±2.52*	11.50±2.75*
	CON	Baseline	66.46±12.55	37.00±7.56	24.15±4.94	14.48±3.84	18.97±3.51
		Nitro	42.25±11.56*	27.53±4.14*	11.47±3.13*	5.30±2.30*	10.61±1.79*
	AG	Baseline	63.99±12.94	37.59±9.73	23.37±5.31	13.77±3.39	18.59±3.89
		Nitro	43.16±13.49*	28.34±6.75*	11.95±4.25*	6.21±3.66*	11.77±2.39*
CCA	PRE	Baseline	26.45±9.62	70.61±8.38	18.33±6.28	7.00±8.38	17.23±3.33
		Nitro	10.78±12.26*	65.85±11.33*	6.06±8.74*	-0.62±8.09*	15.56±3.96
	CON	Baseline	26.24±10.90	78.72±20.90	19.03±6.77	8.44±20.90	17.61±4.71
		Nitro	9.90±13.15*	69.38±16.88*	5.24±9.22*	-0.80±9.36*	16.25±5.44
	AG	Baseline	27.26±11.70	73.88±11.50	19.51±7.09	8.74±4.60	17.48±3.68
		Nitro	10.91±11.95*	69.13±10.53*	6.64±8.13*	0.98±7.90*	16.38±4.18

*Values show the mean ± SD (n-11) for the augmentation index (AI) and the differences between inflection points and the end diastolic value (T1). Values after NG stimulation that are statistically different from baseline are denoted by * (P<0.05). No statistically significant differences were seen with HDBR.*

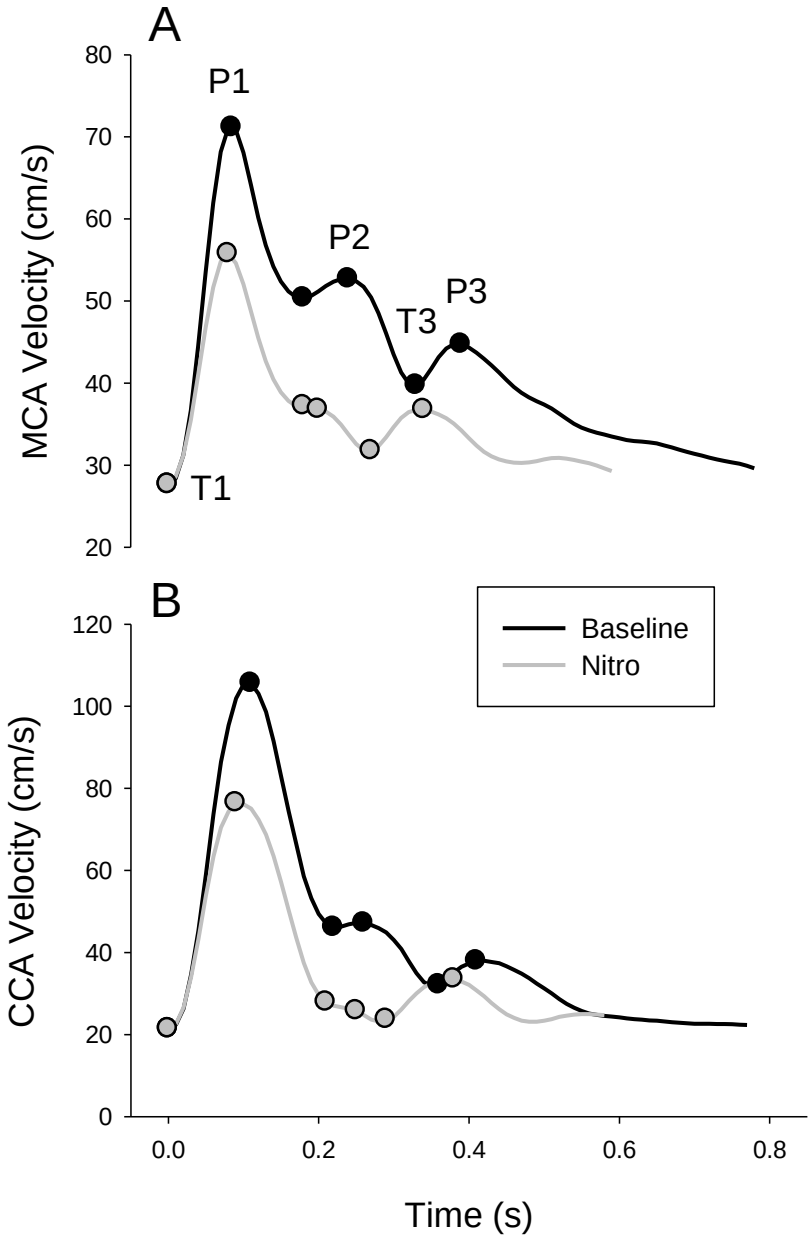

Figure 6.2:Representative MCA and CCA velocity traces

Representative tracing from one individual of the Doppler velocity waves for the MCA (A) and the CCA (B) during resting baseline (black) and after NG stimulation (grey). Points on the waves represent the key inflection points used for the analysis presented in Table 6.2.

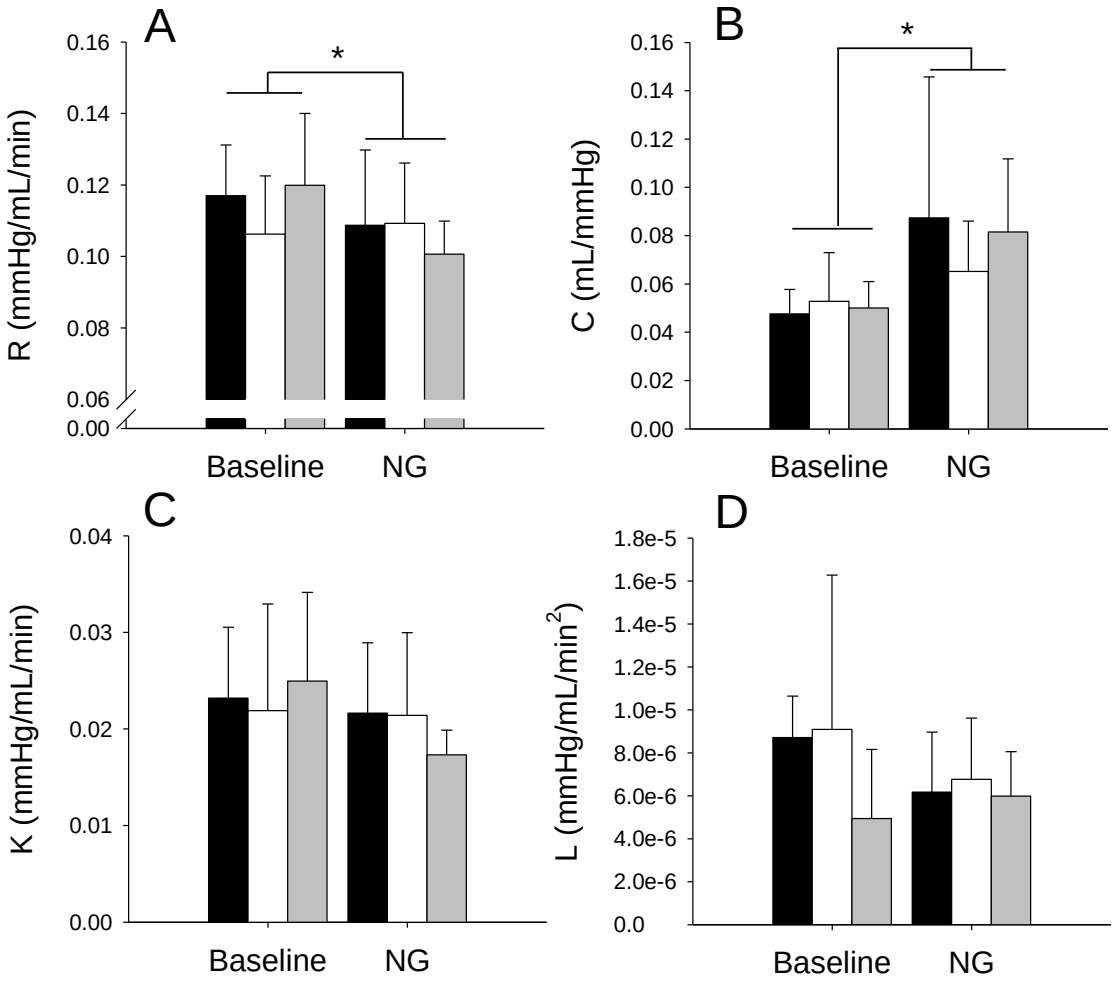

Figure 6.3: RCKL results with NG and HDBR

Values at baseline and in response to NG for RCKL model outputs of resistance (R, panel A), compliance (C, panel B), viscoelastic resistance (K, panel C), inertance (L, panel D). Bars represent PRE (black), CON (white), and AG (grey) (mean ± SD, n=11). Statistical analysis showed significant increases in C and a reduction in R with NG stimulation (P<0.05).*

Table 6.3: CrCP and RAP values with NG and HDBR

		CrCP (mmHg)	RAP
PRE	Baseline	24.90±5.63	1.70±0.30
	Nitro	22.91±6.06	2.13±0.45*
CON	Baseline	27.36±10.32	1.64±0.38
	Nitro	21.85±8.68	2.12±0.39*
AG	Baseline	23.03±6.40	1.78±0.45
	Nitro	20.60±9.57	2.23±0.76*

*Values show the mean ± SD (n-11) for the critical closing pressure (CrCP) and resistance area product (RAP). Values after NG stimulation that are statistically different from baseline are denoted by * (P<0.05). No statistically significant differences were seen with HDBR.*

In response to NG, the RCKL model revealed a reduction in vascular resistance (Figure 6.3 A), an increase in vascular compliance (Figure 6.3 B), and no changes in either viscoelastic resistance (Figure 6.3 C) or inertance (Figure 6.3 D). No differences were seen with HDBR for any model output.

Pre-HDBR RCKL model outputs were compared to MCA velocity wave points, AI, CrCP and RAP using linear regressions both before and after NG stimulation. Results from the analysis showed a strong trend for RAP to be related to R at rest (P=0.058) and significantly related to R after NG. Similarly, P1-T1, or the pulse amplitude of the wave was significantly related to R at rest (P=0.05) and after NG (P=0.002). Results also showed that AI (Figure 6.4 A) and T3-T1 (amplitude of the dicrotic notch, Figure 6.4 B) were significantly related to C both before (P=0.001, and P=0.005 respectively) and after NG (P<0.001 and P=0.002 respectively). P2 was also significantly related to C after NG (P=0.013) with a trend towards the same relationship at baseline (P=0.082). After NG, K was related to RAP (P=0.049) and AI (P=0.015) with a trend towards being related to P1-T1 (pulse amplitude, P=0.088) and T3-T1 (dicrotic notch amplitude, P=0.082). No significant relations were found for the resulting value of L either before or after NG.

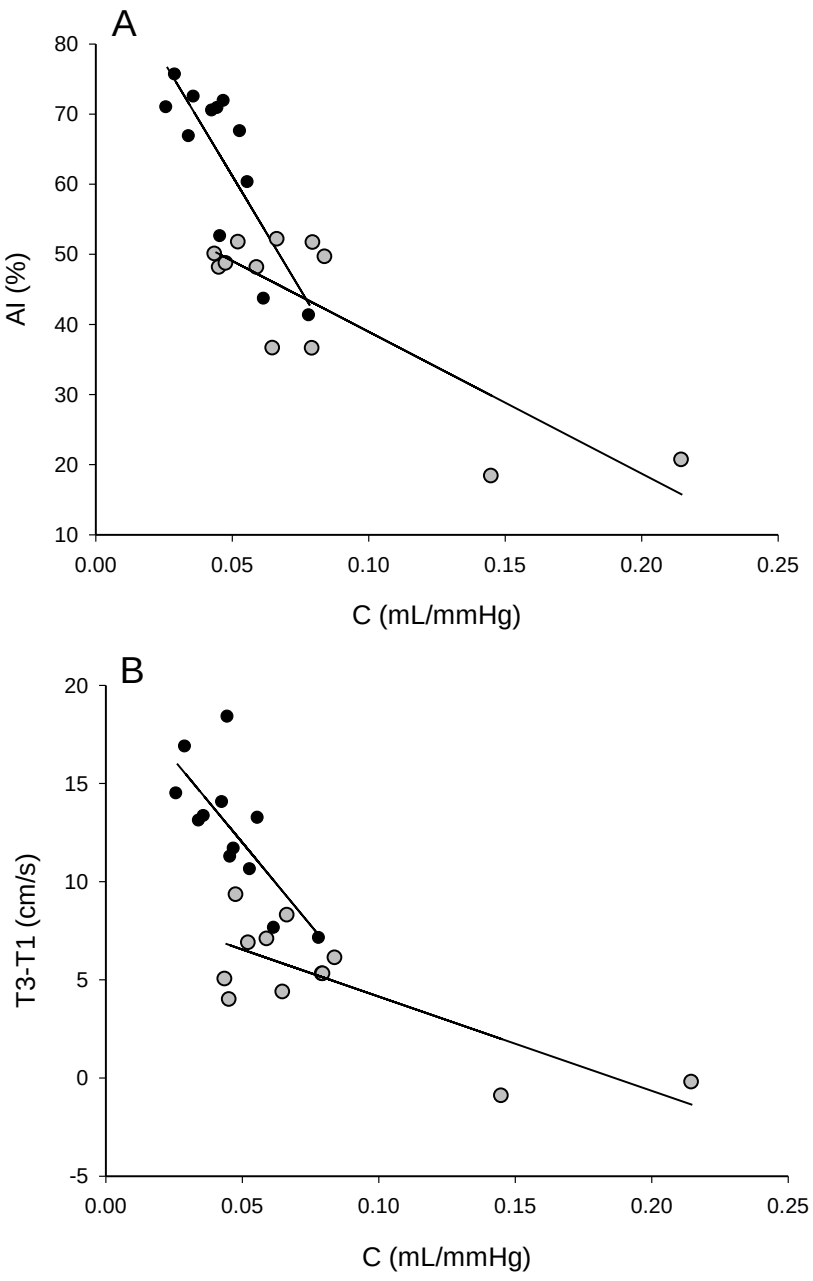

Figure 6.4: Linear regression results for AI and T3-T1 with C

Linear regression results testing the relationship between pre-HDBR resting values (black circles) and NG values (grey circles) of AI (panel A), T3-T1 (the dicrotic notch, panel B) and C (vascular compliance). The results of this analysis showed significant linear relationships between C and both AI and the dicrotic notch before and after NG.

6.5 Discussion

The current study used quantitative measures of cerebral blood flow along with mathematical modeling and waveform inflection point analysis to determine cerebrovascular responses to NG before and after five days of HDBR. In support of the hypothesis, RCKL modeling and assessment of MCA velocity wave form inflection points suggested increased compliance of the cerebrovasculature. Similarly, the changes in MCA velocity waveform inflection points were mirrored in the CCA flow waveform suggesting that change in the CCA reflect alterations in cerebrovascular conditions with NG stimulation. In contrast to the hypothesis, no difference in any variable assessed was seen after HDBR in either the CON or AG conditions.

6.5.1 Blood Flow, Resistance, and Cross-Sectional Area

The use of transcranial Doppler ultrasound allows for the assessment of cerebral blood velocity, but the interpretation of results with respect to cerebral blood flow is dependent on the diameter of the insonated vessel (normally the MCA) remaining constant. Studies have frequently shown reduction in CBFV with NG stimulation (Borisenko & Vlasenko, 1992; Dahl et al., 1989; Siepmann & Kirch, 2000; White et al., 2000) with quantitative assessments of cerebral blood flow showing no changes (Dahl et al., 1989; White et al., 2000; Borisenko & Vlasenko, 1992) and MRI measurements suggesting dilation of the MCA (Hansen et al., 2007). The results of the current study are in agreement with previous work in that reductions in CBFV were observed along with no changes in quantitative measures of cerebral blood flow indicating the dilation of the MCA.

The percent dilation of the MCA was assessed with HDBR and NG using CCA flow measures as a surrogate for cerebral blood flow. One study, which assessed cerebral blood flow with NG, suggested that a 15% dilation of the MCA was required to account for the reduction in velocity and observed measures of cerebral blood flow. Similar results were found with MRI assessments of the MCA after NG stimulation finding a 10-14% dilation of the MCA. The results of the current study were consistent with both of these studies, as a dilation of 13% was found with NG pre-HDBR, and dilations of 16% and 17% post-HDBR.

No previous work has examined potential changes in MCA diameter with HDRB in humans. Animal studies of microgravity exposure have suggested structural changes in cerebral arteries (Wilkerson et al., 1999; Lin et al., 2009; Zhang et al., 2001; Wilkerson et al., 2002) with a reduced lumen cross sectional area (Wilkerson et al., 1999). However, other work has demonstrated that these changes only occurred with simulated microgravity exposure lasting longer than 7 days (Bao et al., 2007; Gao et al., 2009). Therefore, it was unlikely that any structural change would be present after only 5 days of HDBR. The results of this study support this as no changes in calculated MCA diameter were found.

Assessment of vascular resistance showed opposite responses of CVRi and CCA_{VR} to NG. An increase in CVRi was seen with NG; however, the calculation of CVRi is dependent on the assumption that CBFV represents cerebral blood flow. As the MCA was seen to dilate with NG stimulation, the observed increase in CVRi is due to the change in vessel diameter and not changes in cerebrovascular resistance. Conversely, there was a small but significant reduction in CCA_{VR} that served of offset a slight reduction in arterial pressure (data not shown) to maintain CCA blood flow. As the diameter of the MCA is changing, these results highlight the need for caution in interpreting CBFV responses as reflective of cerebral hemodynamics.

6.5.2 Cerebrovascular Tone

This study has demonstrated that the use of CCA blood flow as a quantitative assessment of cerebral blood flow revealed changes in the MCA diameter with NG stimulation. This study also used the quantitative assessment of CCA blood flow to examine potential changes in cerebrovascular tone through the use of waveform analysis and RCKL modelling. Previous work has noted alterations in ophthalmic artery Doppler wave morphology with NG stimulation (Lockhart et al., 2006). It has also been suggested that an augmentation index based on the peak systolic values (P1) and the reflected peak (P2) can be calculated that would be reflective of vascular compliance (Kurji et al., 2006; Robertson et al., 2008). Changes in the augmentation index of the MCA velocity wave have been noted with hypercapnia (Robertson et al., 2008) and aging (Kurji et al., 2006) with both situations

showing an increase in the index suggesting a reduction in cerebrovascular compliance. In the current study, alterations in key inflection points were noted with the MCA and, to a lesser extent, the CCA in that with NG there were reductions in the amplitudes of all inflection points with respect to the end diastolic value (Figure 4, Table 2). In addition, the augmentation index calculated for both the MCA and CCA velocity waves was reduced suggesting an increase in cerebrovascular compliance. These results support the hypothesis that the MCA velocity wave and CCA flow wave would show similar changes in NG and that NG would result in an increase in vascular compliance.

In contrast to the augmentation index results, the calculation of CrCP was not significantly different with NG. Previous work has shown a reduction in CrCP with NG (Moppett et al., 2008) which is in agreement with the augmentation index results suggesting a reduction in cerebrovascular tone with NG. With the current data set, a small but significant reduction in $P_{ET}CO_2$ was noted with NG (data not show). Previous work has shown an increase in CrCP with a reduction in $P_{ET}CO_2$ (Ainslie et al., 2008; Carey et al., 2001; Hsu et al., 2004). Therefore, in the current study the lack of a significant reduction in CrCP may be attributed to the confounding influence of the reduction in $P_{ET}CO_2$.

Of additional consideration is the calculation method used in the current study to determine CrCP. Where previous work has used a linear regression between CBFV and arterial pressure to calculate CrCP (Moppett et al., 2008), the current study utilized a two point method which only involved the calculation of mean and diastolic CBFV and arterial pressure. This method has been shown to have good repeatability (Panerai et al., 2011); however, it may not be as sensitive in detecting changes in vascular tone with NG. The calculation method for CrCP used in this study may also explain the lack of relationship between CrCP and RCKL outputs before and after NG.

Mathematical modeling was used in an attempt to further explain the variation in MCA velocity waveforms with NG stimulation. The RCKL model has been previously used with the peripheral vasculature to show alterations in vascular compliance independent of vascular resistance (Zamir et al., 2007). The results from the current study showed an

increase in cerebrovascular compliance and a reduction in resistance with no changes in viscoeastic resistance or inertance with NG stimulation. The observed increase in cerebrovascular compliance is in agreement with previous investigations showing increased peripheral vascular compliance (Smulyan et al., 1986; Bank & Kaiser, 1998) and results showing a reduction in CrCP suggesting an increase in cerebrovascular compliance (Moppett et al., 2008).

Linear regressions were performed between RCKL model results and MCA velocity wave inflection points at rest pre-HDBR in an attempt to determine the how inflection points relate to cerebrovascular properties. Previous work has related the shape of the MCA velocity waveform for the interpretation of inflection points (Robertson et al., 2008; Aggarwal et al., 2008) but no work has attempted to directly relate these variables to other assessments of cerebrovascular properties. Results of the current study found that the pulse amplitude (P1-T1) of the velocity wave was related to vascular resistance which is consistent with the use of the Doppler resistance indices (Gosling, Lo, & Taylor, 1991) which relate the pulse amplitude of the velocity trace to either the mean velocity (PI) or the peak velocity (RI) to provide an indication of vascular resistance. Interestingly, the vascular compliance output from the RCKL model was significantly related to AI, P2-T1, and T3-T1.

The augmentation index of the velocity wave is based on the assessment of central pressure waves which identified a second systolic peak which was generated from a reflected pressure wave (Nichols et al., 2008). Work with the common carotid artery has demonstrated that the augmentation index calculated from the flow wave was linearly related to the augmentation index calculated from the pressure wave (Hirata, Yaginuma, O'Rourke, & Kawakami, 2006). Therefore, it was expected that AI calculated from the MCA velocity wave and the pulse amplitude of P2, which is due to the reflected wave, would be significantly related to the value of C from the RCKL model.

In addition to the augmentation index, the amplitude of the dicrotic notch was inversely related to vascular compliance. This too can be explained by the velocity of the reflected component of the wave as a greater P2 would serves to increase the pulse amplitude

to the dicrotic notch as a greater amount of the mean flow is occurring in the systolic portion of the velocity wave. Previous work has shown that an increase in the ratio of velocity in the systolic portion of the ophthalmic artery velocity wave to that in the diastolic portion is significantly related to central vascular compliance, such that an increase in the ratio was related to a decrease in central vascular compliance (Maruyoshi et al., 2010). It is unclear how the results presented in this chapter relate to central vascular properties, but they do highlight that changes in the augmentation index, the amplitude of the reflected peak, and the amplitude of the dicrotic notch are all related to changes in vascular compliance downstream from the CCA.

In response to HDBR, no differences in cerebral vascular tone were seen with either the RCKL model results or MCA velocity wave inflection points. Work with animal models of microgravity exposure has suggested increased myogenic tone of cerebral vessels (Wilkerson et al., 2005; Geary et al., 1998; Lin et al., 2009). In contrast, human studies have suggested both increased (Eiken et al., 2008) and decreased (Tuday et al., 2007; Baevsky et al., 2007) arterial compliance with microgravity, but no study has been published examining potential changes in human cerebrovascular tone. The results of the current study show that cerebrovascular tone is well maintained after exposure to 5 days of HDBR.

6.5.3 Limitations

One of the major limitations with this study was with respect to the length of the HDBR period. As the study only involved 5 days of HDBR, it was unlikely that any structural changes in the cerebrovasculature occurred during this time. Animal studies have observed an upregulation of proteins involved in the synthesis of angiotensinogen and of angiotensin-II type-1 receptors in cerebral and carotid arteries that was associated with increased arterial wall thickness after four weeks, but not seven days of hind limb suspension (Bao et al., 2007; Gao et al., 2009) suggesting that longer exposure to simulated microgravity is needed to induce structural changes in cerebral arteries. Therefore, the results of the current study demonstrate that cerebral blood flow and tone were well maintained after 5

days of HDBR; however, it is unclear if this result would be consistent after longer durations of HDBR.

Results of the current study are based on ultrasound assessments of CBFV and CCA diameter and velocity. As such, results are subject to errors inherent in each of these measures. These include the possibility of measurements being taken at different points along the vascular tree, or alterations in the angle of insonation. Care was taken to minimize these errors, however they cannot be completely ruled out as contributing factors in the variability of results.

An additional consideration with the current data is the timing of measures after the administration of NG. Efforts were made to ensure that measures were taken at consistent time points after the administration of NG, but, due to variability in signal acquisition times, measures were taken between 5 and 10 minutes after NG. Previous work has shown that CBFV is reduced up to 30min post NG stimulation (Dahl et al., 1989); therefore, it was thought that the variability in data collection timing post NG would not affect results.

Assessment of cerebrovascular resistance and compliance was done using the RCKL model previously presented (Robertson et al., 2008; Zamir et al., 2007). This model requires the simultaneous assessment of pressure and flow as input variables. To accommodate this, pressure and flow measures were taken from the left and right CCA respectively. Results from the model provide outputs reflecting vascular resistance and compliance downstream from the point of measurement and include the influences of both changes in intracranial and extracranial hemodynamics. No studies have been conducted to determine if differences exist between extracranial and intracranial hemodynamic responses to NG. However, the increase in compliance seen in the current study match changes expected from previously published work which used the calculation of CrCP to determine changes in cerebrovascular tone (Moppett et al., 2008) and from the assessment of peripheral vascular responses (Smulyan et al., 1986; Bank & Kaiser, 1998).

6.6 Conclusion

This study was the first to use quantitative measures of CCA blood flow along with measures of CBFV to assess cerebrovascular responses to NG before and after exposure to five days of HDBR. In support of the hypotheses, alterations in MCA velocity wave inflection points were seen with NG and were reflected in similar alteration in CCA blood flow inflection points. The use of mathematical RCKL modelling showed that NG resulted in a decrease in resistance that was linearly related to the pulse amplitude of the velocity trace, and an increase in vascular compliance related to the calculated augmentation index, the peak of the reflected velocity wave, and the amplitude of the dicrotic notch of the velocity trace. No differences in resting cerebrovascular variables or responses to NG were seen with HDBR. The use of quantitative measures of CCA blood flow as an indication of cerebral blood flow demonstrated that resting cerebrovascular variables and responses to NG are well maintained after exposure to five days of HDBR.

Chapter 7

Common carotid artery blood flow as a quantitative indicator of cerebral blood flow for the assessment of changes in middle cerebral artery diameter

7.1 Overview

The use of transcranial Doppler ultrasound for the assessment of cerebral hemodynamics is dependent on the diameter of the insonated vessel remaining constant. As this may not be the case under all conditions, the purpose of the current study was to use measures of common carotid artery (CCA) blood flow to determine potential changes in middle cerebral artery (MCA) diameter with nitroglycerin (NG) and acute changes in the partial pressure of end tidal carbon dioxide ($P_{ET}CO_2$). Data were collected from 12 subjects who performed 30s of breath-hold after a normal inspiration and 20s of breath-hold following 30s of hyperventilation. Data were also collected from these same subjects before and after stimulation with NG. MCA and CCA velocity were continuously recorded throughout the test. CCA flow was calculated from diameter measures taken at rest, after the 30s of hyperventilation, after each of the breath holds, and every 30s after NG for 9 minutes. Regression analysis was performed to determine the relationship between MCA velocity and CCA flow for both NG and acute changes in $P_{ET}CO_2$. No relationship was found between CCA flow and CBFV with NG confirming the dilation of the MCA with NG. With changes in $P_{ET}CO_2$ a significant non-linear relationship was found between MCA velocity and CCA flow suggesting the dilation of the MCA with acute changes in $P_{ET}CO_2$. Using CCA flow as a quantitative measure of cerebral blood flow, a 13% dilation of the MCA was found with NG. With alterations in $P_{ET}CO_2$, the MCA diameter was found to increase by 8% with hypoventilation and decrease by 7% with hyperventilation. The results of this study demonstrate that the diameter of the MCA does not remain constant with NG or acute changes in $P_{ET}CO_2$ emphasizing the need to quantitative measures of cerebral blood flow.

7.2 Introduction

Transcranial Doppler ultrasound (TCD) is frequently used as a method for the non-invasive estimation of cerebral blood flow. However, TCD is limited in that the diameter of the insonated vessel, traditionally the middle cerebral artery (MCA) is not known and therefore, cerebral blood flow velocity (CBFV) is measured and not quantitative measures of cerebral blood flow. As the diameter of the MCA may not remain constant under all conditions, the quantitative assessment of blood flow in vessels supplying the cerebral circulation may provide a more complete picture of changes in cerebrovascular hemodynamics including calculations of potential changes in MCA diameter.

The common carotid artery (CCA) is a readily accessible vessel which provides a non-invasive indication of cerebral blood flow. The CCA bifurcates to form the internal (ICA) and external (ECA) carotid arteries with approximately 65% of blood flow going to the cerebral circulation via the ICA at rest (Sato, Ogoh, Hirasawa, Oue, & Sadamoto, 2011). Recently, Sato et al. (Sato et al., 2012) have demonstrated that ECA flow does not change with hyper- and hypo-capnia which suggests that the observed changes in ICA flow are reflected in CCA flow. Therefore, these results suggest that the CCA provides a quantitative assessment of cerebral blood flow with changes in CO_2.

Nitroglycerin has been frequently used in research settings as a method to elicit maximal vasodilation independent of the endothelium (Bleeker et al., 2005; Bonnin et al., 2001; Platts et al., 2009). With respect to the cerebral circulation, studies have consistently shown a reduction in CBFV with NG (Bishop et al., 1986; Poeppel et al., 2007; Ulrich et al., 1995; Dahl et al., 1992; Muller et al., 1995; Dahl et al., 1994). However, this reduction has been shown to result from dilation of the MCA (Hansen et al., 2007) with no changes in cerebral blood flow (Borisenko & Vlasenko, 1992; White et al., 2000). In addition to the assumption of no change in cerebral blood flow with NG, the MCA diameter change can also be calculated using CCA flow as a quantitative indication of cerebral blood flow.

In a recent study, Willie et al. (Willie et al., 2012) showed that with change in the arterial partial pressure of carbon dioxide ($PaCO_2$), CBFV measures underestimated the

change in cerebral blood flow as measured by internal carotid artery blood flow, thus suggesting the potential dilation or constriction of the MCA. This is in contrast to other work that has suggested that the diameter of the MCA remains constant with changes in $PaCO_2$ (Giller et al., 1993; Serrador et al., 2000; Valdueza et al., 1997). Willie et al. (Willie et al., 2012) utilized 15 minute step changes in PaCO2 to assess CBFV and ICA blood flow responses which could influence the CBFV responses to hyper- and hypo-capnia. Therefore, it is unclear if similar changes in MCA diameter would be observed over a shorter time frame, or if the observed changes are due to the duration of the CO_2 stimulus.

The purpose of this study was to assess CBFV responses along with quantitative measures of CCA blood flow to determine potential MCA diameter changes with NG and acute changes in $PaCO_2$. It was hypothesized that no relationship would exist between CCA blood flow and CBFV with NG indicating the dilation of the MCA. With changes in $PaCO_2$, it was hypothesized that a non-linear relationship would be seen between CBFV and CCA blood flow indicating changes in MCA diameter with acute changes in $PaCO_2$.

7.3 Methods

Twelve individuals were tested (six men) with a mean age of 26±4 years (mean ± SD). All experimental procedures were approved by the University of Waterloo, Office of Research Ethics, and protocol conducted in accordance with the declaration of Helsinki. All participants signed informed consent and were aware of their right to withdraw from the study at any time without prejudice.

Participants were requested to abstain from consuming caffeine for 12 hours and food for two hours before the start of the testing session. All testing took place with participants at supine rest. Variations in ventilation were used to manipulate end tidal CO_2 ($P_{ET}CO_2$) thought to reflect alterations in $PaCO_2$. Two bouts of hypoventilation and two bouts of hyperventilation, each separated by 1.5 minutes of rest, were performed by the participants. Hypoventilation consisted of 30s of breath hold in which subjects were instructed to start the breath hold at the end of a normal inspiration. For hyperventilation testing, subjects were

instructed to increase tidal volume and slightly increase breathing frequency to achieve a low level of hyperventilation. This breathing pattern was maintained for 30s immediately after which subjects performed a 20s breath hold which was initiated at the end of an inspiration. Expired CO_2 was measured (Colin, Pilot, San Antonio, TX) from a nasal cannula. Values were recorded as percent CO_2 and later converted to mmHg based on ambient temperature and barometric pressure.

Subjects always performed the NG testing following the manipulations in $P_{ET}CO_2$. Previous work has shown the effects of NG stimulation on CBFV persisting for, on average, 30 minutes after stimulation (Dahl et al., 1989). Therefore, the testing was done in this order to avoid any confounding effects on NG on the CO_2 testing. For the NG testing, two minutes of supine rest were recorded for baseline measures after which 0.4mg of NG was administered sublingually (Nitrolingual ®). Data were recorded continuously for 10 minutes after NG stimulation.

7.3.1 Cardiovascular Variables

Heart rate (HR) was determined using a standard three lead electrocardiogram and arterial blood pressure continuously recorded using finger photoplethysmography (Finometer, Finapres Medical, Amsterdam). TCD was used for the assessment of CBFV with a 2MHz Doppler ultrasound probe fixed in place using a head band over the temporal window allowing for the insonation of the right MCA (Multigon Industries, New York, NY). Blood velocity was assessed in the ipsilateral common carotid artery using a 4MHz Doppler probe with a fixed 45° angle (Multigon Industries, New York, NY). It was assumed that the common carotid artery was parallel to the skin surface and, therefore, velocity measures were corrected for a 45° angle of insonation. The beat-by-beat means of the outer envelopes of the MCA and CCA velocity signals were determined for analysis.

Echo Doppler ultrasound imaging (MicroMaxx, SonoSite Inc, USA) of the left CCA was conducted for the measurement of CCA diameter which was used with the measures of CCA velocity for the calculation of blood flow. For diameter measurement, an M-mode tracing of the left CCA was obtained approximately 2cm away from the carotid bifurcation

and diameter measured from the recorded M-mode tracing using edge detection software. Systolic (maximum) and diastolic (minimum) diameters were determined from the M-mode tracing and CCA diameter calculated as: Diameter = (1/3)*Systolic + (2/3)*Diastolic. Diameter measures were determined at the start and end of each bout of hyper- and hypoventilation, the beginning of breath hold following hyperventilation, at baseline before NG, and ever 30s for 9 minutes following NG administration.

7.3.2 Data Analysis

The protocol consisted of each subject performing two trials of hyperventilation and hypoventilation; however, due to probe movement during hyperventilation, two subjects only had a single hyperventilation trial. Therefore, 24 hypoventilation trials and 22 hyperventilation trials were used to assess the relationship between CCA blood flow and CBFV. Mean arterial pressure (MAP) was determined as the mean over a cardiac cycle. Similarly, CCA blood velocity and CBFV were determined as the mean of the outer envelope of the Doppler spectrum over a cardiac cycle. Vascular resistance of the CCA was calculated as CCA_{VR} = MAP / CCA flow. Similarly, an index of cerebrovascular resistance was calculated at CVRi = MAP / CBFV.

Resting values were determined as 10s averages taken before each bout of hyper- and hypo-ventilation. Similarly, peak responses were determined as 5s averages after breath hold, or at the end of hyperventilation. Resting $P_{ET}CO_2$ values were determined and compared to peak responses defined as the average of the last three end tidal values of the hyperventilation, and the first end tidal value after breath hold.

With respect to the NG responses, a 30s average was taken during the resting baseline period and compared to values four minutes after the administration of NG. For these data, two different methods of assessing changes in MCA diameter were used. First, as previously suggested (Borisenko & Vlasenko, 1992; White et al., 2000) cerebral blood flow was assumed to remain constant with the administration of NG and the percent change in MCA diameter was calculated as previously described (Dahl et al., 1989; Borisenko & Vlasenko, 1992) using the following equation:

(Equation 1) $$\Delta d\% = \left(\sqrt{\frac{CBFV_1}{CBFV_2}} - 1\right) \times 100$$

Where $CBFV_1$ is the resting baseline value and $CBFV_2$ is the value four minutes after NG stimulation. The second method assumed that changes in cerebral blood flow might have occurred with NG and CCA blood flow was used as a surrogate of cerebral blood flow to calculate the theoretical change in MCA diameter as:

(Equation 2) $$\Delta d\% = \left(\sqrt{\frac{CCA_2}{CBFV_2} \times \frac{CBFV_1}{CCA_1}} - 1\right) \times 100$$

Where, again, $CBFV_1$ and CCA_1 are baseline averages of cerebral blood velocity and common carotid artery blood flow respectively, and $CBFV_2$ and CCA_2 are values four minutes after NG stimulation.

Beat-by-beat data was linearly interpolated to second-by-second values and averaged across both trials for each subject. Hypo- and hyperventilation data was combined and linear regressions analysis was performed on these data for each subject to determine the relationship between CCA flow and CBFV with changes in $P_{ET}CO_2$ (SigmaPlot 11.0, Systat Software Inc., Chicago, IL) Data for NG testing were averaged over 30s periods and linear regressions performed for each subject using the 30s averages to test for a relationship between CCA flow and CBFV using linear regression.

Beat-by-beat data for hyper- and hypoventilation were linearly interpolated to second-by-second values and averaged across both trials for each subject. Hypo- and hyperventilation data was combined and regressions analysis was performed on these data for each subject to determine the relationship between CCA flow and CBFV with changes in $P_{ET}CO_2$ (SigmaPlot 11.0, Systat Software Inc., Chicago, IL). Two different curves (linear and a four component sigmoid curve) were used to fit the CCA flow and CBFV relationship with the resulting fits compared using an F ratio. For this test, the residual sum of squares (RSS) for each curve was compared to determine the F ratio as:

(Equation 3) $$F = \frac{(RSS_1 - RSS_2)/(DF_1 - DF_2)}{RSS_2/DF_2}$$

For this equation, RSS_1 and RSS_2 are the residual sums of squares for the linear and sigmoid curves with DF_1 and DF_2 degrees of freedom respectively.

General hemodynamic responses to changes in CO_2 and NG were assessed using a one-way repeated measures analysis of variance (SigmaStat 3.5, Systat Software Inc., Chicago, IL). For all test, statistical significance was set at $p<0.05$.

7.4 Results

Cardiovascular responses to changes in $P_{ET}CO_2$ and NG, presented in Table 7.1, indicated that HR was not changed with either hypo- or hyperventilation. Conversely, MAP was seen to increase with hypoventilation and decrease with hyperventilation. Hemodynamic responses in Table 7.2 showed that hypoventilation elicited approximately a 32% increase in CBFV and a 14% increase in CCA flow where hyperventilation served to decrease CBFV and CCA by 31% and 16% respectively and NG decreased CBFV by 13% with no change in CCA flow. No changes were seen with CCA_{VR} but CVRi was increased 27% with hyperventilation and decreased 19% with hypoventilation.

Results from the assessment of CBFV and CCA blood flow responses, presented in Figure 7.1, showed a reduction in CBFV but no change in CCA blood flow. Linear regression analysis of the CBFV and CCA flow relationship with NG showed weak, but significant relationship ($P<0.05$) for 4 of the 12 subjects with an average R^2 value of 0.299±0.107. For the remaining 8 subjects, no significant relationships were seen between CBFV and CCA flow ($P>0.05$) with an average R^2 of 0.038±0.056. The results from NG stimulation suggest that, as expected the MCA dilated with NG producing a reduction in CBFV with no change in cerebral blood flow as seen by the lack of change in CCA flow and the lack of linear relationships between CBFV and CCA flow. The calculation of MCA diameter change with NG stimulation resulted in a 13.2±6.1% dilation.

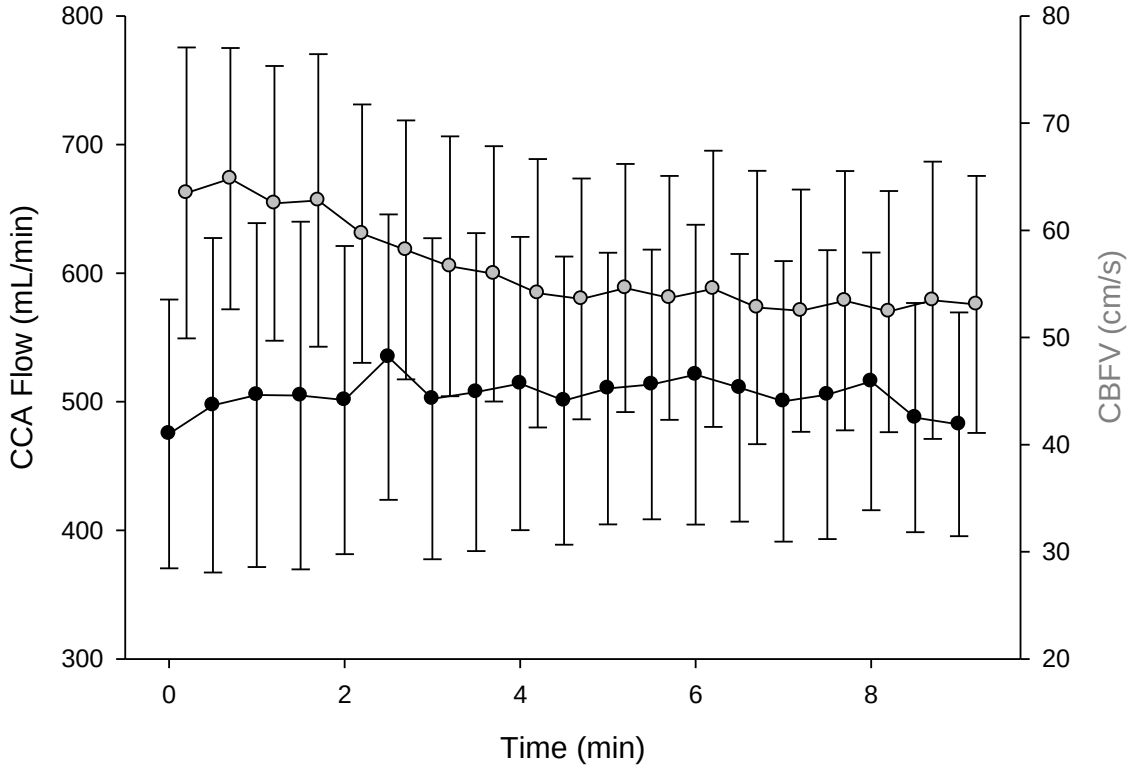

Figure 7.1:CCA and MCA response to NG

Responses to NG of CCA flow (black circles) and CBFV (grey circles) (mean ± SD). Statistical analysis was conducted on values at 4 and 9 minutes (Table 7.2) showing no changes in CCA flow, but a decrease in CBFV.

With alterations in $P_{ET}CO_2$, all 12 subjects showed a significant linear relationship with an average R^2 value of 0.795±0.196. Although all subjects showed significant linear relationships between CBFV and CCA flow with hyper- and hypo-ventilation, inspection of the resulting residuals (Figure 7.2 A) suggested a non-linear relationship. Therefore, non-linear regression analysis using a four parameter sigmoid curve was conducted showing significant relationships for all subjects with an average R^2 of 0.825±0.167. For each individual, the linear and non-linear curve fits were compared using the F ratio. Results found that the nonlinear curve provided a better fit for the data for 9 of the 12 individuals ($P<0.05$) with strong trends for 2 of the remaining 3 ($P=0.075$ and $P=0.077$). A representative

data set is presented in Figure 7.2, which shows the linear regression model (Figure 7.2 A) and the sigmoid regression model (Figure 7.2 B) suggesting a better fit with the non-linear regression. Using CCA flow as a surrogate measure of cerebral blood flow, the calculated MCA diameter changes using Equation 2 were -6.8±2.7% and 7.8±7.2% for hyper- and hypoventilation respectively.

Table 7.1: Cardiovascular responses to $P_{ET}CO_2$ and NG

	$P_{ET}CO_2$ (mmHg)	HR (bpm)	MAP (mmHg)
Baseline	37.02±3.06	62.60±10.78	93.16±7.38
Hypoventilation	42.92±2.81*	65.88±20.48	98.31±8.28*
Hyperventilation	23.07±4.96*	65.74±13.08	81.77±8.80*
Nitro	37.54±4.00	60.38±7.88	90.98±5.80

*Values show the mean ± SD with values that are statistically different from baseline denoted by * ($P<0.05$).*

Table 7.2: Hemodynamic responses to $P_{ET}CO_2$ and NG

	CCA Flow (mL/min)	CBFV (cm/s)	CCA_{VR} (mmHg/mL/min)	CVRi (mmHg/cm/s)
Baseline	486.93±99.79	62.52±13.02	0.199±0.044	1.57±0.44
Hypoventilation	553.77±113.43*	82.74±20.12*	0.184±0.035	1.27±0.39*
Hyperventilation	397.11±116.23*	43.05±9.04*	0.223±0.070	1.99±0.57*
Nitro	514.20±114.02	54.13±12.52*	0.184±0.036	1.79±0.55*

*Values show the mean ± SD with values that are statistically different from baseline denoted by * ($P<0.05$).*

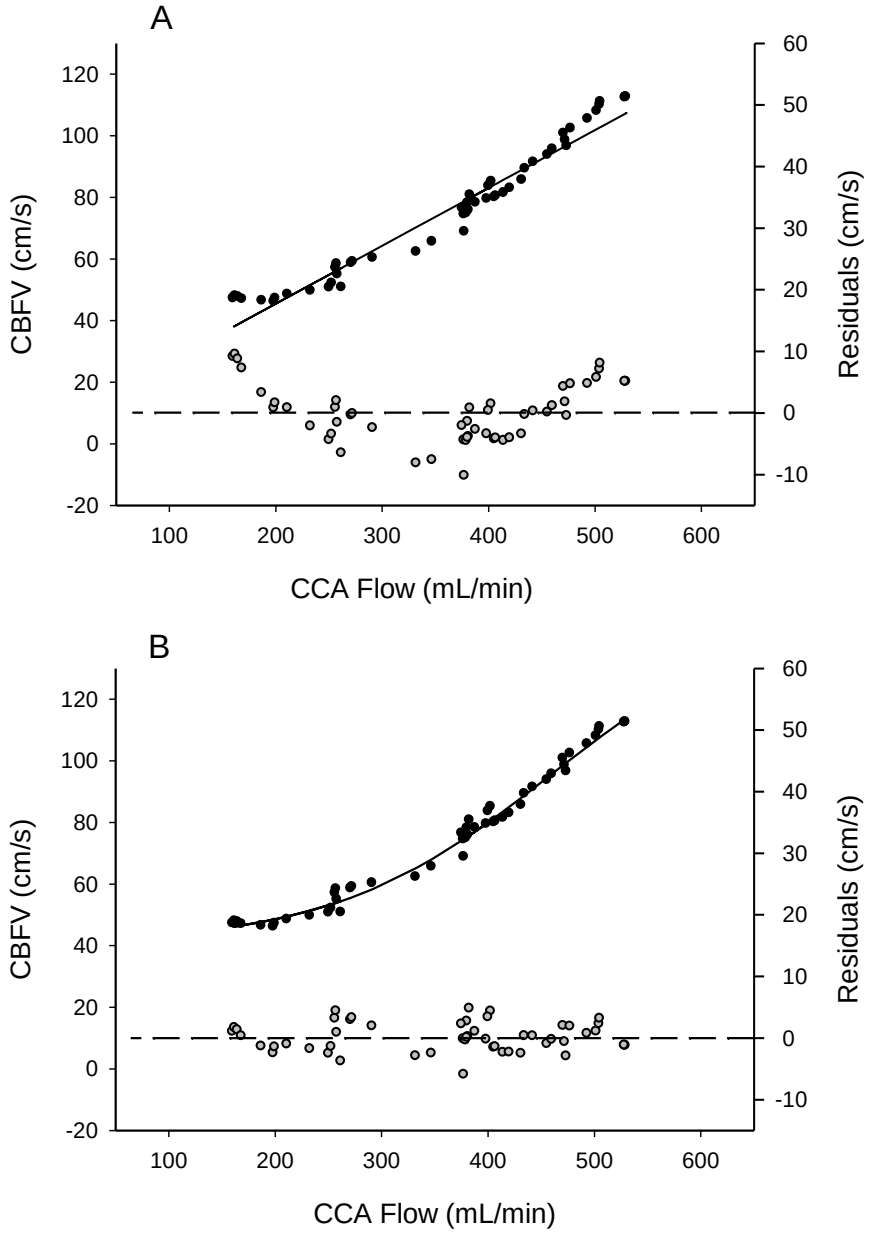

Figure 7.2:Linear verses non-linear curve fit

Representative regression results (black dots) with data from hyper- and hypo-ventilation. Linear regression results (Panel A) were statistically significant (P<0.0001) with an R^2 value of 0.952. Non-linear regression results of the same data (Panel B) were also statistically significant (P<0.0001) with a larger R^2 value of 0.988. Calculation of the F ratio of this data showed that the non-linear curve provided a better fit with a more random distribution of residuals (grey dots).

7.5 Discussion

This study provided the opportunity to study simultaneously the responses of cerebral blood flow velocity in the middle cerebral artery and blood flow in the common carotid artery with alterations in $P_{ET}CO_2$ and NG stimulation. In support of the hypotheses, the results of this study found a sigmoid relationship between CCA blood flow and CBFV with change in $P_{ET}CO_2$, and no relationship between CCA blood flow and CBFV with NG stimulation suggesting, in both instances, changes in the diameter of the MCA. This is the first study to show a non-linear relationship between CBFV and CCA blood flow with acute changes in $P_{ET}CO_2$ suggesting a change in the diameter of the MCA.

7.5.1 MCA and NG

Consistent with the hypothesis, no relationship was seen between CBFV and CCA flow with NG stimulation, as CCA flow was not changed, which suggested dilation of the MCA with NG. This result is consistent with previously reported data that showed reductions in MCA velocity with no changes in cerebral blood flow (Dahl et al., 1989; Dahl et al., 1990; Borisenko & Vlasenko, 1992; White et al., 2000). Previous work by Dahl et al. (Dahl et al., 1989) using regional blood flow calculated that a diameter increase of the MCA of 15% was necessary to account for the reduction in CBFV with no change in cerebral blood flow. More recently, a study by Hansen et al (Hansen et al., 2007) used MRI to directly measure the diameter of the MCA after NG stimulation finding diameter increases of 10-14%. The current study, using CCA blood flow to calculate the changes in MCA diameter, found a 13% dilation of the vessel which is consistent with the previous studies.

7.5.2 MCA and $P_{ET}CO_2$

The literature has been split on whether the MCA changes diameter with alterations in $PaCO_2$. Several studies have suggested that the diameter remains constant as a strong relationship has been seen between cerebral blood flow and CBFV with acetazolamide testing (Dahl et al., 1992; Muller et al., 1995; Ulrich et al., 1995), hypercapnia (Bishop et al., 1986; Muller et al., 1995; Poeppel et al., 2007), and hypocapnia (Poeppel et al., 2007). In addition, MRI studies have also suggested no change in the diameter of the MCA with

acetazolamide testing (Schreiber et al., 2000) and changes in $P_{ET}CO_2$ (Serrador et al., 2000; Valdueza et al., 1997). However, limitations in the measurement methods may have contributed to this lack of observable change.

One of the most cited papers suggesting that the diameter of the MCA remains constant with manipulations in $P_{ET}CO_2$ is that of Serrador et al. (Serrador et al., 2000). In this study, the diameter of the MCA was measured under manipulations of $P_{ET}CO_2$ and with the application of lower body negative pressure; however, questions remain as to the ability of this study to detect small changes in MCA diameter. In this study, it was reported that the pixel resolution of images was 0.47mm (Serrador et al., 2000). With a reported average MCA diameter of 2.5mm (Serrador et al., 2000), the pixel resolution would equate to approximately 19% of the diameter of the vessel. Even assuming that the employed measurement techniques were able to improve this resolution, it is still unlikely that they were able to accurately detect changes in the MCA diameter less than 0.25mm, or 10% of the resting MCA diameter. This does have implications for TCD studies a 10% change in diameter with velocity remaining constant would equate to a 21% change in cerebral blood flow. Similarly, if cerebral blood flow is constant, a 10% change in diameter could offset a 17% change in velocity.

Several studies have suggested that the diameter of the MCA does not remain constant with manipulation in $P_{ET}CO_2$. Work by Valdueza et al. (Valdueza et al., 1999) quantified cerebral blood flow by using simultaneous Doppler measures of MCA and sphenoperietal sinus blood velocity. Through comparison of arterial and venous blood velocity, it was concluded that increases in $P_{ET}CO_2$ can result in change in MCA diameter. In a separate study, Dahl et al. (Dahl et al., 1994) found no correlation between changes in cerebral blood flow and CBFV with acetazolamide, again, suggesting a change in MCA diameter. Although MCA diameter was not directly assessed, work by Poeppel et al. (Poeppel et al., 2007) showed variations in changes in regional cerebral blood flow and CBFV also suggesting changes in MCA diameter to account for this difference. Finally, in a study by Eicke et al. (Eicke et al., 1999), similar to the current study, CBFV was compared to CCA blood flow showing a linear relationship between the two variables with changes in

$P_{ET}CO_2$. However, when CCA flow was used to calculated percent changes in MCA diameter, a 6% increase and a 4.5% decrease were found with increased and decreased $P_{ET}CO_2$ respectively. Most recently, Willie et al. (Willie et al., 2012) showed that CBFV measures underestimated changes in cerebral blood flow with 15 minute step increases and decreases in $PaCO_2$. However, the current study is the first to suggest that changes in MCA diameter can occur within 30s of breath hold or hyperventilation.

7.5.3 Limitations

The most noteworthy limitation of this study was the use of blood flow in the common carotid artery as a surrogate for cerebral blood flow. Blood flow in the MCA is supplied by the ICA which is in turn supplied by the CCA. However, the CCA also provides blood flow through the ECA. It is possible that changes in flow distribution between the ICA and ECA may have accounted for some of the variation in result. However, the recent study by Sato et al. (Sato et al., 2012) showed that ECA blood flow was not changed with variation in $PaCO_2$. Therefore, it is believed that the observed changes in CCA flow in the current study were indicative of changes in cerebral blood flow.

7.6 Conclusion

Consistent with the hypotheses, this study was able to demonstrate a strong relationship between CCA blood flow and CBFV with changes in $P_{ET}CO_2$ and no relationship between these variables with NG stimulation suggesting dilation of the MCA. In addition, this was the first study to show that the relationship between CCA blood flow and CBFV with acute changes in $P_{ET}CO_2$ was non-linear thereby suggesting changes in MCA diameter. This study highlights the need to quantitative assessments of cerebral blood flow, as the diameter of the MCA appears to be changing with acute manipulations in $P_{ET}CO_2$.

Chapter 8

Cerebral blood velocity responses to changes in CO_2 and the relationship to carotid artery blood flow

8.1 Overview

Transcranial Doppler ultrasound has been used to assess cerebral blood velocity (CBFV) in the middle cerebral artery (MCA) with characteristics of the within beat velocity profile being used as a potential method for determining cerebrovascular tone. However, changes in MCA diameter and cerebral blood flow may distort these measures. Therefore, the purpose of this study was to simultaneously assess MCA velocity and common carotid artery (CCA) velocity to determine potential changes in cerebrovascular tone with changes in the partial pressure of end tidal carbon dioxide ($P_{ET}CO_2$). Data were collected from 12 individuals who performed 30s of hyperventilation and 30s of breath-hold to manipulate $P_{ET}CO_2$. Arterial pressure, MCA velocity, and CCA velocity were continuously measured throughout the test. Velocity waves were assessed to determine key inflection point which allowed for the calculation of the Doppler resistance indices (RI=(systolic-diastolic)/systolic and PI=(systolic-diastolic)/mean), the augmentation index (AI=(reflected peak-diastolic)/(systolic-diastolic) x 100%), and critical closing pressure. The Doppler resistance indices calculated for the MCA and CCA both showed an increase and decrease with hyper- and hypoventilation respectively. However, only the MCA showed variation in other velocity wave inflection points, the calculation of AI, and the calculation of CrCP suggesting that alterations in the cerebral circulation are not reflected in the CCA velocity wave. Assessment of the augmentation index suggested an increase and decrease in cerebrovascular compliance with hyper- and hypoventilation respectively. In contrast the calculation of CrCP suggested a reduction in cerebrovascular tension with hypoventilation and an increase with hyperventilation. These results suggest that in the cerebral circulation, vascular tension changes independently from cerebrovascular compliance with changes in $P_{ET}CO_2$ and highlight that cerebrovascular tone is comprised of multiple factors that may be independently changing within the confines of the skull.

8.2 Introduction

Assessment of the within beat characteristics of the middle cerebral artery (MCA) blood velocity trace provides a potential method for the determination of cerebrovascular tone. It has been suggested that both the augmentation index (AI) (Robertson et al., 2008) and critical closing pressure (Panerai, 2003) reflect changes in cerebrovascular tone. However, little work has been done to systematically relate changes in the MCA velocity trace to quantitative measures of cerebral blood flow or other within beat characteristic with changes in cerebral blood flow.

Studies have looked at changes in cerebral blood velocity waveforms in a number of conditions including hypercapnia (Robertson et al., 2008) and stimulation with nitroglycerin (Lockhart et al., 2006). Previous work has shown and increase in the augmentation index, calculated from the MCA velocity wave profile, with aging (Kurji et al., 2006) and hypercapnia (Robertson et al., 2008) suggesting a reduction in pulse wave transit time with an early return of the reflected wave potentially due to an increase in vascular tone and reduction in vascular compliance. Conversely, work with critical closing pressure (CrCP) has shown a decrease in CrCP with hypercapnia (Ainslie et al., 2008; Panerai, 2003; Panerai et al., 1999) suggesting a decrease in vascular tone and increase in vascular compliance. The quantitative assessment of cerebral blood flow may help to explain the discrepancy between CrCP and AI interpretations of cerebrovascular tone with changes in CO_2.

The common carotid artery (CCA) may provide a readily accessible artery for the assessment of cerebral blood flow and potential assessment of cerebrovascular tone. Previous work has dilation and constriction of the MCA with changes in the partial pressure of end tidal carbon dioxide ($P_{ET}CO_2$) using CCA blood flow as a surrogate for cerebral blood flow (Chapter 7). Assessment of within beat characteristics of the MCA and CCA velocity waves has suggested that alterations in MCA waveform shape with nitroglycerin are reflected in similar alterations in the CCA waveform (Chapter 6). To date, no work has looked at the simultaneous assessment of MCA velocity waveforms and CCA velocity waves to determine if CCA measure can be used to describe changes in cerebrovascular properties and

potentially explain the apparently contradictory results between changes in the MCA velocity wave profile and the calculation of CrCP with changes in $P_{ET}CO_2$.

In this study, it was hypothesized that the MCA velocity wave would show changes in key inflection points with alterations in $P_{ET}CO_2$ and that these changes would be reflected in the CCA flow waveform. Therefore, the purpose of this study was to characterize changes in the MCA and CCA velocity waves in hope that the assessment of the CCA velocity wave would help to explain the apparent conflicting cerebrovascular tone results between the calculation of the augmentation index and critical closing pressure.

8.3 Methods

Data for this study were acquired during the same study as Chapter 7. Therefore, the experimental protocol was as previously described (Chapter 7) with the additional data analysis as follows.

8.3.1 Data Analysis

The protocol consisted of each subject performing two trials of hyperventilation and hypoventilation; however, due to probe movement during hyperventilation, two subjects only had a single hyperventilation trial. Therefore, 24 hypoventilation trials and 22 hyperventilation trials were used to assess the relationship between CCA blood flow and CBFV. Mean arterial pressure (MAP) was determined as the mean over a cardiac cycle. Similarly, CCA blood velocity and CBFV were determined as the mean of the outer envelope of the Doppler spectrum over a cardiac cycle. Vascular resistance of the CCA was calculated as CCA_{VR} = MAP / CCA flow. Similarly, an index of cerebrovascular resistance was calculated at CVRi = MAP / CBFV.

For the assessment of velocity wave characteristics of both the MCA and CCA, ten consecutive cardiac cycles were averaged to produce a representative wave for each resting period before hyper- and hypo-ventilation and at each peak response point for hyper- and hypoventilation. The representative waves were then assessed for key inflection points shown in Figure 8.1. All inflection points were assessed with respect to end diastolic velocity, T1, as

P1-T1, T2-T1, P2-T1, T3-T1, and P3-T1 where T represents at trough and P represents a peak inflection point of the wave to provide an indication of the shape of the waveform. As previously described (Robertson et al., 2008; Kurji et al., 2006), the peaks P1 and P2 of the velocity wave were used with the end diastolic value T1 for the calculation of an augmentation index as AI = (P2-T1) / (P1-T1) x 100%. The Doppler resistance indices, RI and PI, were calculated as RI = (P1-T1) / P1, and PI = (P1-T1) / Vmean, where Vmean was the mean velocity calculated from the average CCA or MCA blood velocity wave.

For each of the ten cardiac cycles used to generate the representative waveform, CrCP was calculated using a two point method of mean arterial pressure CBFV and diastolic pressure and velocity as previously described (Panerai et al., 2011). Briefly, the slope of the relationship between CBFV and MAP was calculated as a = (CBFVmean – CBFVdia) / (MAP – DBP). RAP was then calculated as RAP = 1 / a and CrCP calculated as CrCP = MAP – (CBFVmean / a). Using this same, method an index of CrCP was also calculated using the CCA velocity wave.

Inflection point and CrCP changes with $P_{ET}CO_2$ were assessed using a one-way repeated measures analysis of variance (SigmaStat 3.5, Systat Software Inc., Chicago, IL).

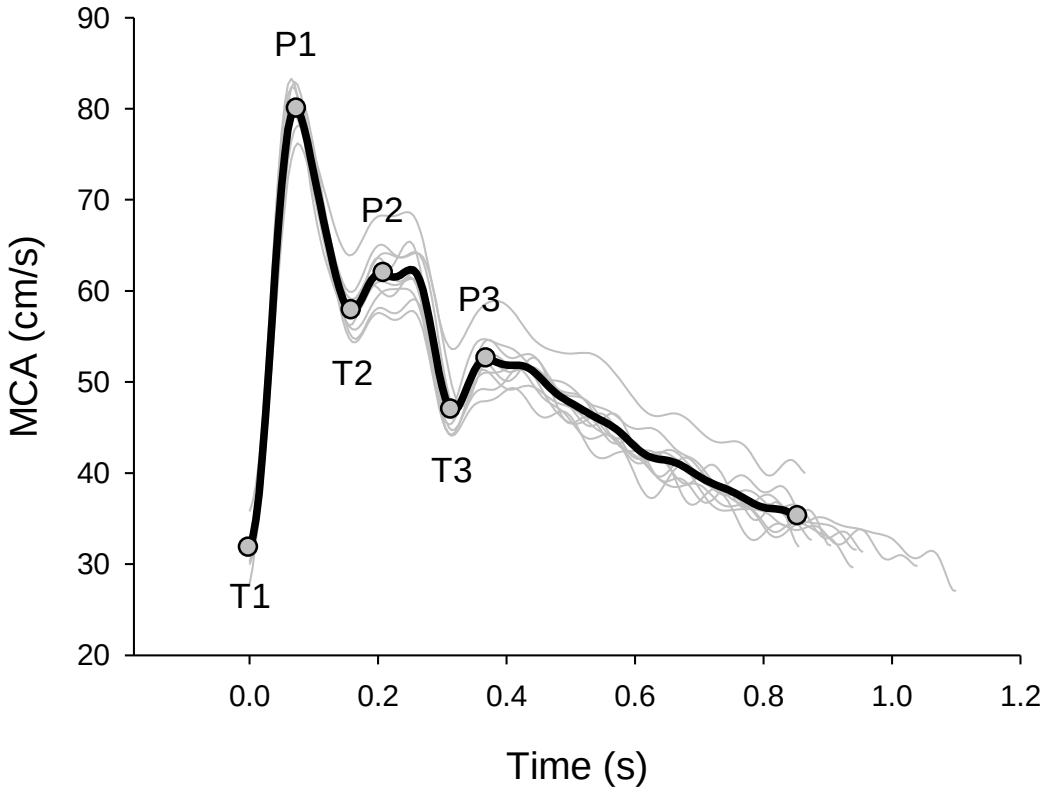

Figure 8.1: Representative average MCA velocity wave

The figure depicts 10 beats of MCA velocity (grey lines) that were averaged to produce the representative wave (black line). The velocity wave was then assessed for key inflection points; end diastolic velocity (T1), the systolic peak (P1), the following trough (T2), reflected peak (P2), dicrotic notch (T3), and the following peak (P3). Changes in waveform shape with alterations in CO_2 were then determined by comparing inflection points to the end diastolic, T1, value.

8.4 Results

Average velocity waveforms for a representative subject are shown from the MCA (Figure 8.2 A and B) and the CCA (Figure 8.2 C and D) during baseline rest, hypoventilation, and hyperventilation. Changes in $P_{ET}CO_2$ produced changes in mean velocity and end diastolic velocity. Therefore, to assess changes in the waveform shape, key

inflection points were assessed with respect to the end diastolic velocity (T1). Results from the assessment of the inflection points, presented in Table 8.1, show significant changes in all inflection points of the MCA with respect to T1 during changes in $P_{ET}CO_2$. In contrast to the MCA results, only the peak CCA velocity point was significantly increased with hyperventilation and no other differences were found with any of the other inflection points or the calculation of the augmentation index.

For both the CCA and MCA the Doppler resistance indices (RI and PI), AI, CrCP, and RAP are presented in Table 8.2. Both CCA and MCA RI and PI were increased with hyperventilation and reduced with breath hold. The MCA AI was significantly increased with hypoventilation decreased with hyperventilation but no changes were seen in CCA AI. MCA CrCP was increased with hyperventilation and reduced with hypoventilation but again, no changes were seen in CrCP calculated with the CCA velocity wave. RAP was not changed with hypo- and hyperventilation when calculated with either the MCA or the CCA.

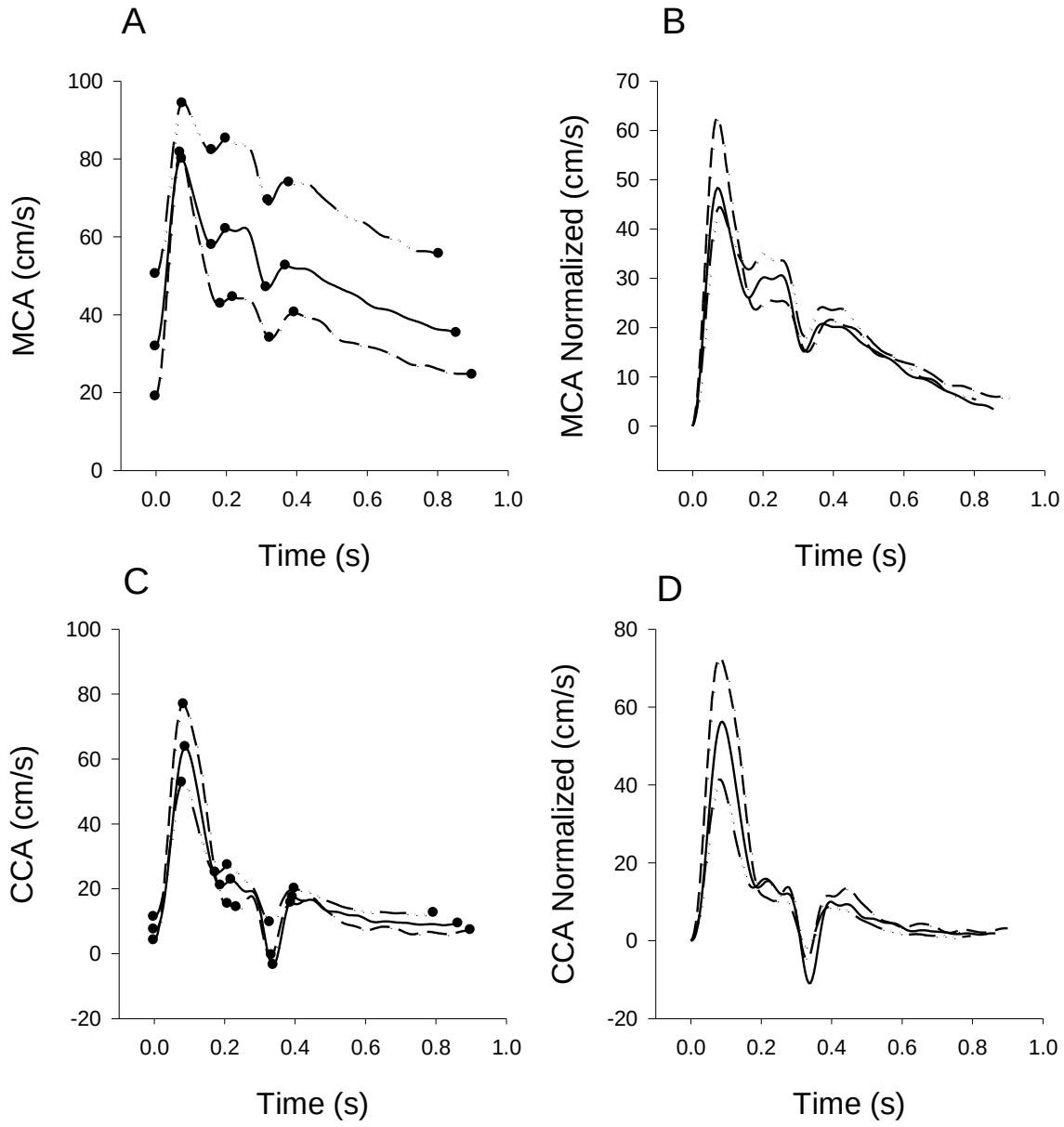

Figure 8.2: Representative MCA and CCA waves

Representative data from one individual for average MCA (panel A and B) and CCA (panel C and D) velocity waves at rest (solid black line), hypoventilation (dashed dotted line), and hyperventilation (dashed line). Key points are identified as dots on the corresponding waves in panels A and C. Panels B and D show the same velocity waves from panels A and C normalized to end diastolic velocity so that waves started at 0cm/s.

Table 8.1: Velocity wave inflection points with changes in $P_{ET}CO_2$

		P1-T1 (cm/s)	T2-T1 (cm/s)	P2-T1 (cm/s)	T3-T1 (cm/s)	P3-T1 (cm/s)
MCA	Baseline	54.12±15.08	34.57±9.29	35.57±7.12	20.30±6.41	28.00±6.47
	Hypoventilation	51.92±16.50	41.60±11.96*	44.18±12.16*	26.01±8.45*	32.71±8.57*
	Hyperventilation	64.21±20.15*	29.36±10.60*	28.40±9.51*	11.02±5.78*	25.33±5.35
CCA	Baseline	42.82±11.11	15.77±8.43	15.23±6.87	0.72±3.99	11.40±2.61
	Hypoventilation	36.31±10.11	14.80±6.64	15.26±4.93	1.48±3.36	10.60±2.56
	Hyperventilation	58.64±16.40*	18.13±15.89	16.62±12.39	-2.89±7.70	13.75±6.47

*Values show the mean ± SD for differences between inflection points and the end diastolic value (T1). Values that are statistically different from baseline are denoted by * (P<0.05).*

Table 8.2: AI, resistance, and CrCP responses to changes in $P_{ET}CO_2$

		AI (%)	RI	PI	CrCP (mmHg)	RAP (mmHg/cm/s)
MCA	Baseline	69.56±14.57	0.575±0.061	0.887±0.187	30.4±8.2	1.11±0.36
	Hypoventilation	88.50±19.49*	0.477±0.063*	0.644±0.163*	23.0±8.4*	1.00±0.30
	Hyperventilation	46.70±16.55*	0.733±0.068*	1.520±0.346*	39.2±6.7*	1.08±0.37
CCA	Baseline	36.49±15.84	0.838±0.052	2.586±0.632	49.6±10.9	2.70±0.92
	Hypoventilation	43.96±14.95	0.754±0.069*	1.864±0.684*	44.0±12.4	3.00±0.82
	Hyperventilation	26.97±16.18	0.938±0.045*	3.780±0.801*	54.4±6.7	2.02±0.77

*Values show the mean ± SD with values that are statistically different from baseline denoted by * (P<0.05).*

A different view of the changes in waveform shape is presented in Figure 8.3. In this figure, the average wave for all subjects is presented for hyperventilation (red) and hypoventilation (blue) (Figure 8.3 A and B). Assuming the resting average wave represents 0cm/s, the middle panels show the differences between the resting wave and the hyperventilation and hypoventilation waves. Finally, the bottom panels show the same differences accounting for the pressure wave. From this it can be seen that changes in the velocity waves are dependent on the phase of the cardiac cycle. In addition, it can be seen that the majority of change for the CCA occurred during the systolic phase (P1-T1) where the MCA showed change throughout the cardiac cycle. When the pressure wave shape was taken into consideration, it can be seen that the majority of change in the MCA velocity wave occurred during the systolic portion of the cardiac cycle (Figure 8.3 E and F).

To further examine the influence of the pressure wave on the velocity wave, the relationship between the averaged, normalized velocity waves were plotted against the averaged, normalized pressure waves (Figure 8.4). From these plots it can be seen that with hypoventilation Figure 8.4 C), the relationship between MCA velocity and pressure was closer, compared to the relationship with hyperventilation (Figure 8.4 E) which showed a large ‘loop’ portion corresponding to the systolic portion of the waves. Conversely, there appear to be limited differences with the CCA wave to pressure wave relationship.

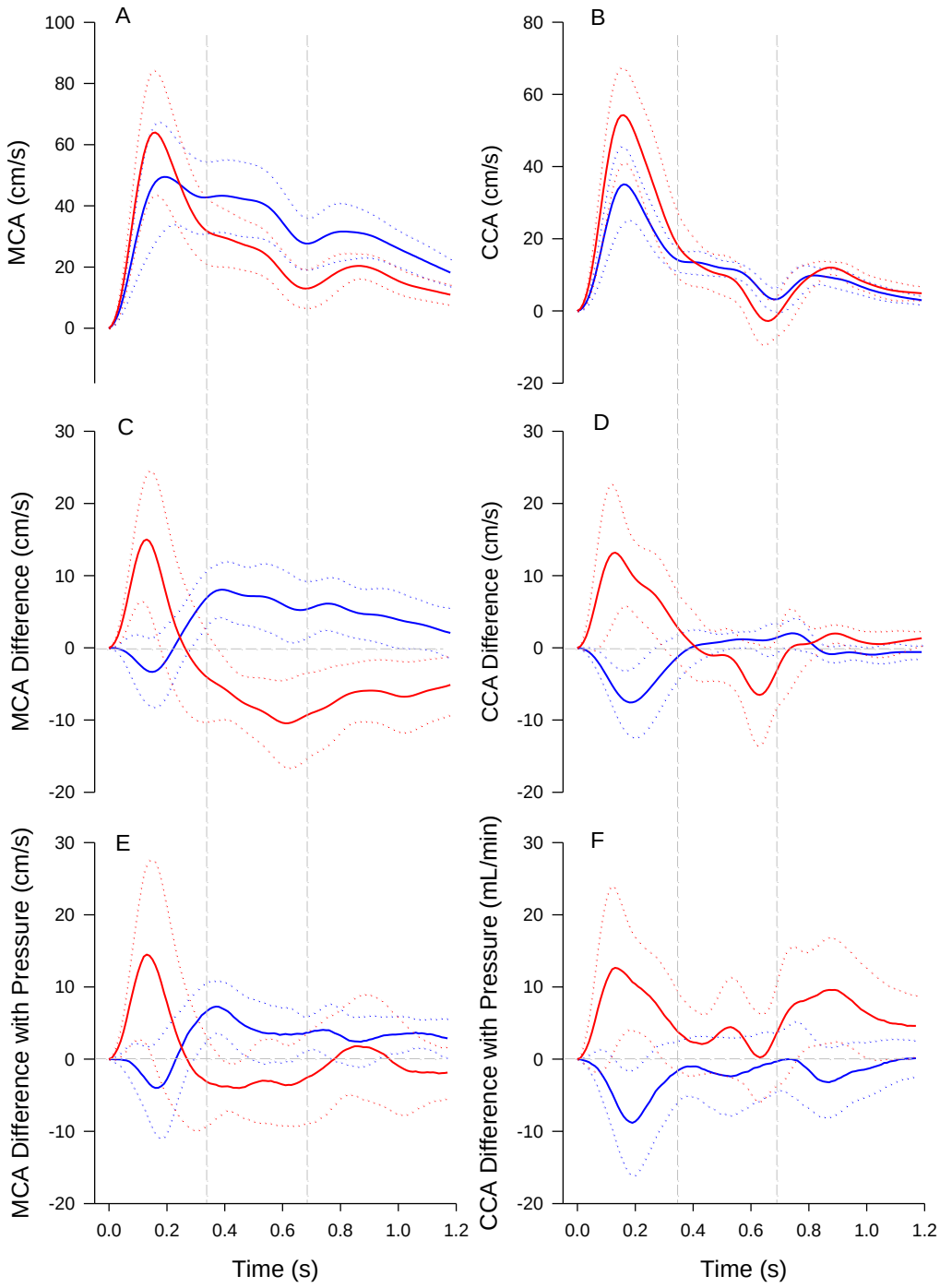

Figure 8.3: Changes in velocity waves

Averages velocity waves (solid) ± SD (dotted) for the raw waveform (A and B) for hyper- (red) and hypoventilation (blue), differences from baseline velocity waves (C and D), and differences from baseline with respect to the pressure wave (E and F).

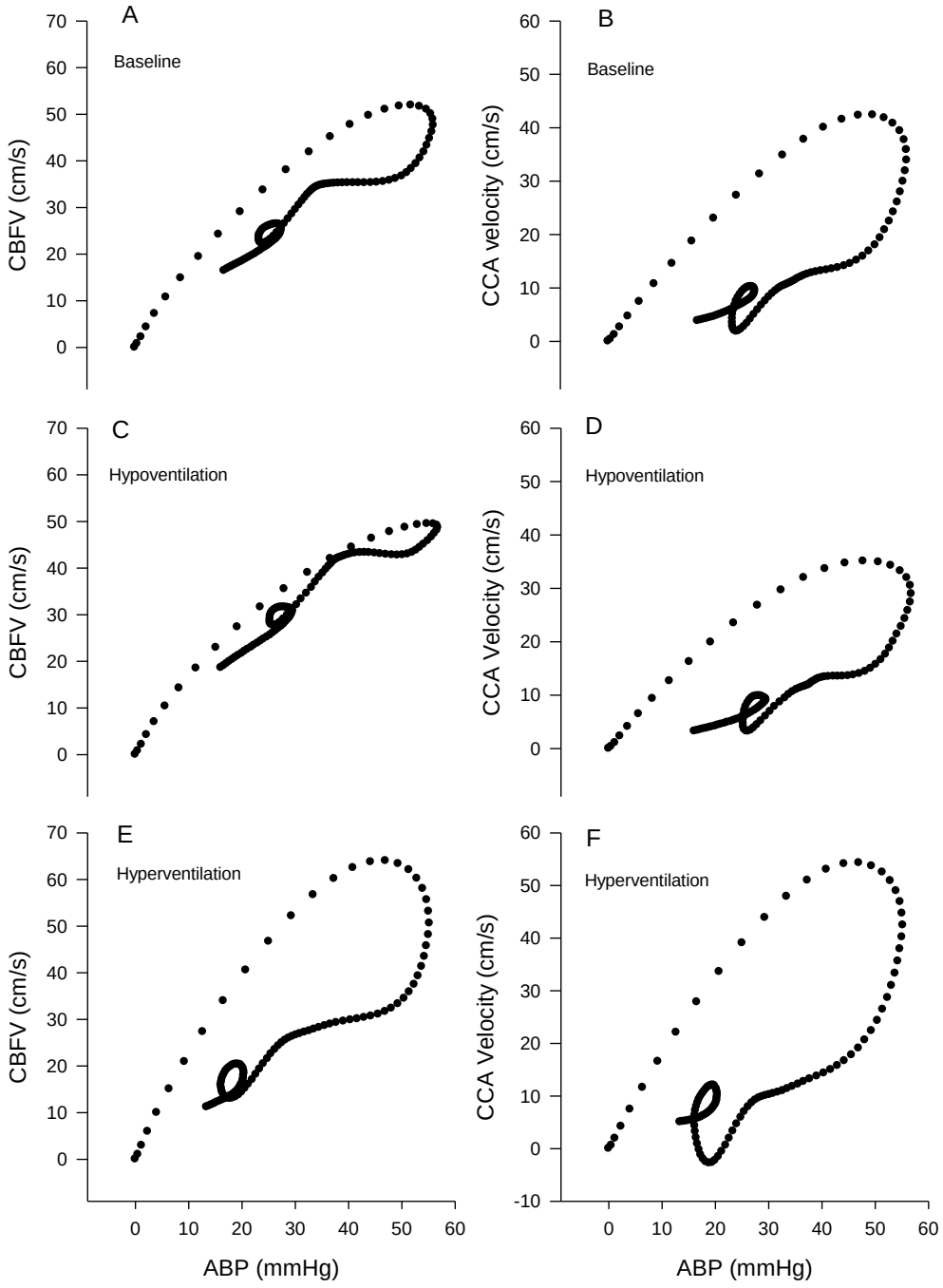

Figure 8.4: MCA and CCA velocity waves versus the arterial pressure wave

Relationships between MCA velocity waves (A, C, and E) and CCA velocity waves (B, D, and F) with the arterial pressure wave at rest (A and B), with hypoventilation (C and D), and with hyperventilation (E and F).

8.5 Discussion

The purpose of the current study was to utilize quantitative measures of CCA blood flow to describe changes in cerebrovascular hemodynamics with changes in $P_{ET}CO_2$. Therefore, CCA blood flow was assessed simultaneously with CBFV during hyper- and hypoventilation. In contrast to the hypotheses, the observed changes in MCA velocity waveform morphology were not seen in the CCA velocity wave. More in depth examination of the MCA velocity wave compared to the CCA velocity wave and the arterial pressure wave suggested that alterations in the systolic portion of the velocity wave may be influencing the interpretation of changes in vascular tone with hyper- and hypoventilation.

8.5.1 Velocity and Flow Wave Inflection Points

Previous work has examined the CBFV wave profile under varying conditions (Robertson et al., 2008; Kurji et al., 2006; Albina et al., 2004; Lockhart et al., 2006). However this is the first that has attempted to associate observed changes in CBFV velocity wave inflection points with similar alterations in the CCA flow wave. To accomplish this, five inflection points were assessed (three peaks and two troughs) with respect to end diastolic velocity or flow. Significant alterations were seen for all points in of the MCA velocity trace, but contrary to the hypothesis, only the systolic peak of the CCA flow wave showed a similar increase with hyperventilation which contributed to alterations in the Doppler resistance indices.

The calculation of the Doppler resistance indices, RI and PI rely on the observation that changes in downstream vascular resistance serve to change the pulse amplitude of the velocity trace (Gosling et al., 1991). Therefore, an increase in the pulse amplitude of the velocity, or flow, trace with respect to systolic value (RI) or the mean of the wave (PI) is thought to reflect an increase in downstream vascular resistance. In this study, hypo- and hyperventilation produced a respective decrease an increase in RI and PI for both the MCA velocity wave and the CCA velocity wave suggesting that changes in downstream vascular resistance serve to produce similar changes in the pulse amplitudes of both the MCA velocity and CCA flow waveform. However, when only the P1-T1 variable was assessed, differences

in the CCA velocity wave were only different with hyperventilation suggesting that the Doppler resistance indices are dependent on more than just the pulse amplitude of the velocity wave.

Contrary to the hypothesis, and observed results with nitroglycerin (Chapter 6), assessment of the other waveform inflection points only showed variation in the MCA trace and not the CCA trace. This was especially evident when the velocity traces were assessed over the cardiac cycle with respect to the resting baseline traces (Figure 8.3 C and D). Vertical lines on this figure represent the troughs of the inflection points and serve to divide the velocity trace into three distinct sections where the first section represents the systolic component, the second section influenced by the reflected wave, and the third section indicating the diastolic decay portion after the dicrotic notch. From this figure it can be seen that changes in the velocity wave trace change to different extents throughout the cardiac cycle where the MCA tended to show differences throughout the cardiac cycle, the CCA only showed change in the systolic component. The differences in these responses are reflected in the lack of change in the CCA velocity wave inflection points.

Several factors could account for the variation in responses between the MCA and CCA velocity traces. Most notably is the fact that the MCA is much further down the arterial tree than the CCA. Some studies have been conducted which have examined flow wave shape at different points of the carotid vascular tree finding large variations in waveform morphology at different measurement points (Gwilliam et al., 2009; Schubert et al., 2011). Therefore, it is possible that changes MCA velocity waveform morphology due to small variations in vascular tone are not translated up the vascular tree to the CCA.

Possible changes in MCA diameter with hyper- and hypo-ventilation may also have contributed to the observed changes in velocity waveform morphology. Previous work has suggested the possibility of changes in MCA diameter (Chapter 7). However, the CCA diameter was only significantly changed with hyperventilation (Chapter 7); therefore, it is possible that the variation in MCA diameter and lack of change in CCA diameter could have contributed to the differences in responses.

8.5.2 Augmentation Index and CrCP

Similar to data reported by Robertson et al. (Robertson et al., 2008), this study showed that hypoventilation resulted in an increase in the calculated augmentation index of the MCA. The current study also demonstrated that the reverse is also true in that hyperventilation resulted in a reduction of the augmentation index. The augmentation index represents an increase in the ratio of P2-T1 to P1-T1 or rather an increase in the ratio of the second peak, thought to represent a reflected wave, to the systolic peak (Robertson et al., 2008; Kurji et al., 2006). Based on observations from arterial pressure waves (Nichols et al., 2008), it is thought that the augmentation index of the cerebral blood velocity traces represents constructive interference of a reflected wave such that an increase in the augmentation index would represent a faster return of the reflected velocity wave and thus an increase in vascular tone (Robertson et al., 2008; Kurji et al., 2006). Work with the CCA flow wave and pressure has shown that the augmentation index calculated from the flow wave was similar to that calculated with the pressure wave (Hirata et al., 2006) which lends support to the concept that changes in the augmentation index of the MCA velocity wave is reflective of changes in cerebrovascular tone. However, the observed augmentation index results are in contrast to the observed CrCP results.

Consistent with previous reports, this study found an increase in CrCP with hyperventilation and a reduction in CrCP with hypoventilation (Ainslie et al., 2008; Panerai et al., 1999; Panerai, 2003). Thought to be directly related to vascular wall tension (Panerai, 2003), these changes in CrCP suggest that hyper- and hypoventilation result in decreased and increased vascular tension respectively. The observed changes in vascular tension are consistent with the metabolic influences of changes in CO_2, such that an increase in CO_2 results in a relaxation of vascular smooth muscle and a reduction in vascular wall tension. However, the results of the current study suggest that cerebrovascular compliance is changing independent of the changes in vascular tone.

If blood flow circulation was a purely resistive system, the arterial pressure wave would equal the flow wave (Zamir, 2005). In the current study, differences in the pressure-flow relationship were seen with both hyper- and hypoventilation (Figure 8.3 E and Figure

8.4 A, C, and E) suggesting alterations in vascular compliance. One research group, which has attempted to quantify cerebrovascular compliance with hypercapnia has shown conflicting results with animal data demonstrating an increase in compliance (Czosnyka et al., 2012) where human data suggested a reduction (Carrera et al., 2011; Kasprowicz et al., 2012). Previous work with sublingual NG has shown that the calculation of AI was negatively related to vascular compliance (Chapter 6). Therefore, considering the AI result of the current study, it would appear that vascular compliance is changing independently of cerebrovascular tension as determined by the calculation of CrCP.

8.5.3 Limitations

The current study utilized hyperventilation and breath-holds to manipulate $P_{ET}CO_2$. The results showed that this experimental manipulation was successful in altering $P_{ET}CO_2$; however, the magnitude of change was not controlled. Therefore, some of the variability seen in the current work could be a reflection of individual differences in the degree of hyperventilation, or the ability to perform the 30s breath-hold.

The calculation method used for critical closing pressure may also have influenced the results. This study used a two point method using mean and diastolic values of CBFV and ABP as this method has been shown to provide good repeatability (Panerai et al., 2011). It has been noted that the calculation of CrCP using the linear relationship between CBFV and ABP only provides an estimate of the true CrCP and does not account for changes in cerebrovascular compliance (Panerai, 2003). Therefore, it is possible that some of the CrCP results reflecting cerebral arterial wall tension may be distorted by the changes in cerebrovascular compliance.

8.6 Conclusions

The current study assessed simultaneous recordings of MCA and CCA blood velocity with changes in $P_{ET}CO_2$ for the assessment of cerebrovascular tone. In support of the hypothesis, significant changes in the MCA velocity trace were seen with hyper- and hypo-ventilation; however, in contrast to the hypothesis, these variations were not reflected in the

CCA velocity trace. Further examination of the velocity waves showed that where the CCA velocity wave is only altered in the systolic portion of the cardiac cycle, the MCA wave shows variation throughout which may be reflective of changes in cerebrovascular compliance with changes in $P_{ET}CO_2$. The calculation of the augmentation index of the MCA velocity wave suggested an increase and decrease in cerebrovascular compliance with hyper- and hypoventilation respectively. These results contrasted with the calculation of CrCP which suggested an increase and decrease in cerebrovascular tension with hyper- and hypoventilation. Therefore, the results of this study suggest that in the cerebral circulation cerebrovascular compliance, and cerebral arterial tension change independently with alterations in $P_{ET}CO_2$.

Chapter 9

General Conclusions

In the presented studies, the general purpose was to examine cerebrovascular properties under varying conditions with particular emphasis on the within beat variation of the cerebral blood velocity trace. It was hypothesized that information about the cerebrovasculature, including changes in vascular tone, could be learned from examining within beat variation that would not otherwise be considered with just traditional measures of mean CBFV or CVRi. To test this general hypothesis, CBFV and CBFV Doppler waveform morphology were assessed after long duration spaceflight, in response to orthostasis before and after exposure to 5 days HDBR, in response to changes in $P_{ET}CO_2$, and in response to sublingual NG.

9.1 Spaceflight

Exposure to microgravity and simulated microgravity provide interesting models for the examination of cerebral blood flow control as these situations may promote remodelling of the cerebrovasculature without the confounding influences of systemic pathological conditions including, but not limited to cardiovascular disease, diabetes, and hypertension. Recently, two studies have been published noting vision alterations associated with structural changes of the eye in astronauts after long duration spaceflight which have been attributed to increased intracranial pressure during flight (Kramer et al., 2012; Mader et al., 2011). To date, it is still unknown to what extent intracranial pressure is increased in astronauts and what affect this has on the cerebrovasculature.

Much of what is known with respect to cerebrovascular adaptations to microgravity comes from animal work which has shown significant remodelling of the cerebrovasculature. Cerebral arteries of rats after HLU have shown vascular smooth muscle hypertrophy (Wilkerson et al., 1999; Lin et al., 2009; Zhang et al., 2001; Wilkerson et al., 2002) with a smaller luminal cross-sectional area (Wilkerson et al., 1999) and increased myogenic tone

(Wilkerson et al., 2005; Geary et al., 1998; Lin et al., 2009) thought to be related to the nitric oxide (Prisby et al., 2006; Lin et al., 2009; Wilkerson et al., 2005) or renin-angiotension system (Bao et al., 2007). Functionally, these alterations have been associated with reductions in cerebral blood flow (Wilkerson et al., 2002; Wilkerson et al., 2005). In human studies, no changes have been seen in resting CBFV or CVRi suggesting a lack of changes in human cerebrovasculature (Blaber et al., 2011; Iwasaki et al., 2007; Tobal et al., 2001). However, CBFV is only representative of cerebral blood flow if the diameter of the insonated vessel is not changing. To date, no studies have been conducted in humans to assess whether the MCA diameter changes after exposure to real or simulated microgravity. However, the results of animal models suggest that there is remodelling of the cerebrovasculature with spaceflight.

The results of Chapter 2 also showed no differences in resting CBFV after spaceflight. However, it is possible that this lack of change was the result of reduced cerebral blood flow through a smaller vessel which was suggested in the results of Chapter 3. The study presented in Chapter 3 looked to examine potential changes in CBFV Doppler waveform morphology with spaceflight, where Chapter 2 was primarily focused on potential changes in the functional regulation of cerebral blood flow. Contrary to the hypothesis, the key inflection points of the CBFV wave were not different pre to post spaceflight likely due to large variability in individual responses. Conversely, results from the calculation of CrCP after spaceflight showed an increase in CrCP which suggests an increase in cerebrovascular tone, a reduction in MCA resting diameter, or a combination of these two alterations. Although it cannot be confirmed with the measurements made in the current studies, it would appear that cerebrovascular remodelling did occur with long duration spaceflight which could contribute to the observed functional changes in cerebral blood flow regulation.

The main findings of Chapter 2 showed that cerebrovascular autoregulation and cerebrovascular CO_2 reactivity were both blunted after long duration spaceflight. This is in contrast to results of short duration spaceflight presented by Iwasaki et al. (Iwasaki et al., 2007) which showed no change, or even slight improvements in cerebrovascular autoregulation and potentially work by Blaber et al. (Blaber et al., 2011) that demonstrated

impairments in cerebrovascular autoregulation only in those astronauts that exhibited post flight orthostatic intolerance; however orthostatic tolerance was not assessed in the current study. It is possible that the variations in cerebrovascular results after spaceflight are due to individual differences in adaptation responses. In the current study, although the direction of change in cerebrovascular autoregulation and cerebrovascular CO_2 reactivity responses were similar, the magnitudes of the responses were very different. Similarly, the recent studies of vision changes with long duration spaceflight show a large amount of individual variation (Kramer et al., 2012; Mader et al., 2011). However, results do suggest that to varying degrees, idiopathic intracranial hypertension associated with long duration spaceflight results in cerebrovascular adaptations for all individuals.

9.2 Orthostasis

Reductions in orthostatic tolerance have frequently been seen after spaceflight (Buckey et al., 1996; Waters et al., 2002) and with simulated microgravity exposure (Arbeille et al., 2008; Zhang et al., 1997). As syncope ultimately results from cerebral hypoperfusion, it follows that alterations in the cerebrovasculature may contribute to changes in orthostatic tolerance. The studies presented in Chapter 4 and Chapter 5 both examined the cerebrovascular responses to sustained orthostasis and the progression towards syncope before and after exposure to five days of HDBR. Both studies, to some extent looked at the within beat variation in the MCA velocity trace to further understand the cerebrovascular responses to orthostasis.

It has been frequently documented that transition to an upright results in reductions in BP_{MCA}, CBFV, and $P_{ET}CO_2$ (Immink et al., 2006; O'Leary et al., 2007; Cencetti et al., 1997; Serrador et al., 2006) and a progressive reduction in $P_{ET}CO_2$ with prolonged head up tilt (O'Leary et al., 2007; Razumovsky et al., 2003; Howden, Lightfoot, Brown, & Swaine, 2004; Cencetti et al., 1997). With the progression towards syncope, several studies have observed paradoxical increases in cerebrovascular resistance before syncope (Serrador et al., 2006; Bondar et al., 1995; Levine et al., 1994) which could be due to the reduction in arterial CO_2 (Serrador et al., 2006; Blaber et al., 2001). The results in Chapter 4 support the hypothesis of

a reduction in $P_{ET}CO_2$ being significantly related to the reduction in CBFV and the increase in CVRi with the progression towards syncope independent of changes in BP_{MCA}. In addition, this chapter also demonstrated a progressive increase in CrCP with the progression towards syncope which suggests that changes in cerebrovascular tone contribute to the reduction in cerebral blood flow. The calculation of CrCP in this chapter utilized a two point method of mean and diastolic BP_{MCA} and CBFV; however, similar results were showed by Carey et al. (Carey et al., 2001) who used the linear regression method which is dependent on the shape of the entire velocity and pressure waveforms. Therefore, it is conceivable that this change in cerebrovascular tone with the progression towards syncope contributed to the collapse of small blood vessels within the brain thus leading to a reduction in cerebral blood flow and the development of syncope.

The calculation of CrCP is dependent on the relationship between BP_{MCA} and CBFV and is affected to by the shape of the cerebral blood velocity waveform. The work presented in Chapter 5 in part attempted to expand on the CrCP results by examining the MCA velocity waveform with the progression towards syncope. Originally intended as an extension of a previously published study with the same subjects in which the temporal artery Doppler waveform morphology was examined with approaching syncope (Arbeille et al., 2012), Chapter 5 examined both the temporal artery and the MCA velocity waves with the progression towards syncope in an attempt to relate these changes to potential alterations in cerebrovascular autoregulation in those individuals with marked orthostatic intolerance after HDBR. Previous work examining the MCA velocity trace has shown a deepening of the dicrotic notch portion of the MCA velocity trace (Albina et al., 2004) which was also found in the current study. However, contrary to the hypothesis, although there was a reduction in orthostatic tolerance, there were no observed changes in cerebrovascular autoregulation, changes in temporal artery or MCA velocity profiles, or the ratio of temporal artery velocity to CBFV with HDBR. These results suggest that although changes in the MCA velocity trace occur with the progression towards syncope, this response is well maintained and is not related to the development of orthostatic intolerance after five days of HDBR.

Due to the CrCP results presented in Chapter 4, it is likely that the observed reduction in the dicrotic notch point of the MCA velocity wave presented in Chapter 5 was due to alterations in cerebrovascular tone. However, other physiological changes with the progression towards syncope may have also contributed to changes in MCA waveform morphology including alterations in vascular resistance, changes in cerebral blood flow, and alterations in MCA diameter. Therefore, later chapters of this thesis have used quantitative measures of cerebral blood flow and mathematical modeling in attempt to explain the physiological relevance of the observed changes in MCA velocity waveform morphology.

9.3 RCKL Modelling

Mathematical modeling, applied to the cerebral circulation, may provide an indication of cerebrovascular properties that can be used to assess the observed changes in velocity waveform morphology. Previously described by Zamir et al. (Zamir et al., 2007) to describe changes in the peripheral circulation, the RCKL model uses a modified Windkessel model placing vascular resistance (R) and vascular compliance (C) in parallel with viscoelastic (K) resistance and inertance (L) in series with C. In a pilot study, the RCKL model was used with CCA blood flow and pressure recordings to detect changes in cerebrovascular properties with aging (Robertson et al., 2008). The results of this thesis further examined the feasibility of using CCA measures and the RCKL model for detecting change in cerebrovascular variables and determining the relationship to alteration in MCA velocity wave inflection points.

Preliminary work with the RCKL model presented in Appendix A showed good repeatability of the RCKL outputs. Although the CV values were greater than 20% for each of R, C, K, and L a power analysis determined that a change of one half the within-subject standard deviation would require a sample size of only 11 individuals. Therefore, it is likely that observed changes in the RKCL results presented in Chapter 6 are due to changes in vascular properties and not the error of the measurement. Of additional consideration with respect to the use of the RCKL model was the calculation of flow values for the common carotid artery. With the ultrasound assessment of CCA blood flow, studies have commonly used a single measure of CCA diameter for the calculation of flow (Sato et al., 2011; Eicke et

al., 1999; Arbeille et al., 2001). However, as the CCA is a very pulsatile artery, it was unclear what effect a single diameter measure versus continuous diameter measures would have on the calculation of CCA flow within a cardiac cycle and therefore the results of RCKL modelling. The results presented in Appendix B show that although the use of continuous diameter measures of CCA flow affect the shape of the resultant CCA flow wave and the corresponding responses to NG, the use of continuous diameter measures did not affect the results of the RCKL model. Therefore, considering the results of Appendix A and Appendix B, the RCKL model was used to determine cerebrovascular responses to HDBR and NG.

Use of the RCKL model with NG and HDBR presented in Chapter 6 showed that R was decreased and C was increased after NG and there was no effect of HDBR on any of the RCKL results. The lack of change in NG response after five days of HDBR was expected as previous work, presented in Appendix C, looking at women after 56 days of HDBR also found no change in the cerebrovascular responses to NG (Zuj et al., 2012b). In addition, the results from this chapter also found no differences in CCA diameter, or calculated MCA diameter after HDBR or in the dilation response to NG which further supports the results from Chapter 4 and Chapter 5 which all indicate that cerebrovascular hemodynamics are not changed after only 5 days of HDBR.

In Chapter 6, RCKL results were then compared to observed changes in the MCA velocity wave. This analysis revealed that both before and after NG the augmentation index of the MCA velocity, the reflected peak (P2), and the amplitude of the dicrotic notch (T3) were all related to the value of C from the RKCL model. Previous work has suggested that the augmentation index of the MCA velocity wave corresponds to cerebrovascular compliance such that an increase in the index is associated with a reduction in vascular compliance (Robertson et al., 2008; Kurji et al., 2006). The work presented in chapter 6 confirmed that the augmentation index is related to cerebrovascular compliance as determined through the use of the RCKL model. This work suggests that the determination of the amplitude of the dicrotic notch and the calculation of the augmentation index may be used as indicators of cerebrovascular compliance potentially providing another index that can

be determined from the MCA velocity trace for the assessment of cerebrovascular hemodynamics.

The use of NG for the assessment of changes in cerebrovascular properties presents a situation where there is a dilation of the middle cerebral artery with no changes in cerebral blood flow. However, changes in $P_{ET}CO_2$ as seen in previous chapters of this thesis have been known to result in changes in cerebral blood flow. Therefore, the last section examined the relationship between CCA blood flow and MCA blood velocity with acute changes in $P_{ET}CO_2$.

9.4 Cerebrovascular tone, tension, and compliance

The use of transcranial Doppler ultrasound for the assessment of cerebral blood flow relies on the assumption that the MCA does not change diameter. However, the MCA is not a static vessels and has been shown to dilate with NG (Hansen et al., 2007). Recent work has also suggested changes in MCA diameter with 15min step changes in $PaCO_2$ (Willie et al., 2012). Therefore, Chapter 7 looked at assessing potential changes in MCA diameter with NG and acute changes in $P_{ET}CO_2$ using measures of CCA flow. Results from both Chapter 6 and Chapter 7 both confirm that assessment of CCA blood flow with NG provides a calculated dilation of the MCA that is consistent with what was observed in the study by Hansen et al. (Hansen et al., 2007). In addition the results of Chapter 7 also showed that with acute changes in $P_{ET}CO_2$ there are changes in cerebral blood flow and calculated MCA diameter that may have implications for alterations in cerebrovascular tone.

Throughout this thesis, and in the literature, the term "cerebrovascular tone" has been used as a nebulous concept incorporating the influences of changes in active and elastic cerebrovascular tension, cerebrovascular compliance, and to some extent potential changes in the luminal diameter of cerebral vessels. However, results from the assessment of MCA and CCA wave properties with acute changes in $P_{ET}CO_2$ suggest that this concept of tone with respect to velocity wave morphology and the calculation of critical closing pressure may not be appropriate for describing the cerebral circulation. While it can be said that

cerebrovascular tone influences the morphology of the MCA velocity trace, it would appear that some waveform assessments, particularly the augmentation index and CrCP, would be better used to describe changes in cerebrovascular compliance and tension.

Results from Chapter 8 demonstrated that with an increase in $P_{ET}CO_2$, there is an increase in the augmentation index suggesting an increase in cerebrovascular tone, and a decrease in CrCP suggesting a reduction in cerebrovascular tone with the opposite true for a reduction in $P_{ET}CO_2$. However, results from Chapter 6 suggested that AI was reflective of cerebrovascular compliance consistent with the interpretation from previously published work (Robertson et al., 2008; Kurji et al., 2006) where the descriptions of CrCP have emphasized that CrCP is reflective of cerebrovascular tension (Burton, 1951; Panerai, 2003). Therefore, with changes in $P_{ET}CO_2$ it appears that the tension and compliance of the cerebrovasculature are changing independently potentially due to the changes in cerebral blood flow within the confined space of the skull. These results suggest the need for further clarification in the concept of cerebrovascular tone with relationships to MCA velocity waveform morphology and the calculation of CrCP.

9.5 Summary and future directions

The results presented in this thesis represent initial work with respect to the analysis of MCA velocity wave morphology for the assessment of cerebrovascular hemodynamics. Results have demonstrated the malleability of the MCA velocity waveform and have suggested that assessment of various components of velocity wave including the overall pulse amplitude, the amplitude of the reflected peak, and the amplitude of the dicrotic notch reflect variation in cerebrovascular tone. However, additional analysis has demonstrated that care must be taken in the interpretation of cerebrovascular tone as different vascular properties affecting cerebral blood flow generally included in the concept of ‘tone’ may be changing independently.

Results from this thesis have also highlighted the need for quantitative assessments of cerebral blood flow. TCD provides a relatively simple and reproducible method for the

assessment of cerebral blood flow velocity. However, results presented have demonstrated that the MCA is not a static vessel and diameter changes may be confounding interpretation of CBFV results with respect to cerebral blood flow. Studies that have used MRI to visually assess the MCA diameter have been limited by the resolution of the technology available and may not have been able to detect small variations in MCA diameter (Valdueza et al., 1997; Schreiber et al., 2000; Serrador et al., 2000). Therefore, additional work is required to assess potential changes in MCA diameter using the improved imaging systems that are available.

Future studies are needed to further explore the relationships between cerebral blood velocity wave characteristics and cerebrovascular hemodynamics. Mathematical modelling using the RCKL model may provide additional insight into the physiological meaning of velocity wave characteristics. The RKCL model was used to describe the changes in the MCA velocity wave with NG finding relations between output variables and waveform characteristics (Chapter 6); however, it is unclear if these relationships would be consistent with changes in $P_{ET}CO_2$ or under other conditions. Therefore, additional work is required to expand the use of the RCKL model for the assessment of cerebrovascular hemodynamics and for the interpretation of changes in MCA velocity wave morphology in various situations.

One of the major limitations of work presented in this study was the use of the CCA for quantitative assessments of cerebral blood flow. In ideal situations, analysis of ICA blood flow and waveform morphology may provide a better indication of cerebrovascular responses. However, the use of the ICA may be limited by the anatomical situation of the vessel preventing the non-invasive assessment of pressure. Therefore, the CCA was used in the presented studies as this vessel provided an easily imaged vessel with the potential for simultaneous non-invasive measures of pressure. Some studies assessing the CCA have suggested that the changes in CCA diameter over the cardiac cycle are reflective of CCA pressure (Sugawara, Niki, Furuhata, Ohnishi, & Suzuki, 2000; Niki et al., 2002; Hirata et al., 2006). Therefore, if future studies determine that a similar relationship between diameter and pressure exists for the ICA, the continuous assessment of ICA diameter and flow may provide a better indication of changes in cerebrovascular hemodynamics.

Of final consideration is the length of HDBR utilized for the studies presented in Chapter 4, Chapter 5, and Chapter 6. HDBR may be used as an Earth based analogue of microgravity exposure; however, the lack of changes found in the current studies are likely due to the HDBR only lasting 5 days. This prevents comparison to the long duration spaceflight study presented in Chapter 2 and Chapter 3 and even comparison to other spaceflight studies which have involved 1-2 weeks of flight (Blaber et al., 2011; Iwasaki et al., 2007; Waters et al., 2002). Therefore, studies are required with longer duration HDBR periods to determine potential influences of microgravity on human cerebrovascular structure and function with particular focus on potential changes in cerebrovascular tone.

Appendix A

Repeatability of a method for determining cerebrovascular properties

A.1 Introduction

The cerebral circulation presents the unique challenge of being contained within the skull and, therefore, prevents non-invasive, direct assessment of cerebral circulation in humans. To address this issue, the use of mathematical modeling may help to provide further information about cerebrovascular properties. It is well known that blood flow is affected by downstream vascular conditions. The simplification of the Poiseuille equation to relate flow to resistance and the pressure gradient is one example of this. However, it has been noted that if blood flow was a purely resistive system, the blood flow and pressure waves would be identical (Zamir, 2005). As may not be the case in the cerebral circulation, additional variables, such as vascular compliance, must be taken into consideration. In 2007, Zamir et al. (Zamir et al., 2007) presented a model for the assessment of peripheral hemodynamic properties. Based on a modified Windkessel model, the presented model (RCKL) placed resistance (R) and capacitance (C) in parallel with viscoelastic resistance (K) and inertance (L) in series with C. Theses researchers showed that the model was very effective in assessing properties of peripheral circulation; however, it is still unknown if the RCKL model can be applied to assess the cerebral circulation.

The RCKL model required the simultaneous input of pressure and blood flow measures to calculate the outputs of R, C, K, and L. With respect to the cerebral circulation, non-invasive measures of both pressure and flow can be made using the common carotid artery (CCA). Preliminary work using the RCKL model and CCA measures of pressure and blood flow has shown that RCKL is able to demonstrate large changes in cerebrovascular properties associated with age (Robertson et al., 2008). However, it is unclear how sensitive this model is for detecting changes in cerebral vascular properties, or what the variability is within the measure. Therefore, this study is intended as pilot work to determine the repeatability of RCKL outputs using CCA measures for model input.

A.2 Methods

Data were collected on five participants recruited for this pilot work. Participants were asked to come into the lab on three separate days with efforts being made to ensure that each participant was in a similar physiological state for each testing day; that is, participants were asked to come into the lab at the same time of day each of the three days and will have eaten similar meals during the day and performed similar amounts of physical activity. All data were collected with the participants resting in a supine position.

The use of RCKL requires the simultaneous assessment of pressure and flow in the conduit artery of interest. To accomplish this task in humans, two non-invasive methods were employed. Pressure was determined via tonometry with the use of a Millar pressure transducer. Briefly, a trained experimenter manually held the probe in place over the artery of interest and applied pressure so that the probe was firmly against the artery but not altering blood flow in the artery. At this point, the pressure waveforms recorded by the Millar probe can be considered representative of arterial pressure. The experimenter aimed to maintain a constant pressure on the probe throughout the testing. The absolute pressure values recorded by the Millar probe are dependent on the hold-down pressure applied by the experimenter; therefore, the Millar pressure tracing were normalized to recorded diastolic arterial pressure readings. Arterial blood pressure (ABP) was determined continuously through the use of finger photoplesthysmography (Finometer, Finapres Medical, Amsterdam). A three lead ECG was used for the assessment of heart rate.

Blood velocity in the common carotid artery was determined using Doppler ultrasound (Multigon Industries, New York, NY). A 4MHz, pulsed wave, Doppler ultrasound probe was used to assess continuous velocity in the common carotid artery (CCA). The outer envelope of the Doppler spectrum was recorded for analysis. Echo Doppler ultrasound (MicroMaxx, Sonosite Inc.) was used to determine the diastolic diameter of the common carotid artery. This diameter was then used to calculate arterial cross sectional area which was used to convert the Doppler blood velocity trace to blood flow.

Data collection started after the participant had been resting supine for five minutes. Data were collected so that three distinct sections of usable data, at least ten cardiac cycles in length, were recorded. Usable data were defined as 10 consecutive cardiac cycles where both the velocity and pressure tracing showed consistent waveforms with minimal variation in baseline (hold-down pressure of Millar probe) or spikes in the ultrasound signal. This data collection was repeated on each of the three days that the participant was in the lab. Therefore, each participant had three RCKL measures on each day of testing for a total of nine measures.

A.2.1 Data Analysis

RCKL modeling was used to assess cerebrovascular hemodynamic properties for each of the nine trials (three on each day). For each trial, mean values of CCA flow, CCA arterial blood pressure, R, C, K, and L were determined. A one way repeated measures analysis of variance was conducted to determine the residual mean square error representative of within-subject variance. Measurement error was determined through the calculation of within-subject standard deviation (SW) which is equivalent to the square root of within-subject variance (Bland & Douglas, 1996a). Repeatability was then calculated at 2.77 x SW (Bland & Douglas, 1996a). The coefficient of variation (CV), expressed as a percentage, was also calculated as the ratio of SW and overall mean (Bland & Douglas, 1996b).

A.3 Results

Data were successfully collected for each individual on each testing day. Mean data for CCA flow, CCA arterial pressure, R, C, K, and L are presented in Table A.1. No differences were seen between data trials for either mean CCA blood flow, or mean CCA arterial pressure. Results from the repeated measures analysis of variance also showed no difference between data sections for R, C, K, or L ($P>0.05$). Results for the calculation of repeatability and CV are shown in Table A.2.

Table A.1: Average RCKL and CCA pressure and flow values for each trial

Data Trial	R (mmHg/mL/min)	C (mL/mmHg)	K (mmHg/mL/min)	L (mmHg/mL/min^2)	CCA Flow (mL/min)	CCA ABP (mmHg)
T1	0.537 ± 0.175	0.0127 ± 0.0065	0.0412 ± 0.012	7.73E-6 ± 5.22E-6	183.7 ± 72.7	88.6 ± 6.97
T2	0.529 ± 0.176	0.0140 ± 0.0066	0.0605 ± 0.031	7.44E-6 ± 3.30E-6	185.4 ± 77.5	87.4 ± 9.40
T3	0.506 ± 0.188	0.0162 ± 0.0089	0.0514 ± 0.035	7.32E-6 ± 5.98 E-6	193.9 ± 85.2	86.1 ± 7.98
T4	0.434 ± 0.0949	0.0142 ± 0.0066	0.0353 ± 0.014	7.57E-6 ± 2.05E-6	204.7 ± 64.1	84.5 ± 7.04
T5	0.430 ± 0.0868	0.0148 ± 0.0069	0.0294 ± 0.009	6.44E-6 ± 4.62E-6	203.4 ± 55.1	84.2 ± 7.99
T6	0.459 ± 0.0403	0.0126 ± 0.0051	0.0357 ± 0.019	5.25E-6 ± 4.12E-6	191.5 ± 34.0	87.2 ± 12.0
T7	0.414 ± 0.0699	0.0162 ± 0.0047	0.0242 ± 0.008	5.10E-6 ± 4.18E-6	208.7 ± 52.7	84.7 ± 16.0
T8	0.434 ± 0.066	0.0132 ± 0.0029	0.0303 ± 0.016	5.99E-6 ± 3.79E-6	202.8 ± 49.1	86.8 ± 17.5
T9	0.451 ± 0.0716	0.0143 ± 0.0046	0.0418 ± 0.009	6.31E-6 ± 3.39E-6	203.9 ± 56.9	89.2 ± 16.7

Values show the mean ± SD for each data section. Results of the repeated measures analysis of variance showed no differences between the data trials for any variable.

Table A.2: Repeatability and CV values for RCKL outputs

Variable	Repeatability	CV
R	0.235mmHg/mL/min	18.2%
C	0.00923mL/mmHg	23.4%
K	0.0518mmHg/mL/min	48.1%
L	4.81E-5mmHg/mL/min^2	264.0%

Table shows results of repeatability analysis with values for repeatability and the coefficient of variation.

A.4 Discussion

RCKL modelling has previously been used to describe changes in the peripheral vasculature (Zamir et al., 2007). The major finding of the current work was that RCKL modelling of the cerebral circulation produced repeatable outputs, suggesting that observed changes in model outputs are the result of alteration in the cerebrovasculature and that this model can be applied to provide a greater understanding of cerebrovascular hemodynamics.

The assessment of repeatability involves determining the degree of within-subject variation. This was determined through the calculation of repeatability and CV. In general, the smaller the values for repeatability and CV the better the repeatability of the measure. The current study showed values for CV that at first assessment seemed large. Therefore, sample size calculations were conducted to determine how these repeatability numbers translated to practical application. Calculations were conducted to determine the minimum sample size required to detect a change of half of the repeatability with a standard deviation equal to SW, power of 0.8, and an alpha level of 0.05. To detect a change in R, a sample size of 10 was required, where only 9 were required for C, K, and L. These results suggest that despite larger than desired values for CV, only a relatively small sample sizes are required to detect changes in RCKL outputs.

A.4.1 Limitations

In this study, hemodynamic data collected from the common carotid artery were thought to reflect changes in cerebral blood flow. However, the CCA supplies both the intracranial circulation via the internal carotid artery and the extracranial circulation via the external carotid artery. The use of RCKL modeling provides indications of total downstream vascular condition. Therefore, the use of the CCA for RCKL modelling is influenced by both the cerebral and extracranial circulation. Future studies need to be conducted to determine potential differences between intracranial and extracranial responses and how these responses relate to RCKL outputs.

As the data acquisition of common carotid artery pressure and flow are to be done simultaneously, this required pressure to be collected on one side of the neck and flow to be determined on the opposite side. The left and right common carotid arteries do possess slightly different characteristics; however, pilot work conducted in the Neurovascular Research Laboratory at Western University, has shown no differences in RCKL measure when pressure was collected on the right side with flow on the left versus pressure collected on the left side and flow on the right (data not shown). For consistency purposes, Millar pressure data were always collected from the left CCA and velocity and flow measures from the right CCA.

Doppler ultrasound was used for the assessment of CCA velocity; however, the use of this method does not allow for the determination of the exact angle of insonation. It is believed that this did not pose an issue for this work, as each individual was acting as his/her own control, and the structure of the common carotid artery was not expected to change over a 3 day period. This assumption may serve to increase variability between subjects; however, this testing was intended to assess repeatability within subjects and the assumption of a constant angle of insonation was believed to be appropriate.

In the current work, only the end diastolic diameter value was used for the calculation of flow. However, there is a large variation in CCA diameter throughout the cardiac cycle. Currently it is unclear how the use of continuous diameter for the calculation of flow will

influence results for RCKL modelling and future work will have to address this consideration.

The current study was designed solely to test the repeatability of RCKL outputs using CCA pressure and flow measures as model inputs. As such, it is not possible to tell from the current data set what variables might have contributed to the variability of RCKL outputs. Previous work has suggested alterations in vascular tone with changes in carbon dioxide (Ogoh et al., 2010; Panerai et al., 2010; Panerai, 2003). It is possible that spontaneous fluctuations in CO_2 contributed to the variability seen in this study. Future work is required to determine potential variables that contribute to within subject variation of RCKL outputs.

A.5 Conclusion

The current work presented repeatability data for RCKL modelling using flow and pressure inputs measured in the common carotid artery. Although values calculated for CV seem large, the sample size required to detect a minimum change of half the repeatability was small suggesting good repeatability of the measures. In summary, the results of this work support the use of RCKL modelling with inputs from the CCA for the assessment of hemodynamic properties.

Appendix B

The impact of continuous common carotid artery diameter measures on the calculation of flow and flow waveform morphology with nitroglycerin stimulation

B.1 Introduction

The use of Doppler ultrasound for the assessment of blood flow has traditionally utilized single diameter measures for the calculation of vessel cross sectional area and resulting flow. In many cases the end diastolic diameter is used or a mean diameter is calculated as Davg = ((1/3) x Dsys) + ((2/3) x Ddia). However, in addition to differences between systolic (Dsys) and diastolic (Ddia) diameter, throughout the cardiac cycle the diameter of blood vessels change with alterations in pressure and are potentially dependent on vascular compliance and viscoelastic resistance. This is particularly evident when studying the common carotid artery (CCA) as changes in vessel diameter are relatively large and can be easily seen in real time B-mode ultrasound video. The use of continuous diameter measurements will have an influence on the calculation of mean blood flow, but could also have a profound influence in results when the variation in flow is assessed within a cardiac cycle, particularly in situations where CCA vascular tone is changing.

Nitroglycerin (NG) is commonly used in clinical settings as a method to reduce the work of the heart through venodilation and potentially through dilation of coronary blood vessels (Abrams, 1996). In research settings NG is often used to determine maximal nitric oxide (NO) dependent dilation of conduit arteries independent of the endothelium (Bleeker et al., 2005; Bonnin et al., 2001; Guazzi et al., 2004). However, NG also influences vascular tone as previous work has shown an increase in peripheral vascular compliance (Smulyan et al., 1986; Bank & Kaiser, 1998) and a reduction in cerebrovascular tone (Moppett et al., 2008) with NG. It is conceivable that the CCA also responds in a similar fashion thus altering the diameter profile throughout a cardiac cycle and potentialy calculations of flow and vascular resistance.

Previous work has utilized mathematical modeling for the determination of downstream vascular properties. The RCKL model, based on a modified Winkessel model, placed resistance (R) and compliance (C) in parallel with viscoelastic resistance (K) and inertance (L) in series with C and has been used to assess changes in the peripheral vasculature (Zamir et al., 2007) and the cerebrovasculature with aging (Robertson et al.,

2008). However, these studies only utilized single diameter measures for the calculation of flow. Therefore the purpose of the current study was to continuously assess the diameter for the CCA at rest and after NG stimulation to determine if alterations exist in the CCA flow profile that affect calculations of flow, vascular resistance, and RCKL model outputs.

This study looked at the calculation of CCA blood flow and resistance with a single diastolic diameter measure of the CCA and with continuous assessment of CCA diameter both before and after NG stimulation. In addition RCKL model outputs were also assessed with the two calculated CCA flow waves. It was hypothesized the different methods for calculating CCA blood flow would result in statistically different absolute values, but would not affect the calculated responses to NG. However, it was also hypothesized that the use of continuous CCA diameter for the RCKL model would produce significantly different compliance and viscoelastic resistance results to those utilizing single diameter measures for the calculation of flow both at rest and with NG stimulation.

B.2 Methods

Data for this project were collected as a part of the STBR-2010 project with general methods and instrumentation presented in Chapter 6.

B.2.1 Data Analysis

The assessment of CCA diameter was conducted using video analysis, wall detection software. This software was designed to use a threshold detection technique for the identification of vessel walls providing a diameter measure for each frame of video collected. Video was recorded at 25 frames per second which allowed for the detection of diastolic (Ddia) diameter points with a diameter measure calculated for each frame of video. Continuous diameter measures (Dcont) values were spline interpolated to 100Hz to match CCA velocity which was also calculated at 100Hz. The outer envelope of the CCA Doppler velocity trace was used as an indication of CCA blood velocity and combined with diameter measures for the calculation of CCA flow. Therefore, two different values for flow were determined using Ddia and Dcont.

Differences in the CCA flow waves with the different calculation methods were assessed by looking at key inflection points as shown in Figure B.1 and assessed with respect to the end diastolic velocity value, T1, as P1-T1, T2-T1, P2-T1, T3-T1, and P3-T1. Similar to previously described (Robertson et al., 2008; Kurji et al., 2006), the peaks P1 and P2 of the velocity wave were used with the end diastolic value T1 for the calculation of an augmentation index as AI = (P2-T1) / (P1-T1) x 100%.

Mean flow was determined as the mean of each calculated flow wave over a cardiac cycle. Vascular resistance (VR) was determined as mean arterial pressure divided by mean flow. In addition, the two Doppler resistance indices were calculated from the CCA flow waves as RI = (CCAsys-CCAdia)/CCAsys and PI = (CCAsys-CCAdia)/CCAmean.

RCKL modeling was conducted as previously presented by Zamir et al. (Zamir et al., 2007). Briefly, simultaneous flow and pressure measures of the CCA were used as model inputs both before and after NG stimulation for the calculation of downstream R, C, K, and L.

B.2.2 Statistical Analysis

Values presented show the mean ± SD. Data were assessed using a two-way repeated measures analysis of variance (SigmaStat 3.5, Systat Software Inc., Chicago, IL) for the main effects of NG stimulation and flow calculation method as well as any potential interactions between NG and calculation method. For all tests, significance was set at $P<0.05$.

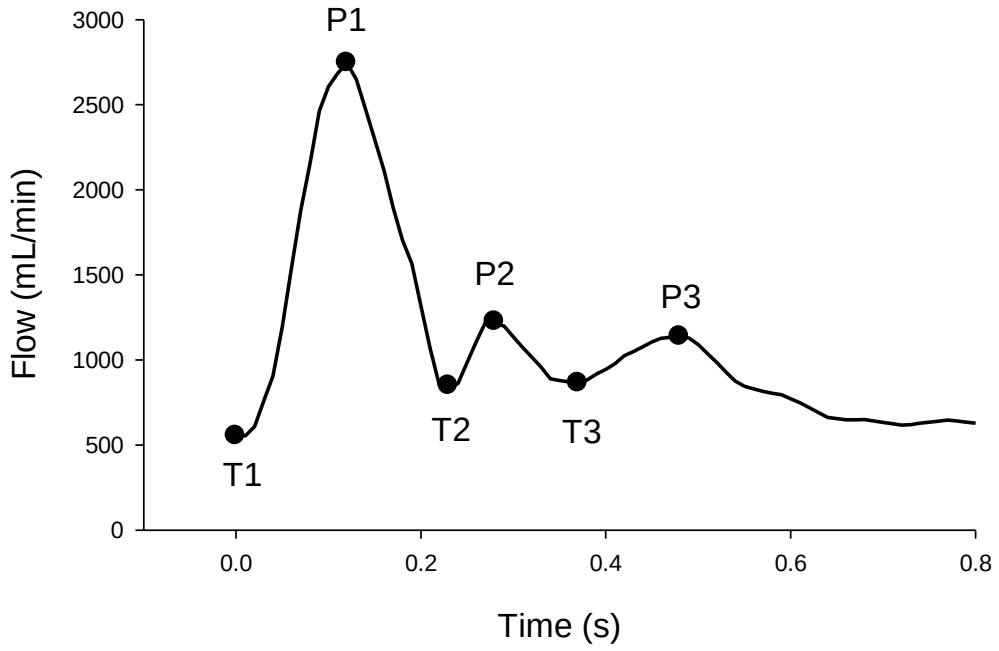

Figure B.1: Representative CCA flow wave

CCA flow waveform with key inflection points marked as T1, P1, T2, P2, T3, and P3.

B.3 Results

Representative tracings are shown in Figure B.2 for CCA pressure (Figure B.2 A), CCA diameter (Figure B.2 B), and CCA flow calculated using the continuous diameter measure (Figure B.2 C). Calculated CCA blood flow (Figure B.3 A) and vascular resistance (Figure B.3 B) showed the main effect of measure indicating that the absolute value of CCA blow flow and VR were dependent on the diameter measure used. Statistical analysis also found main effect of NG with CCA_{VR} being reduced with NG administration. With respect to the Doppler resistance indices, RI (Figure B.3 C) and PI (Figure B.3 D) both showed interaction effects between the use of Ddia or Dcont and NG stimulation. Post hoc testing showed that with Ddia, PI was greater after NG stimulation (P=0.037) and there was a strong trend for an increase in RI (P=0.051). Conversely, when Dcont was used for the calculation of flow, there were no changes in either RI or PI with NG.

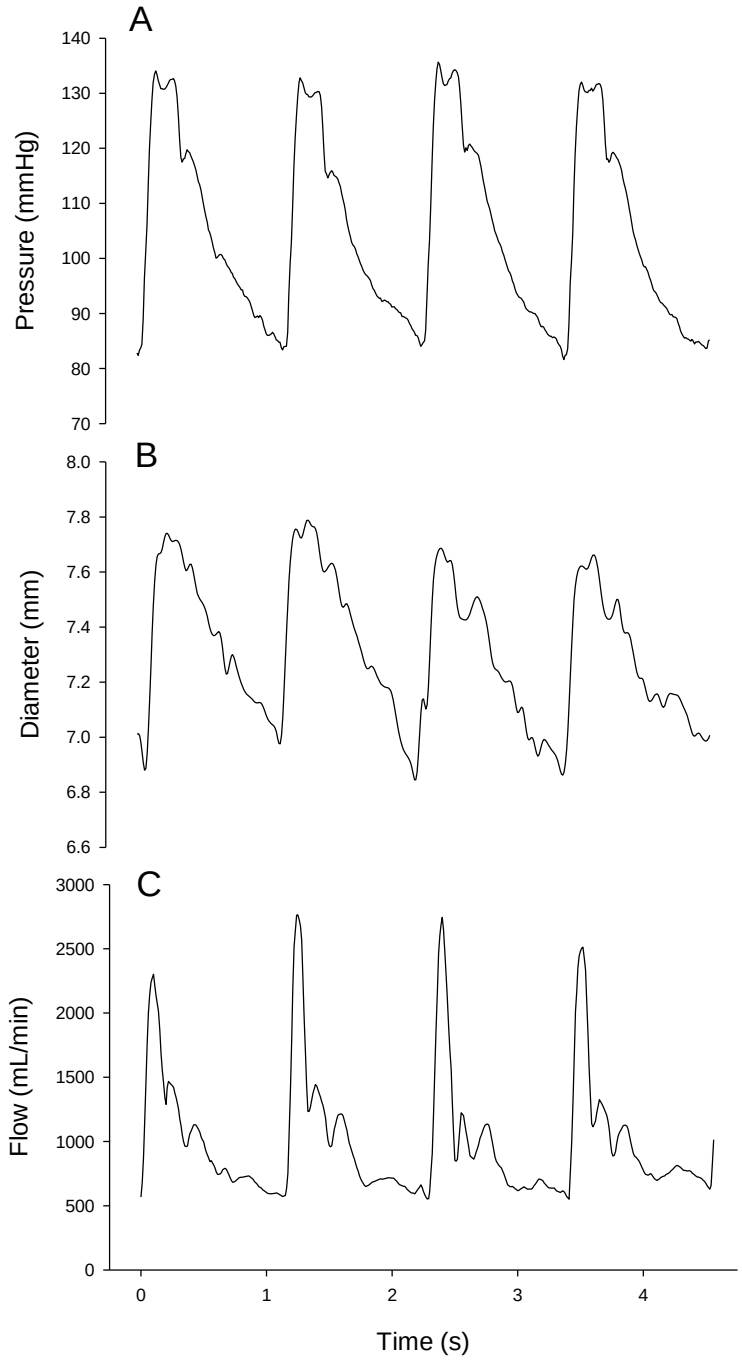

Figure B.2: Individual raw data

Raw data from one individual with CCA pressure (A), diameter (B) and CCA flow calculated with the continuous diameter measure (C).

Representative CCA flow waves are show in Figure B.4 for baseline rest (Figure B.4 A) and after NG stimulation (Figure B.4 B) with waves normalized to an end diastolic value of 0mL/min. From this figure it can be seen that the diameter measure used for the calculation of CCA blood flow influences the shape of the resultant flow wave. Statistically significant results were found for each of the flow wave inflection points assessed (Figure B.5). Significant interactions were found for T2-T1 (Figure B.5 B), P2-T1 (Figure B.5 C), and T3-T1 (Figure B.5 D). Post hoc analysis showed that values calculated with Dcont were different from Ddia with a greater response to NG for flow waves calculated with Dcont. P1-T1 (Figure B.5 A) also showed a main effect of measure with only Dcont values showing a significant increase with NG. However, the interaction did not reach statistical significance potentially due to large individual variability in the direction of NG responses. P3-T1 (Figure B.5 E) showed a significant effect of the measurement method, but no effects of NG. Analysis of AI showed significant differences between Dcont and Ddia values and a significant reduction with NG; however there was no interaction between these variables.

RCKL modelling results showed differences in the values for R (Figure B.6 A), C (Figure B.6 B), and L (Figure B.6 D) dependent on the diameter measure used for the calculation of flow. The calculated value of K (Figure B.6 C) was not dependent on the diameter measure used. Only C showed a significant change with NG stimulation; however, no interactions were found between the diameter measure used and NG stimulation.

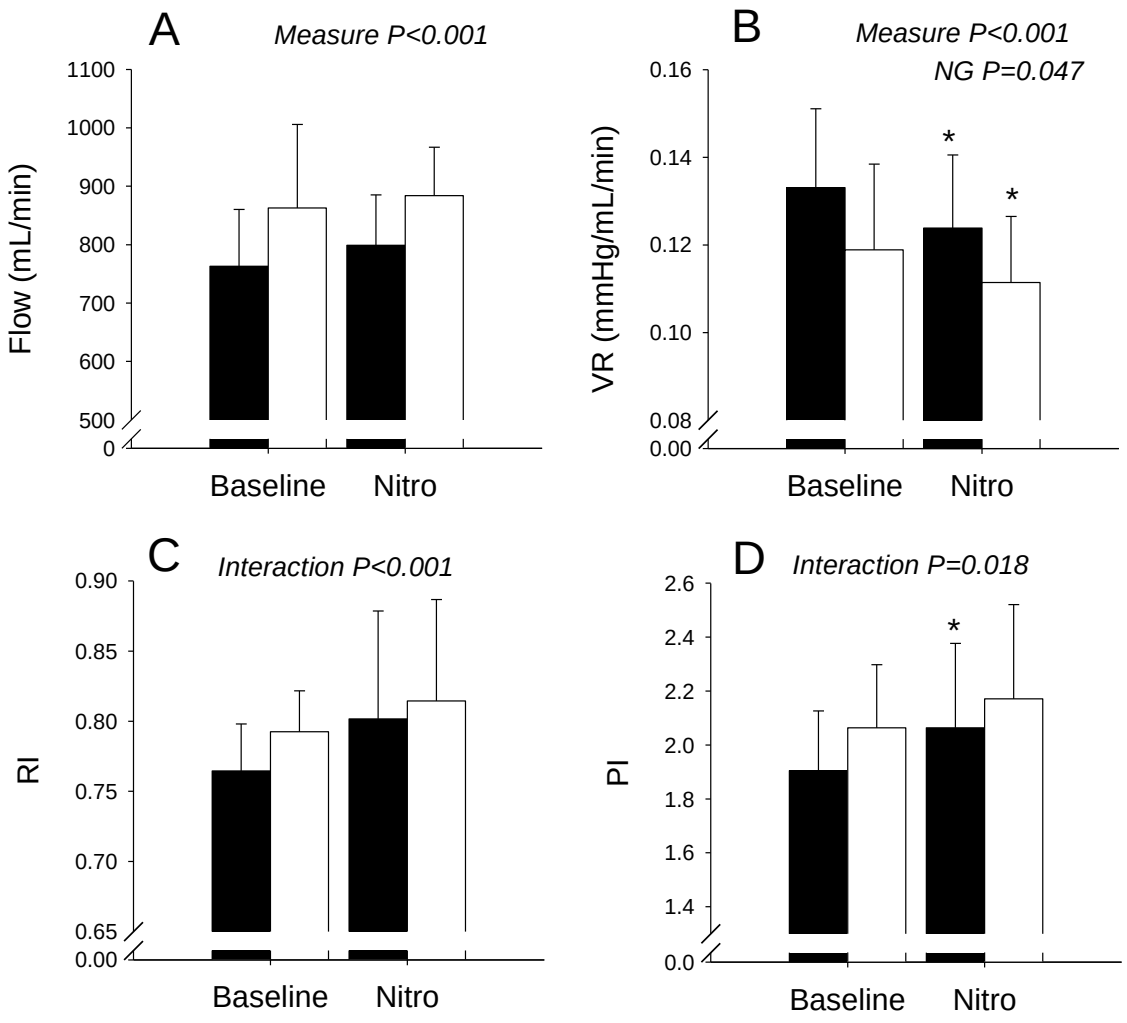

Figure B.3: Calculated CCA flow and vascular resistance

*Results for calculated CCA flow (panel A), vascular resistance (panel B), RI (panel C), and PI (panel D) calculated with Ddia (black bars) and Dcont (white bars). All values are mean ± SD with P values on the graphs showing the main effects of the two-way repeated measures ANOVA. Values that are statistically different with NG compared to corresponding baseline values are denoted by * P<0.05.*

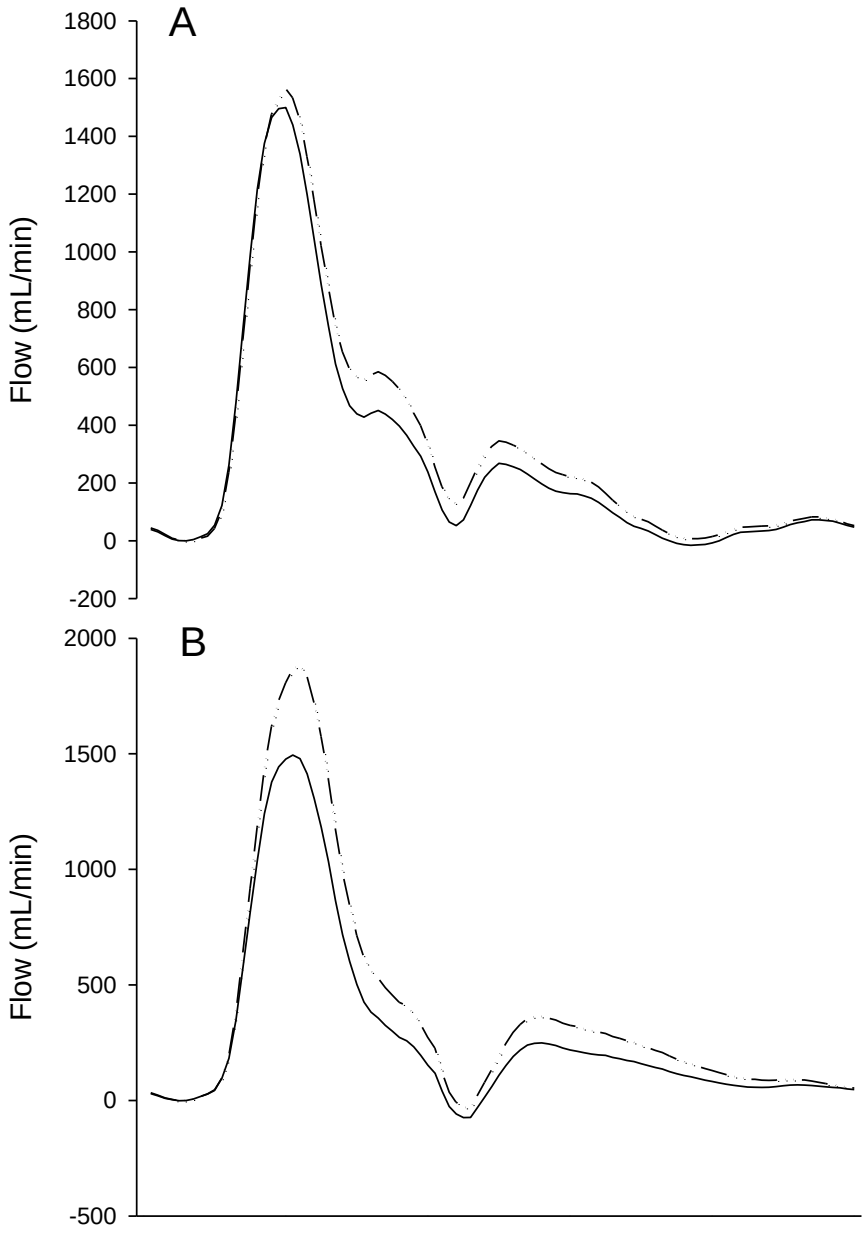

Figure B.4: Representative CCA flow waves

Representative CCA flow waveforms for one individual at rest (panel A) and after NG (panel B). Lines show flow waves calculated with Ddia (solid) and Dcont (dashed dotted).

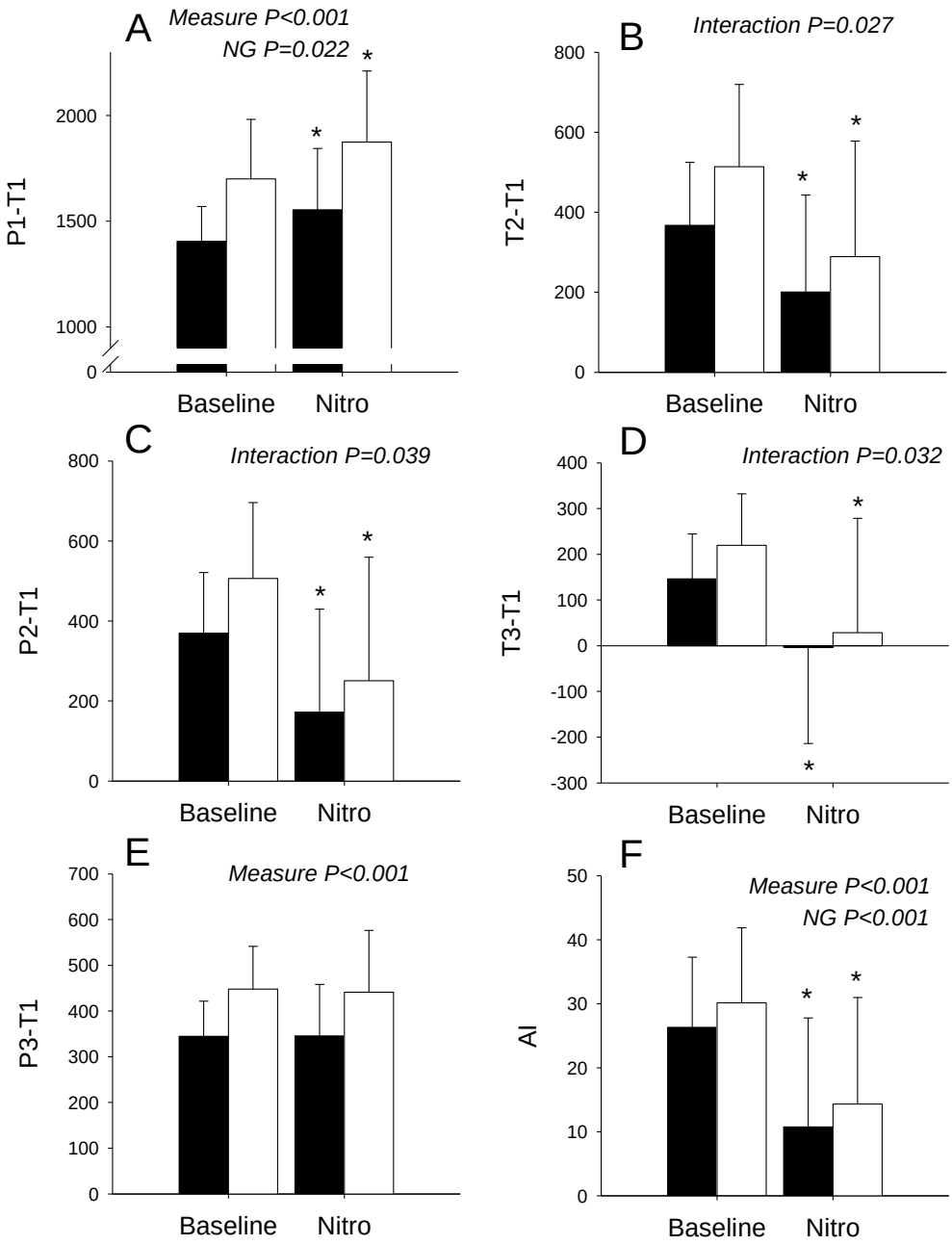

Figure B.5: Wave inflection point results

*Flow wave inflection point results (mean ± SD) for Ddia (black bars) and Dcont (white bars). P values on the graphs showing the main effects of the two-way repeated measures ANOVA. Values statistically different with NG are denoted by * P<0.05.*

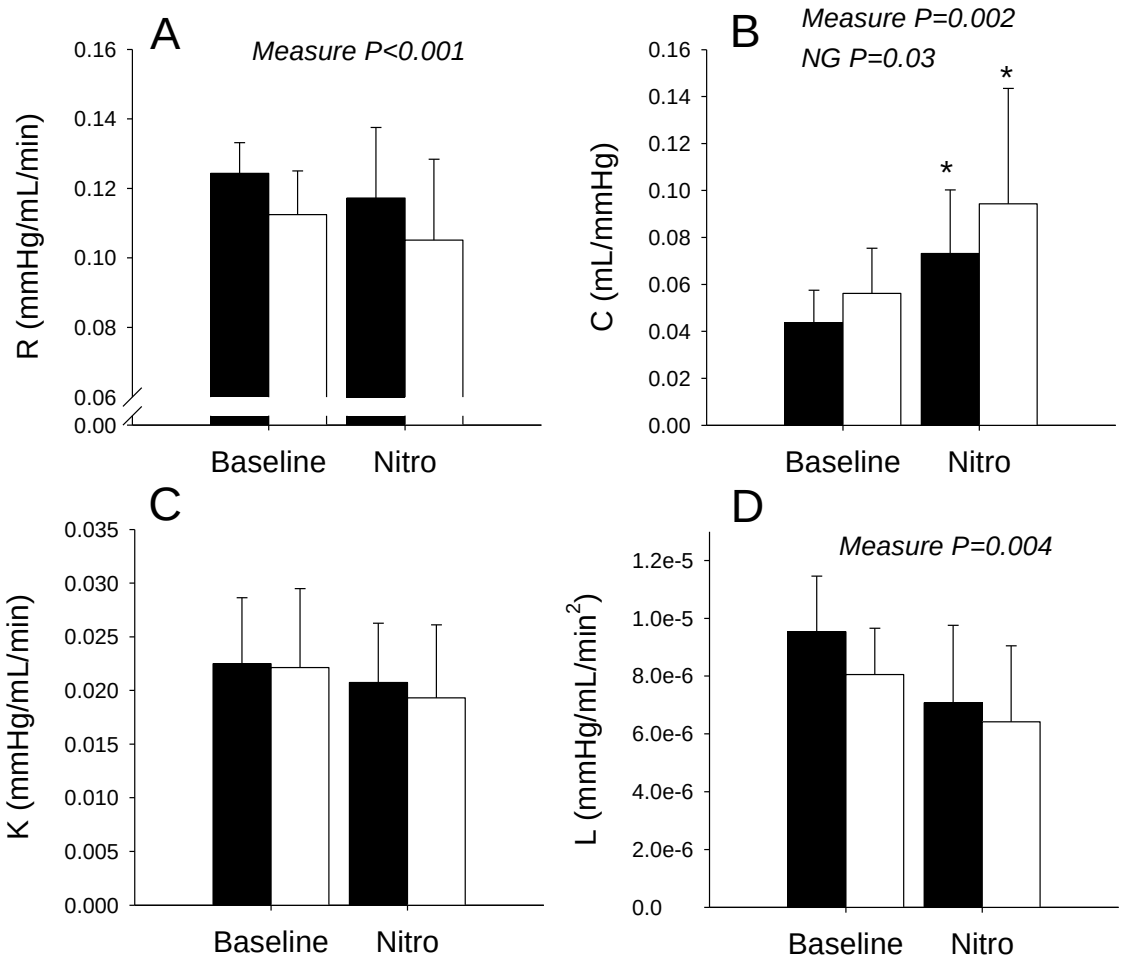

Figure B.6: RCKL results

*Results from the RCKL modeling analysis using flow waves calculated with Ddia (black bars) and Dcont (white bars). All values are mean ± SD with P values on the graphs showing the main effects of the two-way repeated measures ANOVA. Values that are statistically different with NG compared to corresponding baseline values are denoted by * P<0.05.*

B.4 Discussion

The current study utilized two different assessments of CCA diameter for the calculation of CCA flow to determine how each diameter measure affected the resultant CCA flow waveform and responses to NG. In support of the hypothesis, the results showed differences in calculated flow and resistance values with the different diameter measures; however, responses to NG were similar for each diameter measure used. Also in support of the hypotheses, assessment of the CCA flow waveform morphology showed significant differences with the different diameter measures and showed greater responses to NG when continuous diameter measures were used compared to single measures. The different calculated flow waves also resulted in differences in the RCKL model results; however, in contrast to the hypothesis, no differences in RCKL model results with NG were seen.

Studies using the ultrasound assessment of CCA blood flow have frequently used a single diameter measure for the calculation of flow (Sato et al., 2011; Eicke et al., 1999; Arbeille et al., 2001). The results of the current study support this method for determining changes in mean CCA flow, but also demonstrate that continuous measure of vessel diameter are needed when changes are assessed within a cardiac cycle. Some work has been conducted with continuous diameter assessments of the CCA (Hirata et al., 2006; Niki et al., 2002; Hirata et al., 2006) and brachial artery (Green, Cheetham, Reed, Dembo, & O'Driscoll, 2002) but these studies did not attempt to show the difference between a flow wave calculate with a single diameter measure versus that with the continuous diameter measures.

Surprisingly, no differences in the RCKL outputs were seen between the two flow calculations. The RCKL model generates a modelled flow wave from the measured pressure wave with changes in R, C, K, and L so that the modelled flow wave matches measured flow wave. Analysis of the flow wave inflection points found that the use of continuous diameter measures altered the shape of the flow wave; therefore, alterations in the RCKL outputs were expected. As this was not the case, it is possible that the RCKL model, which is a simplified estimate of downstream hemodynamic conditions, was not sensitive enough to be affected by the small but significant alterations in the CCA flow waveform.

B.4.1 Limitations

In the current study, ultrasound video was collected and used for analysis which provided a diameter measure for each frame of video. Therefore, diameter measures were collected at 25Hz for comparison to a velocity trace assessed at 100Hz. Diameter measures were spline interpolated to match the velocity collection frequency; however this interpolation may introduce an additional error into the calculation of flow using continuous diameter. As ultrasound technology continues to progress, it is possible that collecting diameter measures at a higher collection frequency will show more variation in the diameter wave thus further contributing to alteration in the calculated flow waveform.

B.5 Conclusion

The current study showed that different methods of CCA diameter measures have a significant effect on the resultant calculated CCA flow, vascular resistance, and RCKL model output. However, contrary to the hypothesis, the different diameter measure did not affect the responses of these variables. Conversely, in support of the hypothesis, several flow waveform inflection points and the calculation of RI and PI showed significant interactions. These results suggest that when using ultrasound assessments of CCA flow and resistance, as long as the diameter used is consistent, minimal differences will be seen. However, in cases where the morphology of the waveform within a cardiac cycle is important, a continuous diameter measure would be required.

Appendix C

Responses of women to sublingual nitroglycerin before and after 56 days of 6° head down bed rest

This chapter was published as:

Zuj KA, Arbeille Edgell H, Shoemaker JK, Custaud MA, Arbeille Ph, and Hughson RL (2012). Responses of women to sublingual nitroglycerin before and after 56 days of 6° head down bed rest. *J Appl Physiol* 113(3) 434-441.

C.1 Overview

This study tested the hypothesis that cardiovascular effects of sublingual nitroglycerin (NG) would be exaggerated after 56 days of 6° head down bed rest (HDBR) in women, and that an aerobic and resistive exercise countermeasure (EX, n=8) would reduce the effect compared to HDBR without exercise (CON, n=7). Middle cerebral artery maximal blood flow velocity (CBFV), cardiac stroke volume (SV), and superficial femoral artery blood flow (Doppler ultrasound) were recorded at baseline rest and for five minutes following 0.3 mg sublingual NG. Post-HDBR, NG caused greater increases in heart rate (HR) in CON compared to EX (+24.9±7.7, and +18.8±6.6bpm respectively, $P<0.0001$). The increase in HR combined with reductions in SV to maintain cardiac output. Systolic, mean and pulse pressures were reduced 5-10mmHg by NG, but total peripheral resistance was only slightly reduced at 3min after NG. Reductions in CBFV of -12.5±3.8cm/s were seen after NG, but a reduction in the Doppler resistance index suggested dilation of the middle cerebral artery with no differences after HDBR. The femoral artery dilated with NG and blood flow was reduced ~50% with the appearance of large negative waves suggesting marked increase in downstream resistance, but there were no effects of HDBR. In general, responses of women to NG were not altered by HDBR; the greater increase in HR in CON but not EX was probably a consequence of cardiovascular deconditioning. These results contrast with the hypothesis and a previous investigation of men after HDBR by revealing no change in cardiovascular responses to exogenous nitric oxide.

C.2 Introduction

The vasodilatory actions of nitric oxide (NO) work in conjunction with sympathetic vasoconstrictor activity and other vasoactive hormones in the regulation of blood pressure and blood flow (Delp & Laughlin, 1998; Mombouli & Vanhoutte, 1999). Acute alterations in NO effects on blood vessels have been noted under conditions that simulate spaceflight in animals (Prisby et al., 2006; Wilkerson et al., 2005; Sangha, Vaziri, Ding, & Purdy, 2000; Vaziri, Ding, Sangha, & Purdy, 2000) and humans (Rudnick et al., 2004; Bleeker et al., 2005; Platts et al., 2009; Bonnin et al., 2001; Salanova, Schiffl, Püttmann, Schoser, & Blottner, 2008). These results suggest that alterations in hemodynamic responses with exposure to real or simulated microgravity may be due to changes in NO mediated mechanisms.

Animal models of simulated microgravity have shown elevated nitric oxide synthase (NOS) activity increasing NO production that could dilate peripheral vessels and reduce vascular responsiveness to norepinephrine (Sangha et al., 2000; Vaziri et al., 2000). In contrast, cerebral arteries of hind limb suspended rats show reduced eNOS protein (Wilkerson et al., 2005) and reduced middle cerebral artery endothelial dependent dilation (Prisby et al., 2006). These results from animal studies point towards potential regional differences in hemodynamic responses to NO after simulated microgravity; a topic which has not been studied in humans.

Focusing on isolated regions, studies involving humans suggest changes in the NO system after simulated microgravity. Expression of NOS isoforms in leg skeletal muscle was altered in men following 90 days of head down bed rest (HDBR) (Rudnick et al., 2004) and in the women reported in the current study after 60 days of HDBR (Salanova et al., 2008). In peripheral vascular beds, a trend has been observed for greater flow mediated dilation (FMD) responses after HDBR (Bleeker et al., 2005; Platts et al., 2009) thought to be mediated by NO mechanisms (Green, 2005). However, different responses have been observed with respect to the dilatory effects of sublingual nitroglycerin (NG) where two studies have shown no effect (Bonnin et al., 2001; Platts et al., 2009) compared to enhanced dilation after 52 days

of horizontal bed rest (Bleeker et al., 2005). It has been speculated that changes in NO mediated mechanisms of blood flow regulation might contribute to orthostatic intolerance observed after spaceflight and spaceflight simulation (Bonnin et al., 2001; Guazzi et al., 2004). A greater heart rate response to NG has been reported after seven days of HDBR (Bonnin et al., 2001) but little information is available on the systemic and regional responses to this NO donor.

The current experiments were conducted within the WISE-2005 spaceflight analogue study which involved women who completed 56 days of continuous 6° HDBR with or without exercise countermeasures. We hypothesized that 56 days of HDBR would exaggerate cardiovascular responses to NG reflecting poorer orthostatic tolerance following HDBR and that the aerobic and resistive exercise countermeasure would attenuate these effects.

C.3 Methods

C.3.1 WISE-2005

The Women's International Simulation for Space Exploration (WISE) was an international collaborative study between the Centre National d'Etudes Spatiales (CNES), European Space Agency (ESA), Canadian Space Agency (CSA), and the National Aeronautics and Space Administration (NASA). This study reports on fifteen healthy women between the ages of 25 and 40 years of age who completed 60 days of continuous 6° HDBR with the experiments for this study completed on day 56 of HDBR. The research was conducted in Toulouse, France, at the MEDES Space Medicine Research Facility of CNES and approved by the Comité Consultatif de Protections des Personnes dans la Recherche Biomédicale, Midi-Pyrénées (France), Committee for the Protection of Human Subjects at Johnson Space Center, and local ethics committees including the Office of Research Ethics, University of Waterloo. All study protocols were in accordance with the declaration of Helsinki. Each subject signed an informed consent form and was aware of her right to withdraw from the study without prejudice.

C.3.2 Countermeasures and Exercise Schedule

Subjects were randomly assigned to either the control (CON), or exercise (EX) group after first stratifying them according to maximal oxygen uptake. Participants were recreationally active with an average height of 164.3±6.2cm and weight of 58.2±5.0kg. Maximal oxygen uptake data have been previously presented (Schneider, Lee, Macias, Watenpaugh, & Hargens, 2009; Guinet et al., 2009) with averages of 38.9±6.8mL/min/kg and 37.9±4.0mL/min/kg for CON and EX respectively. One participant in the CON group did not complete the NG testing post-HDBR and was excluded from all analysis. The CON group (n=7) did not receive any countermeasure during the 56 days of bed rest, while the subjects in the EX group (n=8) performed two types of exercise. Three to four times per week, the EX group exercised for 40 minutes between 40-80% of their peak oxygen uptakes on a treadmill inside a lower body negative pressure (LBNP) chamber with LBNP applied to provide a ground reaction force of 1-1.2 body weight (Cao et al., 2005). Treadmill exercise was followed by 10 minutes of static LBNP. Every third day of the bed rest period, the EX group completed flywheel resistance exercise (Rittweger et al., 2005).

C.3.3 Physiological Measures

Heart rate (HR) was determined using a standard three lead electrocardiogram. Finger photophlethysomography (Finometer, Finapres Medical, Amsterdam) was used for the determination of arterial pressure. Mean arterial pressure (MAP), systolic pressure (SBP), diastolic pressure (DBP), and pulse pressure (PP) were determined from the recorded pressure wave forms. Data were recorded on a PowerLab (ADInstruments, Colorado Springs, USA) data collection system.

Aortic blood velocity was determined using a 2MHz probe oriented to determine the velocity of blood at the aortic root (Multigon, New York, NY). Ultrasound imaging (Acuson 128XP, Paris, France) was used to assess the cross-sectional area of the aortic root which was then combined with velocity measures to determine cardiac stroke volume (SV). Cardiac output (Q) was determined as the product of SV and HR. Total peripheral resistance (TPR) was calculated as TPR = MAP / Q.

Superficial femoral artery blood velocity was determined using a 4MHz pulsed Doppler probe (CardioLab, ESA-CNES device, France). Echo Doppler ultrasound (Acuson 128XP, Paris, France) was used to provide images of the superficial femoral artery for the determination of vessel cross-sectional area and the calculation of femoral blood flow. Blood flow data were normalized to 100mL of lower limb lean tissue calculated from magnetic resonance imaging (S. Trappe and T. Trappe, personal communication). Femoral vascular conductance (FC) was calculated as FC = femoral flow / MAP. Vascular conductance was calculated for this study as the calculation of vascular resistance (MAP / flow) had a skewed distribution with some extremely high values as, in some individuals, femoral blood flow was reduced to near zero with NG stimulation.

Echo Doppler imaging of the portal vein (Acuson 128XP, Paris, France) was used for the assessment of portal vein cross sectional area. Due to technical issues, the data from only eight of the subjects was analyzed for pre-HDBR responses.

Transcranial Doppler ultrasound was performed for the assessment of cerebral blood flow velocity (CBFV). A 2MHz pulsed Doppler probe (CardioLab, ESA-CNES device, France) was positioned over the temporal window allowing for the insonation of the middle cerebral artery (MCA). Throughout the test, the probe was held in place using a head band. The outer envelope of the Doppler spectrum was recorded and CBFV was determined as the mean of the outer envelope over a cardiac cycle. Two indexes of cerebral vascular resistance, CVRi and RI, were calculated from the waveform. CVRi was determined from CVRi = MAP / CBFV, whereas RI was calculated from RI = (CBFVsys – CBFVdia) / CBFVsys where CBFVsys and CBFVdia are the maximum and minimum points of the wave respectively during a cardiac cycle.

C.3.4 Testing Protocol

Data were collected seven days before the start of HDBR (pre-HDBR) and on the 56th day of the bed rest period (post-HDBR), approximately 24 hours after a treadmill in LBNP exercise session for the EX group. All measures were made in a supine posture. Physiological measures were recorded continuously for two minute baseline period and five

minutes after the sublingual administration of 0.3mg of nitroglycerin (Natispray, Proctor & Gamble Pharmaceuticals, France). Imaging of the portal vein was performed at baseline, two, and four minutes after NG stimulation for 8 of the 15 participants, pre-HDBR. Diameter measures of the superficial femoral artery were taken at baseline and five minutes after NG.

C.3.5 Statistical Analysis

The analysis of HDBR responses used a three-way repeated measures analysis of variance with the main effects for this analysis being HDBR (pre, post), countermeasure group (EX n=8, CON n=7), and time after drug. Responses to NG were determined every minute after NG and compared to baseline values before NG stimulation. SAS 9.1.3 analysis software was used for all statistical analysis with significance set at $p<0.05$. Values in the text are expressed as mean ± SD.

C.4 Results

C.4.1 Pre-HDBR Response to NG

No differences were seen for any measured variable between EX and CON pre-HDBR (filled symbols in figures). MAP was slightly reduced the first minute, decreased significantly (-4.9±3.0mmHg, Figure C.1 A) for the second minute, and remained lower for the remainder of the test. A decrease in SBP (-5.5±4.5mmHg, Figure C.1 B) combined with a slight increase in DBP to produce a decrease in PP (-5.8±4.9mmHg, Figure C.1 C). SBP recovered back towards baseline after four minutes, but the small, significant increase in DBP (1.7±3.4mmHg, Figure C.1 D) served to maintain the decrease in PP.

HR pre-HDBR increased significantly in the first minute after NG (4.2±4.2bpm, Figure C.2 A) then increased further at two minutes (11.8±3.9bpm) and remained elevated. SV decreased significantly by the second minute and Q was elevated only at the third minute (Figure C.2 B and D respectively). TPR was reduced at the third minute in response to NG (Figure C.2 C). The average baseline diameter of the portal vein was 10.9±1.7mm. Diameter

increased at two minutes to 11.9±1.9mm and remained dilated after four minutes with an average value of 12.0±1.7mm (n=8, $p<0.05$).

CBFV decreased over the first two minutes of NG (-9.0±2.3cm/s, Figure C.3 A) then remained lower throughout the observation period. Two calculated resistance indices revealed opposite effects. CVRi increased at two minutes (0.30±0.15mmHg/cm/s, Figure C.3 B) then remained elevated until the end of the test. However, the Doppler resistance index, RI, remained constant for the first two minutes and decreased significantly at three minutes after NG stimulation (-0.025±0.042, Figure C.3 C).

Femoral blood flow was reduced by 49.1±22.1mL/min/100mL tissue (Figure C.4 A, $p<0.05$). This resulted primarily though a large reduction in downstream vascular conductance (Figure C.4 B, $p<0.05$) as the diameter of the superficial femoral artery increased after NG (11.7±6.6% and 15.9±10.2% for EX and CON respectively, Figure C.4 C, $p<0.05$). The pattern of the blood velocity waveform (Figure C.5) changed dramatically during NG with the forward flow followed immediately by a large negative component.

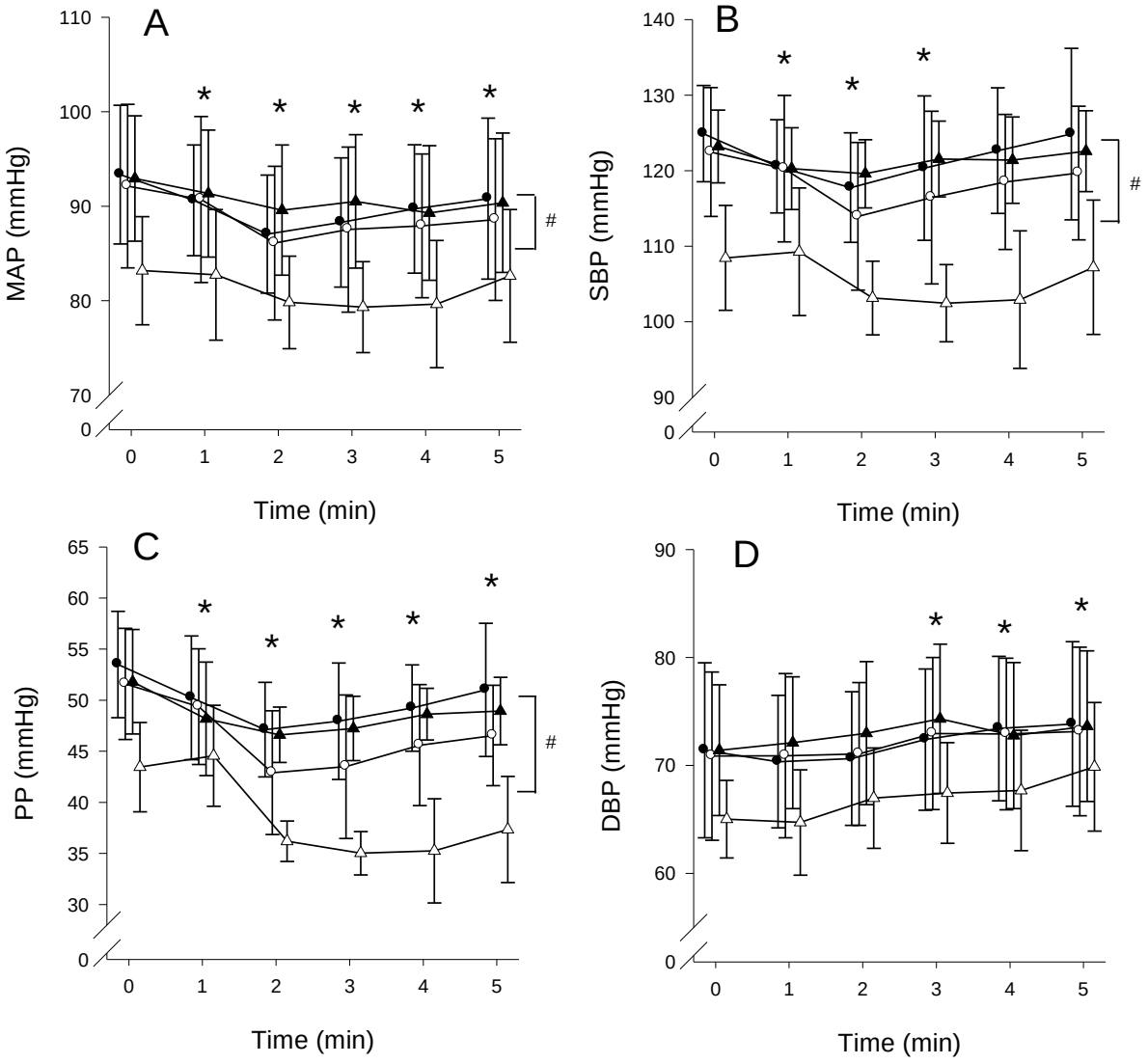

Figure C.1: Arterial pressure responses to NG

Responses of MAP (A), SBP (B), PP (C) and DBP (D) to 0.3mg sublingual nitroglycerin (NG) administered at time = 0. Pre- (solid symbols) and post-HDBR (open symbols) for exercise (EX, ●) and control (CON, ▲) groups. The assessment of NG effects are shown as differences from time = 0 (, $p<0.05$). Group x HDBR interactions showed significant reductions in MAP, SBP, and PP in CON post-HDBR compared to pre-HDBR (#, $p<0.05$). HDBR x NG interactions were found for both SBP and PP ($p<0.05$) indicating greater reductions in these variables post-HDBR. CON n=7, EX n=8.*

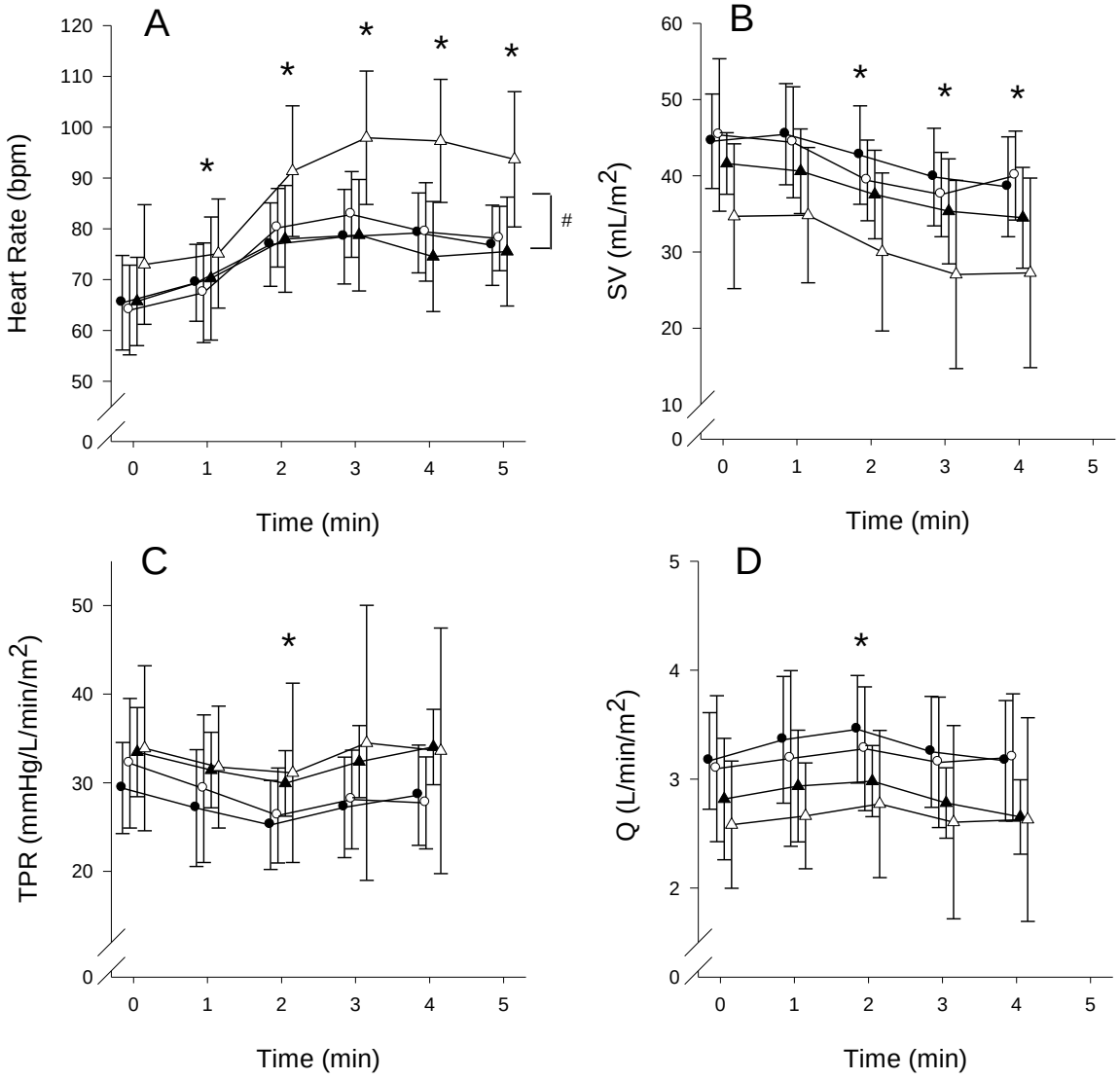

Figure C.2: HR, SV, TPR, and Q responses to NG

Responses of HR (A), SV (B), TPR (C), and Q (D) to NG administered at time = 0 before and after HDBR (symbols as in Figure C.1). The assessment of NG effects are shown as differences from time = 0 (, $p<0.05$). A significant 3 ways interaction (HDBR x Group x NG) was found for HR ($p<0.05$) indicating a greater response to NG in CON post-HDBR (CON n=7, EX n=8). No HDBR effects were found for SV, TPR, or Q (CON n=5, EX n=5).*

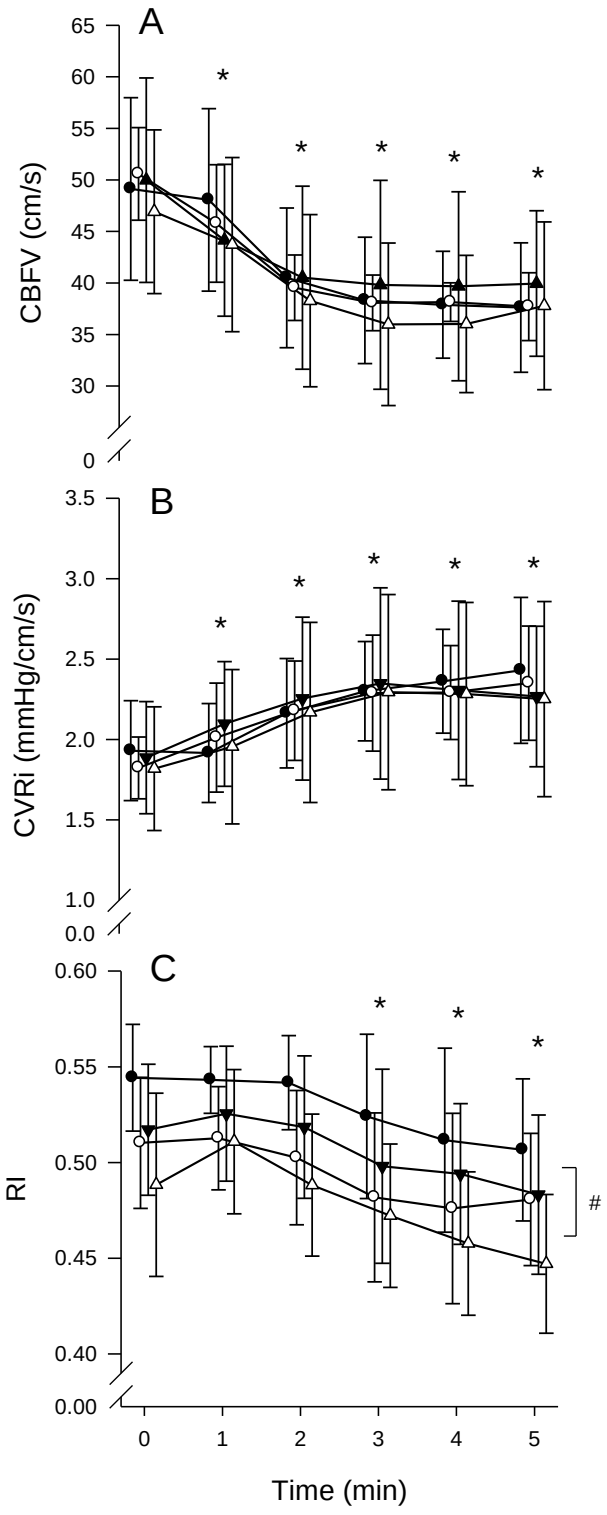

Figure C.3: Cerebrovascular responses to NG

Responses of CBFV (A), CVRi (B), and RI (C) to NG administered at time = 0 before and after HDBR (symbols as in Figure C.1). The assessment of NG effects are shown as differences from time = 0 (, $p<0.05$). No HDBR effects were found with either CBFV or CVRi; however, post-HDBR, RI was significantly reduced (#, $p<0.05$). CON n=6, EX n=7*

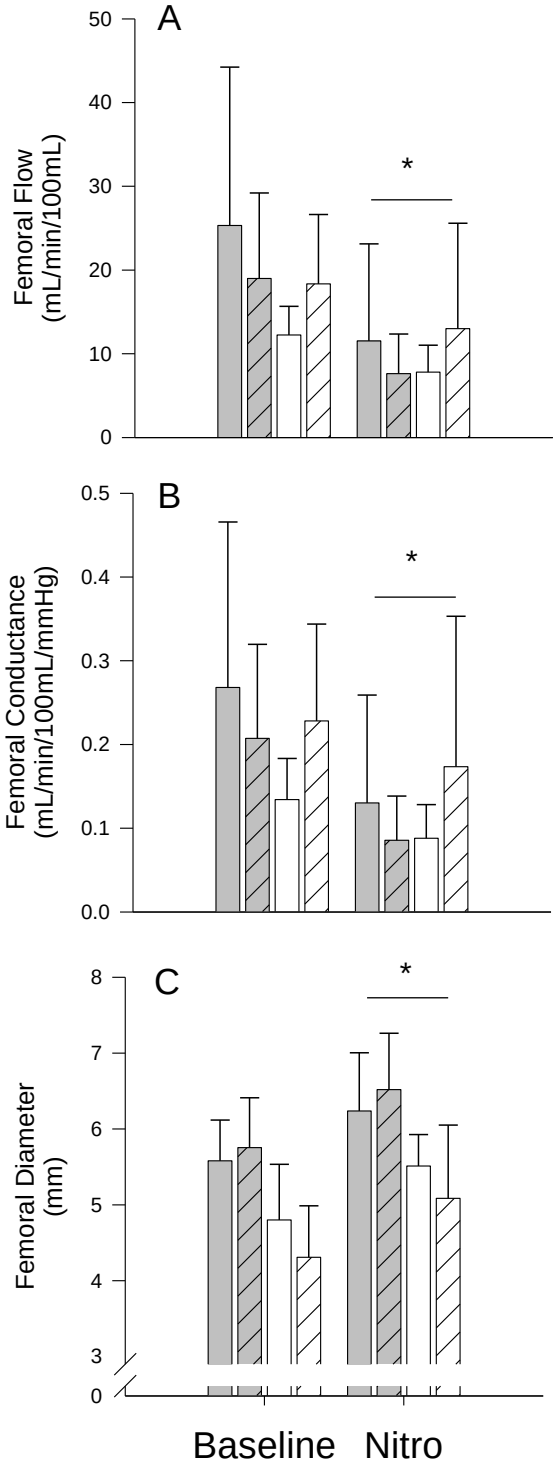

Figure C.4: Femoral artery responses to NG *Responses of superficial femoral artery flow (A), conductance (B), and diameter (C) in response to NG pre-HDBR (solid bars) and post-HDBR (hatched bars) for EX (grey) and CON (white). All variables showed a significant effect of NG (*, $p<0.05$). No HDBR effects were found for femoral flow, conductance, or diameter. CON n=5, EX n=6.*

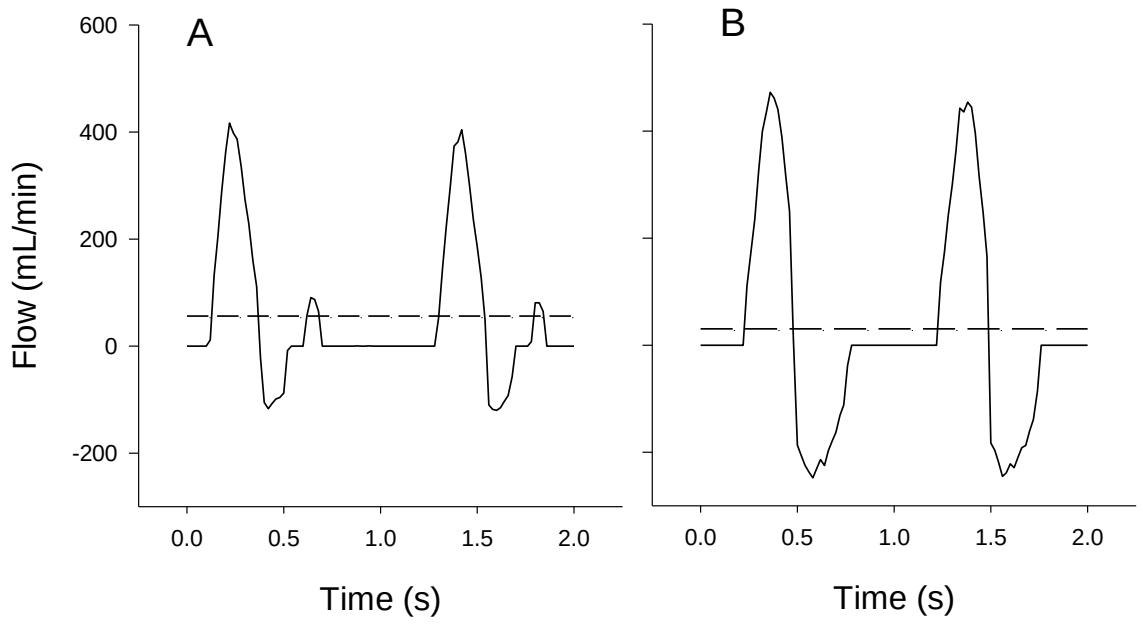

Figure C.5: Representative femoral blood flow trace

Representative tracings of the waveforms for a single subject of femoral blood flow (product of measured instantaneous velocity and vessel cross-sectional area) at baseline (A) and after NG stimulation (B). Mean flow, shown by dashed horizontal lines, was greater at baseline (56.1 mL/min) than after NG (30.1 mL/min) primarily due to a large increase in negative flow.

C.4.2 Effects of HDBR

After HDBR, resting MAP, SBP, and PP were lower in the CON group with no change in the EX group (Figure C.1). A significant HDBR x NG interaction effect ($p<0.05$) was detected for SBP and PP whereby both variables decreased more in post-HDBR compared to pre-HDBR.

The HR responses to NG after HDBR were characterized by a significant three-way interaction of HDBR x Group x NG effect (Figure C.2). Further analysis of this interaction showed that baseline HR, measured before NG stimulation, was elevated in CON but not in the EX group. In response to NG, both groups had greater HR increases post-HDBR. Peak increases in HR pre-HDBR (13.7±5.8 bpm and 13.0±5.2 bpm for EX and CON respectively) were significantly less than post-HDBR with a smaller HDBR increase for EX than CON

(18.8±6.6 bpm and 24.9±7.7 bpm for EX and CON respectively, Figure C.2). There were no HDBR effects for SV (Figure C.2 B), Q (Figure C.2 D), or TPR (Figure C.2 C).

After HDBR, CBFV and CVRi responses to NG were not statistically different from pre-HDBR (Figure C.3). There was a significant reduction in RI post-HDBR in both the EX and CON groups (HDBR main effect), but there was no difference in the response to NG. Baseline femoral blood flow, conductance, and diameter were not significantly different post-HDBR and the responses to NG including the change in diameter (13.9±13.6% and 18.6±17.2% for EX and CON respectively) were also not changed (Figure C.4).

C.5 Discussion

Sublingual nitroglycerin was used in the current study to investigate the overall cardiovascular response to an exogenous source of NO and to determine if the responses were altered after 56 days of HDBR. The pre-HDBR responses to NG were consistent with previous research with an increase in heart rate (Bonnin et al., 2001), reduction in cardiac stroke volume (Soma, Angelsen, Aakhus, & Skjaerpe, 2000), and lower arterial systolic, mean, and pulse pressure (Soma et al., 2000; Smulyan et al., 1986; Lai, Koyanagi, Shaw, & Takeshita, 1998). A novel observation was the almost 50% reduction in femoral blood flow that reflected a marked reduction in downstream vascular conductance as demonstrated by the large reverse (negative) component, shown in Figure C.5, of the Doppler ultrasound trace (Arbeille et al., 1995). Mean cerebral blood flow velocity was reduced in response to NG, but the reductions in the Doppler resistance index suggested that brain blood flow might have increased or at least remained constant as observed previously using other imaging techniques (Borisenko & Vlasenko, 1992; Dahl et al., 1989; Dahl et al., 1990; White et al., 2000).

This is the first study to explore the potential effects of an exercise countermeasure on the hemodynamic responses to NG in women after HDBR. Consistent with our hypothesis and in agreement with a shorter duration HDBR study of men (Bonnin et al., 2001), there was a greater increase in HR with NG stimulation that was attenuated by the exercise

countermeasure. Conversely, post-HDBR there was a greater reduction in both systolic blood pressure and arterial pulse pressure that was not affected by the exercise countermeasure. No effects of HDBR were seen for any of the cerebrovascular indicators examined in this study. Similarly, there were no differences in femoral artery dilation responses to NG which was consistent with results from two studies (Bonnin et al., 2001; Platts et al., 2009) but contrasted with the results from the Berlin Bed Rest Study in men (Bleeker et al., 2005). Overall, these data revealed only small changes in the cardiovascular responses to NG after HDBR which tend to contrast with previously reported data from both human males and rodent models.

C.5.1 Overall Responses to Nitroglycerin

This study provided a comprehensive view of the cardiovascular response of young, healthy, women to sublingual NG both before and after 56 days of HDBR. Previous work has focused on regional responses to NG in men. NG is an NO donor acting primarily on vascular smooth muscle (Chung & Fung, 1990; Ignarro et al., 1981), but potentially affecting the endothelium (Munzel, 2001). The major clinical application of NG has been to alleviate the effects of angina by reducing the preload on the heart through venodilation and by the direct action of dilating coronary arteries (Abrams, 1996). In research settings, NG is used extensively in the study of vasodilatory properties of conduit arteries as a method for eliciting maximal vasodilation independent of the endothelium (Bleeker et al., 2005; Bonnin et al., 2001; Guazzi et al., 2004). In the current study, NG was used to determine hemodynamic responses to NO both before and after HDBR.

There was evidence in the current study from the decline in SV that the cardiac preload was reduced by NG. The decline in SV was consistent with data from hypertensive men (Soma et al., 2000) but in contrast to that study Q was elevated at three minutes, potentially as a function of the increase in HR resulting from baroreflex compensation for the decline in SBP and MAP. The different responses could reflect a sex difference in the effect of NG or could simply reflect the contrast between hypertensive patients and the healthy subjects of the current study.

The peripheral vascular responses to NG suggested the dilation of conduit arteries but also a marked peripheral vasoconstriction as seen by the dilation of the superficial femoral artery, but reduction in superficial femoral blood flow. In spite of this local effect, the overall change in TPR was very small only significantly reduced at three minutes when Q was elevated suggesting that other vascular beds, possibly the splanchnic (see below) had directionally opposite changes in vascular resistance than the peripheral vasculature. Similar increases in vascular resistance in the limbs has been previously reported in studies examining blood flow control in the dog (Bogaert, Herman, & De Schaepdryver, 1970; O'Hara, Ono, Oguro, & Hashimoto, 1981), and is probably resultant from an initial elevation in muscle sympathetic nerve activity with NG (Nordin, Fagius, & Waldenlind, 1997). To the best of our knowledge, this is the first study to demonstrate a marked reduction in femoral vascular conductance in response to NG in women.

The overall maintenance of TPR with clear indications of increased local vasoconstriction in the legs suggests that other vascular beds must have had reduction in resistance. The increase in portal vein diameter was expected due to the venodilator actions of NG (Abrams, 1996). Given a positive relationship between portal vein diameter and blood flow (Arbeille, Besnard, Kerbeci, & Mohty, 2005) it is possible that portal vein flow increased with NG as found previously in humans (Reiss et al., 1994) and pigs (Morse & Rutlen, 1994) potentially do to a reduction in splanchnic vascular resistance thereby offsetting the observed increase in peripheral vascular resistance and allowing for the maintenance of TPR; however, an incomplete data set with no measures of velocity suggests caution in interpreting the impact on portal vein blood flow.

There were marked reductions in CBFV after sublingual NG. While it is often assumed that the cross-sectional area of the middle cerebral artery does not change during an experimental manipulation and that observed changes in velocity are proportional to changes in volume flow. This does not appear to be correct under the current conditions as MRI angiography has confirmed the dilation of the MCA with NG (Hansen et al., 2007). This study provides further support for the dilation of the MCA with NG in that the Doppler resistance index (RI) indicated a reduction in resistance in contrast to the calculated CVRi

which increased. The reduced RI coincident with lower MAP after NG might suggest relatively unchanged cerebral blood flow which is consistent with observations from PET scanning techniques following NG stimulation (Borisenko & Vlasenko, 1992; White et al., 2000).

C.5.2 Effects of NG after HDBR

Long duration HDBR as used in the current study is associated with a general cardiovascular deconditioning (Pavy-Le Traon et al., 2002). The current study was designed with an exercise countermeasure (EX) intervention to contrast with the control (CON) group that simply rested in bed throughout the entire 56 days. The EX group showed preservation of baseline values of HR and SV in the post-HDBR baseline condition while there was a significant increase in HR in the CON group. Post-HDBR, SV for the CON group was reduced by 16% compared to pre-HDBR values but this was not significant as technical problems limited the sample size. However, other data sets for different experiments conducted on these same women found significant reductions in SV in the CON group (Edgell et al., 2007; Guinet et al., 2009) as well as evidence of reduced left ventricular volume and mass in the CON group and a significant increase in mass for the EX group (Dorfman et al., 2007). In combination with these results, reductions in total blood volume of -9% for CON and -4% for EX (Guinet et al., 2009) probably contributed to the elevation in HR required to maintain cardiac output in the CON group as observed in this study.

There were no differences in the diameter of the superficial femoral artery, blood flow, or vascular conductance as a function of HDBR. Also, there were no changes in the response to sublingual NG in either the CON or the EX groups with HDBR. Previous research with men found reduction in leg artery diameter after 52 days horizontal bed rest (Bleeker et al., 2005) and after 60 days HDBR with or without resistance or vibration exercise countermeasures (van Duijnhoven et al., 2010). It is possible that the women in the current study were not as physically active prior to HDBR as the men so there was less difference between pre- and post-HDBR values, but technical difficulties reduced the sample size to 5 so the negative findings in the women should be viewed with caution. In the current

study, the EX group showed no differences in pre- and post-HDBR baseline diameter values suggesting that the exercise countermeasures, which included treadmill running, were sufficient to maintain vascular properties, while resistance or vibration exercise in men was not sufficient to maintain femoral artery diameter (van Duijnhoven et al., 2010).

The findings of no difference in response to NG after HDBR in the women of the current study contrast with data from the study of men in horizontal bed rest (Bleeker et al., 2005), but are similar to the findings for the tibial (Platts et al., 2009) and brachial (Bonnin et al., 2001) arteries of men after HDBR. In another investigation of the same subjects in the current study, Demiot et al (Demiot et al., 2007) showed that microvascular dilation of skin vessels to sodium nitroprusside was not affected by HDBR suggesting that peripheral vascular responses to NO from donor molecules was not altered by HDBR in women. Although there are no data for potential changes in the nitric oxide synthase (NOS) expression of the conduit arteries studied in the current study, muscle biopsy samples from these same women revealed that the exercise countermeasures were associated with an increased number of capillaries and greater total endothelial NOS (Salanova et al., 2008). No changes in the relative density of endothelial NOS were reported but sarcolemmal-associated NOS1 was reduced in the CON and increased in the EX women.

No HDBR effect was observed for CBFV or CVRi for either baseline values or in responses to NG, but there was a significant baseline reduction in RI post-HDBR. The interpretation of the differences between CVRi and RI response to NG could suggest a dilation of the MCA, but interpretation of HDBR effects remain uncertain. Unchanged CBFV has been previously reported with HDBR and spaceflight (Zhang et al., 1997; Arbeille et al., 2001; Pavy-Le Traon et al., 2002) and has been taken to reflect no changes in cerebral blood flow as indicated by measures of common carotid artery flow in cosmonauts (Arbeille et al., 2001). However, the common carotid artery supplies both cerebral and extracranial vascular beds and therefore, might not reflect changes in cerebral blood flow. Animal models of microgravity exposure have shown vascular smooth muscle hypertrophy of cerebral blood vessels (Wilkerson et al., 1999; Lin et al., 2009; Zhang et al., 2001; Wilkerson et al., 2002) and a smaller luminal cross-sectional area (Wilkerson et al., 1999) that is associated with

reduced cerebral blood flow (Wilkerson et al., 2002; Wilkerson et al., 2005). The different cerebrovascular response to head-down position between animals and humans might be due to the application of quantitative methods in animals compared to indirect indicators of brain blood flow in humans. These differences could potentially be resolved by application of quantitative ultrasound techniques to assess blood flow through the internal carotid artery.

C.5.3 Limitations

The WISE bed rest study was conducted as a large, multi-investigator study of the effects of long duration HDBR and the potential benefits of exercise countermeasures. Technical issues related to the acquisition of the Doppler signals for cardiac stroke volume and leg blood flow reduced the sample size and it was impossible to repeat the measurements. Therefore, while the statistical analysis did not find significant bed rest on effects on cardiac SV and femoral artery blood flow it is possible that the main effects would have been found with a larger sample size.

C.6 Conclusion

In response to NG, post-HDBR there was an augmented HR response, especially in the CON group. The HR responses likely serve to offset reductions in SV as Q was maintained. Cerebral blood velocity decreased with NG but this was most likely the result of dilation of the middle cerebral artery. A novel finding was, contrary to previous work in men, no changes were seen resting superficial femoral diameter post-HDBR and no differences were seen in the femoral vascular response to NG which included a large reduction in femoral vascular conductance. These data indicate that the primary impact of HDBR on the women of this study was on cardiovascular deconditioning and that there were no changes in the response to NG as an exogenous source of NO.

References

Aaslid, R., Lindegaard, K. F., Sorteberg, W., & Nornes, H. (1989). Cerebral autoregulation dynamics in humans. *Stroke, 20,* 45-52.

Aaslid, R., Markwalder, T. M., & Nornes, H. (1982). Non-invasive transcranial Doppler ultrasound recording of flow velocity in basal cerebral-arteries. *J Neurosurg, 57,* 769-774.

Abrams, J. (1985). Hemodynamic-effects of nitroglycerin and long-acting nitrates. *Am Heart J, 110,* 216-224.

Abrams, J. (1996). Beneficial actions of nitrates in cardiovascular disease. *Am J Cardiol, 77,* 31C-37C.

Adamson, S. L., Morrow, R. J., Langille, B. L., Bull, S. B., & Ritchie, J. W. K. (1990). Site-dependent effects of increases in placental vascular-resistance on the umbilical arterial velocity waveform in fetal sheep. *Ultrasound Med Biol, 16,* 19-27.

Aggarwal, S., Brooks, D. M., Kang, Y., Linden, P. K., & Patzer, J. F. (2008). Noninvasive monitoring of cerebral perfusion pressure in patients with acute liver failure using transcranial Doppler ultrasonography. *Liver Transplant, 14,* 1048-1057.

Ainslie, P. N., Celi, L., McGrattan, K., Peebles, K., & Ogoh, S. (2008). Dynamic cerebral autoregulation and baroreflex sensitivity during modest and severe step changes in arterial PCO_2. *Brain Res, 1230,* 115-124.

Ainslie, P. N., Murrell, C., Peebles, K., Swart, M., Skinner, M. A., Williams, M. J. et al. (2007). Early morning impairment in cerebral autoregulation and cerebrovascular CO_2 reactivity in healthy humans: Relation to endothelial function. *Exp Physiol, 92,* 769-777.

Albina, G., Cisneros, L. F., Laino, R., Nobo, U. L., Ortega, D., Schwarz, E. et al. (2004). Transcranial Doppler monitoring during head upright tilt table testing in patients with suspected neurocardiogenic syncope. *Europace, 6,* 63-69.

Arbeille, P., Berson, M., Achaibou, F., Bodard, S., & Locatelli, A. (1995). Vascular-resistance quantification in high-flow resistance areas using the Doppler method. *Ultrasound Med Biol, 21,* 321-328.

Arbeille, P., Fomina, G., Roumy, J., Alferova, I., Tobal, N., & Herault, S. (2001). Adaptation of the left heart, cerebral and femoral arteries, and jugular and femoral veins during short- and long-term head-down tilt and spaceflights. *Eur J Appl Physiol, 86,* 157-168.

Arbeille, P., Kerbeci, P., Mattar, L., Shoemaker, J., & Hughson, R. (2008). Insufficient flow reduction during LBNP in both splanchnic and lower limb areas is associated with orthostatic intolerance after bedrest. *Am J Physiol Heart Circ Physiol, 295,* H1846-H1854.

Arbeille, P., Sigaudo, D., Le Traon, A. P., Herault, S., Porcher, M., & Gharib, C. (1998). Femoral to cerebral arterial blood flow redistribution and femoral vein distension during orthostatic: Tests after 4 days in the head-down tilt position or confinement. *Eur J Appl Physiol Occup Physiol, 78,* 208-218.

Arbeille, P., Zuj, K., Shoemaker, K., & Hughson, R. (2012). Temporal artery Doppler spectrum morphology responses to tilt and LBNP as an early indicator of syncope. *Aviat Space Environ Med, 83,* 394-402.

Arbeille, P. P., Besnard, S. S., Kerbeci, P. P., & Mohty, D. M. (2005). Portal vein cross-sectional area and flow and orthostatic tolerance: a 90-day bed rest study. *J Appl Physiol, 99,* 1853-1857.

Baevsky, R. M., Baranov, V. M., Funtova, I. I., Diedrich, A., Pashenko, A. V., Chernikova, A. G. et al. (2007). Autonomic cardiovascular and respiratory control during prolonged spaceflights aboard the International Space Station. *J Appl Physiol, 103,* 156-161.

Bagian, J. P. & Hackett, P. (1991). Cerebral blood-flow - comparison of ground-based and spaceflight data and correlation with space adaptation syndrome. *J Clin Pharmacol, 31,* 1036-1040.

Bank, A. J. & Kaiser, D. R. (1998). Smooth muscle relaxation - effects on arterial compliance, distensibility, elastic modulus, and pulse wave velocity. *Hypertension, 32,* 356-359.

Bao, J. X., Zhang, L. F., & Ma, J. (2007). Angiotensinogen and AT1R expression in cerebral and femoral arteries during hindlimb unloading in rats. *Aviat Space Environ Med, 78,* 852-858.

Battisti-Charbonney, A., Fisher, J., & Duffin, J. (2011). The cerebrovascular response to carbon dioxide in humans. *J Physiol, 589,* 3039-3048.

Beasley, M. G., Blau, J. N., & Gosling, R. G. (1979). Changes in internal carotid-artery flow velocities with cerebral vasodilation and constriction. *Stroke, 10,* 331-335.

Bednarczyk, E. M., Wack, D. S., Kassab, M. Y., Burch, K., Trinidad, K., Haka, M. et al. (2002). Brain blood flow in the nitroglycerin (GTN) model of migraine: measurement using positron emission tomography and transcranial Doppler. *Cephalalgia, 22,* 749-757.

Bishop, C. C. R., Powell, S., Rutt, D., & Browse, N. L. (1986). Transcranial Doppler measurement of middle cerebral-artery blood-flow velocity - a validation-study. *Stroke, 17,* 913-915.

Blaber, A. P., Bondar, R. L., Moradshahi, P., Serrador, J. M., & Hughson, R. L. (2001). Inspiratory CO_2 increases orthostatic tolerance during repeated tilt. *Aviat Space Environ Med, 72,* 985-991.

Blaber, A. P., Goswami, N., Bondar, R. L., & Kassam, M. S. (2011). Impairment of cerebral blood flow regulation in astronauts with orthostatic intolerance after flight. *Stroke, 42,* 1844-1850.

Bland, J. M. & Douglas, G. A. (1996a). Statistics Notes: Measurement error. *BMJ, 313,* 744.

Bland, J. M. & Douglas, G. A. (1996b). Statistics Notes: Measurement error proportional to the mean. *BMJ, 313,* 106.

Bleasdale, R. A., Mumford, C. E., Campbell, R. I., Fraser, A. G., Jones, C. J. H., & Frenneaux, M. P. (2003). Wave intensity analysis from the common carotid artery: a new noninvasive index of cerebral vasomotor tone. *Heart Vessels, 18,* 202-206.

Bleeker, M. W. P., De Groot, P. C. E., Rongen, G. A., Rittweger, J., Felsenberg, D., Smits, P. et al. (2005). Vascular adaptation to deconditioning and the effect of an exercise countermeasure: Results of the Berlin Bed Rest study. *J Appl Physiol, 99,* 1293-1300.

Bogaert, M. G., Herman, A. G., & De Schaepdryver, A. F. (1970). Effects of nitroglycerin (trinitrin) on vascular smooth muscle. *Eur.J Pharmacol., 12,* 215-223.

Bondar, R. L., Kassam, M. S., Stein, F., Dunphy, P. T., Fortney, S., & Riedesel, M. L. (1995). Simultaneous cerebrovascular and cardiovascular-responses during presyncope. *Stroke, 26,* 1794-1800.

Bondar, R. L., Stein, F., Vaitkus, P. J., Johnston, K. W., Chadwick, L. C., & Norris, J. W. (1990). Transcranial Doppler studies of flow velocity in middle cerebral-artery in weightlessness. *J Clin Pharmacol, 30,* 390-395.

Bonnin, P., Ben Driss, A., Benessiano, J., Le Traon, A. P., Maillet, A., & Levy, B. I. (2001). Enhanced flow-dependent vasodilatation after bed rest, a possible mechanism for orthostatic intolerance in humans. *Eur J Appl Physiol, 85,* 420-426.

Borisenko, V. V. & Vlasenko, A. G. (1992). Assessment of cerebrovascular reactivity with low-doses of nitroglycerin - transcranial Doppler and cerebral blood-flow. *Cerebrovasc Dis, 2,* 58-60.

Brown, G. G., Perthen, J. E., Liu, T. T., & Buxton, R. B. (2007). A primer on functional magnetic resonance imaging. *Neuropsychol Rev, 17,* 107-125.

Buckey, J. C., Lane, L. D., Levine, B. D., Watenpaugh, D. E., Wright, S. J., Moore, W. E. et al. (1996). Orthostatic intolerance after spaceflight. *J Appl Physiol, 81,* 7-18.

Burton, A. C. (1951). On the physical equilibrium of small blood vessels. *Am J Physiol, 164,* 319-329.

Cao, P. H., Kimura, S., Macias, B. R., Ueno, T., Watenpaugh, D. E., & Hargens, A. R. (2005). Exercise within lower body negative pressure partially counteracts lumbar spine deconditioning associated with 28-day bed rest. *J Appl Physiol, 99,* 39-44.

Carey, B. J., Eames, P. J., Panerai, R. B., & Potter, J. F. (2001). Carbon dioxide, critical closing pressure and cerebral haemodynamics prior to vasovagal syncope in humans. *Clin Sci, 101,* 351-358.

Carey, B. J., Manktelow, B. N., Panerai, R. B., & Potter, J. F. (2001). Cerebral autoregulatory responses to head-up tilt in normal subjects and patients with recurrent vasovagal syncope. *Circulation, 104,* 898-902.

Carrera, E., Kim, D. J., Castellani, G., Zweifel, C., Smielewski, P., Pickard, J. D. et al. (2011). Effect of hyper- and hypocapnia on cerebral arterial compliance in normal subjects. *J Neuroimaging, 21,* 121-125.

Cencetti, S., Bandinelli, G., & Lagi, A. (1997). Effect of PCO_2 changes induced by head-upright tilt on transcranial Doppler recordings. *Stroke, 28,* 1195-1197.

Chan, G. S., Ainslie, P. N., Willie, C. K., Taylor, C. E., Atkinson, G., Jones, H. et al. (2011). Contribution of arterial Windkessel in low-frequency cerebral hemodynamics during transient changes in blood pressure. *J Appl Physiol, 110,* 917-925.

Chung, S. J. & Fung, H. L. (1990). Identification of the subcellular site for nitroglycerin metabolism to nitric-oxide in bovine coronary smooth-muscle cells. *J Pharmacol Exp Ther, 253,* 614-619.

Claassen, J. A., Zhang, R., Fu, Q., Witkowski, S., & Levine, B. D. (2007). Transcranial Doppler estimation of cerebral blood flow and cerebrovascular conductance during modified rebreathing. *J Appl Physiol, 102,* 870-877.

Clivati, A., Ciofetti, M., Cavestri, R., & Longhini, E. (1992). Cerebral vascular responsiveness in chronic hypercapnia. *Chest, 102,* 135-138.

Cooke, W. H., Ryan, K. L., & Convertino, V. A. (2004). Lower body negative pressure as a model to study progression to acute hemorrhagic shock in humans. *J Appl Physiol, 96,* 1249-1261.

Czosnyka, M., Richards, H. K., Reinhard, M., Steiner, L. A., Budohoski, K., Smielewski, P. et al. (2012). Cerebrovascular time constant: dependence on cerebral perfusion pressure and end-tidal carbon dioxide concentration. *Neurological Research, 34,* 17-24.

Dahl, A., Lindegaard, K. F., Russell, D., Nyberghansen, R., Rootwelt, K., Sorteberg, W. et al. (1992). A comparison of transcranial Doppler and cerebral blood-flow studies to assess cerebral vasoreactivity. *Stroke, 23,* 15-19.

Dahl, A., Russell, D., Nyberghansen, R., & Rootwelt, K. (1989). Effect of nitroglycerin on cerebral-circulation measured by transcranial Doppler and spect. *Stroke, 20,* 1733-1736.

Dahl, A., Russell, D., Nyberghansen, R., & Rootwelt, K. (1990). Cluster headache - transcranial Doppler ultrasound and rCBF studies. *Cephalalgia, 10,* 87-94.

Dahl, A., Russell, D., Nyberghansen, R., Rootwelt, K., & Mowinckel, P. (1994). Simultaneous assessment of vasoreactivity using transcranial Doppler ultrasound and cerebral blood-flow in healthy-subjects. *J Cereb Blood Flow Metab, 14,* 974-981.

Davis, M. J. & Hill, M. A. (1999). Signaling mechanisms underlying the vascular myogenic response. *Physiol Rev, 79,* 387-423.

de Riva, N., Budohoski, K., Smielewski, P., Kasprowicz, M., Zweifel, C., Steiner, L. et al. (2012). Transcranial Doppler pulsatility index: What it is and what it isn't. *Neurocrit Care,* 1-9.

Delp, M. D. & Laughlin, M. H. (1998). Regulation of skeletal muscle perfusion during exercise. *Acta Physiol Scand, 162,* 411-419.

Demiot, C., Dignat-George, F., Fortrat, J. O., Sabatier, F., Gharib, C., Larina, I. et al. (2007). WISE 2005: chronic bed rest impairs microcirculatory endothelium in women. *Am J Physiol Heart Circ Physiol, 293,* H3159-H3164.

Djurberg, H. G., Seed, R. F., Evans, D. A. P., Brohi, F. A., Pyper, D. L., Tjan, G. T. et al. (1998). Lack of effect of CO_2 on cerebral arterial diameter in man. *J Clin Anesth, 10,* 646-651.

Donald, I. & Levi, S. (1976). *Present and future of diagnostic ultrasound*. New York: Wiley.

Dorfman, T. A., Levine, B. D., Tillery, T., Peshock, R. M., Hastings, J. L., Schneider, S. M. et al. (2007). Cardiac atrophy in women following bed rest. *J Appl Physiol, 103,* 8-16.

Dumville, J., Panerai, R. B., Lennard, N. S., Naylor, A. R., & Evans, D. H. (1998). Can Cerebrovascular Reactivity Be Assessed Without Measuring Blood Pressure in Patients With Carotid Artery Disease? *Stroke, 29,* 968-974.

Edgell, H., Zuj, K. A., Greaves, D. K., Shoemaker, J. K., Custaud, M. A., Kerbeci, P. et al. (2007). WISE-2005: adrenergic responses of women following 56-days, 6 degrees head-down bed

rest with or without exercise countermeasures. *Am J Physiol Regul Integr Comp Physiol, 293,* R2343-R2352.

Edwards, M. R., Devitt, D. L., & Hughson, R. L. (2004). Two-breath CO_2 test detects altered dynamic cerebrovascular autoregulation and CO_2 responsiveness with changes in arterial PCO_2. *Am J Physiol Regul Integr Comp Physiol, 287,* R627-R632.

Edwards, M. R., Shoemaker, J. K., & Hughson, R. L. (2002). Dynamic modulation of cerebrovascular resistance as an index of autoregulation under tilt and controlled $P_{ET}CO_2$. *Am J Physiol Regul Integr Comp Physiol, 283,* R653-R662.

Edwards, M. R., Topor, Z. L., & Hughson, R. L. (2003). A new two-breath technique for extracting the cerebrovascular response to arterial carbon dioxide. *Am J Physiol Regul Integr Comp Physiol, 284,* R853-R859.

Eicke, B. M., Buss, E., Bahr, R. R., Hajak, G., & Paulus, W. (1999). Influence of acetazolamide and CO_2 on extracranial flow volume and intracranial blood flow velocity. *Stroke, 30,* 76-80.

Eiken, O., Kolegard, R., & Mekjavic, I. B. (2008). Pressure-distension relationship in arteries and arterioles in response to 5 wk of horizontal bedrest. *Am J Physiol Heart Circ Physiol, 295,* H1296-H1302.

Evans, D. H., Levene, M. I., Shortland, D. B., & Archer, L. N. J. (1988). Resistance index, blood-flow velocity, and resistance area product in the cerebral-arteries of very low birth-weight infants during the 1st week of life. *Ultrasound Med Biol, 14,* 103-110.

Fathi, A. R., Yang, C., Bakhtian, K. D., Qi, M., Lonser, R. R., & Pluta, R. M. (2011). Carbon dioxide influence on nitric oxide production in endothelial cells and astrocytes: Cellular mechanisms. *Brain Res, 1386,* 50-57.

Fogarty, J. (2011). Risk of microgravity-induced visual alterations/intracranial pressure (ICP). NASA Human Research Roadmap [On-line]. Available: http://humanresearchroadmap.nasa.gov/Risks/?i=105

Forster, B. B., Mackay, A. L., Whittall, K. P., Kiehl, K. A., Smith, A. M., Hare, R. D. et al. (1998). Functional magnetic resonance imaging: The basics of blood-oxygen-level dependent (BOLD) imaging. *J Can Assoc Radiol, 49,* 320-329.

Frey, M. A. B., Mader, T. H., Bagian, J. P., Charles, J. B., & Meehan, R. T. (1993). Cerebral blood velocity and other cardiovascular-responses to 2 days of head-down tilt. *J Appl Physiol, 74,* 319-325.

Gao, F., Bao, J., X, Xue, J., Huang, J., Huang, W., Wu, S., X et al. (2009). Regional specificity of adaptation change in large elastic arteries of simulated microgravity rats. *Acta Physiol Hung, 96,* 167-187.

Geary, G. G., Krause, D. N., Purdy, R. E., & Duckles, S. P. (1998). Simulated microgravity increases myogenic tone in rat cerebral arteries. *J Appl Physiol, 85,* 1615-1621.

Giller, C. A., Bowman, G., Dyer, H., Mootz, L., Krippner, W., Loftus, C. M. et al. (1993). Cerebral arterial diameters during changes in blood-pressure and carbon-dioxide during craniotomy. *Neurosurgery, 32,* 737-742.

Gosling, R. G., Lo, P. T. S., & Taylor, M. G. (1991). Interpretation of pulsatility index in feeder arteries to low-impedance vascular beds. *Ultrasound Obst Gyn, 1,* 175-179.

Green, D. (2005). Point: Flow-mediated dilation does reflect nitric oxide-mediated endothelial function. *J Appl Physiol, 99,* 1233-1234.

Green, D., Cheetham, C., Reed, C., Dembo, L., & O'Driscoll, G. (2002). Assessment of brachial artery blood flow across the cardiac cycle: retrograde flows during cycle ergometry. *J Appl Physiol, 93,* 361-368.

Guazzi, M., Lenatti, L., Tumminello, G., Puppa, S., Fiorentini, C., & Guazzi, M. D. (2004). The behaviour of the flow-mediated brachial artery vasodilatation during orthostatic stress in normal man. *Acta Physiol Scand, 182,* 353-360.

Guinet, P., Schneider, S. M., Macias, B. R., Watenpaugh, D. E., Hughson, R. L., Le Traon, A. P. et al. (2009). WISE-2005: effect of aerobic and resistive exercises on orthostatic tolerance during 60 days bed rest in women. *Eur J Appl Physiol, 106,* 217-227.

Gwilliam, M. N., Hoggard, N., Capener, D., Singh, P., Marzo, A., Verma, P. K. et al. (2009). MR derived volumetric flow rate waveforms at locations within the common carotid, internal carotid, and basilar arteries. *J Cereb Blood Flow Metab, 29,* 1975-1982.

Hainsworth, R. (2004). Pathophysiology of syncope. *Clin Auton Res, 14,* 18-24.

Hansen, J., Pedersen, D., Larsen, V., Sanchez-del-Rio, M., Linera, J., Olesen, J. et al. (2007). Magnetic resonance angiography shows dilatation of the middle cerebral artery after infusion of glyceryl trinitrate in healthy volunteers. *Cephalalgia, 27,* 118-127.

Hargens, A. R. & Watenpaugh, D. E. (1996). Cardiovascular adaptation to spaceflight. *Med Sci Sports Exercise, 28,* 977-982.

Haubrich, C., Czosnyka, Z., Lavinio, A., Smielewski, P., Diehl, R. R., Pickard, J. D. et al. (2007). Is there a direct link between cerebrovascular activity and cerebrospinal fluid pressure-volume compensation? *Stroke, 38,* 2677-2680.

Hetzel, A., Braune, S., Guschlbauer, B., & Dohms, K. (1999). CO2 Reactivity Testing Without Blood Pressure Monitoring? *Stroke, 30,* 398-401.

Hida, W., Kikuchi, Y., Okabe, S., Miki, H., Kurosawa, H., & Shirato, K. (1996). CO_2 response for the brain stem artery blood flow velocity in man. *Resp Physiol, 104,* 71-75.

Hirata, K., Yaginuma, T., O'Rourke, M. F., & Kawakami, M. (2006). Age-related changes in carotid artery flow and pressure pulses - Possible implications for cerebral microvascular disease. *Stroke, 37,* 2552-2556.

Hirayanagi, K., Iwase, S., Kamiya, A., Watanabe, Y., Shiozawa, T., Yamaguchi, N. et al. (2005). Alternations of static cerebral and systemic circulation in normal humans during 14-day head-down bed rest. *Med Sci Monit, 11,* CR570-CR575.

Hoskins, P. R. (1990). Measurement of arterial blood-flow by Doppler ultrasound. *Clin Phys Physiol Meas, 11,* 1-26.

Howden, R., Lightfoot, J. T., Brown, S. J., & Swaine, I. L. (2004). The effects of breathing 5% CO_2 on human cardiovascular responses and tolerance to orthostatic stress. *Exp Physiol, 89,* 465-471.

Hsu, H. Y., Chao, A. C., Chen, Y. T., Wong, W. J., Chern, C. M., Hsu, L. C. et al. (2005). Comparison of critical closing pressures extracted from carotid tonometry and finger plethysmography. *Cerebrovasc Dis, 19,* 369-375.

Hsu, H. Y., Chern, C. M., Kuo, J. S., Kuo, T. B. J., Chen, Y. T., & Hu, H. H. (2004). Correlations among critical closing pressure, pulsatility index and cerebrovascular resistance. *Ultrasound Med Biol, 30,* 1329-1335.

Hu, X. A., Alwan, A. A., Rubinstein, E. H., & Bergsneider, M. (2006). Reduction of compartment compliance increases venous flow pulsatility and lowers apparent vascular compliance: Implications for cerebral blood flow hemodynamics. *Med Eng Phys, 28,* 304-314.

Hughson, R. L., Edwards, M. R., O'Leary, D. D., & Shoemaker, J. K. (2001). Critical analysis of cerebrovascular autoregulation during repeated head-up tilt. *Stroke, 32,* 2403-2408.

Hughson, R. L., Shoemaker, J. K., Blaber, A. P., Arbeille, P., Greaves, D. K., Pereira-Junior, P. P. et al. (2011). Cardiovascular regulation during long-duration spaceflights to the International Space Station. *J Appl Physiol*.

Ide, K., Eliasziw, M., & Poulin, M. J. (2003). Relationship between middle cerebral artery blood velocity and end-tidal PCO_2 in the hypocapnic-hypercapnic range in humans. *J Appl Physiol, 95,* 129-137.

Ignarro, L. J., Lippton, H., Edwards, J. C., Baricos, W. H., Hyman, A. L., Kadowitz, P. J. et al. (1981). Mechanism of vascular smooth-muscle relaxation by organic nitrates, nitrites, nitroprusside and nitric-oxide - Evidence for the involvement of S-nitrosothiols as active intermediates. *J Pharmacol Exp Ther, 218,* 739-749.

Immink, R. V., Secher, N. H., Roos, C. M., Pott, F., Madsen, P. L., & van Lieshout, J. J. (2006). The postural reduction in middle cerebral artery blood velocity is not explained by $PaCO_2$. *Eur J Appl Physiol, 96,* 609-614.

Iwasaki, K. i., Levine, B. D., Zhang, R., Zuckerman, J. H., Pawelczyk, J. A., Diedrich, A. et al. (2007). Human cerebral autoregulation before, during and after spaceflight. *J Physiol, 579,* 799-810.

Kasprowicz, M., Diedler, J., Reinhard, M., Carrera, E., Steiner, L. A., Smielewski, P. et al. (2012). Time constant of the cerebral arterial bed in normal subjects. *Ultrasound in medicine & biology, 38,* 1129-1137.

Kawai, Y., Murthy, G., Watenpaugh, D. E., Breit, G. A., Deroshia, C. W., & Hargens, A. R. (1993). Cerebral blood-flow velocity in humans exposed to 24-h of head-down tilt. *J Appl Physiol, 74,* 3046-3051.

Kirkham, F. J., Padayachee, T. S., Parsons, S., Seargeant, L. S., House, F. R., & Gosling, R. G. (1986). Transcranial measurement of blood velocities in the basal cerebral-arteries using pulsed Doppler ultrasound - velocity as an index of flow. *Ultrasound Med Biol, 12,* 15-21.

Klabunde, R. E. (2007). Cardiovascualr physiology concepts. http://www.cvphysiology.com/Blood%20Pressure/BP004.htm [On-line].

Kleiser, B., Scholl, D., & Widder, B. (1995). Doppler CO_2 and diamox test - decreased reliability by changes of the vessel diameter. *Cerebrovasc Dis, 5,* 397-402.

Kramer, L. A., Sargsyan, A. E., Hasan, K. M., Polk, J. D., & Hamilton, D. R. (2012). Orbital and intracranial effects of microgravity: Findings at 3-T MR imaging. *Radiology, 263,* 819-827.

Krejza, J., Rudzinski, W., Pawlak, M., Tonnaszewski, M., Ichord, R., Kwiatkowski, J. et al. (2007). Angle-corrected imaging transcranial Doppler sonography versus imaging and nonimaging transcranial Doppler sonography in children with sickle cell disease. *Am J Neuroradiol, 28,* 1613-1618.

Ku, D. N. (1997). Blood flow in arteries. *Annu Rev Fluid Mech, 29,* 399-434.

Kurji, A., Debert, C. T., Whitelaw, W. A., Rawling, J. M., Frayne, R., & Poulin, M. J. (2006). Differences between middle cerebral artery blood velocity waveforms of young and postmenopausal women. *Menopause, 13,* 303-313.

Lai, C. P., Koyanagi, S., Shaw, C. K., & Takeshita, A. (1998). Evaluation of the early stage of carotid atherosclerosis using the vascular response to nitroglycerin and high-resolution ultrasonography. *Jpn Circ J, 62,* 494-498.

Lavi, S., Egbarya, R., Lavi, R., & Jacob, G. (2003). Role of nitric oxide in the regulation of cerebral blood flow in humans - chemoregulation versus mechanoregulation. *Circulation, 107,* 1901-1905.

Lavi, S., Gaitini, D., Milloul, V., & Jacob, G. (2006). Impaired cerebral CO_2 vasoreactivity: association with endothelial dysfunction. *Am J Physiol Heart Circ Physiol, 291,* H1856-H1861.

LeLorier, P., Klein, G. J., Krahn, A., Yee, R., Skanes, A., & Shoemaker, J. K. (2003). Combined head-up tilt and lower body negative pressure as an experimental model of orthostatic syncope. *J Cardiovasc Electrophysiol, 14,* 920-924.

Levine, B. D., Giller, C. A., Lane, L. D., Buckey, J. C., & Blomqvist, C. G. (1994). Cerebral versus systemic hemodynamic during graded orthostatic stress in humans. *Circulation, 90,* 298-306.

Lewis, N., Atkinson, G., Lucas, S., Grant, E., Jones, H., Tzeng, Y. et al. (2010). Diurnal variation in time to presyncope and associated circulatory changes during a controlled orthostatic challenge. *Am J Physiol Regul Integr Comp Physiol, 299,* R55-R61.

Lin, L. J., Gao, F., Bai, Y. G., Bao, J. X., Huang, X. F., Ma, J. et al. (2009). Contrasting effects of simulated microgravity with and without daily -G(x) gravitation on structure and function of cerebral and mesenteric small arteries in rats. *J Appl Physiol, 107,* 1710-1721.

Lindegaard, K. F., Lundar, T., Wiberg, J., Sjoberg, D. I. K., Aaslid, R., & Nornes, H. (1987). Variations in middle cerebral-artery blood-flow investigated with noninvasive transcranial blood velocity-measurements. *Stroke, 18,* 1025-1030.

Lockhart, C. J., Gamble, A. J., Rea, D., Hughes, S., McGivern, R., Wolsley, C. et al. (2006). Nitric oxide modulation of ophthalmic artery blood flow velocity waveform morphology in healthy volunteers. *Clin Sci, 111,* 47-52.

Mader, T. H., Gibson, C., Pass, A. F., Kramer, L. A., Lee, A. G., Fogarty, J. et al. (2011). Optic disc edema, globe flattening, choroidal folds, and hyperopic shifts observed in astronauts after long-duration space flight. *Ophthalmology, 118,* 2058-2069.

Maruyoshi, H., Kojima, S., Kojima, S., Nagayoshi, Y., Horibata, Y., Kaikita, K. et al. (2010). Waveform of ophthalmic artery Doppler flow predicts the severity of systemic atherosclerosis. *Circulation Journal, 74,* 1251-1256.

Mathew, R. J. (1996). Postural syncope and autoregulation of cerebral blood flow. *Biol Psychiatry, 40,* 923-926.

McVeigh, G. E., Bratteli, C. W., Morgan, D. J., Alinder, C. M., Glasser, S. P., Finkelstein, S. M. et al. (1999). Age-related abnormalities in arterial compliance identified by pressure pulse contour analysis - aging and arterial compliance. *Hypertension, 33,* 1392-1398.

Micieli, G., Bosone, D., Costa, A., Cavallini, A., Marcheselli, S., Pompeo, F. et al. (1997). Opposite effects of L-arginine and nitroglycerin on cerebral blood velocity: Nitric oxide precursors and cerebral blood velocity. *J Neurol Sci, 150,* 71-75.

Mitsis, G. D., Poulin, M. J., Robbins, P. A., & Marmarelis, V. Z. (2004). Nonlinear modeling of the dynamic effects of arterial pressure and CO_2 variations on cerebral blood flow in healthy humans. *IEEE Trans Biomed Eng, 51,* 1932-1943.

Mombouli, J. V. & Vanhoutte, P. M. (1999). Endothelial dysfunction: From physiology to therapy. *J Mol Cell Cardiol, 31,* 61-74.

Moppett, I. K., Sherman, R. W., Wild, M. J., Latter, J. A., & Mahajan, R. P. (2008). Effects of norepinephrine and glyceryl trinitrate on cerebral haemodynamics: transcranial Doppler study in healthy volunteers. *Brit J Anaesth, 100,* 240-244.

Morse, M. A. & Rutlen, D. L. (1994). Influence of nitroglycerin on splanchnic capacity and splanchnic capacity cardiac-output relationship. *J Appl Physiol, 76,* 112-119.

Muller, M., Voges, M., Piepgras, U., & Schimrigk, K. (1995). Assessment of cerebral vasomotor reactivity by transcranial Doppler ultrasound and breath-holding - a comparison with acetazolamide as vasodilatory stimulus. *Stroke, 26,* 96-100.

Munzel, T. (2001). Editorial comment - Does nitroglycerin therapy hit the endothelium? *J Am Coll Cardiol, 38,* 1102-1105.

Nariai, T., Suzuki, R., Hirakawa, K., Maehara, T., Ishii, K., & Senda, M. (1995). Vascular reserve in chronic cerebral-ischemia measured by the acetazolamide challenge test - comparison with positron emission tomography. *Am J Neuroradiol, 16,* 563-570.

Nichols, W. W., Denardo, S. J., Wilkinson, I. B., McEniery, C. M., Cockcroft, J., & O'Rourke, M. F. (2008). Effects of arterial stiffness, pulse wave velocity, and wave reflections on the central aortic pressure waveform. *J Clin Hypertens, 10,* 295-303.

Niki, K., Sugawara, M., Chang, D., Harada, A., Okada, T., Sakai, R. et al. (2002). A new noninvasive measurement system for wave intensity: evaluation of carotid arterial wave intensity and reproducibility. *Heart Vessels, 17,* 12-21.

Nordin, M., Fagius, J., & Waldenlind, E. (1997). Sympathetic vasoconstrictor outflow to extremity muscles in cluster headache. Recordings during spontaneous and nitroglycerin-induced attackse. *Headache, 37,* 358-367.

Nornes, H. & Wikeby, P. (1977). Cerebral arterial blood-flow and aneurysm surgery .7. Local arterial flow dynamics. *J Neurosurg, 47,* 810-818.

O'Hara, N., Ono, H., Oguro, K., & Hashimoto, K. (1981). Vasodilating effects of perhexiline, glyceryl trinitrate, and verapamil on the coronary, femoral, renal, and mesenteric vasculature of the dog. *J Cardiovasc.Pharmacol., 3,* 251-268.

O'Leary, D., Hughson, R., Shoemaker, J., Greaves, D., Watenpaugh, D., Macias, B. et al. (2007). Heterogeneity of responses to orthostatic stress in homozygous twins. *J Appl Physiol, 102,* 249-254.

O'Leary, D. D., Kimmerly, D. S., Cechetto, A. D., & Shoemaker, J. K. (2003). Differential effect of head-up tilt on cardiovagal and sympathetic baroreflex sensitivity in humans. *Exp Physiol, 88,* 769-774.

Ogoh, S., Brothers, R., Jeschke, M., Secher, N. H., & Raven, P. B. (2010). Estimation of cerebral vascular tone during exercise; evaluation by critical closing pressure in humans. *Exp Physiol, 95,* 678-685.

Pandit, J. J., Mohan, R. M., Paterson, N. D., & Poulin, M. J. (2007). Cerebral blood flow sensitivities to CO_2 measured with steady-state and modified rebreathing methods. *Respir Physiol Neurobiol, 159,* 34-44.

Panerai, R., Salinet, A., Brodie, F., & Robinson, T. (2011). The influence of calculation method on estimates of cerebral critical closing pressure. *Physiol Meas, 32,* 467-482.

Panerai, R. B., Dineen, N., Brodie, F., & Robinson, T. (2010). Spontaneous fluctuations in cerebral blood flow regulation: contribution of $PaCO_2$. *J Appl Physiol, 109,* 1860-1868.

Panerai, R. B. (1998). Assessment of cerebral pressure autoregulation in humans - a review of measurement methods. *Physiol Meas, 19,* 305-338.

Panerai, R. B. (2003). The critical closing pressure of the cerebral circulation. *Med Eng Phys, 25,* 621-632.

Panerai, R. B., Dawson, S. L., & Potter, J. F. (1999). Linear and nonlinear analysis of human dynamic cerebral autoregulation. *Am J Physiol Heart Circ Physiol, 277,* H1089-H1099.

Panerai, R. B., Deverson, S. T., Mahony, P., Hayes, P., & Evans, D. H. (1999). Effect of CO_2 on dynamic cerebral autoregulation measurement. *Physiol Meas, 20,* 265-275.

Paulson, O. B., Strandgaard, S., & Edvinsson, L. (1990). Cerebral autoregulation. *Cerebrovasc Brain Metab Rev, 2,* 161-192.

Paulson, O. B., Waldemar, G., Schmidt, J. F., & Strandgaard, S. (1989). Cerebral-circulation under normal and pathologic conditions. *Am J Cardiol, 63,* C2-C5.

Pavy-Le Traon, A., Costes-Salon, M. C., Vasseur-Clausen, P., Bareille, M. P., Maillet, A., & Parant, M. (2002). Changes in kinetics of cerebral autoregulation with head-down bed rest. *Clin Physiol Funct Imaging, 22,* 108-114.

Platts, S. H., Martin, D. S., Stenger, M. B., Perez, S. A., Ribeiro, L. C., Summers, R. et al. (2009). Cardiovascular adaptations to long-duration head-down bed rest. *Aviat Space Environ Med, 80,* A29-A36.

Poels, M. M., Ikram, M. A., Vernooij, M. W., Krestin, G. P., Hofman, A., Niessen, W. J. et al. (2008). Total cerebral blood flow in relation to cognitive function: The Rotterdam Scan Study. *J Cereb Blood Flow Metab, 28,* 1652-1655.

Poeppel, T., Terborg, C., Hautzel, H., Herzog, H., Witte, O., Mueller, H. et al. (2007). Cerebral haemodynamics during hypo- and hypercapnia - determination with simultaneous O-15-butanol-PET and transcranial Doppler sonography. *Nuklearmed, 46,* 93-100.

Portella, G., Cormio, M., Citerio, G., Contant, C., Kiening, K., Enblad, P. et al. (2005). Continuous cerebral compliance monitoring in severe head injury: Its relationship with intracranial pressure and cerebral perfusion pressure. *Acta Neurochir, 147,* 707-713.

Poulin, M. J., Liang, P. J., & Robbins, P. A. (1996). Dynamics of the cerebral blood flow response to step changes in end-tidal PCO_2 and PO_2 in humans. *J Appl Physiol, 81,* 1084-1095.

Poulin, M. J. & Robbins, P. A. (1996). Indexes of flow and cross-sectional area of the middle cerebral artery using Doppler ultrasound during hypoxia and hypercapnia in humans. *Stroke, 27,* 2244-2250.

Powers, W. J. (1991). Cerebral hemodynamics in ischemic cerebrovascular-disease. *Ann Neurol, 29,* 231-240.

Prisby, R. D., Wilkerson, M. K., Sokoya, E. M., Bryan, R. M., Wilson, E., & Delp, M. D. (2006). Endothelium-dependent vasodilation of cerebral arteries is altered with simulated microgravity through nitric oxide synthase and EDHF mechanisms. *J Appl Physiol, 101,* 348-353.

Rakebrandt, F., Palombo, C., Swampillai, J., Schon, F., Donald, A., Kozakova, M. et al. (2009). Arterial wave intensity and ventricular-arterial coupling by vascular ultrasound: Rationale and methods for the automated analysis of forwards and backwards running waves. *Ultrasound Med Biol, 35,* 266-277.

Raviele, A., Gasparini, G., Dipede, F., Menozzi, C., Brignole, M., Dinelli, M. et al. (1994). Nitroglycerin infusion during upright tilt - a new test for the diagnosis of vasovagal syncope. *Am Heart J, 127,* 103-111.

Razumovsky, A. Y., DeBusk, K., Calkins, H., Snader, S., Lucas, K. E., Vyas, P. et al. (2003). Cerebral and systemic hemodynamics changes during upright tilt in chronic fatigue syndrome. *J Neuroimaging, 13,* 57-67.

Reiss, W. G., Bauer, L. A., Horn, J. R., Zierler, B. K., Easterling, T. R., & Strandness, D. E. (1994). Acute effects of sublingual nitroglycerin on hepatic blood-flow in healthy-volunteers. *J Clin Pharmacol, 34,* 912-918.

Reneman, R. S., Hoeks, A., & Spencer, M. P. (1979). Doppler ultrasound in the evaluation of the peripheral arterial circulation. *Angiology, 30,* 526-538.

Rittweger, J., Frost, H. M., Schiessl, H., Ohshima, H., Alkner, B., Tesch, P. et al. (2005). Muscle atrophy and bone loss after 90 days' bed rest and the effects of flywheel resistive exercise and pamidronate: Results from the LTBR study. *Bone, 36,* 1019-1029.

Robertson, A. D., Zuj, K. A., Zamir, M., Hughson, R. L., & Shoemaker, J. K. (2008). Mathematical modelling shows changes in multiple cerebrovascular properties of older adults. *Appl Physiol Nutr Metab, 33,* S83-S84.

Robertson, J. W., Debert, C. T., Frayne, R., & Poulin, M. J. (2008). Variability of middle cerebral artery blood flow with hypercapnia in women. *Ultrasound Med Biol, 34,* 730-740.

Rudnick, J., Puttmann, B., Tesch, P. A., Alkner, B., Schoser, B. G. H., Salanova, M. et al. (2004). Differential expression of nitric oxide synthases (NOS 1-3) in human skeletal muscle following exercise countermeasure during 12 weeks of bed rest. *Faseb Journal, 18,* 1228-1230.

Salanova, M., Schiffl, G., Püttmann, B., Schoser, B. G., & Blottner, D. (2008). Molecular biomarkers monitoring human skeletal muscle fibres and microvasculature following long-term bed rest with and without countermeasures. *J Anat, 212,* 306-318.

Sangha, D. S., Vaziri, N. D., Ding, Y., & Purdy, R. E. (2000). Vascular hyporesponsiveness in simulated microgravity: role of nitric oxide-dependent mechanisms. *J Appl Physiol, 88,* 507-517.

Sato, K., Ogoh, S., Hirasawa, A., Oue, A., & Sadamoto, T. (2011). The distribution of blood flow in the carotid and vertebral arteries during dynamic exercise in humans. *J Physiol, 589,* 2847-2856.

Sato, K., Sadamoto, T., Hirasawa, A., Oue, A., Subudhi, A. W., Miyazawa, T. et al. (2012). Differential blood flow responses to CO_2 in human internal and external carotid and vertebral arteries. *J Physiol, 590,* 3277-3290.

Schmetterer, L., Findl, O., Strenn, K., Graselli, U., Kastner, J., Eichler, H. G. et al. (1997). Role of NO in the O_2 and CO_2 responsiveness of cerebral and ocular circulation in humans. *Am J Physiol Regul Integr Comp Physiol, 273,* R2005-R2012.

Schneider, S. M., Lee, S. M. C., Macias, B. R., Watenpaugh, D. E., & Hargens, A. R. (2009). WISE-2005: Exercise and nutrition countermeasures for upright VO_2pk during bed rest. *Med Sci Sports Exercise, 41,* 2165-2176.

Schreiber, S. J., Gottschalk, S., Weih, M., Villringer, A., & Valdueza, J. M. (2000). Assessment of blood flow velocity and diameter of the middle cerebral artery during the acetazolamide

provocation test by use of transcranial Doppler sonography and MR imaging. *Am J Neuroradiol, 21,* 1207-1211.

Schubert, T., Santini, F., Stalder, A. F., Bock, J., Meckel, S., Bonati, L. et al. (2011). Dampening of blood-flow pulsatility along the carotid siphon: Does form follow function? *Am J Neuroradiol, 32,* 1107-1112.

Seals, D. R. (2003). Habitual exercise and the age-associated decline in large artery compliance. *Exercise Sport Sci Rev, 31,* 68-72.

Serrador, J. M., Hughson, R. L., Kowalchuk, J. M., Bondar, R. L., & Gelb, A. W. (2006). Cerebral blood flow during orthostasis: role of arterial CO_2. *Am J Physiol Regul Integr Comp Physiol, 290,* R1087-R1093.

Serrador, J. M., Picot, P. A., Rutt, B. K., Shoemaker, J. K., & Bondar, R. L. (2000). MRI measures of middle cerebral artery diameter in conscious humans during simulated orthostasis. *Stroke, 31,* 1672-1678.

Siepmann, M. & Kirch, W. (2000). Effects of nitroglycerine on cerebral blood flow velocity, quantitative electroencephalogram and cognitive performance. *Eur J Clin Invest, 30,* 832-837.

Smulyan, H., Mookherjee, S., & Warner, R. A. (1986). The effect of nitroglycerin on forearm arterial distensibility. *Circulation, 73,* 1264-1269.

Soma, J., Angelsen, B. A. J., Aakhus, S., & Skjaerpe, T. (2000). Sublingual nitroglycerin delays arterial wave reflections despite increased aortic "stiffness" in patients with hypertension: A Doppler echocardiography study. *J Am Soc Echocardiog, 13,* 1100-1108.

Sorond, F. A., Serrador, J. M., Jones, R. N., Shaffer, M. L., & Lipsitz, L. A. (2009). The sit-to-stand technique for the measurement of dynamic cerebral autoregulation. *Ultrasound Med Biol, 35*, 21-29.

Stewart, J. M., Medow, M. S., Messer, Z. R., Baugham, I. L., Terilli, C., & Ocon, A. J. (2012). Postural neurocognitive and neuronal activated cerebral blood flow deficits in young chronic fatigue syndrome patients with postural tachycardia syndrome. *Am J Physiol Heart Circ Physiol, 302*, H1185-H1194.

Strandgaard, S. & Paulson, O. B. (1984). Cerebral autoregulation. *Stroke, 15*, 413-416.

Sugawara, M., Niki, K., Furuhata, H., Ohnishi, S., & Suzuki, S. (2000). Relationship between the pressure and diameter of the carotid artery in humans. *Heart Vessels, 15*, 49-51.

Sun, X. Q., Yao, Y. J., Yang, C. B., Jiang, S. Z., Jiang, C. L., & Liang, W. B. (2005). Effect of lower-body negative pressure on cerebral blood flow velocity during 21 days head-down tilt bed rest. *Med Sci Monit, 11*, CR1-CR5.

Tobal, N., Roumy, J., Herault, S., Fomina, G., & Arbeille, P. (2001). Doppler measurement of cerebral and lower limb flow during a lower body negative pressure test for predicting orthostatic intolerance. *J Ultrasound Med, 20*, 1207-1217.

Tuday, E. C., Meck, J. V., Nyhan, D., Shoukas, A. A., & Berkowitz, D. E. (2007). Microgravity-induced changes in aortic stiffness and their role in orthostatic intolerance. *J Appl Physiol, 102*, 853-858.

Ulrich, P. T., Becker, T., & Kempski, O. S. (1995). Correlation of cerebral blood-flow and MCA flow velocity measured in healthy-volunteers during acetazolamide and CO_2 stimulation. *J Neurol Sci, 129,* 120-130.

Valdueza, J. M., Balzer, J. O., Villringer, A., Vogl, T. J., Kutter, R., & Einhaupl, K. M. (1997). Changes in blood flow velocity and diameter of the middle cerebral artery during hyperventilation: Assessment with MR and transcranial Doppler sonography. *Am J Neuroradiol, 18,* 1929-1934.

Valdueza, J. M., Draganski, B., Hoffmann, O., Dirnagl, U., & Einhaupl, K. M. (1999). Analysis of CO_2 vasomotor reactivity and vessel diameter changes by simultaneous venous and arterial Doppler recordings. *Stroke, 30,* 81-86.

van Duijnhoven, N. T. L., Green, D. J., Felsenberg, D., Belavy, D. L., Hopman, M. T. E., & Thijssen, D. H. J. (2010). Impact of bed rest on conduit artery remodeling effect of exercise countermeasures. *Hypertension, 56,* 240-246.

Vaziri, N. D., Ding, Y., Sangha, D. S., & Purdy, R. E. (2000). Upregulation of NOS by simulated microgravity, potential cause of orthostatic intolerance. *J Appl Physiol, 89,* 338-344.

Waters, W. W., Ziegler, M. G., & Meck, J. V. (2002). Postspaceflight orthostatic hypotension occurs mostly in women and is predicted by low vascular resistance. *J Appl Physiol, 92,* 586-594.

White, R. P., Deane, C., Hindley, C., Bloomfield, P. M., Cunningham, V. J., Vallance, P. et al. (2000). The effect of the nitric oxide donor glyceryl trinitrate on global and regional cerebral blood flow in man. *J Neurol Sci, 178,* 23-28.

Wilkerson, M. K., Colleran, P. N., & Delp, M. D. (2002). Acute and chronic head-down tail suspension diminishes cerebral perfusion in rats. *Am J Physiol Heart Circ Physiol, 282,* H328-H334.

Wilkerson, M. K., Lesniewski, L. A., Golding, E. M., Bryan, R. M., Amin, A., Wilson, E. et al. (2005). Simulated microgravity enhances cerebral artery vasoconstriction and vascular resistance through endothelial nitric oxide mechanism. *Am J Physiol Heart Circ Physiol, 288,* H1652-H1661.

Wilkerson, M. K., Muller-Delp, J., Colleran, P. N., & Delp, M. D. (1999). Effects of hindlimb unloading on rat cerebral, splenic, and mesenteric resistance artery morphology. *J Appl Physiol, 87,* 2115-2121.

Willie, C. K., Macleod, D. B., Shaw, A. D., Smith, K. J., Tzeng, Y. C., Eves, N. D. et al. (2012). Regional brain blood flow in man during acute changes in arterial blood gases. *J Physiol, 590,* 3261-3275.

Wintermark, M., Sesay, M., Barbier, E., Borbely, K., Dillon, W. P., Eastwood, J. D. et al. (2005). Comparative overview of brain perfusion imaging techniques. *Stroke, 36,* 2032-2033.

Zamir, M. (2005). *The Physics of Coronary Blood Flow*. New York: Springer Science+Business Media, Inc.

Zamir, M., Goswami, R., Salzer, D., & Shoemaker, J. (2007). Role of vascular bed compliance in vasomotor control in human skeletal muscle. *Exp Physiol, 92,* 841-848.

Zhang, L. F. (2001). Vascular adaptation to microgravity: What have we learned? *J Appl Physiol, 91,* 2415-2430.

Zhang, L. N., Zhang, L. F., & Ma, J. (2001). Simulated microgravity enhances vasoconstrictor responsiveness of rat basilar artery. *J Appl Physiol, 90,* 2296-2305.

Zhang, R., Zuckerman, J. H., Pawelczyk, J. A., & Levine, B. D. (1997). Effects of head-down-tilt bed rest on cerebral hemodynamics during orthostatic stress. *J Appl Physiol, 83,* 2139-2145.

Zhang, R., Zukerman, J. H., Giller, C. A., & Levine, B. D. (1998). Transfer function analysis of dynamic cerebral autoregulation in humans. *Am J Physiol Heart Circ Physiol, 274,* H233-H241.

Zhang, R., Behbehani, K., & Levine, B. D. (2009). Dynamic pressure-flow relationship of the cerebral circulation during acute increase in arterial pressure. *J Physiol, 587,* 2567-2577.

Zhang, Y. R., Liu, M. W., Wang, M. L., Zhang, L., Lv, Q., Xie, M. X. et al. (2010). Wave intensity analysis of carotid artery: A noninvasive technique for assessing hemodynamic changes of hyperthyroid patients. *Journal of Huazhong University of Science and Technology-Medical Sciences, 30,* 672-677.

Zhu, Y. S., Tseng, B. Y., Shibata, S., Levine, B. D., & Zhang, R. (2011). Increases in cerebrovascular impedance in older adults. *J Appl Physiol, 111,* 376-381.

Zimmermann, C. & Haberl, R. L. (2003). L-arginine improves diminished cerebral CO_2 reactivity in patients. *Stroke, 34,* 643-647.

Zuj, K. A., Arbeille, P., Shoemaker, J. K., Blaber, A. P., Greaves, D. K., Xu, D. et al. (2012a). Impaired cerebrovascular autoregulation and reduced CO_2 reactivity after long duration spaceflight. *Am J Physiol Heart Circ Physiol, 302,* H2592-H2598.

Zuj, K. A., Edgell, H., Shoemaker, J. K., Custaud, M. A., Arbeille, P., & Hughson, R. L. (2012b). WISE 2005: Responses of women to sublingual nitroglycerin before and after 56 days of 6-degree head down bed rest. *J Appl Physiol, 113,* 434-441.

Zwiebel, W. J. & Pellerito, J. S. (2005). *Introduction to Vascular Ultrasonography*. (Fifth ed.) Philadelphia: Elsevier Inc.